Design of a universal phantom for quality assurance in diagnostic radiology x-ray imaging

by

Annemari Groenewald

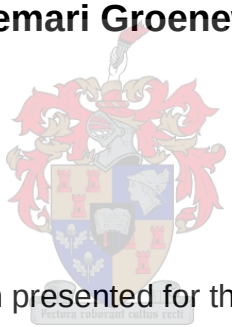

Dissertation presented for the degree of
Doctoral (Medical Physics)
in the Faculty of Health Sciences at Stellenbosch University

Radiodiagnosis Division
Department of Medical Imaging and Clinical Oncology
Faculty of Medicine and Health Sciences

Supervisor: Dr Willem Adolf Groenewald
Date: December 2017

Declaration

By submitting this dissertation electronically, I declare that the entirety of the work contained therein is my own, original work, that I am the sole author thereof (save to the extent explicitly otherwise stated), that reproduction and publication thereof by Stellenbosch University will not infringe any third party rights and that I have not previously in its entirety or in part submitted it for obtaining any qualification.

Date: December 2017

Abstract

Introduction

In medical X-ray imaging several diagnostic x-ray imaging modalities are applied to enable disease diagnosis, i.e. general projection radiography, fluoroscopy, mammography and Computed Tomography (CT) scanning. X-ray images must be of sufficient quality to enable accurate diagnosis. Image quality is quantified using suitable phantoms to ensure that equipment failure is detected before patient care is affected.

A variety of phantoms are commercially available. However, these are modality specific, expensive and often complicated to use. In resource limited institutions, like many in Africa including South Africa, three problems are identified in the field of diagnostic radiology X-ray image quality control (QC). These are cost, man power and expertise and time constraints. A gap thus exists in the market for a single universal image quality assurance (QA) phantom, capable of doing all required QC tests for all X-ray imaging modalities. A phantom, answering to this requirement, in addition must be user-friendly and cost- and time-efficient.

Aim

To design, develop, manufacture, test and validate a universal image QA phantom for diagnostic radiology X-ray imaging. The phantom must be compact, unique, universal (i.e. not modality specific), easy and quick to use and manufactured at a substantially reduced cost compared to the commercially available options.

Materials and methods

Using literature studies on existing commercial phantoms for guidance, a prototype universal phantom was designed, manufactured and tested for all X-ray imaging modalities. From the prototype results, adjustments were made and the universal image quality phantom was developed and manufactured. The phantom is made from high density polyethylene and houses several inserts of different materials to asses

sensitometry, image uniformity, limiting resolution, image noise, i.e. signal-to-noise (SNR) and contrast-to-noise (CNR) ratios, geometry and measurement tools, standard signal, low contrast detectability, positioning and alignment, artefacts and visual image quality inspection. For CT scanning the phantom measures slice thickness and for mammography masses, fibres and micro-calcifications are evaluated. Data analysis software was developed for analysis of obtained images and a complete step-by-step user's manual was prepared. Reproducibility testing was performed on the phantom, using Department of Health (DoH) specified limits. Independent validation of the phantom package (i.e. phantom, software and manual) was done by three independent medical physicists. They compared the phantom to the commercial phantoms in general use in their institutes.

Results

The universal image QA phantom and accompanying data analysis software produced reproducible results for all imaging modalities, within the accepted DoH tolerance levels. The independent validation results proofed that the phantom package was easy to transport, light weight and compact, easy to set-up and use, versatile, cost effective and user friendly.

Discussion and conclusion

From the reproducibility testing and independent validation results it may be concluded that the universal image QA phantom, with accompanying data analysis software and user's manual, offers an acceptable single phantom solution for medical X-ray imaging. The universal phantom is a cost and time saver and as such could fill a gap in the existing market. In addition, the phantom could also be used by radiographers in resource limited institutions.

Opsomming

Inleiding

Mediese X-straalbeelding gebruik verskeie diagnostiese X-straal beeldingsmodaliteite om siekte te diagnoseer. Dít sluit algemene projeksieradiografie, fluoroskopie, mammografie en rekenaartomografie- (RT-)skandering in. Die X-straalbeelde moet van ’n voldoende gehalte wees om akkurate diagnose moontlik te maak. Beeldgehalte word met behulp van geskikte fantome gekwantifiseer om te sorg dat onklaar toerusting opgespoor word voordat dit pasiëntesorg beïnvloed.

’n Verskeidenheid fantome is kommersieel verkrygbaar. Tog is dit metodespesifiek, duur en dikwels ingewikkeld om te gebruik. By hulpbronbeperkte instellings, waaronder baie instellings in Afrika, wat Suid-Afrika insluit, word veral drie probleme met die gehaltebeheer van diagnostiese X-straalbeelding ondervind, naamlik koste, menslike hulpbronne en kundigheid, en tydsbeperkinge. Daar is dus ’n leemte in die mark vir ’n enkele, universele beeldgehalteversekeringsfantoom wat alle nodige gehaltebeheertoetse vir alle X-straalbeeldingsmetodes kan uitvoer. Daarbenewens moet so ’n fantoom gebruikersvriendelik en sowel koste- as tyddoeltreffend wees.

Doelwit

Die doelwit is om ’n universele beeldgehalteversekeringsfantoom vir diagnostiese radiologie-X-straalbeelding te ontwerp, te ontwikkel, te vervaardig, te toets en te staaf. Die fantoom moet kompak, uniek en universeel (d.w.s. nie metodespesifiek nie) wees, sowel as maklik en vinnig om te gebruik. Boonop moet dit aansienlik goedkoper wees om te vervaardig as die huidige kommersieel verkrygbare fantome.

Materiaal en metodes

Aan die hand van ’n literatuurstudie oor bestaande kommersiële fantome is ’n prototipe- universele fantoom vir alle X-straalbeeldingsmetodes ontwerp, gebou en getoets. Die ontwerp is op grond van die prototiperesultate aangepas, waarna die universele beeldgehaltefantoom ontwikkel en vervaardig is. Die fantoom word

gemaak van hoëdigtheid-poliëtileen en bestaan uit verskeie invoegsels van verskillende materiale vir die evaluering van sensitometrie, beeldeenvormigheid, resolusiebeperking, beeldgeruis (met ander woorde sein-tot-geruis- en kontras-tot-geruis-verhoudings), geometrie en meetgereedskap, standaardsein, laekontrasopsporing, posisionering en belyning, artefakte, en visuele beeldgehalte. Vir RT-skandering meet die fantoom snitdikte, en vir mammografie word die opsporing van gewasse, vesels en mikroverkalkings geëvalueer. Dataontledingsagteware is ontwikkel om opgeneemde beelde te ontleed, en ’n volledige stapsgewyse gebruikershandleiding is saamgestel. Herhaalbaarheidstoetse is aan die hand van die Departement van Gesondheid se gespesifiseerde perke met die fantoom uitgevoer. Drie onafhanklike mediese fisici het die fantoompakket (d.w.s. fantoom, sagteware en handleiding) onafhanklik gestaaf. Hulle het die fantoom vergelyk met die kommersiële fantome wat hulle onderskeie instellings oor die algemeen gebruik.

Resultate

Die universele beeldgehaltesekerheidsfantoom en gepaardgaande dataontledingsagteware lewer herhaalbare resultate vir alle beeldingsmetodes op, wat ook binne die Departement van Gesondheid se toleransieperke val. Die onafhanklike geldigheidsresultate bewys dat die fantoompakket maklik vervoer, liggewig en kompak is, maklik is om op te stel en te gebruik, en boonop veelsydig en kostedoeltreffend is.

Bespreking en gevolgtrekking

Die herhaalbaarheidstoetse en onafhanklike geldigheidsresultate dui daarop dat die universele beeldgehaltesekerheidsfantoom, tesame met die gepaardgaande dataontledingsagteware en gebruikershandleiding, ’n aanvaarbare enkele fantoomoplossing vir mediese X-straalbeelding bied. Die universele fantoom spaar geld en tyd, en kan dus ’n leemte in die bestaande mark vul. Dit kan veral goed te pas kom vir radiografiste in hulpbronbeperkte instellings.

Dedication

This thesis is dedicated to Blue.

Acknowledgements

I am grateful to my supervisor and co-supervisor, Dr Wilhelm Groenewald and Dr Harry Delis, for their guidance, valuable input and much appreciated support.

A special word of thanks to Johan Braasch, of Gebrateq Advanced Engineering, for his assistance in the design and manufacturing of the proposed phantom, and to Ernst Uys for development of the data analysis software. I also thank the Medical Physics Divisions at Groote Schuur, Charlotte Maxeke Johannesburg Academic and Inkosi Albert Luthuli Central Hospitals for independent validation of the phantom package. Thank you to Elsie Bester and the team from Winelands Radiology in Vergelegen Medi Clinic for allowing and arranging imaging of the phantom. Thank you to Dr Alan Chamberlain for proof reading the thesis.

Grateful acknowledgement is made to the following instances:
Harry Crossley bursary fund for awarding me a bursary for my research.
Innovus for registration of the international patent PCT/IB2016/051165.
Chris Vine-Soanes, from Gartech Equipment, for the assistance and supply of different plastics and specifications.
Hendrik de Vos, of Netcare, for supplying commercial phantoms for validation of the phantom.
Cobus Visser and Wayne Swart from the Department of Mechanical and Mechatronic Engineering at Stellenbosch University for 3-D printing of inserts.
The staff of the radiology and medical physics departments at Tygerberg Academic Hospital for their assistance and for allowing me to conduct the study in their departments.
Equra Health for allowing me to conduct research during office hours.

A final word of thanks to anyone who supported me in any way throughout the project.

Table of contents

Appendices

List of Figures

Figure **Page**

List of Tables

List of abbreviations

AAPM	American Association of Physicists in Medicine
ABC	Automatic Brightness Control
ABS	Acylonitrile Butadiene Styrene
ACR	American College of Radiology
AEC	Automatic exposure control
ALARA	As low as reasonably achievable
arb.	Arbitrary
CCD	Charge-coupled device
cm	Centimetre
CNR	Contrast to noise ratio
CT	Computed tomography
CR	Computed radiography
DoH	Department of health
DR	Digital Radiography
ESF	Edge spread function
FOV	Field of view
FWHM	Full width at half maximum
HDPE	High density polyethylene
HU	Hounsfield unit
IBs	Inspection bodies
kV	Kilo voltage
lp/cm	Line pairs per centimetre
lp/mm	Line pairs per millimetre
LSF	Line spread function
mAs	Milli-ampere seconds
mm	Millimetre
MTF	Modulation transfer function
OD	Optical Density
PLA	Poly Lactic Acid

PMMA	Poly-methyl methacrylate
PMT	Photo-multiplier tube
PSF	Point spread function
PSP	Photo-stimulable phosphor
SOP	Standard operating procedure
QA	Quality assurance
QMS	Quality management system
QC	Quality control
ROI	Region of interest
SANAS	South African National Accreditation System
SDNR	Signal-difference-to-noise ratio
SID	Source-to-image distance
SNR	Signal-to-noise ratio
USA	United States of America
WL	Window level
WW	Window width
2-D	Two dimensional
3-D	Three dimensional

Chapter 1

Introduction

Medical imaging requires the application of radiation, for example x-rays, that have the ability to penetrate the tissues of the human body. X-rays are able to enter the body and interact with tissues, producing an image of the internal anatomy of the body.[1] These images, produced by different imaging modalities in diagnostic radiology, assist radiologists to diagnose and follow up a wide variety of diseases and pathologies.

To ensure that the obtained images are of acceptable quality, i.e. can be used clinically for accurate diagnosis, image quality should be evaluated and maintained. Image quality is a subjective concept that requires certain measures to be objectively quantified. Quantification may be done by using phantoms during routine quality control.

In a radiology practice a framework for a Quality Management System (QMS) plays an essential role. The QMS considers the objectives and policies of the division, whether documents and procedures in line with these objectives and policies are available, provides practical written instructions for staff and monitors, records, audits and corrects all procedures and practises. Quality assurance (QA) covers all factors affecting the intended outcome, which is an accurate clinical diagnosis in the field of diagnostic radiology. QA thus includes all actions needed to ensure that equipment satisfies quality requirements. In diagnostic radiology the aim will specifically be to perform the most appropriate x-ray investigation for correct diagnosis, with optimised exposure factors, giving consistent high quality images with acceptable patient doses. A QA program will be designed and implemented to maintain quality and safety of imaging techniques. Quality control (QC) involves the processes through which relevant performance parameters are measured and compared to existing standards, baseline values and accepted tolerances. QC also includes actions taken to correct

out-of-tolerance results. Quality standards are a set of accepted criteria used for assessing the quality of activities.[2]

The clinical performance of imaging systems may be assessed by applying a good QC program, under a comprehensive QA system. QA provides a framework for continuous improvement through routine feedback and assists in identification of deviations from ideal performance, which could negatively impact patient care. Possible staff training needs may also be identified. An effective QA program is easy to implement clinically and its proposed tests would enable subjective and objective evaluation of the entire imaging system. The program should also be cost effective and easy to maintain.[3] The QA program for equipment should cover acceptance testing and commissioning, periodic testing, corrective action when results are out of tolerance, record keeping of all procedures, results and actions and finally optimisation of QA protocols through review and auditing as time goes by.[2]

Acceptance testing or commissioning is important to ensure that equipment conforms to specifications and meets legal requirements and it is done prior to clinical use. The results obtained from the commissioning process will form the baseline values for comparison to routine QC results, and deviations from these baseline values serve as indications of possible problems. If equipment was already installed and acceptance testing results were unavailable, new baseline values should be determined. If a problem was identified in routine testing with deviations from baseline values, its cause should be determined using more sophisticated tests.[4]

Commissioning ensures that equipment is ready for clinical use and establishes baseline values to which periodic QC results can be compared. These baseline values are re-established after any major intervention on the equipment. Routine or periodic QC testing determines whether equipment performance has changed and whether corrective action would be needed. Equipment maintenance and routine QC are complimentary.[2]

Radiology equipment should be appropriate for the task it must perform. It must also be able to perform this task accurately at an acceptable cost to patients and the hospital or clinic, considering monetary expenses and down time. Routine evaluation

of equipment, in the form of a formal QC program, is necessary to ensure continued and reliable performance by detecting changes that could influence patient diagnosis, treatment or care.[5] X-ray equipment does drift out of calibration and develop defects. This is detected with routine QC.[5]

The frequency at which QC is done, depends on the purpose, age, reliability and frequency of use of the equipment and its importance in the medical imaging field.[5] The stability of the QC parameter being assessed and its importance on the overall imaging system performance also influences the frequency of QC test performance. QC tests vary in frequency from daily to yearly and can be divided into essential, i.e. the recommended minimum standard, and desirable, i.e. testing at best practise level.[2] Variable processes should be monitored more frequently, as do older and less reliable equipment that are less stable. Establishing baseline values for QC are not only important for comparison to future QC results, but also gives valuable experience in use and operation of equipment. QC test frequencies should be increased from recommendations in literature when setting baseline values and after component failure to ensure that corrective action taken was appropriate.[5] The performance standards can be acceptable, i.e. performance within accepted limits, and achievable, i.e. the level of performance that should be achieved. Test types include repeatability, which shows that results are within limits for several measurements done at the same time, and consistency, which shows that results are not changing over time.[2]

All QC results should be meticulously recorded and kept for analysis. The performance of each unit must be evaluated and units should be compared to each other to determine consistency between devices.[6] An individual equipment record must be compiled and maintained for every equipment device. This includes the unit make and model, licence number, date of installation, user's manual, acceptance and routine QC test results, dates and details of services and replacements and details of persons performing tests, upgrades or services. A QC manual and in house developed standard operating procedures (SOPs), describing the tests in a step-by-step manner, must be available.[7]

According to the literature "Image quality depends only on intrinsic, objective physical characteristics of an imaging system, and can be measured independently of an

observer.[6]" This implies that it should be objective and only equipment dependent. Clinical image quality "is whatever the observer says it is (i.e. it is a subjective perception of the image, 'in the eye of the beholder')[6]", which implies that it also depends on the observer or interpreter. And it "is defined by an observer's ability to achieve an acceptable level of performance for a specified task[6]", hence certain limits or minimum achievable standards exist. Image quality therefore depends on imaging technology, proper equipment design, proper set-up of equipment parameters, proper utilisation of equipment and knowledge and skill of the person operating the equipment. It is also influenced by observer knowledge, ability, skill and viewing conditions. By using image quality indices, from suitable phantoms for example, observer dependence is minimised. The obtained image quality is described in terms of contrast, noise, sharpness, saturation and artefacts.[6] QA and QC ensure image quality within specified limits. The importance of investigating image quality with routine QC is therefore clear, i.e. ensuring accurate diagnosis in diagnostic radiology. However, many limitations occur in actual practise.

In resource limited institutions and countries, such as many in Africa and including South Africa, three main problems may be identified in the field of image quality assessment. These are firstly cost, secondly man power and expertise and thirdly time constraints. A variety of commercially available phantoms, as discussed in Chapter 3 in this dissertation, are in use. However, these are often expensive and modality specific. This results in a multitude of phantoms to be purchased at substantial costs to enable the radiology practice to do comprehensive image quality assurance. Evaluation and interpretation of results from these phantoms are complicated and take time. In addition it is recommended that QA programs should be developed, implemented, overseen and managed by a qualified medical physicist.[5] However, resource limited institutions are already understaffed and rarely employ sufficiently trained personnel, like medical physicists, to work with the complicated phantoms. The solution for these institutions could be a universal image quality assurance phantom, capable of doing all required routine image quality control consistency tests on the existing diagnostic radiology x-ray imaging equipment, including, x-ray units (fixed and mobile), fluoroscopy, mammography and computed tomography (CT) scanning.

The aim of this research is to design, develop, manufacture, test and validate a universal image quality assurance phantom for diagnostic radiology x-ray image quality assurance, i.e. for equipment commissioning in setting baseline values and for routine image QC comparing obtained results to the set baseline values. This phantom should be cost effective and easy and quick to use. To achieve this a prototype phantom will be planned, produced and tested. The shortcomings of the prototype will be addressed and a final version of the phantom will be developed. This phantom will be tested for reproducibility of results and compared to commercially available phantoms by independent evaluators, to determine if its image quality assessment results are adequate, if it is easy to use and cheaper to acquire compared to other phantoms. To aid this evaluation, semi-automatic data analysis software will be developed and a user's manual for the phantom and the analysing software will be written. For the research to remain unique, a patent will be registered, protecting the concept.

The proposed phantom, user's manual and data analysis software would be designed by a qualified medical physicist and optimised for easy implementation, maintenance and record keeping by radiography personnel in the division. A complete user's manual, Appendix A in this dissertation, would be included as part of the research as well as semi-automatic data analysis software, as described in Chapter 5 and Appendix B. The data analysis software would simplify the QC process, resulting in less needed involvement of medical physicists and better information communication to technologists for repairs. Periodic, remote review of results by a medical physicist would be considered sufficient. The proposed universal phantom, user's manual and data analysis software would be simple to use and implement, with clear instructions, ensuring suitability for the full spectrum of diagnostic radiology practices and clinics. Practices that would benefit, include those with maximum workload using CT, mammography, general x-rays (including mobile x-ray units) and fluoroscopy, to small clinics using a single or only a few imaging units with fewer patients. The proposed universal phantom would be compact, robust, easy to use and cheaper to manufacture, addressing the above mentioned problems in resource limited institutions.

The basic physics involved in the production of radiographic x-ray images is discussed in Chapter 2. Image quality is defined and evaluators of image quality are discussed. Mention is made of the state of affairs in diagnostic radiology in South Africa. The current image quality assurance solutions are detailed in Chapter 3. The commercially available phantoms, required improvements and proposed solutions for each modality are explored and the need for a universal phantom solution is identified. The design and development of such a phantom is discussed in Chapter 4 and its relevance to general x-ray imaging, fluoroscopy, mammography and CT scanning is explored in Chapter 5. Chapter 6 discusses the reproducibility testing of the universal phantom and Chapter 7 the independent evaluation of the universal image quality assurance phantom, its user's manual and data analysis software. The semi-automatic data analysis software is described in Appendix B, with a complete user's manual presented in Appendix A. The dissertation concludes with recommendations in Chapter 8.

Chapter 2

Diagnostic radiology imaging and quality assurance

Image quality assurance, in terms of acceptance testing, commissioning of equipment and routine QC, is an essential tool in the identification of faulty equipment and maintenance of clinically acceptable image quality for accurate disease diagnosis, follow up and minimising repeat exposures. For improved patient care, image quality assurance should therefore be part of the basic operations of a diagnostic radiology practice. This chapter considers the physics involved in the formation of x-ray images, describes the measures of image quality and the importance of routine image quality control in diagnostic radiology, with reference to the South African situation.

2.1 The physics of x-ray imaging

The quality of a radiological image is essentially determined by the physics of image formation. The formation of an image can be described in four stages, i.e. the interaction of x-rays with the detector to generate a detectable response, the temporary storage of the response, measurement of the response and erasing of the image for subsequent use in digital systems. It involves detecting objects of which the size and contrast are limited by quantum statistics and the efficiency of the image receptor in detecting incident x-ray quanta.[8]

2.1.1 X-rays

Radiation is energy in movement. X-rays are electromagnetic radiation. X-rays are photons with no mass, constant speed in a vacuum and are not affected by electric or magnetic fields. X-rays are described by the wave-particle duality, i.e. in terms of both waves or discrete quanta of energy called photons. X-rays are ionising radiation, as it could produce ionised atoms and molecules by removing electrons from atomic shells during interactions.[9]

X-rays are produced when electrons with high kinetic energies interact with materials and kinetic energy is converted to electromagnetic radiation. An x-ray tube contains an electron source, i.e. the cathode, and a target, i.e. the anode. These are housed in a vacuum, with a high voltage supplied by an x-ray generator, for the acceleration of the electrons from the cathode to the anode. A schematic representation of an x-ray tube is included in Figure 2.1.

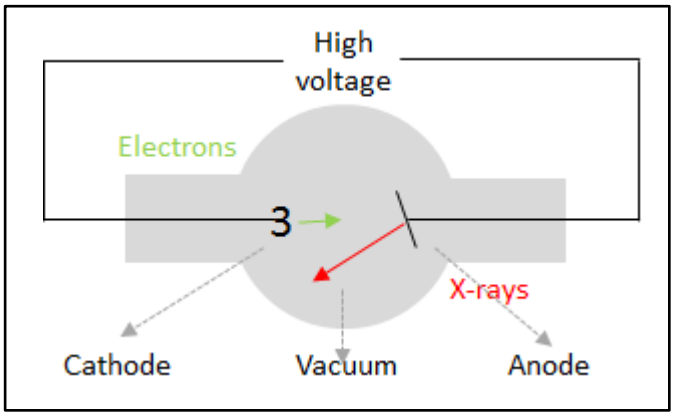

Figure 2.1: Basic schematic representation of an x-ray tube.

An x-ray spectrum consists of Bremsstrahlung and characteristic x-rays, as shown in Figure 2.2. Bremsstrahlung radiation is produced when the positively charged nucleus attracts the negatively charged electron, slowing it down. Kinetic energy is lost and converted to a Bremsstrahlung x-ray. The incident accelerated electron can eject an inner shell electron, leaving a vacancy. This vacancy is filled by an electron from an adjacent higher shell. The difference in binding energy of the shells is emitted as a characteristic x-ray photon.[10]

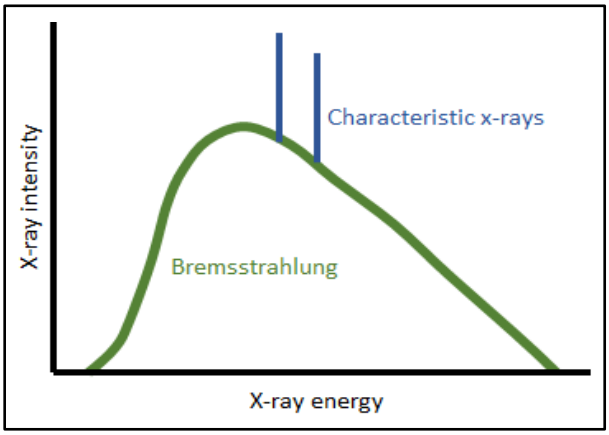

Figure 2.2: An x-ray spectrum.

2.1.2 Interactions of x-rays with matter

As x-rays pass through matter they interact with the atomic electrons of the material causing ionisations and excitations. Ionisation interactions are classified as photoelectric attenuation and incoherent (or Compton) scattering. Excitation transfers energy to an inner shell electron, exciting it to a higher energy level and shell and leaving a vacancy in the original shell. If the transferred energy is more than the binding energy of the shell, the electron is ejected from the atom and ionisation occurs. The inner shell vacancy is filled by an electron from an outer shell, which creates a vacancy in this shell. This cascade process continues and the energy released in each transition is emitted as characteristic x-rays and the outer shell electron ejected from the atom is called an Auger electron. The released energy is the difference in the binding energies between the inner and outer shells. Charged particles can also have inelastic interactions with atomic nuclei of the material they pass through, resulting in the particle path being deflected and the energy transferred to a photon which is emitted as Bremsstrahlung.[1]

2.1.2.1 Raleigh scatter

In coherent, classical or Rayleigh scattering no energy is lost by the incident photon, but it is scattered through an angle, i.e. its path is changed.[11] The incident photon interacts with the atom as a whole. The incident photon's electromagnetic wave transfers energy to all the electrons in the interaction atom, causing in phase oscillation. This energy is radiated by the electrons as a photon with the same energy,

but in a different direction. As electrons are not ejected, ionisation does not occur. It occurs at low energies, for example those used in mammography. This interaction is more likely to occur with high atomic number materials and at low photon energies. At high photon energies, coherent scatter occurs mostly in a forwards direction with a small angle of deflection. Raleigh scattering is shown in Figure 2.3.[12]

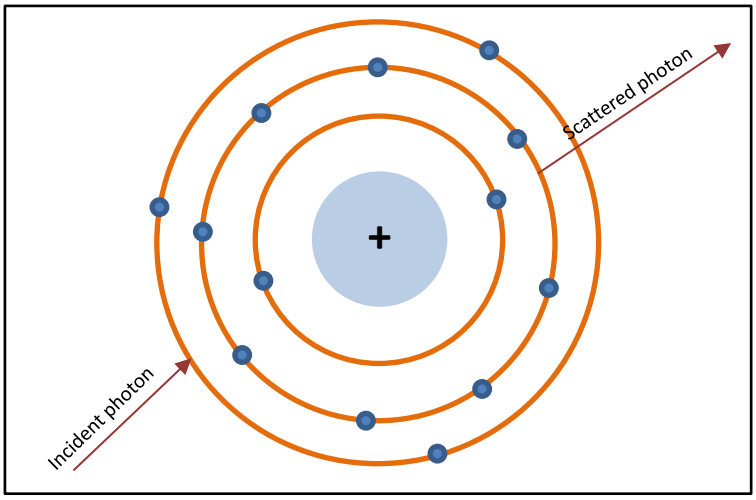

Figure 2.3: Raleigh scatter.

When scattered photons are detected, image quality is degraded. Object contrast and image sharpness are decreased by scatter, as a general mottled background noise is caused on the image. Scatter does not contribute to image formation, but increases patient absorbed dose if attenuated in the patient.

2.1.2.2 Compton scatter

In Compton scattering, the incident photon interacts with a free electron and energy is transferred to the electron.[11] Compton scatter is also called inelastic, incoherent or non-classical scatter. In the diagnostic radiology range, this is the most common type of interaction. It occurs between a photon and an outer shell electron, i.e. a valence electron, which is ejected from the atom, causing ionisation. The photon is scattered with reduced energy. The energy of the incident photon must be greater than the binding energy of the valence electron for Compton scatter to occur. Compton scatter is illustrated in Figure 2.4.[12]

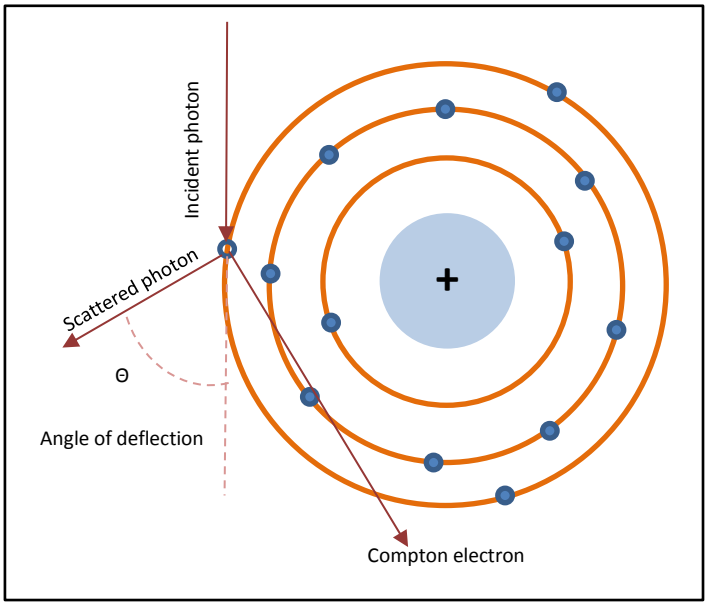

Figure 2.4: Compton scatter.

The probability of Compton interactions depends on the number of electrons in the atom, i.e. on the density of the material and the number of electrons per unit mass of the material. The number of electrons per unit mass is relatively constant for different materials, thus the probability of Compton interactions is dependent on the density of the interacting material. Compton interaction probability is independent of material atomic number and incident photon energy. These interactions therefor occur at all energies applicable in the diagnostic radiology range. Compton scatter decreases image spatial resolution, thus reducing image quality. It adds a background haze to the image, which obscures small attenuation differences and causes blurred object borders.

2.1.2.3 Photoelectric effect

In this interaction, all of the incident photon's energy is transferred to an inner shell electron, which is ejected from the atom. This is called a photoelectron. The atom is left in an ionised state. The energy of the incident photon must be greater than the binding energy of the inner shell electron. The created vacancy is filled by an electron from a shell with a lower binding energy. The difference in binding energies of the shells is emitted as a characteristic x-ray or Auger electron. The resultant vacancy is filled with an electron from a shell with even lower binding energy and the filling and emission process continues in a cascade.[12] The photoelectric effect depends directly

on atomic number and inversely on photon energy, i.e. $\frac{Z^3}{E^3}$ where Z is the atomic number and E is the photon energy.[11] The probability of a photoelectric interaction increases with increasing atomic number and decreases with increased incident photon energy. There are no scattered photons, which degrade image quality, with photoelectric effect. Figure 2.5 shows the photoelectric effect.[12]

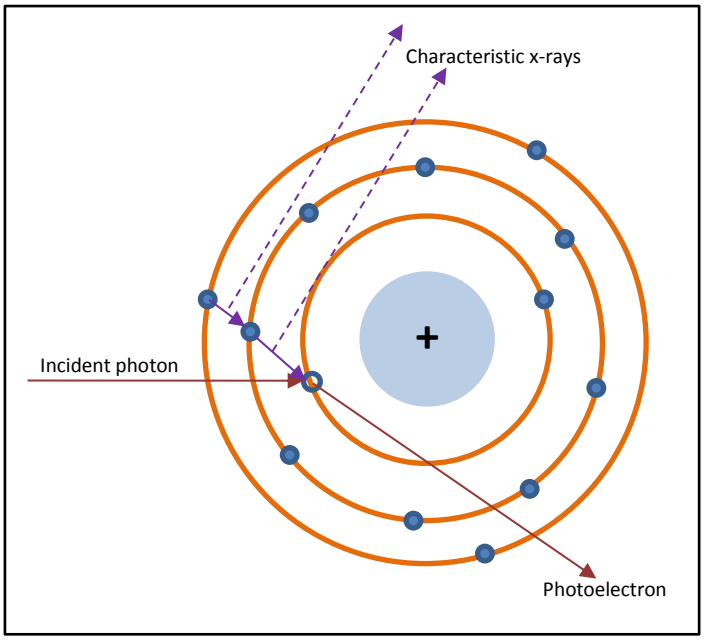

Figure 2.5: The photoelectric effect.

At the binding energy of an electron shell, the absorption coefficient increases as more electrons are available for the interaction. This energy is called the absorption edge and it is characteristic for every material. The photoelectric effect dominates at lower photon energies and Compton scatter for the rest of the diagnostic energy range.[11]

The photoelectric effect assists in the development of image contrast. The absorption differences between soft tissues, like muscle, is enhanced by the photoelectric effect, due to the strong dependence of interaction probability on material atomic number. In diagnostic radiology, the strong inverse dependence of photoelectric interactions on incident photon energy decreases the attenuation difference between bone and soft tissue. To counteract this the kV is reduced, increasing contrast, however this also increases the absorbed dose to the patient. A delicate balance between image quality and patient dose thus exists. A practical example is chest radiography, where bone,

at lower incident photon energies, will attenuate strongly through photoelectric interactions, obscuring visualisation of the lungs. Due to the higher atomic number of bone, photoelectric interactions occur in bone preferentially, compared to surrounding soft tissues. These attenuation differences determine the contrast of the chest x-ray image.

Another interaction mechanism is pair production. It only occurs at energies of 1022 keV or more and is therefore not significant in diagnostic radiology.[11]

2.1.3 X-ray attenuation coefficients

Attenuation is the removal of photons from the x-ray beam as it transverses matter through absorption and scattering of the photons. When the x-ray beam is mono-energetic the linear attenuation coefficient, μ, in units of cm^{-1}, refers to the fraction of photons removed from the incident photon beam per unit thickness of traversed material. It depends on the number of atoms per unit distance, i.e. the density of the material.[12] The attenuation of the incident photons is governed by the mass attenuation coefficient, $\frac{\mu}{\rho}$, which is independent of the density, ρ, and has units of cm^2/g. The total mass attenuation coefficient is the sum of the mass attenuation coefficients of each of the individual interaction mechanisms, as shown in Equation 2.1. Here $\frac{\tau}{\rho}$ is the photoelectric effect mass attenuation coefficient, $\frac{\mu_{coh}}{\rho}$ and $\frac{\mu_{inc}}{\rho}$ are the mass attenuation coefficients for Rayleigh and Compton scattering and $\frac{\omega}{\rho}$ is the mass attenuation coefficient for pair production.

$$\frac{\mu}{\rho} = \frac{\tau}{\rho} + \frac{\mu_{coh}}{\rho} + \frac{\mu_{inc}}{\rho} + \frac{\omega}{\rho} \qquad \text{[Equation 2.1]}$$

For compounds and mixtures, the mass attenuation coefficient is the weighted sum of the constituent elements, as in Equation 2.2, where w_i is the weight fraction of element i.[11]

$$\frac{\mu}{\rho} = \sum_i w_i \left(\frac{\mu}{\rho}\right)_i$$ [Equation 2.2]

2.2 Evaluation of image quality metrics

The advantage of a digital image is that post acquisition image processing can be applied to improve the quality of the displayed image, for example by adjusting the windowing and levelling of the image. Images are displayed with a range of grey scale values, determined by the window width and level settings. Window width is the range grey scale values, white to black, represented by the mapped values. Window level is the middle grey scale value within the selected window width. This is illustrated in Figure 2.6. Different window width and level settings are used by different observers and with different imaging studies.[13] By adjusting the windowing the contrast display of the image is changed. A viewer can select the full range of available pixel values in the image, or set a certain threshold displaying only a portion of the pixel values. All pixel values below the threshold is displayed as the darkest value.[14]

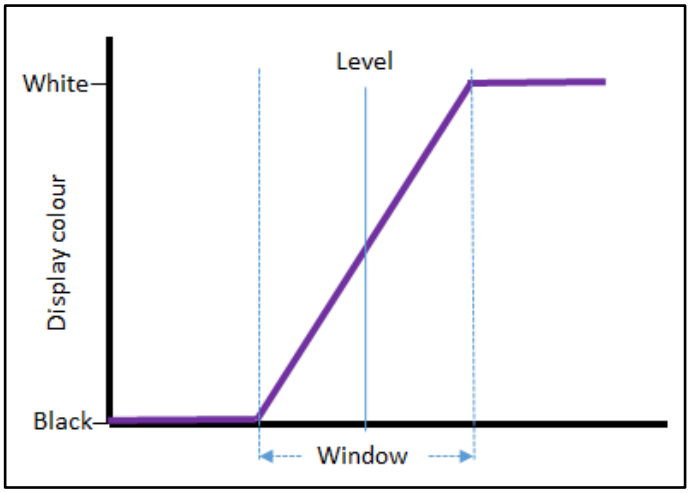

Figure 2.6: Window width and window level in digital imaging.

An x-ray is a radon transform of the object. This incorporates the different attenuations of the different materials in the object. From the resultant image interpretations about the inside of the object can be made. Simply put, an x-ray image represents of the inside of an object pictorially. This representation is an approximation, with the image having an associated error, i.e. the difference between the image and the actual

object. Therefore, two images of the same object, taken with the same imaging system, will not be identical due to inherent image noise. In order to determine how accurately an image represents the actual object the quality of the image must be determined in a quantifiable manner.[15] Image quality is quantified in terms of image contrast, resolution and noise.

2.2.1 Image contrast

Image contrast is defined as differences in the grey scale values of adjacent areas in an image. A uniformly grey image exhibits no contrast. High contrast is depicted in images with sharp transitions between dark and light grey. Contrast is produced by differences in tissue composition, i.e. densities, atomic numbers and mass energy attenuation and absorption coefficients.[9] The contrast of an object depends on the thickness of the object and is different for objects with different mass attenuation coefficients and densities. The contrast is inversely proportional to the effective energy kilovolt (kV) setting, as the mass attenuation coefficient decreases as the kV setting increases. At low kV the contrast is high as the photoelectric effect dominates. However, the incident low energy photons have little penetration ability and this increases the radiation dose delivered to the patient. At higher kV settings the contrast is reduced due to the predominance of scatter interactions, although the delivered patient dose will also be decreased.[16] The image quality and delivered radiation dose relationship is therefore demonstrated when considering image contrast.

Both the photoelectric effect and Compton scatter interactions influence image contrast. From sections 2.1.2.2 and 2.1.2.3 above it is seen that the probability for Compton scatter depends on material density and photoelectric effect on material atomic number and incident photon energy. If image contrast results from differences in material densities, it is due to Compton interactions and independent of photon energy and material atomic number. If a difference in atomic numbers and changes in photon energy, i.e. kV, results in changes in image contrast, it is due to the predominance of photoelectric interactions. In practice this means that kV changes for soft tissues does not affect image contrast substantially, unless low kV settings are considered. In materials like bone, with high atomic numbers, the kV dependence of contrast is seen over a wider range of kV settings.

Contrast can be defined as the ratio of a difference in signal to the average signal. A small difference is therefore negligible if the average signal is large, but it is visible if the average signal is small. The goal in medical imaging is to achieve a high contrast so that abnormal structures can easily be seen.[15]

2.2.1.1 Local (weber) contrast

The local, or Weber, contrast is given by Equation 2.3, where f_f and f_b are the signals of the feature and background.[15]

$$C = \frac{f_f - f_b}{f_b} \quad \text{[Equation 2.3]}$$

Weber contrast is usually used when small structures are present in a background area of uniformity. Modulation or Michelson contrast, as in Equation 2.4, describes patterns of dark and bright structures in an image and is used in image Fourier analysis. Here f_{min} is the lowest and f_{max} the highest signal.[15]

$$C_W = \frac{f_{max} - f_{min}}{f_{max} + f_{min}} \quad \text{[Equation 2.4]}$$

2.2.1.2 Subject contrast

Subject or physical contrast is the local or modulation contrast of the structure in the imaged object. With x-ray imaging it depends on the x-ray spectrum and the attenuation of the structure and the object.[15] It describes the differences in x-ray intensities exiting the patient as a result of different degrees of photoelectric interactions in different materials, i.e. it maps attenuation in the patient. Therefore it depends on material thickness, density and atomic number. As the photoelectric effect is also incident photon energy dependent, subject contrast also depends on the energy, improving with a decrease in kV and resulting in increased absorbed dose.

2.2.1.3 Image contrast

Image or detector contrast depends on the subject contrast and the imaging detector characteristics. It expresses the subject contrast attenuation differences as recorded in the produced x-ray image. In x-ray imaging it is influenced by the x-ray spectrum, the image detector thickness, composition and grey scale characteristics, i.e. film or digital. The display contrast is the final contrast of the image, as it is viewed. It depends on the image contrast and image processing.[15]

When image blurring does not occur the ratio of image to subject contrast is called the transfer function of the imaging system. Blurring spreads the signal laterally, causing a focused point to become a diffused point, thus decreasing the contrast of small structures. This lateral diffusion only occurs if the size of the structure is smaller than the width of the blurring function, hence larger structures are not as severely affected.[15] This decreases images sharpness.

2.2.2 Image resolution

Spatial resolution describes an imaging system's ability to display two objects, close together, as separate, or as the ability to visualise small detail in an image. If a system can display smaller structures, the spatial resolution is high, and vice versa. The maximum spatial frequency, for which modulation is maintained without aliasing, or the smallest object the imaging system can resolve, is referred to as the limiting spatial resolution. For most imaging systems the limiting spatial resolution where the modulation transfer function (MTF) reaches 10 %.[9,14]

The MTF illustrates an object's percentage contrast recorded by the imaging system as a function of the size of the object.[17] Figure 2.7 shows examples of MTFs.

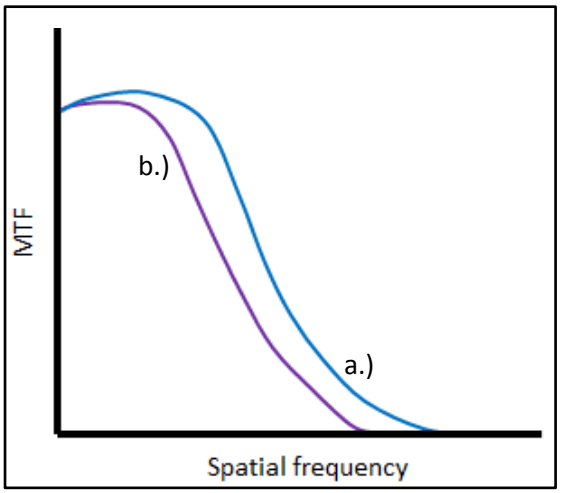

Figure 2.7: a.) MTF for a system with a higher resolution, i.e. can display smaller objects. b.) MTF for a system with a lower resolution.

A basic measure of resolution properties of an imaging system is point spread function (PSF). The PSF is the response of the imaging system to an input point source, like a small ball. The line spread function (LSF) is the response of the imaging system to a line source, e.g. a slit in attenuating material. When a sharp edge is used as stimulus, an edge spread function (ESF) results from the edge gradient. By calculating the Fourier transform of a PSF, LSF or ESF a curve called the MTF is obtained. This is shown in Equation 2.5 where the modulation transfer function, $MTF(f)$, is the modulus of the Fourier transform of the line spread function, $LSF\ (f)$, and $i = \sqrt{-1}$.[18] The MTF is a complete descriptor of spatial resolution.[14]

$$MTF\ (f) = \sqrt{\left(\int_{-\infty}^{\infty} LSF(x)e^{-2\pi i \int x} dx\right)^2} \qquad \text{[Equation 2.5]}$$

Resolution is measured with high contrast objects with sharp edges, like bar phantoms, and is expressed in line pairs per unit length.[15] It is influenced by image detector characteristics and by factors unrelated to the detector, like geometrical unsharpness, x-ray source size and motion blurring.[8] The ability to detect and resolve a structure therefore depends on the signal to noise ratio of the structure.[15]

2.2.3 Image noise

Images are degraded by noise.[15] Quantum mottle or white noise, is inherently present in images and can be quantified with region of interest (ROI) analysis using the equations described below.

Contrast resolution describes the ability to detect and distinguish small grey scale changes from background noise. It is described by the signal-to-noise ratio (SNR).[14] High contrast resolution is restricted by imaging system blurring. Low contrast structures, even large ones, may not be visible due to the signal of the structure is lower than the noise in the region surrounding the structure. The quantum SNR is given by Equation 2.6, where $\langle g \rangle$ is the mean and σ_g the standard deviation in a ROI.[15]

$$SNR = \frac{\langle g \rangle}{\sigma_g} \qquad \text{[Equation 2.6]}$$

The amplitude of a signal is compared to the background noise using Equation 2.7, the signal-difference-to-noise ratio (SDNR), where $\langle x_a \rangle$ and $\langle x_b \rangle$ are the mean values of a ROI in structure a compared to background b and σ_b is the standard deviation of the background ROI. This is also called the contrast-to-noise ratio (CNR).[15]

$$SDNR = \frac{\langle x_a \rangle - \langle x_b \rangle}{\sigma_b} \qquad \text{[Equation 2.7]}$$

The CNR is object size independent and a measure of the signal level in the presence of noise.[14] Structure detection is influenced by quantum noise, artefacts, anatomy and the observer.[15]

The amount of scattered radiation depends on the radiographic procedure, x-ray field size, thickness of the object being imaged and position of the object in relation to the x-ray source and image receptor. Scatter interactions dominate in soft tissue, whilst in bone photoelectric interactions occur most often. Scatter increases with x-ray field

size and object thickness, up to an upper cut off point, i.e. the scatter saturates for large fields and thick objects. Scatter can be reduced by using anti-scatter grids, through collimation, i.e. reducing field size carefully as to not exclude objects of interest resulting in retakes and thus additional dose, increasing the distance between the object and image receptor so that divergent scattered photons do not reach the image receptor, and by decreasing object thickness by using compression, which results in a shorter exposure time hence reducing movement blur and allowing for a lower kV setting which improves contrast and SNR.[16]

2.3 Image quality assurance in South African practice

In diagnostic radiology the aim is to obtain clinically useful images, i.e. images with acceptable image quality for accurate diagnosis of different disease conditions, while adhering to the ALARA principle, i.e. the radiation dose delivered to the patient must be kept As Low As Reasonably Achievable (ALARA). The clinical relevance of images can be monitored with quantification of image quality, assessing the parameters as discussed above. For this, routine image quality assurance is required on each imaging device.

In South Africa, the QC requirements for diagnostic radiology equipment image quality are stipulated by the Directorate Radiation Control of the South African Department of Health (DoH), in the document for QC tests for diagnostic x-ray imaging systems.[7] The image quality assurance tests required by DoH are summarised in Table 2.1. As seen from Table 2.1 a good diagnostic radiology QA program involves periodic testing and checking of all components in the image formation chain.

Table 2.1 shows the essential QC tests, i.e. the recommended minimum standards. However, from a best practise level additional testing is desirable.[2] It is clear that these tests require sufficient man power and expertise and are lengthy to conduct, two of the greatest limitations in the South African setting.

Table 2.1: DoH recommendations for image QC for general x-rays and fluoroscopy, unless otherwise stated. (adapted from DoH requirements for QC document[7])

Test	Frequency	Limits
X-ray / light beam centring	Acceptance, 3 monthly	≤ ± 1 cm at 100 cm SID
Constancy or reproducibility	4 monthly	Baseline ± 0.3 OD
Uniformity	Acceptance, 3 monthly Mammography: Acceptance, weekly	Mean ± 10 % (± 5 % for DR) Mammography: Mean pixel value < ± 15 %
Sensitivity	Acceptance, 3 monthly	Baseline ± 25 %
Distance accuracy / scaling errors	Acceptance, 3 monthly	± 0.5 cm or ≤ 2 %
Low and high contrast resolution	Acceptance, 3 monthly Mammography: Acceptance, daily Mammography: Yearly	Limiting spatial resolution baseline minus 25 %, 2.5 – 3 lp/mm Mammography: All patches visible Mammography: 11 - 13 lp/mm
Optical density consistency	Acceptance, 3 monthly	Baseline OD ± 0.20
Image quality visual inspection	Acceptance, 3 monthly Mammography: Weekly	Reproducible Mammography: 4 fibres, 3 spec groups, 3 masses (ACR phantom) (5 fibres, 4 spec groups, 4 masses for DR)
Image noise	Acceptance, daily	CT: Baseline ± 10 %
CT number values	Acceptance, daily	Water: Baseline ± 5 HU Other: Baseline ± 10 HU
Scan plane localisation in CT	Acceptance, 3 monthly	≤ ± 0.2 cm
Reproducibility	Mammography: Acceptance, weekly Acceptance, yearly	Mammography: SNR < ± 10 % Baseline ± 30 % and mean ± 20 %
Artefacts	Mammography: Acceptance, daily	No visible artefacts
Geometrical distortion	Mammography: Acceptance, daily	Mammography: No distortion visible
AEC repeatability	Acceptance, yearly	Mean OD ± 0.2
AEC consistency between chambers	Acceptance, yearly	Baseline ± 30 % and mean ± 20 %
CT slice thickness	Acceptance, yearly	Baseline ± 20 % or ± 0.1 cm

In South Africa 3173 fixed and mobile x-ray units, 1347 fluoroscopy units, 288 mammography units and 297 CT scanners were licenced by DoH. The majority of these were located in state or government sector with a significant number, although fewer, in private practice.[19] (Statistics as at March 2016) According to the secretary of the South African Association for Physicists in Medicine and Biology (SAAPMB), 71 medical physicists registered with the association are employed in state sector and 37 are employed in private sector.[20] (Statistics as at October 2015) It is important to note that not all registered medical physicists are working in diagnostic radiology. The majority of the South Africa medical physicists were employed in radiotherapy at that time, with an estimated 15 employed full time in diagnostic radiology. (as at September 2017)

A clear burden on man power and lack of suitably qualified personnel thus exist in the South African setting. With this burden, time for essential QC is already limited and desirable QC rarely occurs. In addition to these limitations, departmental financial constraints and expensive modality specific commercial QC equipment result in a lack of required basic QC tools. This is to the detriment of patient care. The unfortunate truth is that the situation in the rest of Africa is even more adverse than in South Africa. The three major problems of cost, man power and expertise and time constraints, as identified in Chapter 1, are a reality in South Africa, as well as in the rest of Africa. The proposed solution to this situation could be a cost effective and easy to use universal image quality assurance phantom, as described in Chapter 4.

Chapter 3

Current* image quality assurance systems

Commercially available image quality assessment phantoms are modality specific. In addition, some of these phantoms can only investigate certain image quality parameters. This chapter considers the production of images in general x-rays, fluoroscopy, mammography and CT scanning, introduces the image quality assurance parameters to be assessed in each modality and describes some of the commercially available image quality assurance phantoms in use. These phantoms are used in the design of the universal image quality assurance phantom, as discussed in Chapter 4. Each section concludes with a tabulated comparison between commercially available phantoms and the proposed universal image quality assurance phantom, as described in Chapters 4-7, to indicate that the universal image quality assurance phantom is a useful routine QC tool capable of doing comprehensive image quality control in different x-ray imaging modalities. The universal image quality assurance phantom is intended as a constancy check tool, to compare routine QC values to baseline values set with the phantom. It fills an identified gap in the existing commercial market, with specific focus on resource limited institutions, as mentioned in Chapter 1. It is not intended to replace any of the commercially available phantoms.

3.1 General x-ray imaging

Radiography was the first type of medical imaging that originated with the discovery of x-rays in 1895. The first radiograph is shown in Figure 3.1.[9]

* Current refers to the situation as in 2016

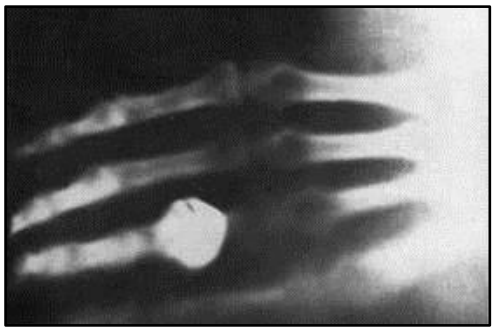

Figure 3.1: The first radiograph by Wilhelm Conrad Roentgen in 1895 (Bushberg *et al*[9])

Projection imaging includes general x-rays, with fixed and mobile x-ray units, mammography and fluoroscopy.

3.1.1 Image formation

The x-ray image is a representation of the attenuation through an object, projected from an x-ray point source onto an image receptor.[10] Radiographs are obtained with the x-ray source on one side of the patient and the image receptor on the opposite side. An almost homogeneous spatial distribution of x-rays enters the patient's body and is modified through different interactions with the body tissues to produce a heterogeneous distribution of x-rays exiting from the body, i.e. the radiographic image. Each location in the image has a grey scale value related to the attenuation properties of the corresponding location in the body.[9] Figure 3.2 illustrates the concept of projection radiography.

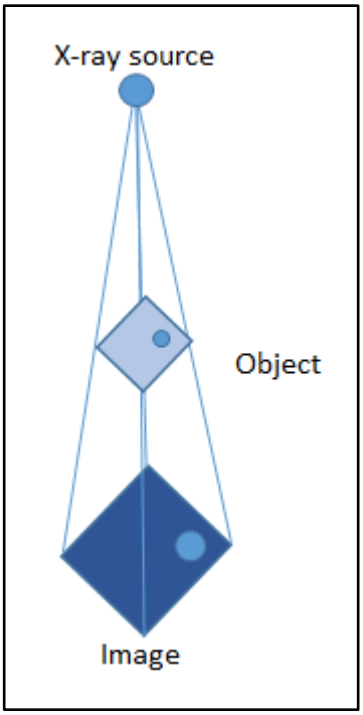

Figure 3.2: The concept of projection radiography.

A radiographic image is a two dimensional (2-D) representation of a three dimensional (3-D) object. Superposition and magnification of anatomy occurs in the 3-D to 2-D projection, which causes loss of image contrast, depth information, uncertainty in object size at different depths and obstruction of objects by overlaying. As the object is a certain distance from the image receptor magnification of the object occurs, reducing image sharpness. Projection radiography also results in shape distortion. In reality the x-ray source is not a point source and scattered radiation is generated in the object, leading to degradation of image quality. By acquiring images with fine focus settings, image resolution may be improved, but this increases tube loading.[10]

Exposure consistency may be increased and repeat exposures reduced by using automatic exposure control (AEC). AEC is possible with digital imaging, like computed radiography (CR) and digital radiography (DR). The x-ray flux is measured at the image receptor and the exposure is stopped when a certain image quality is reached.[18]

3.1.1.1 Film-screen radiography

Film-screen radiography is the historically conventional method of acquiring radiographic images. In screen-film radiography a light sensitive film is placed between intensifying screens in a cassette. The film is a plastic sheet coated with photosensitive emulsion containing silver halide grains. Contact between the screens and film is necessary to prevent artefacts in the image. The screens are made from scintillating phosphor material which emits visible or ultraviolet light upon x-ray interaction. This light primarily causes the darkening of the film. The screens reduce spatial resolution, but also patient dose due to efficient light emission. The front surface of the cassette allows for maximal transmission of incident x-rays. The x-rays and light emitted from the screens interact with the emulsion, changing the chemical bonds to form a latent image. The cassette must be light tight to prevent exposure of the film to ambient light and the film is developed in a dark room to produce the image for viewing. With chemical processing in the dark room the silver halide is converted into silver grains to form the image. With film, increased exposure results in a darker image, i.e. higher optical density (OD). Optical density is a measure of the film transparency is defined in Equation 3.1, where I_0 is the intensity measured with a densitometer in the absence of film and I is the intensity measured through the film.[10]

$$OD = log_{10}\left(\frac{I_0}{I}\right) \qquad \text{[Equation 3.1]}$$

3.1.1.2 Computed Radiography (CR)

CR imaging uses a photostimulable phosphor (PSP) plate housed in a cassette. When the PSP plate is exposed to x-rays, electrons are excited from the valence to the conduction band and are trapped. This forms the latent image, a distribution of electrons trapped in high energy states representative of the amount of energy deposited at each location in the image. Laser light stimulates the release of the trapped energy in the read-out process, with electrons returning to the conduction band and the emission of blue-green light. The intensity of the emitted light is proportional to the absorbed energy from the incident x-rays. This process is shown in Figure 3.3. The PSP plate is then exposed to bright white light for clearing and it can

be reused. The emitted light is detected by photomultiplier tubes (PMTs) which produce a proportional electronic signal. These signals are digitised and displayed.

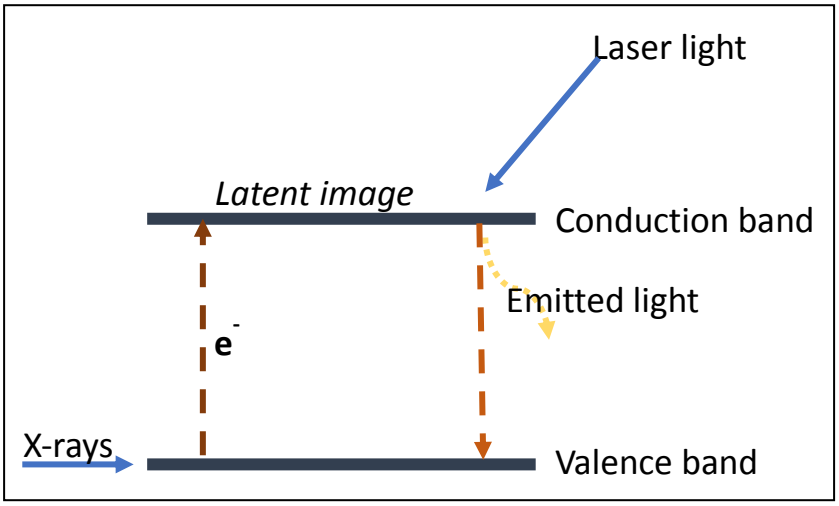

Figure 3.3: Image formation in CR imaging.

3.1.1.3 Digital Radiography (DR)

In DR imaging, digital sensors or flat panel detectors are used and the image is immediately available for display and viewing. Indirect flat panel detectors use an x-ray intensifying screen to convert x-rays to visible light, which is detected. The flat panel consists of several detector elements. Each detector element has a light sensitive area and electronics. With exposure to x-rays charge is build up in each element and stored in a capacitor. The charge is proportional to the amount of light detected. The size of the detector elements determines the spatial resolution of the imaging system. Direct flat panel detectors consist of a thin-film transistor array with a layer of photoconductor material, for example selenium. The electrons produced in the detector layer by incident x-rays are used to directly produce the image by using a negative voltage electrode. The number of produced electrons is proportional to the incident x-ray energy. As electrons travel with high precision in the applied electric field, very little blurring occurs. The electrons are collected at the detector elements and the corresponding image is displayed.[14]

3.1.2 Image quality assurance parameters

Image quality should remain constant and reproducible over time. According to the American Association of Physicists in Medicine (AAPM) and American College of Radiology (ACR) this could be achieved and evaluated with routine imaging of a phantom.[22] Images can be acquired with manual setting of technique factors or with AEC. Where both these options are used, both must be tested in routine quality assurance. AEC should give a constant optical density, or image grey scale, regardless of patient or phantom thickness and this must be verified.[6]

Low and high contrast detectability influence image quality. Low contrast detectability assesses the ability to differentiate objects similar to the background material as they become smaller. High contrast detectability considers small objects of high contrast compared to background and determines the smallest that can be seen. System contrast is assessed monthly and after equipment service using a typical exposure.[23]

Resolution is evaluated in terms of modulation transfer functions or by using suitable bar phantoms, as in the TOR CDR® phantom, discussed in section 3.1.3, for example. Images should also be uniform, i.e. the same grey scale or OD values should be obtained in different areas of an image of a uniform material. As the resultant OD or grey scale value is related to the attenuation, and density, of different materials, sensitometry or grey scale linearity must be assessed to ensure correct display. It is recommended by DoH that these parameters are evaluated three monthly.[7] Image quality is degraded by image noise and the presence of artefacts. These should be assessed quarterly and after service interventions.[23]

In addition to the image quality tests, set-up and geometrical accuracy should be checked by using software measurement tools and comparing the results to the known actual distances. This includes evaluation of the coincidence of the set light field and the delivered x-ray field.

3.1.3 Current* image QA phantoms

For general x-ray imaging quality assurance, a variety of different phantoms are in use. As the TOR CDR® and NORMI 13® phantoms are used more commonly in South Africa, these are discussed below.

3.1.3.1 The TOR CDR® phantom

The phantom is available from Leeds Test Objects provides a continuing check of image quality assurance parameters, with emphasis on parameters that are likely to worsen. Image quality is assessed by identifying the number details and bar-patterns visible. Sensitometry is done with 10 inserts of 5.6 mm diameter each. Resolution is assessed as 0.5 to 14.3 lp/mm. Low contrast and large detail is determined with 17 details of 11 mm diameter and contrast range of 0.002 to 0.075 at 70 kVp and 1mm Cu. The number of details visible is recorded. High contrast and small detail detectability is done visually with 17 inserts of contrast range 0.39 to 0.954 at 70 kVp and 1 mm Cu. The number of visible inserts are counted and recorded. The diameter of these inserts is 0.5 mm.[24] A x-ray image of the phantom is shown in Figure 3.4.

* Current refers to the situation as in 2016

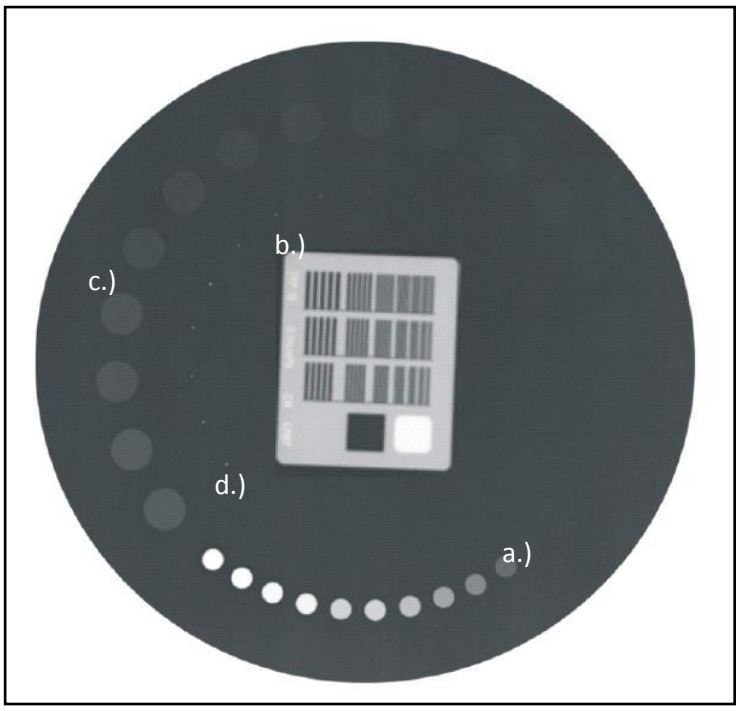

Figure 3.4: An x-ray image of the TOR CDR® phantom. a.) Sensitometry inserts. b.) Bar phantom for spatial resolution. c.) Low contrast large detail inserts. d.) High contrast small detail inserts. (Leads Test Objects Limited[24])

3.1.3.2 The NORMI 13® phantom

Figure 3.5 shows this phantom. It is available from PTW Freiburg GmbH. It is designed for acceptance and constancy tests for digital projection radiography. The phantom tests signal standardisation by measuring the brightness of an image at a central area. It has seven dynamic steps, consisting of different thickness copper plates from 0.0 mm to 2.3 mm, for evaluation of contrast resolution. The steps should be separately identifiable. For low contrast evaluation, six disks with contrasts of 0.8 % to 5.6 % are visually inspected at an image window setting where all seven dynamic steps are depicted differently. At least three low contrast disks must be visible. For homogeneity the optical density or luminance is measured in five different areas, at the centre and at the four corners of the image. The difference between the central and corner values is recorded. Variation from reference values should be less than ± 30 % OD or -50 % to +100 % luminance when AEC is used. A lead foil test pattern is used to evaluate spatial resolution, using a magnifying glass. The lp/mm of the

smallest line group that can be discerned is recorded. Image geometry is assessed by measuring the distances between different lines. A tolerance of ± 3 % is acceptable. These lines are also used to assess scaling and are checked for distortions. The variation between the light field and x-ray field is investigated using the different field size radiopaque field edge marker lines. The image is also evaluated for the presence of artefacts. An additional copper plate is supplied for use with higher kV setting, e.g. 100 kV. The phantom can also evaluate delivered radiation dose by establishing a dose indicator versus image brightness relationship at acceptance testing.[25]

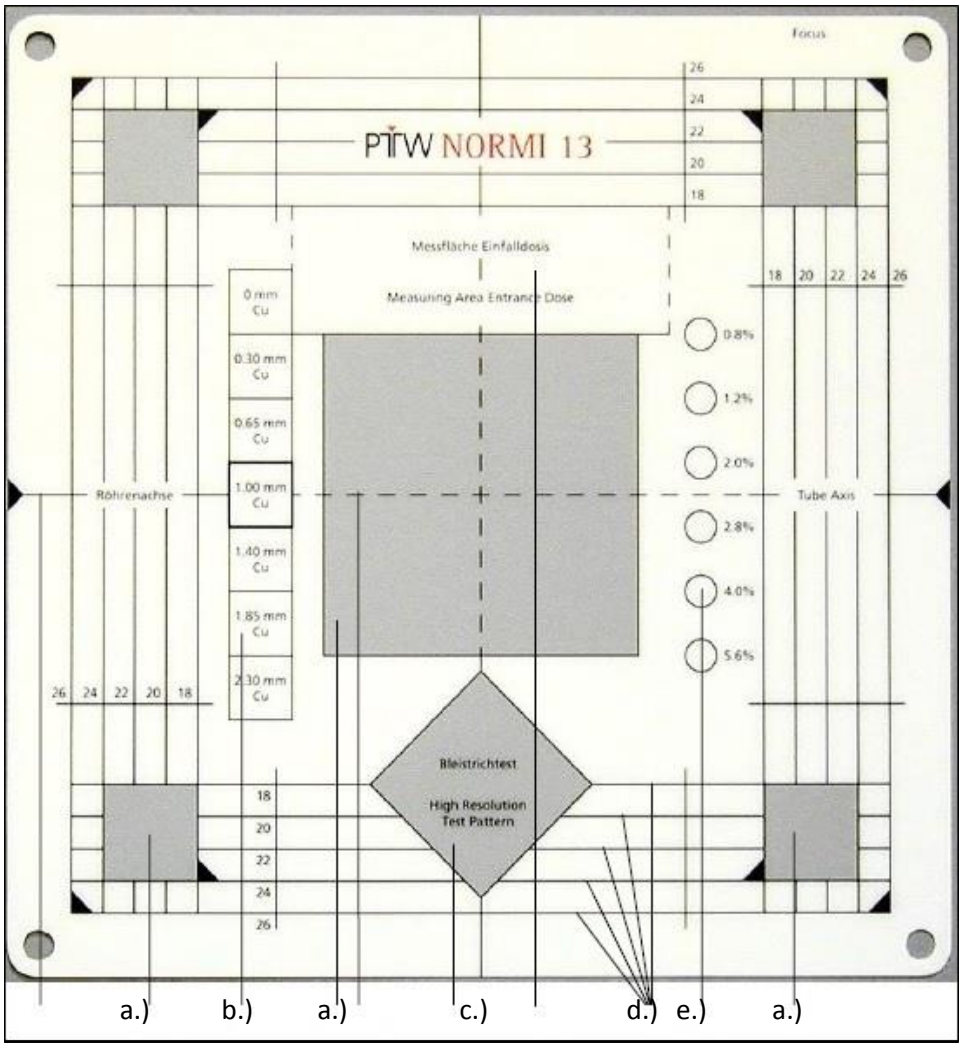

Figure 3.5: The NORMI 13® phantom. a.) Areas used for homogeneity and signal standardisation evaluation. b.) Dynamic contrast resolution steps. c.) Lead foil spatial resolution test pattern. d.) Light field alignment markings. e.) Low contrast disks. (PTW Freiburg GmbH[25]).

Table 3.1 summarises the image quality assurance parameters that can be assessed with the discussed phantoms in comparison to the capabilities of the proposed universal image quality assurance phantom. The universal image quality assurance phantom is at least similar to the commercially available phantoms for routine QC.

Table 3.1: Summary of commercially available modality specific general x-ray phantoms compared to the universal image quality assurance phantom.

Image quality parameter	Sensitometry	Low contrast detectability	Uniformity	Resolution
TOR CDR®	X	X		X
NORMI 13®	X	X	X	X
Universal phantom	**X**	**X**	**X**	**X**
Image quality parameter	Noise	Positioning and alignment	Geometry and measurement tools	Artefacts
TOR CDR®	X		X	X
NORMI 13®	X	X	X	X
Universal phantom	**X**	**X**	**X**	**X**
Image quality parameter	Field size	Standard signal	High contrast resolution	
TOR CDR®		X	X	
NORMI 13®	X	X	X	
Universal phantom	**X**	**X**	**X**	

3.2 Fluoroscopy imaging

Continuous acquisition of a series of x-ray images over a period of time is called fluoroscopy or real time radiography.[9] Fluoroscopy is the main medical imaging contributor of radiation exposure in the United States of America (USA).[6] It is therefore extremely important that image quality is maintained to ensure that additional dose is not needed for satisfactory image formation.

3.2.1 Image formation

Fluoroscopy uses an x-ray beam and a suitable image detector to view images of processes in the human body in real time.[26] Real time imaging gives the appearance

of continuous movement. Fluoroscopy produces real time images at high frame rates and relatively low doses per image.[27] Image detectors or receptors are called x-ray image intensifiers.[26] Modern day image detectors are direct and indirect flat panels. X-ray image intensifiers convert incident photons into visible light photons at the input phosphor, typically made of caesium iodide. The light photons strike a photocathode and electrons are emitted, repelled and accelerated towards an anode, where the electrons are converted to light photons at the output phosphor, characteristically made of zinc cadmium sulphate. The x-ray image is intensified through electronic flux gain, due to the kinetic energy gained by the electrons as they are accelerated, and through magnification gain, due to the reduction of a large x-ray image at the input phosphor to a smaller output phosphor. A measure of system performance is brightness gain, and this is the product of the electronic and magnification gains. The conversion factor is the ratio of the luminance produced at the output phosphor to the incident air Kerma rate at the input phosphor. It decreases over time.[26]

In fluoroscopy, AEC, or Automatic Brightness Control (ABC), controls the incident air Kerma rate on the x-ray image intensifier in order to prevent changes in the brightness of the displayed image, which could alter diagnosis and navigation.[26]

In continuous fluoroscopy the x-ray beam is constantly on. This is a basic approach to fluoroscopy image acquisition. With pulsed fluoroscopy lower radiation doses, improved image quality and reduced tube loading can be achieved.[26] The x-ray generator produces a number of short x-ray pulses, at a certain pulse rate for example 30, 15, 7.5, 4 or 2 pulses per second, which decreases motion artefacts. The frame rate is the image acquisition rate and should be set as low as possible for the examination being done to decrease delivered radiation dose.[27]

3.2.2 Image QA parameters

Routine quality control checks are used as constancy checks. Image quality should be assessed routinely using a phantom that has sufficient attenuation to simulate a patient. Daily assessment before the first patient is imaged for reproducibility is recommended.[23]

Image quality assessment in fluoroscopy includes contrast, noise, sharpness, artefacts, distortions in the image and temporal resolution. These parameters are affected by the design, configuration and use of the fluoroscopic equipment.[26] Grey scales and circular geometry should also be assessed.[28,29] The investigation of these parameters are discussed below.

Spatial resolution and contrast resolution must be evaluated using a suitable phantom with attenuator, wire mesh and a step wedge. The step wedge can also be used to monitor contrast and brightness settings. A line pair phantom with 0.7 – 5.0 line pairs per millimetre (lp/mm) can be used to evaluate spatial resolution. Fluoroscopic contrast resolution is acceptable if 11 mm disks at less than 2 % contrast level can be seen.[6] Contrast resolution in fluoroscopy is low compared to general x-rays, due to low SNR, and can be increased by increasing exposure rates. However, this also increases the radiation dose delivered to the patient. Scattered radiation from the patient also degrades contrast resolution. Fluoroscopic temporal resolution is better than in general x-ray imaging. Several temporal frames are blurred together, improving the SNR, as the x-ray photons from different frames are combined in an image, reducing temporal resolution.[27] The noise levels are generally high due to reduced incident air Kerma rates which are used to minimise patient dose. The image sharpness is influenced by the display and video camera matrix, field of view (FOV), magnification, noise and motion.[26] It is recommended that contrast resolution should be checked monthly.[23]

Fluoroscopic subject contrast is improved by using radiopaque markers and contrast agents, like iodine, barium, gadolinium and carbon dioxide, and by using spectral shaping. In spectral shaping copper filtration is used to attenuate the low energy photons that contribute to patient dose and not to image formation. However this also reduces energy fluence and hence milliampere-seconds (mAs) must be increased.[26] This can be addressed using AEC.

AEC optimises the relationship between patient thickness, copper filtration and tube current by reducing the copper filtration and increasing tube current with increased patient thickness.[26] Obtained phantom images should also be investigated for image blurriness, i.e. the image is not in focus. Automatic brightness control is the ability of

a fluoroscopic system to adjust the mAs and/or kV (and/or pulse width with pulsed fluoroscopy) with patient or phantom thickness to maintain image quality. Image quality of a suitable phantom should be investigated for different thickness of phantom or with different attenuator plates. The visualised image quality should remain almost the same.[5] It is therefore important that different phantom thickness depths are used during QC to ensure the correct operation of AEC.

In fluoroscopy centring is important. Any portion of the fluoroscopic field outside of the image receptor does not contribute to the useful image and hence patient exposure is increased. This alignment should be checked.[30] According to the AAPM and American College of Radiology (ACR) collimation and radiation beam alignment, image artefacts, resolution and phantom image quality should be assessed routinely, in addition to dosimetry quality control.[22] Dose measurements are beyond the scope of this dissertation.

Image quality is also affected by artefacts. A hazy image of which the contrast is reduced, is affected by veiling glare. It is caused by the scatter in the x-ray image intensifier. A fall-off in light intensity towards the image edge is referred to as vignetting. It is caused by deterioration of the video camera and can be reduced by restricting aperture size. Blooming occurs when the signals to the video camera exceed the dynamic range, causing lateral spread in the camera target, resulting in a diffuse image that is larger than the original. This has been addressed in charge-coupled device (CCD) cameras. Enlargement of the image at the image edges is called pincushion distortion and is due to the curvature of the input phosphor. Pincushion effects are reduced by using a smaller FOV. Distortion occurs when straight objects appear curved. This happens when electrons are accelerated in the x-ray image intensifier in the presence of an external magnetic field.[26]

3.2.3 Current* image QA phantoms

The NORMI Rad/Flu® phantom is popular in private practice fluoroscopy image quality assurance in South African catheterization laboratories. It, together with a variety of other commercially available phantoms, are considered below, with comparison to

* Current refers to the situation as in 2016

the proposed universal image quality assurance phantom prototype as described in Chapter 4 section 4.3.

3.2.3.1 TOR 18FG® phantom

Leeds Test Objects medical imaging phantoms has a TOR 18FG® fluoroscopy and fluorography phantom. Constancy checks with the phantom include a grey scale check, resolution limit with 0.5 to 5.0 lp/mm, circular geometry with a lead circle and low-contrast large-detail detectability with 18 inserts of 8 mm diameter at contrast range 0.009 to 0.167 at 70 kVp and 1 mm Cu filtration.[28] The phantom and a x-ray image of the phantom are shown in Figure 3.6.

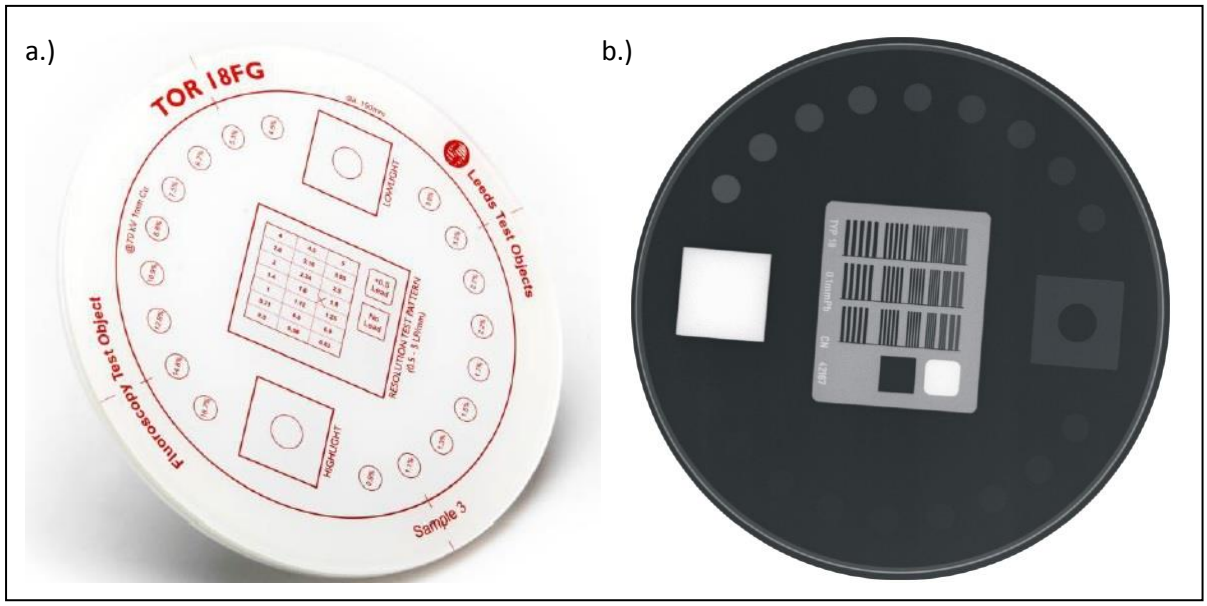

Figure 3.6: a.) The Leads TOR 18FG® phantom. b.) X-ray image of the phantom. (Leads Test Objects Limited[28])

3.2.3.2 RD/FL® contrast-resolution test phantom

The RD/FL® contrast-resolution test phantom, shown in Figure 3.7, is available from CIRS. It contains three mesh patterns ranging from 0.8 to 3.9 lines per mm (20-100 lines per inch) and four low contrast targets of 2, 4, 6 and 8 mm diameter. It allows for the assessment of resolution and contrast in one exposure.[29]

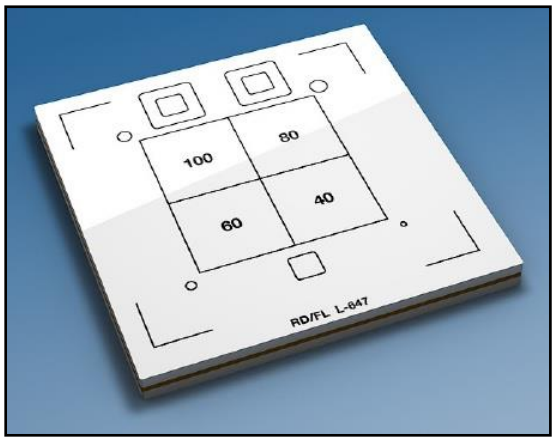

Figure 3.7: The RD/FL® contrast-resolution test phantom. (CIRS Tissue Simulation and Phantom Technology[29])

3.2.3.3 Pro-RF® phantom

JRT Associates supplies several similar fluoroscopic resolution phantoms. The Pro-RF® phantom has eight wire mesh patterns and are available for standard and high resolution systems. Figure 3.8 illustrates the phantom.[31]

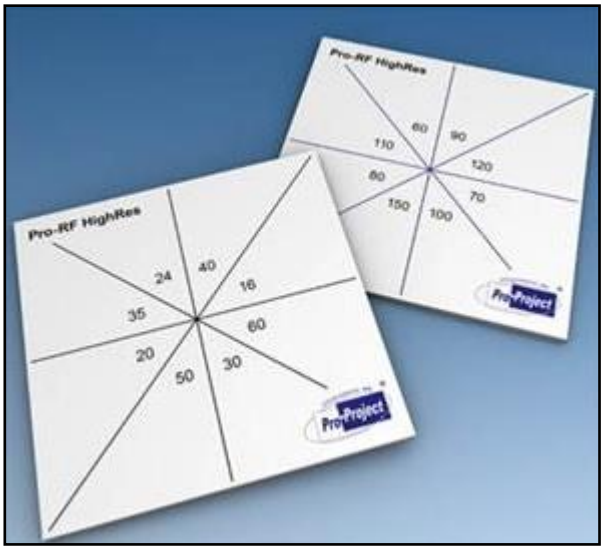

Figure 3.8: The Pro-RF® resolution test phantom. (JRT Associates[31])

3.2.3.4 Fluoro-test resolution tool

This phantom, as shown in Figure 3.9, is available from JR Associates and Fluke Biomedical. It consists of two aluminium plates with arrays of 1.1 cm targets. The targets have different contrasts. Three targets are considered at a time and the threshold contrast is the lowest observed contrast.[32] Large differences in each column are present between adjacent targets for easy decision on target visibility. The threshold contrast is the lowest value seen for the three columns of targets.[33]

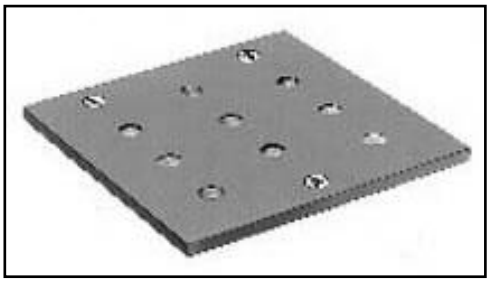

Figure 3.9: The fluoro-test resolution tool. (JRT Associates[32])

3.2.3.5 L600® alignment phantom

Figure 3.10 illustrates the fluoroscopic alignment device, CIRS L600®, consisting of an aluminium plate with four brass strips. The strips are used to define the field edges.[30]

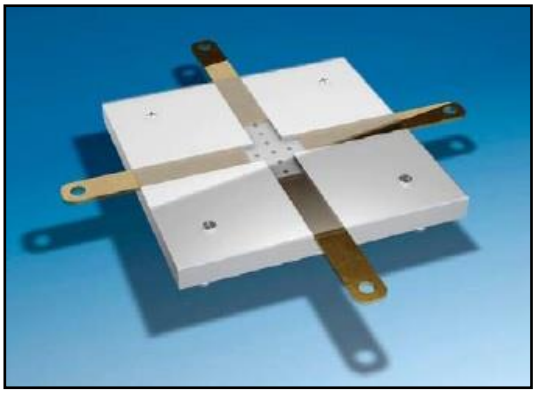

Figure 3.10: CIRS L600® fluoroscopic alignment device. (Universal Medical[30])

3.2.3.6 Fluoroscopy phantom 07-649 CDRH®

Another contrast/resolution test tool is the 07-649 CDRH® fluoroscopic phantom. Figure 3.11 shows it has eight low contrast test holes of 9.5 mm diameter and thicknesses of 0.2 to 1.7 mm. For resolution eight wire meshes of 0.5 – 2.4 lines per mm are included.[34]

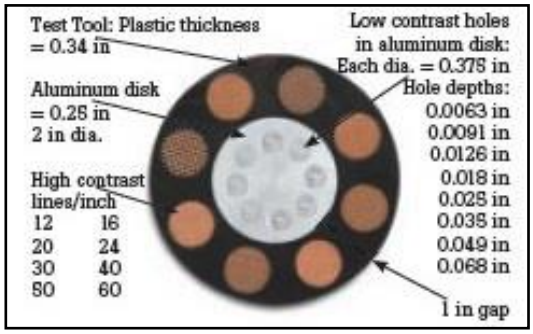

Figure 3.11: The CDRH® test phantom. (Fluke Biomedical[34])

3.2.3.7 SFS set

The SFS set by Radcal® contains different phantoms. Contrast is assessed with 108 inserts, 12 sizes, 0.25 – 11 mm, and 9 contrasts of each size. A step wedge is used to evaluate grey scales and a circle for geometry check. Resolution is 0.5 – 5.0 lp/mm. Figure 3.12 illustrates the set.[35]

3.2.3.8 R/F QC® phantom

The R/F QC® phantom, as in Figure 3.13, has pie shaped wedges with 0.8 – 3.9 lines per mm for high contrast resolution. Four low contrast “masses” of 2, 4, 6 and 8 mm diameter and a density difference patch are used for contrast evaluation. Lines on the phantom are used for alignment with the light field.[36]

Figure 3.12: The SFS® set for fluoroscopy image quality assurance. (Radcal[35])

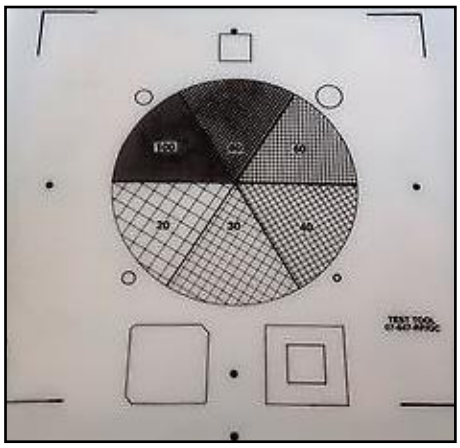

Figure 3.13: The R/F® phantom. (JRT Associates[36])

3.2.3.9 CIRS Model 903® radiography/fluoroscopy QA phantom

The phantom is made from PMMA equivalent epoxy and is 25.4 cm wide and long and 20.7 cm high. It has lead markers at known distances for measurement accuracy. Different depth low contrast holes, 9.5 mm in diameter, in an aluminium disk are used for low contrast assessment. Hole depths range from 1.73 mm to 0.10 mm. High contrast mesh inserts have from 3.15 to 0.47 lines per mm. A contrast detail insert of 9.53 mm thick, 30.00 mm wide and 70.00 mm long is also included. It has 24 holes of 6 different depths and 4 different diameters as shown in Figure 3.14.[37]

Figure 3.14: CIRS Model 903® phantom. (Medical Device Depot Inc[37])

3.2.3.10 Gammex rad/fluoro kit 184D®

Gammex has a similar kit, as in Figure 3.15, the Gammex Rad/Fluoro Kit 184D®, that contains an aluminium step wedge, high and low contrast test tools and beam alignment device.[38]

Figure 3.15: Gammex Rad/Fluoro® kit. (Gammex[38])

3.2.3.11 Fluoroscopic imaging test phantom

Fluke Biomedical's Fluoroscopic Imaging Test Phantom, schematically shown in Figure 3.16, has lead disks to set the black level, white dots for resolution check and grey scale steps.[39]

Grey scale values can be assessed with a perspex step wedge.[40] The grey scale value of each of the steps is recorded and compared to the values at commissioning.[23]

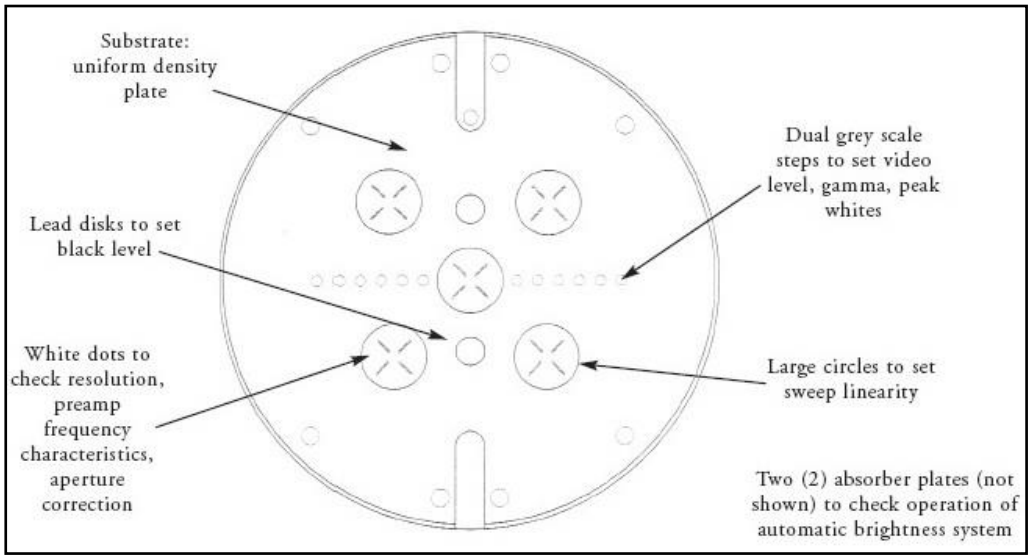

Figure 3.16: The Fluoroscopic Imaging Test Phantom. (Fluke Biomedical[39])

3.2.3.12 NORMI Rad/Flu® phantom

This phantom is used for acceptance and constancy testing in fluoroscopy. It incorporates a copper step wedge for sensitometry assessment, a resolution test pattern, a grid plate and eight low contrast detection inserts.[41] The resolution is assessed visually by reading the lp/mm resolved from the lead-foil grid. Resolutions from 0.6 to 5.0 lp/mm are included. Contrast is visually evaluated with a copper step wedge, with 17 steps of thickness 0.00 to 3.48 mm at depths of 13 mm and 5 mm.[42] The readings and difference between the grey scale values of two specified steps is recorded for signal standardisation and contrast calculation. Contrast detail inserts are visually inspected for visibility.[43] Eight inserts of 10 mm diameter and depth of 0.4 to 4.0 mm are used as well as sixteen inserts, one in each step wedge step, of 4 mm

diameter at 2.5 mm depth.[42] For position verification the distance between the mid-marks on the test object and the centre of the radiation limiting field is measured. The diameter of the object is also measured.[43] A radiograph of the phantom is shown in Figure 3.17.[42]

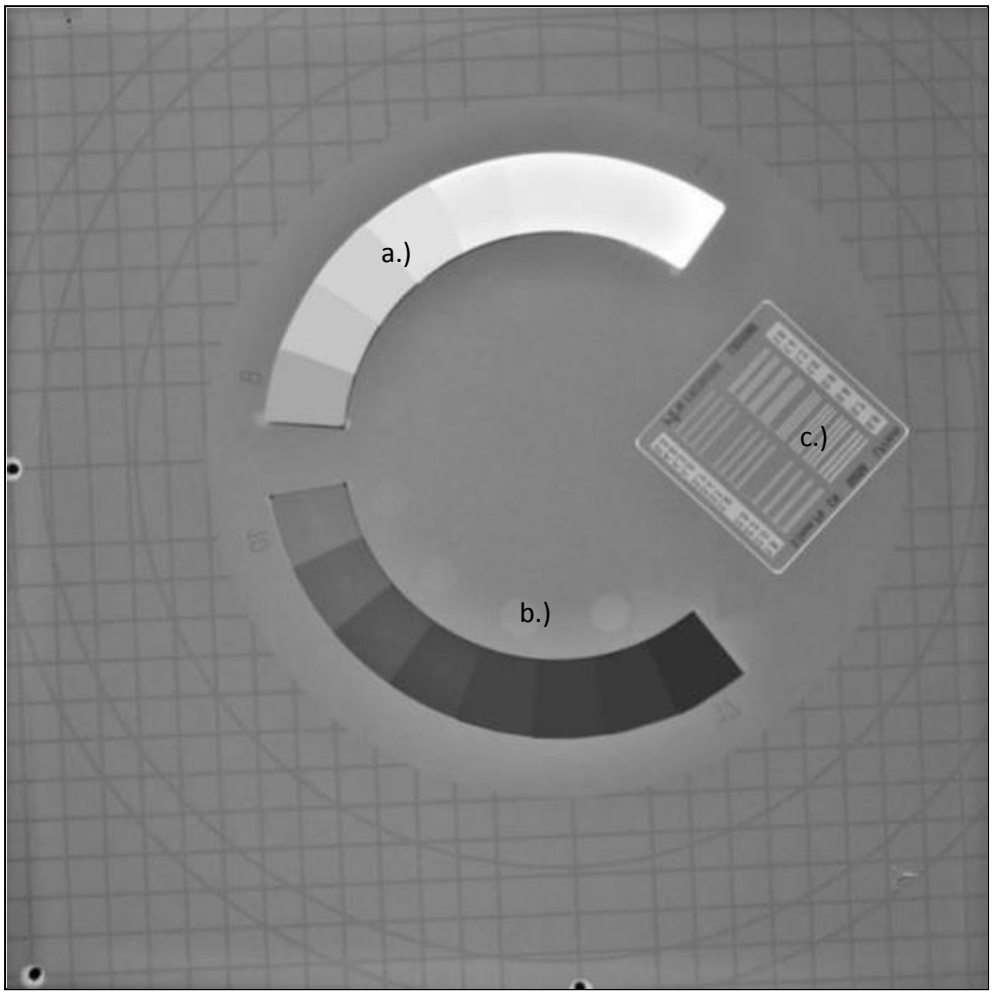

Figure 3.17: The NORMI Rad/Flu® fluoroscopy phantom. a.) Copper step wedge. b.) Contrast detail inserts. c.) Resolution test pattern. (PTW Freiburg GmbH[42])

The routine QC ability of the commercially available phantoms discussed above are summarised in Table 3.2, in comparison to the universal image quality assurance phantom, which is a suitable solution for wide-ranging QC in fluoroscopy.

Table 3.2: Summary of commercially available modality specific fluoroscopy phantoms compared to the universal image quality assurance phantom.

Image quality parameter	Sensitometry	Low contrast detectability	Uniformity	Resolution
TOR 18FG®	X	X	X	X
RD/FL®		X	X	X
Pro-RF®			X	X
Fluoro-Test®		X	X	X
CIRS L600®			X	
CDRH®		X	X	X
SFS Set®	X	X	X	X
RF QC®		X	X	X
CIRS 903®		X	X	X
Gammex Rad/Fluoro®	X	X	X	
Fluke Imaging Test Phantom®	X		X	X
NORMI Rad/Flu	X	X		X
Universal phantom	**X**	**X**	**X**	**X**

Image quality parameter	Noise	Positioning and alignment	Geometry and measurement tools	Artefacts
TOR 18FG®	X		X	X
RD/FL®	X		X	X
Pro-RF®	X		X	X
Fluoro-Test®	X		X	X
CIRS L600®	X		X	X
CDRH®	X		X	X
SFS Set®	X		X	X
RF QC®	X		X	X
CIRS 903®	X		X	X
Gammex Rad/Fluoro®	X	X	X	X
Fluke Imaging Test Phantom®	X		X	X
NORMI Rad/Flu®	X	X	X	X
Universal phantom	**X**	**X**	**X**	**X**

Image quality parameter	Field size	Standard signal	High contrast resolution
TOR 18FG®		X	
RD/FL®			
Pro-RF®			
Fluoro-Test®			
CIRS L600®	X		
CDRH®		X	
SFS Set®			
RF QC®	X		
CIRS 903®			
Gammex Rad/Fluoro®		X	
Fluke Imaging Test Phantom®		X	
NORMI Rad/Flu®	X	X	X
Universal phantom	**X**	**X**	**X**

3.3 Mammography imaging

Mammography is used to detect early stage breast cancer, as diagnostic mammography for symptomatic patients and as screening mammography for asymptomatic individuals. It is also used to localise suspicious areas and as guidance imaging when doing breast biopsies. On a mammogram the distinctive morphology of a tumour mass, patterned appearances of mineral deposits, called micro-calcifications, architectural changes of normal anatomy and differences in the appearance of the same area between the left and right breasts may be indicative of cancer. The image quality of a mammogram must therefore be maintained at a level suitable for these identifications. The resolution of the imaging system must be such that small objects can easily be identified. Breast tissues have low subject contrast, necessitating the use of low energy x-ray spectra to obtain suitable image contrast. Breast tissue is radiation sensitive, and hence the delivered radiation dose must be kept as low as reasonably achievable (ALARA), whilst maintaining acceptable image quality.[44]

Awareness about early detection of breast cancer is increasing. This creates a need for image quality to be optimal, to aid in accurate detection of early stage cancers, minimising false negative results, which in turn requires routine and accurate image quality assurance. A structured quality assurance program monitors performance of mammography equipment and provides a record of machine failure. Quality control procedures should be performed regularly and records meticulously kept, and compared to baseline values, to identify trends and possible equipment issues before patient care is affected. When problems are detected, appropriate action should be taken to correct the problem and further testing should be done to confirm the problem is solved.[45]

3.3.1 Image formation

Due to the unique image quality requirements in mammography, i.e. superior system resolution and contrast from low contrast breast tissues, specific image acquisition parameters are used. For typical breast thicknesses of 3 - 5 cm, best contrast is obtained using molybdenum target with a beryllium window x-ray tube and 0.03 mm molybdenum filtration. Typical exposures for film screen are made at 25 - 35 kVp and 20 - 30 mA for 3 - 6 s. Resolution can be as high as 16 cycles per millimetre with mammography imaging. It is recommended that AEC is used.[45]

Another unique feature of mammography is the use of compression during image acquisition. Compression techniques reduce overlapping anatomy, i.e. spread tissues, and decrease tissue thickness and motion. This reduces scatter, geometric blurring and the delivered radiation dose.[46]

X-ray tube orientation is angled so that a more intense x-ray beam is obtained on chest-wall side, where a greater thickness of breast tissue is encountered, with x-ray intensity fall-off towards the nipple side. The x-ray beam is parallel to the chest-wall to decrease the radiation dose received by the heart. The angled anode absorbs those x-rays parallel to it. The basic concept of mammography imaging is shown in Figure 3.18.

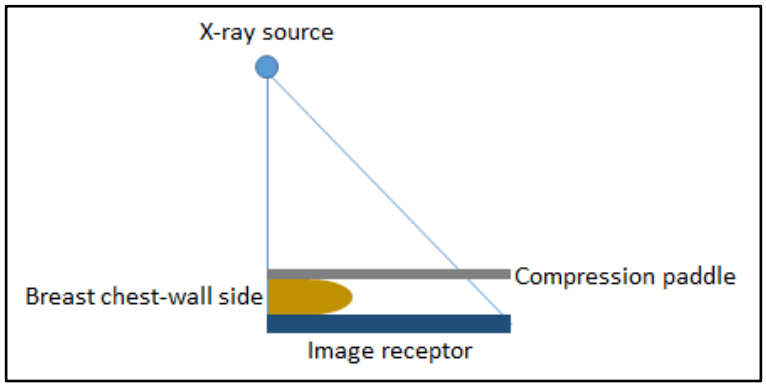

Figure 3.18: Mammography imaging.

Mammography is performed at low tube voltages, below 40 keV, to increase obtained image contrast. Mammography anodes are made from Tungsten or Molybdenum. Tungsten has a higher melting point to accommodate high filament and tube currents, and allows for more efficient x-ray production, due to its higher atomic number. Molybdenum and rhodium are also used, as the K-shell energies are between 17.5 and 22.7 keV, which is optimal for breast imaging.[46]

With screen-film mammography light diffusion results in image blurring. This is influenced by the screen phosphor thickness and particle size, light absorbing dyes and pigments in the screen and by film-screen contact. Single screens can be used to counteract this. Resolution in film-screen mammography is very high. Radiographic noise is caused by film granularity, quantum mottle and screen structure mottle. It results in random optical density variations on a film exposed with a uniform radiation dose.[45] Nowadays CR and DR mammography units are more commonly used than film-screen units.

3.3.2 Image QA parameters

Mammography imaging allows early detection of breast cancer by showing small lesions and micro-calcification details. Changes in breast tissue are subtle and hence mammography image quality must be sensitive enough for accurate detection and diagnosis. Routine image quality evaluation, i.e. image quality consistency testing, is thus very important. Image quality can be evaluated objectively or subjectively. Objective evaluation is done by calculation of SNR, CNR and MTF for example. Mathematical functions give objective and comparable results. Subjective image

quality evaluation is the visual investigation of phantom or clinical images.[47] Image quality is assessed visually, by counting the number of specks, fibres and masses seen and noting the smallest or finest of these that are visible. Images are also investigated for the presence of artefacts. As obtained image quality will depend on the imaging technique factors used, these should be noted and used in future. Image quality analysis then becomes a reproducibility test.

QC in mammography should test image acquisition intensively, image processing according to manufacturer's specifications, and image display, including monitors and printers. Recommended tests include image noise, signal homogeneity, artefacts, contrast and spatial resolution and SNR.[3]

Mammography phantoms should allow for easy assessment of resolution, contrast and overall system performance. Resolution can be tested with a bar phantom with up to 20 cycles per millimetre. Micro-calcifications are simulated with groups of SiC, Al_2O_3 or $CaCO_3$ specks with dimensions 200 - 400 µm. An image of a uniform phantom assesses the uniformity of the x-ray field, the presence of artefacts and the consistency of AEC. Contrast is evaluated using a step wedge of aluminium sheets each of 0.4 mm thickness in 15 steps. Low contrast is assessed with a PMMA disk of 2 - 5 mm thickness.[4] Image contrast is assessed by obtaining the differences in optical density, or image grey scale, behind two selected steps of an aluminium step wedge or behind a PMMA disk and another region in a phantom. Contrast indicates overall changes in system performance. However to diagnose specific issues more specific tests are needed.[45] These tests must be performed for all used manual settings, target/filter combinations and for AEC.

Additionally, for AEC the optical density should remain within ± 0.15 units over the range of different breast thicknesses with uniform phantoms of different thicknesses being imaged.[4]

3.3.3 Current* image QA phantoms

The most commonly used phantom for mammography image quality assurance in South Africa is the Gammex 156® mammographic accreditation phantom. It is the number one phantom listed by the ACR and is the standard phantom used in USA and Canada. The NORMI PAS® phantom is also used in mammography private practice and was used in Chapter 4 section 4.3 for validation of the universal image quality assurance phantom prototype. These phantoms, and a variety of other commercially available phantoms, are described below.

3.3.3.1 Gammex 156® mammographic accreditation phantom

The IAEA recommends the phantom used should contain structures mimicking those found in breast tissue.[3] Figure 3.19 shows the Gammex 156® mammographic accreditation phantom.[48]

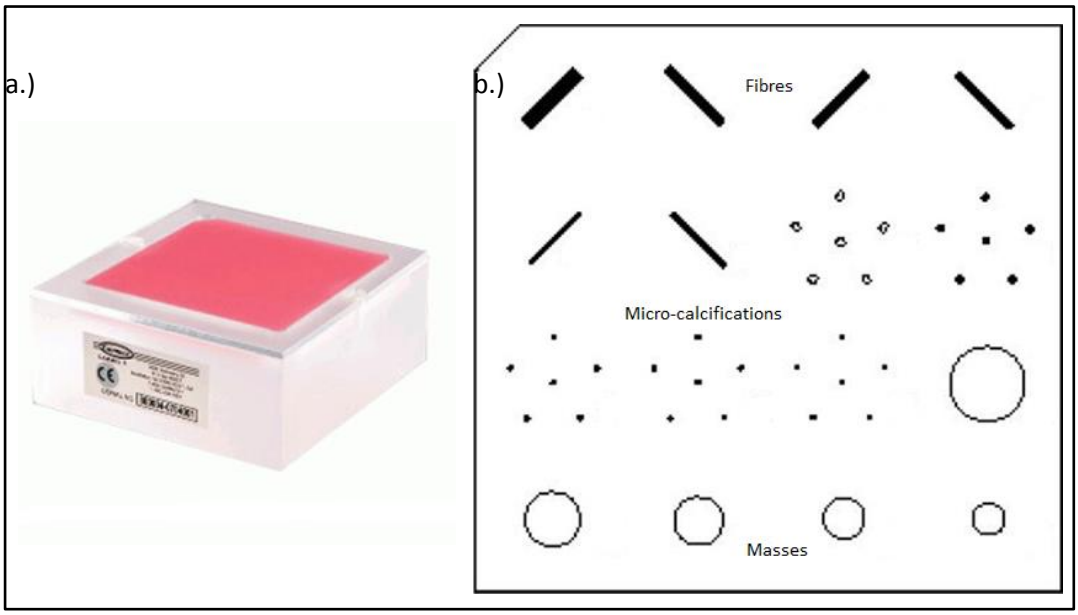

Figure 3.19: a.) The Gammex 156® mammographic accreditation phantom. b.) Insert layout of the phantom. (Gammex[48])

* Current refers to the situation as in 2016

The Gammex 156® phantom simulates 4.2 cm of compressed breast consisting of 50 % glandular and 50 % adipose tissue. Routine imaging of the phantom assists in identifying artefacts and changes in image quality before these become clinically significant. A precision wax insert contains1.56, 1.12, 0.89, 0.75, 0.54 and 0.40 mm nylon fibres, 0.54, 0.40, 0.32, 0.24 and 0.16 mm diameter specks of aluminium oxide simulating micro-calcifications and 0.25, 0.50, 0.75, 1.00 and 2.00 mm diameter lens shaped disks simulating tumorous masses. The insert is enclosed in an acrylic housing.[48,49] Identification of the smallest visible fibres, specks and masses indicate the performance of the system. At least four fibres and three speck groups and masses should be clearly visible. ROI analysis is also used to calculate SNR and CNR.[46]

3.3.3.2 Tissue equivalent model 011A® phantom

CIRS has a similar phantom, the Tissue Equivalent Model 011A® phantom. It simulates a 4.5 cm thick breast of average glandular composition. It contains a 20 lp/mm resolution insert, calcium carbonate grains of 0.130, 0.165, 0.196, 0.230, 0.275 and 0.400 mm for calcification simulation, nylon fibres of 1.25, 0.83, 0.71, 0.53 and 0.30 mm diameter and hemispheric masses of 4.76, 3.16, 2.38, 1.98, 1.59, 1.19 and 0.90 mm thickness.[50] The phantom is available from CIRS and Fluke Biomedical. The phantom is shown in Figure 3.20.

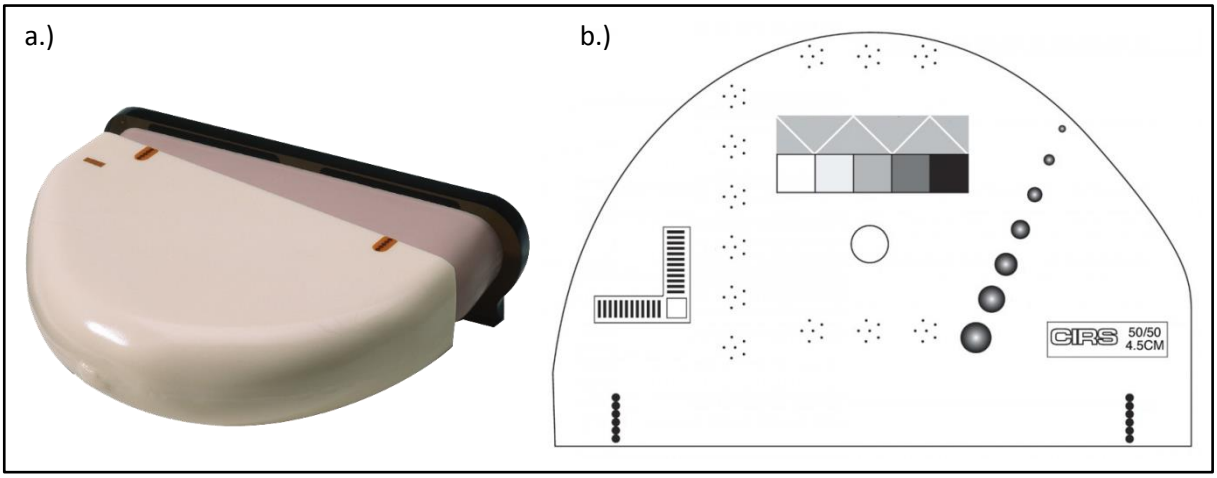

Figure 3.20: a.) The CIRS Tissue Equivalent Model 011A® phantom. b.) Insert layout of the phantom. (JRT Associates[50])

3.3.3.3 Gammex 183® mammographic QC kit

The Gammex 183® routine mammographic QC kit contains, amongst others, a mammographic accreditation phantom (as discussed above) and ACR mammographic quality control manual. The kit allows for image quality, compression force, film-screen contact and processor performance evaluation.[51] A similar kit is offered by CIRS.[52]

3.3.3.4 CIRS high contrast resolution phantoms

The Model 016B® phantom is a bar pattern with 5 to 28 lp/mm. Each bar pattern is positioned at 90 degrees to allow resolution assessment parallel and perpendicular to the anode-cathode direction with a single exposure. It is made from 17.5 micron thick gold-nickel alloy.[53] The CIRS Model 016A®, shown in Figure 3.21, has 5 to 20 lp/mm.[54]

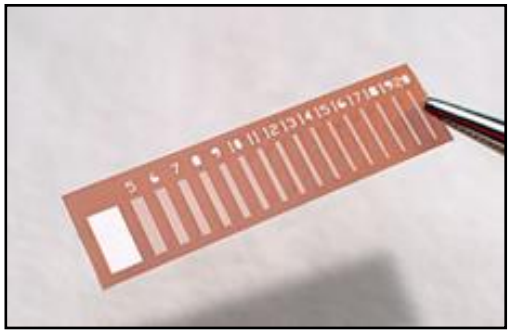

Figure 3.21: The CIRS Model 016B bar phantom. (JRT Associates[54])

3.3.3.5 Artefact identification and contrast detail phantoms

Artefacts can be assessed by imaging a scratch free perspex object. The Artefact Identification Phantom® from JRT Associates is 3.8 x 30.0 x 24.0 cm^3.[55] They also supply a model 18-252 Contrast Detail Mammography Phantom® with 49, in a 7 x 7 matrix, holes with subtle contrast differences. The diameters range from 4.29 to 0.18 mm and contrast from 6.6 % to 0.41 %.[56] These phantoms are shown in Figure 3.22 below.

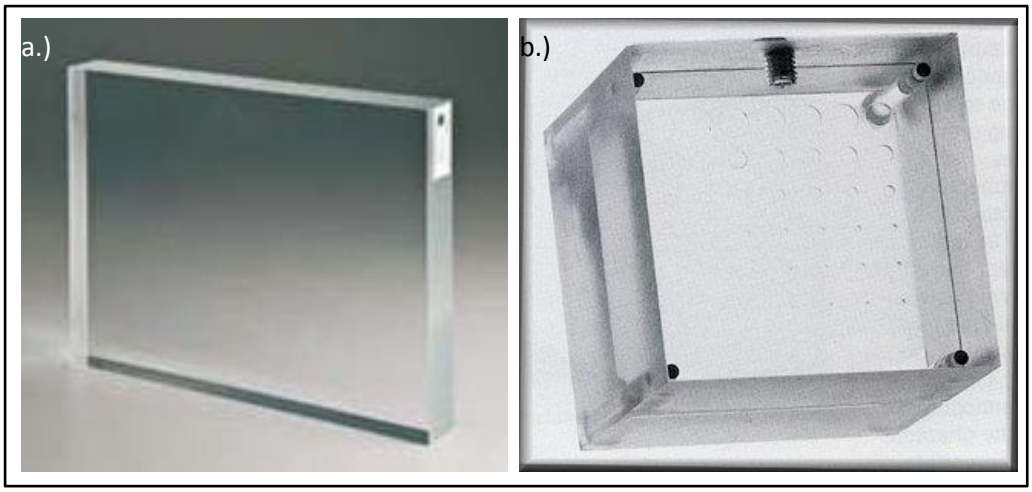

Figure 3.22: CIRS mammography phantoms. a.) The Artefact identification phantom®. (JRT Associates[55]) b.) The 18-252 contrast/detail phantom®. (JRT Associates[56])

3.3.3.6 CIRS model 020 BR3-D® phantom

The phantom consists of 6 half circle slabs with 50 % glandular and 50 % adipose equivalence swirled in each slab. Each slab has a unique swirl pattern, resulting in different backgrounds when stacked together in different thicknesses and combinations. One slab contains calcium carbonate specks of 0.130, 0.165, 0.196, 0.230, 0.275 and 0.400 mm, spheroidal masses of epoxy resin of 1.80, 2.38, 3.18, 3.96, 4.76 and 6.32 mm and fibres of 10 mm length and 0.15, 0.18, 0.23, 0.28, 0.38, 0.41 and 0.60 mm diameter.[57] The phantom is shown in Figure 3.23.

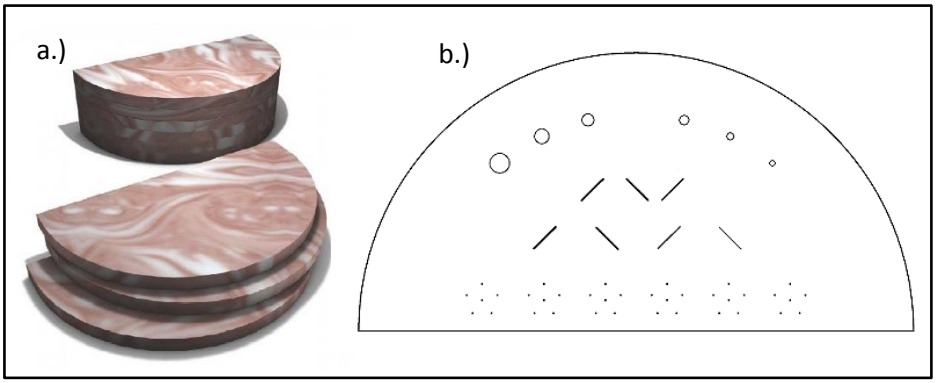

Figure 3.23: a.) The CIRS Model 020 BR3-D phantom®. b.) Insert layout of the phantom. (JRT Assocaites[57])

3.3.3.7 CIRS Mammographic Step Wedge®

Presented in Figure 3.24, the wedge can be used to assess system sensitometry performance quantitatively. It has a 4 cm initial thickness and decreases at 0.25 cm per step over 10 steps.[58]

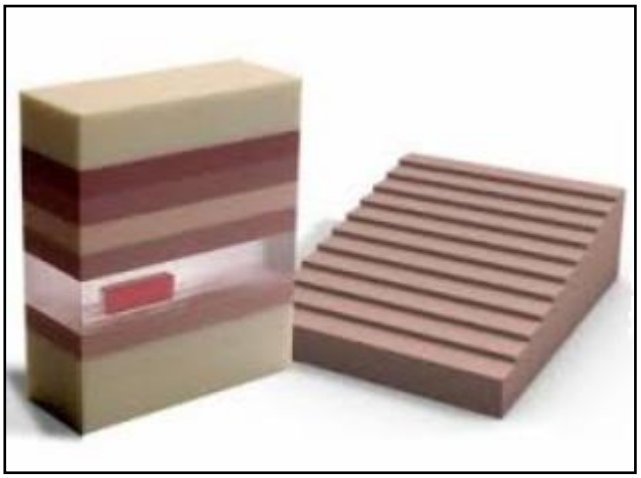

Figure 3.24: CIRS mammographic step wedge®. (JRT Associates[58])

3.3.3.8 NORMI PAS® phantom

The NORMI PAS® phantom is used for image quality assurance on digital mammography units. The base plate of the phantom is semi-circular to simulate breast shape. Two rows of balls are used at chest-wall side to investigate image alignment. An aluminium step wedge can be placed in a cut out in the base plate. The step wedge consists of fourteen steps 0 - 5.2 mm in thickness for sensitometry evaluation. Alternatively a PMMA step wedge with fourteen steps of 0 - 39 mm thickness can be inserted in the cut out. Different test elements can be fitted into the cut out in the structure layer. The PMMA test element is used to assess OD in a ROI. The SDNR is calculated from the SDNR test element, which is used to measure average pixel values for the calculation. The ACR test element contains fibres, micro-calcifications and tumorous masses for visual image quality evaluation. Fibres have diameters of 1.5, 1.1, 0.9, 0.7, 0.55 and 0.4 mm. Masses have thicknesses of 2.0, 1.0, 0.75, 0.5 and 0.25 mm. The speck groups used to simulate micro-calcifications

are 0.5, 0.4, 0.3, 0.2 and 0.12 mm in diameter. A dose detector can also be fitted in the phantom. The NORMI PAS phantom is shown in Figure 3.25.[59]

Figure 3.25: The NORMI PAS® phantom. (PTW Freiburg GmbH[59])

For image quality constancy checks, the NORMI PAS® phantom assesses radiation field limits and centre, average grey scale value, SNR, CNR, artefacts, spatial resolution and contrast resolution.

The commercially available mammography phantoms discussed above are summarised in Table 3.3. Included in the table are the image quality assurance parameters that can be assessed with the universal image quality assurance phantom. The universal image quality assurance phantom therefore presents an acceptable solution for consistency QC in mammography.

Table 3.3: Summary of commercially available modality specific mammography phantoms compared to the universal image quality assurance phantom.

Image quality parameter	Sensitometry	Low contrast detectability (masses)	Uniformity	Resolution
Gammex 156®		X	X	
CIRS tissue equivalent®		X	X	X
CIRS model 016 A & B®				X
CIRS artefact identification®				
CIRS contrast/detail 18-252®				
CIRS 020 BR3-D®		X	X	
CIRS step wedge®	X			
NORMI PAS®	X	X	X	X
Universal phantom	**X**	**X**	**X**	**X**

Image quality parameter	Noise	Positioning and alignment	Geometry and measurement tools	Artefacts
Gammex 156®	X	X	X	X
CIRS tissue equivalent®		X	X	
CIRS model 016 A & B®		X	X	
CIRS artefact identification®		X	X	X
CIRS contrast/detail 18-252®		X	X	
CIRS 020 BR3-D®		X	X	
CIRS step wedge®		X	X	
NORMI PAS®	X	X	X	X
Universal phantom	**X**	**X**	**X**	**X**

Image quality parameter	Standard signal	High contrast resolution	Micro-calcifications	Fibres
Gammex 156®	X	X	X	X
CIRS tissue equivalent®	X		X	X
CIRS model 016 A & B®				
CIRS artefact identification®	X			
CIRS contrast/detail 18-252®	X	X		
CIRS 020 BR3-D®	X		X	X

CIRS step wedge®				
NORMI PAS®	X	X	X	X
Universal phantom	**X**	**X**	**X**	**X**

3.4 Computed Tomography (CT) scanning

CT scanning became available in the 1970s. Its biggest advantage is that anatomical information is displayed as transverse images that, when added, provide a three dimensional representation of the scanned anatomy.[9] The three dimensional image sets, i.e. axial, coronal and sagittal, have isotropic spatial resolution.[19]

3.4.1 Image formation

For CT image formation, a number of transmission profiles through the patient are acquired. The logarithm of the inverse normalised profiles is calculated and the Fourier transform is obtained. The result is filtered and the inverse Fourier transform is calculated. This describes the essence of filtered back projection. Filtered back projection, as opposed to simple back projection, decreases image blurring in the obtained CT slice or image.[15] Figure 3.26 a.) illustrates simple back projection, with filtered back projection shown in Figure 3.26 b.).[60]

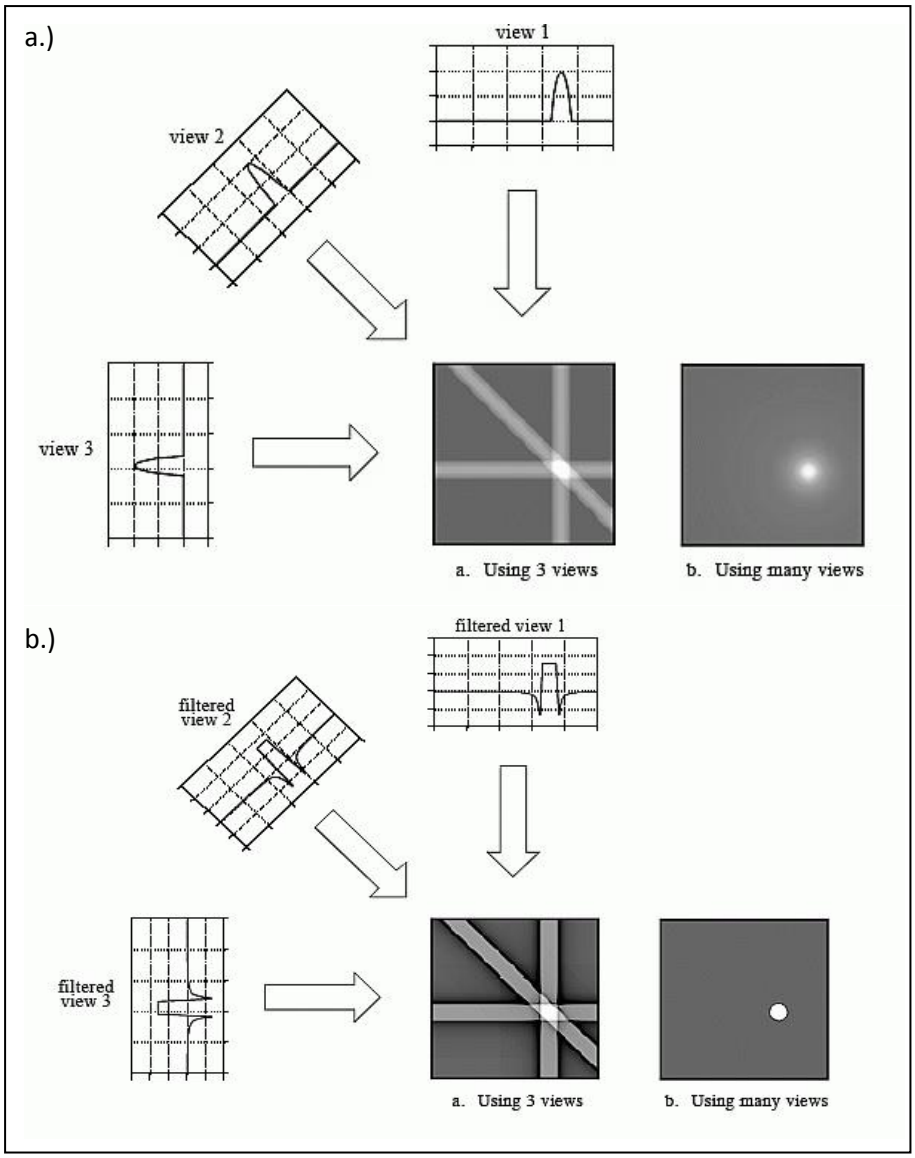

Figure 3.26: a.) Simple back projection. b.) Filtered back projection (Steven *et al*[60])

Simple back projection smears each view along the path it was acquired to form an image, resulting in a blurred version of the correct image. By setting all the pixel values along a ray to the same value and summing the back projected views the final image is obtained. To correct for the blurring effect of simple back projection, filtered back projection is used. As Figure 3.26 b.) shows, each view is filtered before back projection by convolution with a filter kernel to create a set of filtered views. By back projecting the filtered views the resultant image is a better representation of the correct image. Using an infinite number of views will improve the image quality of the resultant image, making it more like the correct one.[60]

A CT scan image is a display of grey scale values derived from the linear attenuation coefficients, μ, of the materials imaged.[61] For a number of different views, the x-ray transmission profiles through the patient are measured in CT scanning. Each view is obtained by rotating the detector and x-ray source around the patient. The transmission profiles are used to reconstruct the CT image, which consists of a matrix of image voxels. Each voxel has a value related to the attenuation of the x-ray beam through the associated tissue, i.e. to the linear attenuation coefficient[15], which depends on the material density, atomic number and x-ray beam energy.[61]

CT scanner attenuation measurements are quoted as relative to water. For small kVp and small atomic number changes the CT-numbers relative to water will remain quite independent of kVp and object size. The mean CT number of water is obtained from ROIs at different locations in an image of a uniform water bath. It should not vary by more than the standard deviation of a centrally placed ROI in such an image.[61] Different tissues have different linear attenuation coefficients. The matrix of linear attenuation coefficients, $\mu_{material}$, is converted to a matrix of CT-numbers, $CTnumber_{material}$, relative to the linear attenuation coefficient of water at room temperature, μ_{water}, by Equation 3.2.[15] CT-numbers are also referred to as Hounsfield Units (HU).

$$CTnumber_{material} = \frac{\mu_{material} - \mu_{water}}{\mu_{water}} \times 1000 \qquad \text{[Equation 3.2]}$$

CT scanners generally use a polychromatic x-ray source, or an x-ray spectrum. The obtained CT-numbers are averaged, based on the linear attenuation coefficients of each material at each x-ray energy. The CT-number of a material, relative to that of water, therefore depends on the size and properties of the object being scanned.[61] CT-numbers are quantitatively meaningful, unlike grey scale values in other x-ray imaging modalities.[19] Differences between expected and obtained CT-numbers may occur as a result of the reconstruction filter and FOV used. Such differences are expected for a scanner over time.[15] Typical CT-number values are shown in Table 3.4, produced from Dance *et al*[15].

Table 3.4: Typical CT-number values and possible CT-number value ranges.[15]

Substance	Typical CT-number	Possible CT-number range
Compact bone	1000	300 to 2500
Muscle	25	10 to 40
Water	0	
Fat	-90	-100 to -80
Lung	-750	-950 to -600
Air	-1000	

The contrast scale of a CT scanner is a measure of the way in which linear attenuation coefficients are converted to CT-numbers. For a certain scanning protocol, the contrast scale, CS, in units of cm^{-1}/HU, can be calculation using Equation 3.3 , where μ_{plex} and μ_{water} are the linear attenuation coefficients of plexiglass and water, the difference being equal to 0.024 cm^{-1}, and HU_{plex} and HU_{water} are the HUs or CT-numbers for plexiglass and water respectively. The image noise is then a percentage of CS and is calculated with Equation 3.4, where σ_{water} is the percentage noise. At 100 – 140 kVp is 0.190 cm^{-1}.[61]

$$CS = \frac{\mu_{plex} - \mu_{water}}{HU_{plex} - HU_{water}} \qquad \text{[Equation 3.3]}$$

$$\sigma_{water} = \frac{\sigma \times CS \times 100}{\mu_{water}} \qquad \text{[Equation 3.4]}$$

With CT scanning, Compton scattering is the most common interaction mechanism in soft tissue. In bone and iodine (with contrast enhancement scanning), a higher proportion of photoelectric interactions will occur due to higher atomic numbers of these materials.[19] The resolution and detectability of low contrast objects depend on the trade-off between spatial resolution and noise versus patient dose and also on inherent image processing to change the appearance of noise in the image.[61]

Post-acquisition image processing and reconstruction, improving the visibility of certain tissues or structures, is possible with CT scanning. Different reconstruction filters can be used, depending on the tissue of importance. Ram-Lak or Ramp filters give ideal spatial resolution with a lot of image noise. These are used to visualise bony structures. A Shepp-Logan filter gives images with less noise and better low contrast resolution for visualisation of soft tissues. The low contrast resolution of CT is superior to planar imaging modalities.[15]

3.4.2 Image QA parameters

The AAPM lists the CT performance tests as noise or contrast scale, spatial resolution in the imaging plane, slice thickness, sensitivity, small lesion detection or low contrast detectability, artefacts (for example motion, beam hardening and alignment artefacts) and image uniformity. The results from these tests must be reproducible over time, i.e. consistency testing.[61] Other image quality assurance parameters of concern in CT scanning include CT-number linearity and CT-number of water consistency.[62,63]

CT spatial resolution is determined by the fundamental resolution properties of acquiring the image and the resolution characteristics of the applied filter and mathematical algorithms.[19] MTFs can be obtained from wedge or spoke phantoms, edge response used to calculate ESF and then MTF or by using an impulse response from a small wire or bead to calculate the MTF from the PSF. Generally resolution is limited by pixel size, therefore the PSF stimulus must be smaller than a pixel. Resolution can also be determined by measuring the disappearance of moderate contrast holes, for example water filled holes in Plexiglass.[61] It can also be tested using rods of different sizes that image as dots or plates of different sizes that image as lines and must be made of a material with significantly higher CT-number than the surrounding phantom material.[6] Spatial resolution of at least 6 line pairs per centimetre (lp/cm) is recommended.[62]

Contrast resolution is affected by exposure technique factors, slice thickness, filtered back projection and reconstruction. Contrast resolution is assessed by visual evaluation of a contrast detail phantom. Smaller objects have lower SNRs and are more difficult to visualise.[19]

The variation in CT numbers among pixels of a scan of a uniform material is referred to as noise. The variation of the CT number among ROIs indicates on image uniformity. Noise must be assessed for all scan protocols, using a uniform phantom, at the centre and periphery of the images, using ROIs containing at least 25 pixels[61] by calculating the standard deviation, σ.[19] As the difference in the attenuation coefficient between normal and pathological tissues is usually small, noise can result in such pathologies being invisible.[61] This necessitates the evaluation of low contrast detectability.

Low contrast detectability, or sensitivity, is investigated with different sized low contrast inserts. Subjectively it is assessed by visualisation and objectively by SNR calculation.[15] It investigates the ability to differentiate between objects with subtle differences in density or attenuation coefficient.[62] Sensitivity hence describes the minimum detectable linear attenuation coefficient difference.[61] Image noise can degrade low contrast objects visibility. If noise is decreased to improve visibility of low contrast objects, patient dose is increased. Detectability therefore depends on object size or spatial resolution, contrast and noise, and therefore on dose.[61]

Slice thickness is defined as the FWHM of the response across the slice.[61] Axial slice width can be measured using a sequence of wires on a ramp at an angle to the axial plane, arranged with 0.5 mm spaces between the wires. By counting the well-seen wires and dividing by 2 the slice width is calculated. This can be done for different slice thicknesses, with an accepted tolerance of 1.5 mm from prescribed width.[62] The AAPM recommends that the width at half maximum response should be used to quantify slice thickness.[61]

Image uniformity ensures an image that is completely even and without artefacts. It is assessed by obtaining the CT-number in identical ROIs in different areas of an image of a homogeneous section of the phantom. The difference should be less than or equal to 5 CT-numbers. Evaluation is done at specified window width and window level settings.[62]

CT-numbers should vary linearly with linear attenuation coefficients. This establishes a constancy of the contrast scale over the range of linear attenuation coefficients of interest clinically. CT-number linearity is assessed using different phantom inserts with different electron and physical densities.[61] Typical inserts include polyethylene, water, PMMA, polycarbonate, nylon, polystyrene and Teflon.[6] Each pixel value in a CT scan image should echo the density of the material imaged in that pixel. In general, the CT-number of water is taken as 0 and that of air as -1000. The CT-numbers of different materials will vary depending on the x-ray spectrum used to obtain the CT scan and is dependent on beam hardening and scatter effects. An average value has been determined for different CT phantom materials, based on different scanners and scanning protocols, accepted with an allowed tolerance. For example water is accepted as 0 ± 7 CT-number. For evaluation of CT-number or CT-number linearity, ROIs are drawn in the inserts and the displayed CT-number is compared to the accepted value. The average CT-number of a material should remain constant for the same exposure protocol.[62]

Images must also be free of artefacts, which could obscure clinically relevant information. Artefacts in CT are acquisition, reconstruction and patient related. Acquisition related artefacts include ring artefacts, due to miscalibration or failure of detector elements. Moire artefact results from under sampling of the projection data. When thick acquisition slices are used, averaging of the linear attenuation coefficients leads to partial volume effects, giving a larger lower density image of a small high density object. Dense bone or metal attenuates the x-ray beam strongly resulting in beam hardening artefacts.[15] As CT x-ray beams are polychromatic, beam hardening artefacts may occur due to unequal filtration in the different image views. It can be assessed by investigating the change in the mean CT-number in a uniform phantom when a variety of higher atomic number objects are introduced in the phantom.[61] Metal or streak artefacts can be so severe that the x-ray beam is almost completely attenuated, giving dark areas in the image surrounding the metal with streaky artefact over the image.[15] Ring artefacts are best evaluated with a narrow window width setting of about 500 – 1000 CT-number.[6] Patient related artefacts can be minimised by reducing patient motion, e.g. breath holding and using short rotation times.[15] Patient misalignment and motion produce streaking from high contrast objects. It can

be evaluated by scanning aluminium pins in a uniform material and setting the WL low and noting any significant streaks from the pins.[61]

The CT-number of water, image noise, image uniformity and artefacts should be evaluated daily. It is recommended that CT number scale stability and accuracy should be evaluated monthly to semi-annually. Spatial resolution should also be evaluated at these intervals. Low contrast detectability is evaluated quarterly to annually and as this is a subjective test, all precautions should be taken to minimise result variability due to subjectivity.[6]

3.4.3 Current image QA phantoms

The most popular phantom for CT image quality control, not only in South Africa but in general, is probably the Catphan® phantom. Different Catphan® phantom models are available, of which more recent models are better suited for advanced multi-slice CT scanner QC.

3.4.3.1 Gammex ACR® phantom

Commercially available CT scanner phantoms include the Gammex ACR® CT phantom, accredited by the ACR Accreditation Program, as shown in Figure 3.27.[63,64]

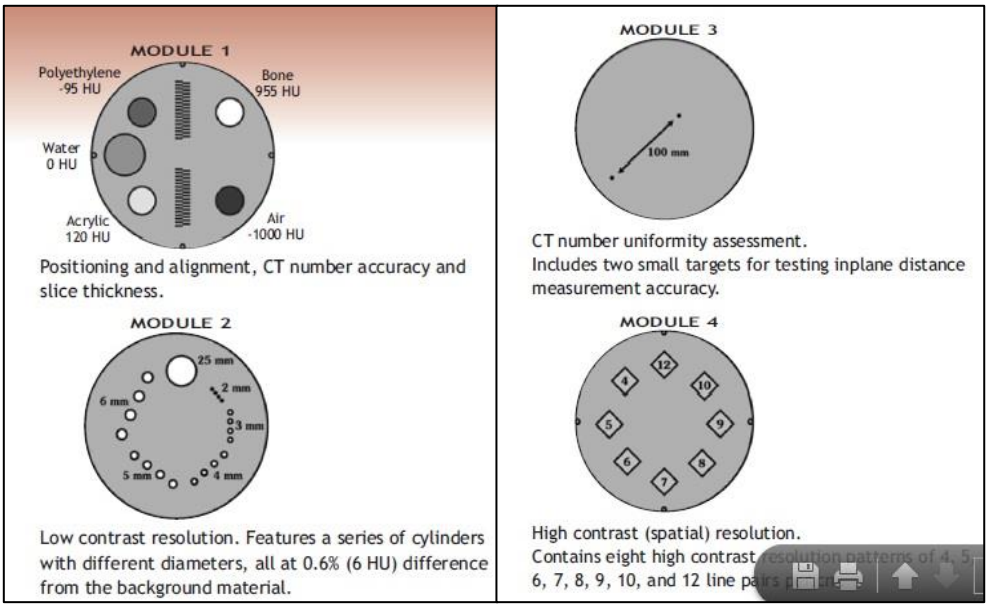

Figure 3.27: The Gammex ACR® CT phantom modules. (Gammex[64])

The Gammex ACR® CT phantom is made from solid water and has a 20 cm diameter and 16 cm length. It contains water equivalent, bone equivalent, acrylic, air and polyethylene inserts for CT-number linearity assessment. A 0.011 mm diameter tungsten carbide bead is used for MTF calculation. Aluminium and polystyrene line pair material is used for resolution assessment with bar phantoms 4, 5, 6, 7, 8, 9, 10 and 12 lp/cm. Steel balls of 1 mm diameter are used for positioning and alignment checks and 0.28 mm ball bearings for distance measurements on an axial slice. A low contrast rod module is used for low contrast resolution with 6, 5, 4, 3 and 2 mm diameter cylinders at a contrast 0.6 % different from background. Four cylinders of each diameter are included. CT-number uniformity is assessed with ROI analysis. Slice thickness is checked with two wire ramps evident in 0.5 mm z-axis increments.[63,64] For analysing low contrast detectability, a set window width (WW) and window level (WL) should be used. The Gammex ACR® CT phantom recommends WW=100 and WL=100 and for uniformity settings of WW=100 and WL=0. With this phantom CT-number linearity is -107 to -87 CT-number for polyethylene, -7 to +7 CT-number for water, +110 to +130 CT-number for acrylic, +850 to +970 CT-number for bone and -1005 to -970 CT-number for air.[62]

3.4.3.2 Gammex 461A® head/body phantom

The Gammex 461A® head/body CT phantom, shown in Figure 3.28, assesses noise, CT number, uniformity, spatial resolution, low contrast detectability, alignment, slice thickness (with 26.6º slope), phantom position and different artefacts. Spatial resolution is assessed from 1.5 to 0.4 mm and low contrast detectability to 0.6%.[65]

Figure 3.28: The Gammex 461A® head/body phantom (Gammex[65])

3.4.3.3 CIRS model 610® AAPM CT performance phantom

Figure 3.29 illustrates the phantom, which can be filled with water, has a 21.59 cm diameter and is 39.37 cm in length. It has inserts for the evaluation of CT-number linearity, high contrast resolution, and slice thickness determination. It can also test noise, uniformity, low contrast sensitivity or detectability (with cavities ranging from 2.54 to 0.32 cm), beam hardening effects, with a bone equivalent ring that fits over the inserts, and has an insert for TLD dose measurements. Its set-up tests mechanical alignment. It is designed based on the AAPM Task Force on CT Scanner Phantoms Report 1, which aims to define the performance of a CT scanner and to describe performance testing using phantoms.[66] According to JRT Associates “one phantom does it all” describes the CIRS phantom for CT QA.[67]

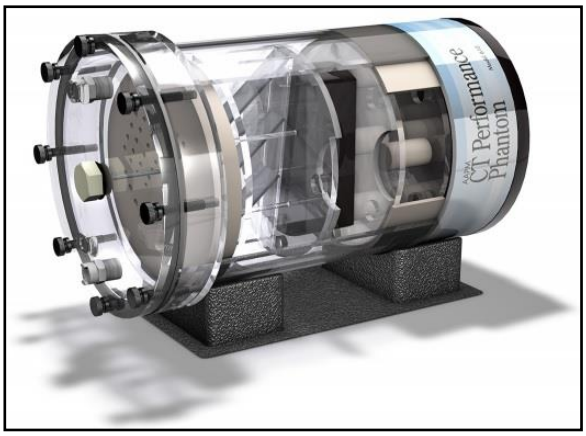

Figure 3.29: The CIRS model 610® AAPM CT performance phantom (CIRS Tissue Simulation and Phantom Technology[66])

3.4.3.4 Spiral/helical CT phantom

The Universal Medical spiral/helical CT phantom is designed for low contrast lesion detection with different scanning protocols. It contains targets with contrast 5, 10 and 20 CT-number above background.[68] It is shown in Figure 3.30.

Figure 3.30: The Universal Medical spiral/helical CT phantom (Universal Medical[68])

3.4.3.5 Catphan phantom

Catphan® phantoms are used for axial, helical and spiral CT QA. The phantoms are constructed of solid-cast materials, eliminating water leaks. It tests slice thickness (in terms of FWHM of a wire ramp), as in Figure 3.31 b.), resolution with 1 to 21 lp/cm, as in Figure 3.31 c.), position verification and alignment check, as in Figure 3.31 b.), low contrast sensitivity, as in Figure 3.31 a.), spatial uniformity, noise, sensitometry and MTF from a PSF of a tungsten carbide bead, as in Figure 3.31 c.). Additionally it investigates sub-slice (with 3, 5, 7 and 9 mm diameter rods of 3, 5 and 7 mm length) and supra-slice (with 40 mm length rods of 2, 3, 4, 5, 6, 7, 8, 9 and 15 mm diameter) low contrast sensitivity, scan incrementation and circular symmetry. CT-number linearity is tested with Teflon, air, low density polyethylene, derlin, acrylic and polymethylpentene inserts. In Catphan 600 slice thickness is assessed using 23° angled ramps with tungsten beads in a 40 mm thick section. The beads are arranged in two opposing ramps, one with 0.3mm diameter beads at 1.0 mm spacing arranged horizontally. The second ramp contains 0.17 mm beads vertically positioned at 0.25 mm spacing. Slice thickness is determined by counting the seen beads and multiplying by the know distance between them.[69,70]

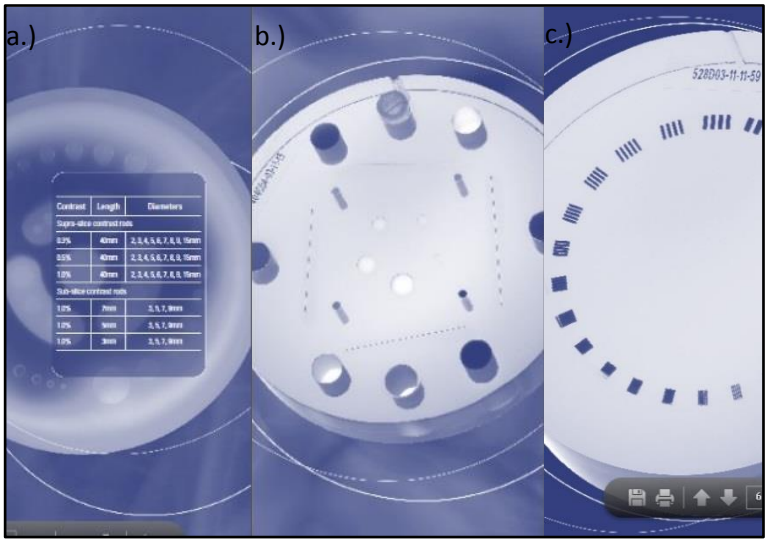

Figure 3.31: The Catphan® phantom. a.) Low contrast detectability module. b.) Sensitometry, alignment and slice thickness module. c.) Resolution module. (The Phantom Laboratory[70])

AAPM Report No. 1[61] provides recommendations on the design of an acceptable CT image quality assessment phantom. Noise assessment phantoms can either be water filled or made from uniform plastic material. It should be circular in cross section, with a diameter of 20.3 cm for a head phantom or 33.0 cm for a body phantom. The wall of the phantom must be thinner than 1.0 cm plexiglass. Changes in the standard deviation in ROIs at least 25 pixels in size located at the centre and periphery of the phantom can be used to assess noise. This should be done for all scanning protocols used. A 2.5 cm diameter plexiglass rod can be positioned in the centre of a water phantom for contrast scale determination. Spatial resolution can be measured with an edge phantom, like a plexiglass block placed in the noise phantom with the surface exactly parallel to the rotational axis of the scanner. Alternatively, a spatial resolution hole phantom can be used, with holes drilled into plexiglass, at a centre to centre distance equal to twice the diameter of the hole, and filled with water. Hole diameters are recommended as 0.75, 1.00, 1.25, 1.50, 1.75, 2.00 and 2.50 mm ± 5 %. Investigation should be done centrally and peripherally in an image. Slice thickness can be assessed by scanning across a 0.5 mm thick x 25.4 mm wide aluminium strip positioned at 45^{o} across the beam. The FWHM can be measured from a profile across the strip and should be assessed at the centre and periphery of an image. For sensitivity assessment pins or holes 3.0 mm to 20.0 mm in diameter can be used. Press fitting pins is difficult and expensive, so liquid solutions in holes are recommended. Linearity evaluation can be done with 2.5 cm diameter cylinders of plexiglass, lexan, nylon, polystyrene and polyethylene at the centre of the noise phantom.[61]

Chiarot *et al*[71] developed a phantom for advanced imaging technology, like multi-detector CT and cone beam CT, evaluation. The phantom addressed shortcomings in current phantoms by having 3-D symmetry using spherical inserts and modules with known contrast simulating real tissue. It is difficult to minimise air pockets, especially around the spherical inserts. The head section contains spheres simulating brain lesions. The left lung's contrast detail spheres approximate lung modules. The right lung is an accessible structure for insertion of different assessment devices and the abdomen simulates kidneys, colon, rectum and prostate. Plastics like Teflon, acetal, acrylic, nylon, polystyrene, polyethylene and polypropylene are used. Sphere diameters are 12.7, 9.5, 8.0, 6.4, 4.8, 3.2 and 1.6 mm. Groups of 12.7 mm diameter

spheres with different contrasts are also incorporated, with one sphere very close to that of the background material. Contrast is manipulated by adding antimony to polyurethane.[71]

Table 3.5 summarises the required CT image quality assurance parameters and indicates which of these can be assessed using the described commercially available phantoms and the universal image quality assurance phantom. The proposed phantom can assess the identified required CT image quality assurance parameters, as an additional tool in routine CT scanning QC.

Table 3.5: Summary of commercially available modality specific CT phantoms compared to the universal image quality assurance phantom.

Image quality parameter	CT-number linearity	Low contrast detectability	Uniformity	Resolution
Gammex ACR®	X	X	X	X
Gammex 461A®	X	X	X	X
CIRS 610®	X	X	X	X
Universal Medical®		X		
Catphan®	X	X	X	X
Universal phantom	**X**	**X**	**X**	**X**

Image quality parameter	Noise	Positioning and alignment	Slice thickness	Geometry and measurement tools
Gammex ACR®	X	X	X	X
Gammex 461A®	X	X	X	X
CIRS 610®	X	X	X	X
Universal Medical®	X			X
Catphan®	X	X	X	X
Universal phantom	**X**	**X**	**X**	**X**

From the results in Tables 3.1, 3.2, 3.3 and 3.5 it may be concluded that the universal phantom could typically measure the same image quality assessment parameters as the commercially available phantoms. In some instances measurements are less elegant and accurate than the commercially available options, as discussed in Chapter 5, but overall the requirements for commissioning of x-ray units, i.e. setting baseline

values, and for routine image QC are satisfied. The outstanding advantage of the universal phantom remains the fact that it offers a single solution phantom covering the full range of x-ray modalities as applied within Diagnostic Radiology.

Chapter 4

Design and development of the universal image quality assurance phantom

Image quality parameters that should be investigated for comprehensive image quality assurance in general x-rays, fluoroscopy, mammography and CT scanning were identified from literature sources as discussed in Chapter 3. These were tabulated in Tables 3.1, 3.2, 3.3 and 3.5 and include sensitometry determination (grey scale linearity or CT number consistency), low contrast detectability, image uniformity, resolution, noise, position and alignment checks, geometry and distance measurements, presence of artefacts, field size or x-to-light field coincidence, standard signal and high contrast resolution. For mammography masses, fibres and micro-calcifications should be considered as well as CT slice thickness in CT scanning. Apart from being able to test all of these parameters, the universal image quality assessment phantom should firstly be of a single unique structure and not a combination of already existing phantoms, secondly be small enough for ease of handling but also large enough to accommodate all the required image quality assessment inserts and thirdly cheap to manufacture and easy to use. The phantom is intended to fill an identified gap in the existing market, as described in Chapter 1, and not to replace any of the commercially available phantoms, with emphasis on cost, man power and expertise and time constraint limitations in resource limited institutions. The design and development of the phantom were based on these requirements. As this study faced a practical problem, requiring a practical approach to finding a solution, experimental iterative derivation of the final phantom was appropriate.

4.1 Initial concepts

The phantom was developed from first principles to be a proper image quality assurance tool based on an extensive literature review of image quality assurance, testing and commercially available phantoms, consultation with medical physicists and

engineers and through experimentation. The process will be discussed in the following sections.

4.1.1 Initial design

The initial concept for the universal image quality assurance phantom is illustrated in Figure 4.1. At the time of the first design, insert and phantom dimensions had not been determined. For planar imaging resolution a bar phantom (1) was included, with its surface perpendicular to the x-ray beam. A small metallic plate (4) was used to calculate MTF from ESF in planar imaging. A small central bead (5) was used to calculate MTF from PSF for resolution in CT scanning. The central bead was also used for set up, i.e. it was perfectly central in the phantom in all dimensions and should therefore be seen on the 0-slice CT scan position and in the centre of a planar image. Spherical inserts were suggested to make use of spherical symmetry, when the phantom was upright (as in Figure 4.1 a.)) for CT scanning and placed flat (as in Figure 4.1 b.)) for planar imaging. Inserts made from materials with different densities (2) were used to assess sensitometry. In CT scanning this is CT number consistency. Another set of inserts, made from the same material but with different radii (3), were used to visually assess low contrast detectability or contrast resolution. These spherical inserts were used in CT scanning and planar imaging. For positioning in CT scanning, a flat side was suggested (as in Figure 4.1 a.)), that would allow the phantom to remain upright without support. The inserts were arranged in different layers to prevent metal or streak artefacts from the bar phantom and metal plate on the spherical insert images during CT scanning.

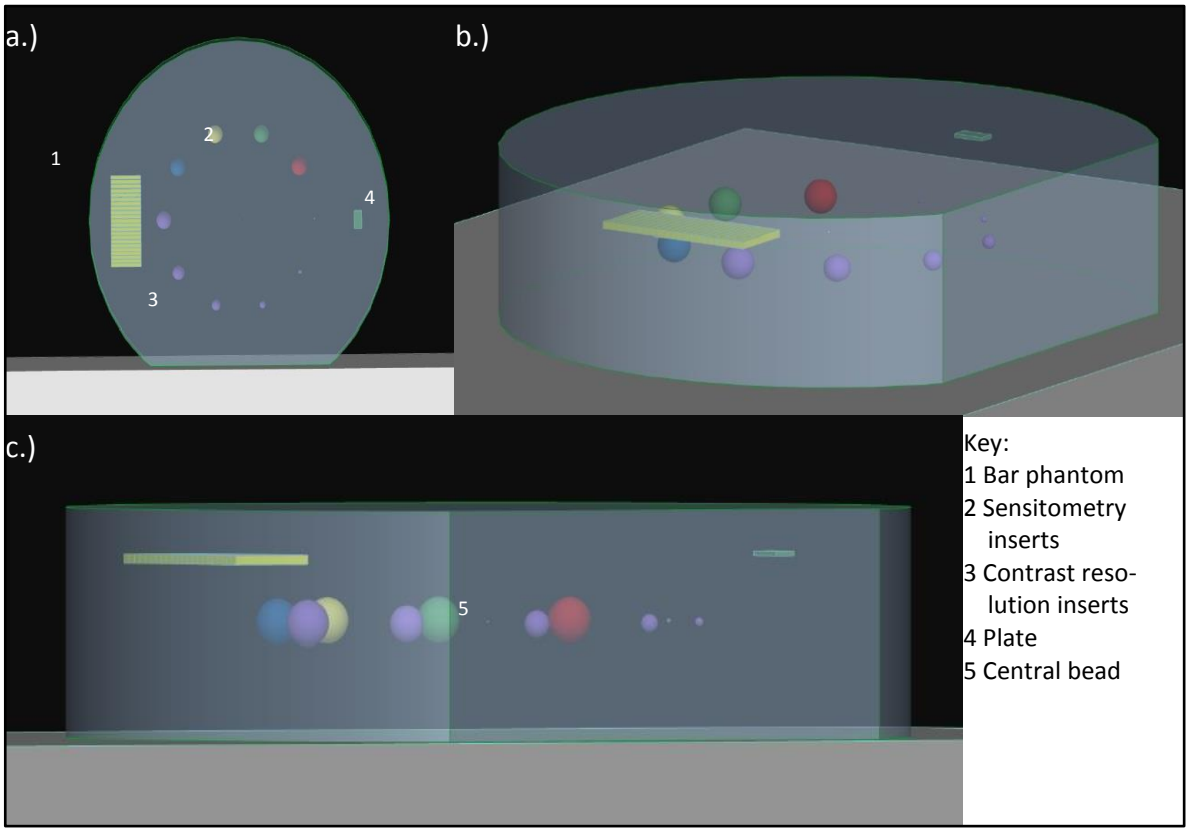

Figure 4.1: Initial universal phantom concept. a.) Set up for CT scanning. b.) Set up for planar imaging. c.) Lateral view showing inserts in different layers.

With reference to Figure 4.1, in general x-rays, fluoroscopy and mammography, i.e. planar imaging, low contrast resolution was assessed with the circular sphere arrangement (3). These spheres were also used to assess masses in mammography. Grey scale linearity was assessed with the spheres of the same size but made from different materials. The MTF was calculated from the central bead (5) PSF and from the ESF of the metal plate (4). High contrast resolution was determined with the bar phantom (1). It was assumed that the bar phantom will additionally be used as fiber analysis tool in mammography. SNRs, CNRs and image uniformity were calculated with the semi-automatic data analysis software, as explained in Chapter 6. Cross wire centering was checked with the bead (5) that was placed exactly centrally, using the scribe lines on the phantom. The bead was also used as micro-calcification assessment tool for mammography. The image quality assurance parameters for CT scanning evaluated with the proposed phantom were low contrast resolution (with circular sphere arrangement) (3), CT-number linearity (with circular sphere arrangement) (2), MTF from PSF of central bead (5), SNR, CNR and uniformity calculation with the semi-automatic data analysis software, 0-slice position (with

centrally placed bead) (5) and checking room lasers used for patient positioning, using scribe lines on the phantom that correspond to the central bead. Further development of the initial concept was necessary, with consideration given to insert sizes and possible materials.

Diagnostic radiology CT scanner table tops are concavely shaped to accommodate the patient. The phantom was adjusted to be a disk with a suitable stand to allow positioning of the phantom in the upright position for CT scanning. The physical and geometrical properties of the different imaging modalities were considered. For CT scanning, the phantom was in an upright position with an acceptable diameter. For planar imaging the phantom was positioned lying flat and with a suitable thickness. Additionally, the diameter was limited by mammography bucky size. For CT scanning the inserts were placed in a circular pattern when the phantom was placed upright on the couch. These inserts should not overlap the planar imaging inserts when the phantom was placed flat. A circular arrangement of spheres was used for low contrast detectability and sensitometry assessment.

Spherical symmetry allowed for the phantom to be used in upright CT and flat planar imaging orientations. However, the machining of perfect spheres was difficult, especially at the small sizes needed, and also very expensive. It was also anticipated that the attenuation of an x-ray beam through a sphere was non-uniform and will result in an image with intensity or grey scale increasing radially outwards from the centre of the object. ROI analysis will therefore consider a ROI in a non-uniform object. To overcome this, the object size must be increased substantially, in order to have a ROI of acceptable size in a uniform region of the object. This is illustrated in Figure 4.2, showing an x-ray image of a golf ball.

Figure 4.2: X-ray image of a golf ball.

For these reasons, i.e. cost, ease of machinability and non-uniform attenuation, the concept of spherical symmetry was abandoned and cuboids were recommended.

4.1.2 Second design

The initial concept was further developed, now employing cubic inserts, and consideration was given to suitable sizes and materials. Tissue equivalence for phantom inserts was extensively researched in the principal investigator's MScMedSc (Medical Physics) dissertation.[72,73] However, as the primary focus of this study was image quality phantom assessment only, tissue equivalence was not important. The adjusted concept is shown in Figure 4.3. In general, the phantom would be circular in planar view with 200 mm diameter and 40 mm thickness. It would be constructed of suitable strength polystyrene or a hard plastic as in Table 4.1. The phantom housing could also be 3-D printed. Printing plastic options are included in Table 4.1.

Table 4.1: Possible phantom housing materials.

Material	Density (gcm^{-3})
Polystyrene	1.05 [74]
Perspex	1.18 [74]
High density polyethylene	0.95 [75]
3-D printing materials	
Acylonitrile Butadiene Styrene (ABS)	1.01 [76]
Hips	1.04 [76]
Poly Lactic Acid (PLA)	1.25 [76]

The inserts for grey scale or CT-number linearity evaluation and low contrast detectability are cuboids, arranged with a face perfectly perpendicular to the phantom top surface for planar imaging and a face perfectly perpendicular to the x-ray beam for rotational imaging, i.e. CT scanning. This ensures that the same thickness of material was seen in each view. One 20 mm thick and two 10 mm thick clear plates, made from the phantom housing material, will be supplied additional to the phantom, to be used with the phantom for automatic exposure control (AEC) and artefact evaluation.

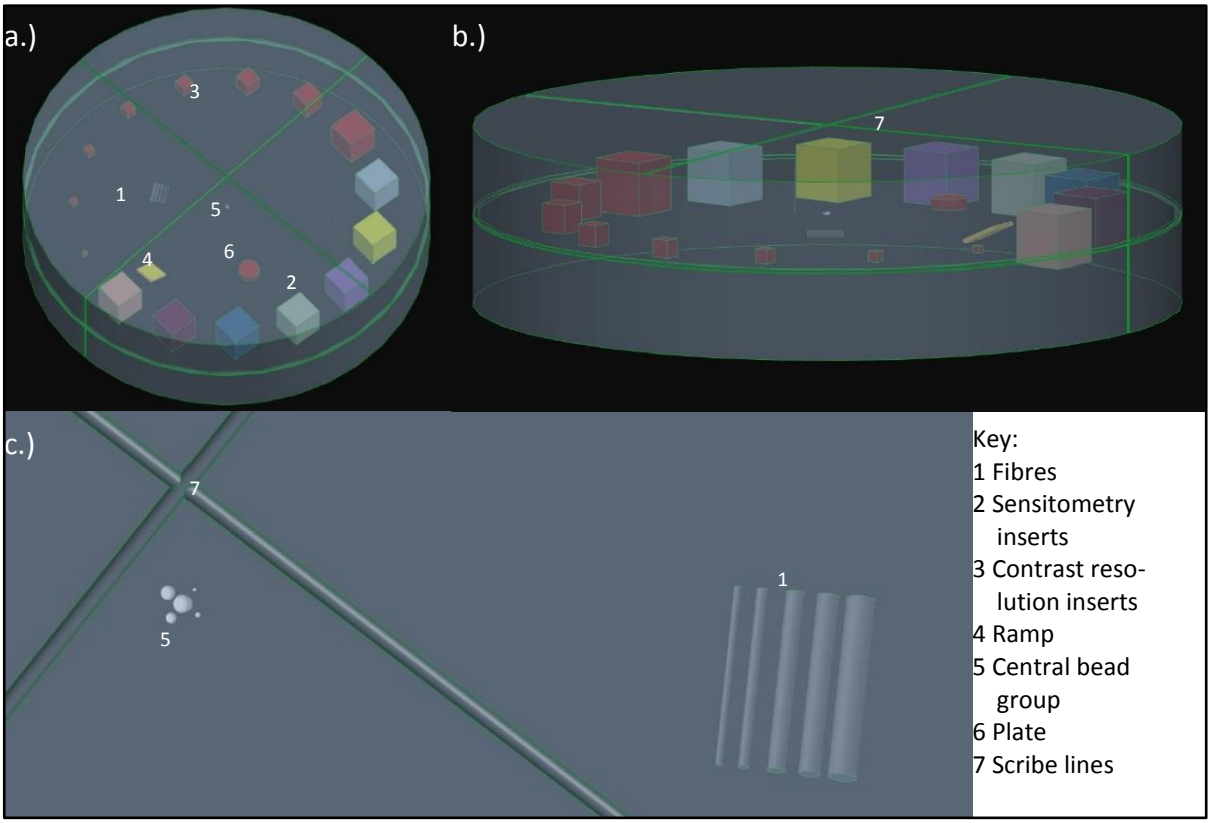

Figure 4.3: Developed universal image quality assurance phantom concept. a.) Perspective showing different inserts. b.) Perspective showing inserts centred in one plane. c.) Zoomed in image of central bead group and fibres.

For low contrast detectability, cubic inserts (3) made from the same material, but with different thicknesses were decided on. Possible materials are included in Table 4.2.

Table 4.2: Possible low contrast detectability materials

Material	Density (gcm^{-3})
Polystyrene	1.05 [74]
Perspex	1.18 [74]
Nylon	1.15 [74]

Seven of these low contrast inserts were used with proposed thicknesses of 2, 3, 4, 6, 8, 10, 20 mm. These sizes corresponded to recommendations in literature and would finally be based on machinability and cost. These cubes were also used to visually inspect masses in mammography imaging.

For grey scale or CT-number linearity seven inserts of a single thickness of 20 mm, but of different materials, were utilized, (2) in Figure 4.3. Proposed materials are included in Table 4.3. All the cubic inserts were arranged along the phantom periphery

Table 4.3: Possible grey scale insert materials.

Material	Density (gcm^{-3})
Acylonitrile Butadiene Styrene (ABS)	1.01 [76]
Hips	1.04 [76]
Poly Lactic Acid (PLA)	1.25 [76]
Polystyrene	1.05 [74]
Perspex	1.18 [74]
Nylon	1.15 [74]
Teflon	2.20 [74]
Gammex SB3 bone tissue equivalent plastic	1.82 [77]
Gammex LN300 lung tissue equivalent plastic	0.30 [77]
Low density polyethylene	0.91 [74]
Gammex solid water	1.05 [77]
Supawood	0.74 *
Air	0.00

* Density as calculated in Appendix C.

A small metallic bead, of 2 mm in diameter, was placed exactly at the center of the phantom, Figure 4.3 (5). Scribe lines (7) were made on the phantom for set-up with lateral and top lasers. Once correctly set-up the scan zero was set at this point. The metallic ball should appear on the central slice, i.e. zero-slice. Position accuracy, zero-slice position and set-up lasers were therefore assessed.

Image uniformity was assessed with ROI analysis with the semi-automatic data analysis software with four ROIs of a specified size at specified different locations in an image. The mean and standard deviation in these ROIs were used to calculate image uniformity, i.e. the values in each of the ROIs must be within a specified percentage of each other. Similarly, the software calculated SNRs and CNRs with Equations 4.1 and 4.2, where S_0 and σ_0 were the mean signal and standard deviation

of the noise of the object of interest and S_B and σ_B were that of the background area in ROIs of the same size inside and right next to the object.

$$SNR = \frac{S_0}{\sigma_0} \quad \text{[Equation 4.1]}$$

$$CNR = \frac{S_0 - S_B}{\sigma_B} \quad \text{[Equation 4.2]}$$

The data analysis software also calculated the MTF from the PSF determined from small metallic balls for evaluation of image resolution. The balls were 1.0, 0.7 and 0.5 mm in diameter, i.e. smaller than the size of a pixel. The software also assessed distance accuracy and geometry by measuring the sizes of certain inserts.

In planar imaging, circular geometry will be assessed with a 20 mm diameter and 3 mm thick plastic insert, made from PMMA, nylon or Teflon, Figure 4.3 (6). The data analysis program will measure the diameter of the imaged circle and compare it to the known diameter.

Images were visually inspected for the presence of artefacts, like streaks, dark or light bands, rings, ghost images, blurring due to motion, lag or residual images from a previous exposure, white specks indicating dead pixels in a digital system and graininess due to quantum mottle.

CT slice width uses a bone equivalent plastic or metal ramp, 20 mm in length, 10 mm wide and 3 mm thick, shown as (4) in Figure 4.3, placed in the phantom at a known angle of 38^o. The slice thickness will be calculated by the data analysis software using the image of the ramp, the known parameters and trigonometry.

Mammography micro-calcifications were simulated with specks of metal, aluminum oxide, calcium carbonate, tungsten or silicon, included at position (5) in Figure 4.3. Suggested diameters ranged between 0.2 and 0.5 mm. Fibrous breast structures were simulated with rubber bands (1) (density of 1.26 gcm^{-3}) (as calculated in Appendix C) or plastic strings, 10 mm in length and between 0.4 and 1.5 mm in

diameter, for example 0.4, 0.6, 0.9, 1.2 and 1.5 mm. Visual inspection was used to determine the smallest inserts visible.

For AEC the image quality as discussed above will be re-evaluated using 40 mm of additional clear attenuator plates, made from the same plastic as the phantom housing material.

3-D printing with different materials was investigated. The results from HIPS and PLA are shown in Figure 4.4. Due to the poor printing resolution these plastics could not be used. The low contrast detectability inserts were accurately 3-D printed from perspex (density of 1.18 gcm^{-3}) and hence high density polyethylene (HDPE) (density of 0.95 gcm^{-3}) was selected as phantom housing material for the prototype.

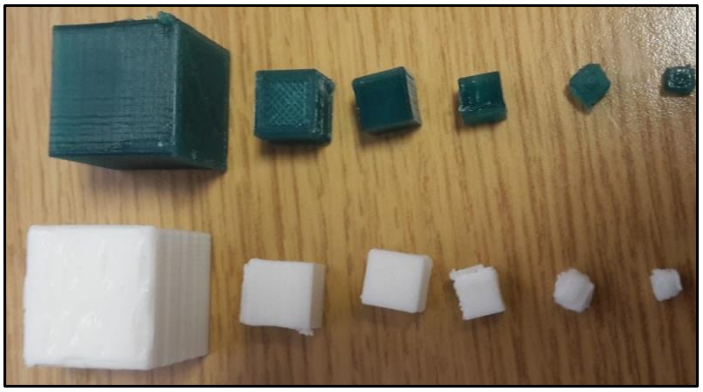

Figure 4.4: 3-D printed PLA (green) and Hips (white) cubes.

4.2 First prototype of the universal phantom

The initial concept was developed and refined into the first working prototype of the universal phantom. The prototype is described in the following sections.

4.2.1 Prototype inserts and materials

The first prototype for the universal image quality assurance phantom is shown diagrammatically in Figure 4.5.

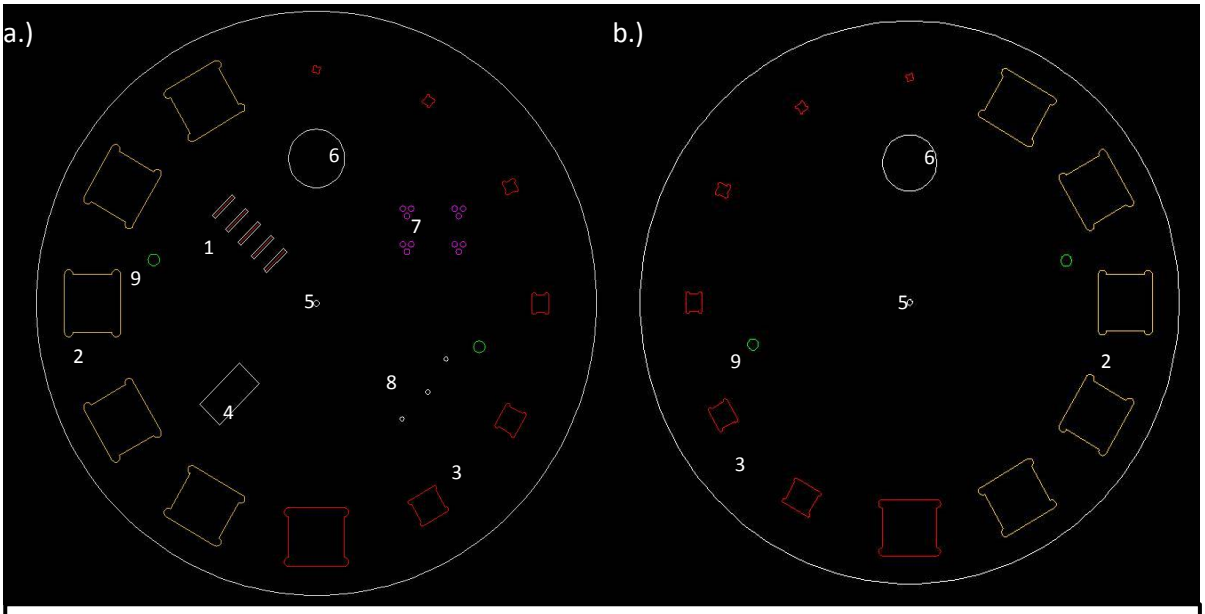

Key: 1 Fibres. 2 Sensitometry inserts. 3 Contrast resolution inserts. 4 Ramp. 5 Central bead. 6 Plate. 7 Micro-calcifications. 8 MTF beads. 9 Distance accuracy holes.

Figure 4.5: Working drawings of the phantom prototype housing. a.) First half of the housing. b.) Mirrored second half of the housing. (created by Gebrateq Advanced Engineering)

The materials and dimensions used in the prototype are indicated in Figure 4.6 with the corresponding densities in Table 4.4. The mammography fibres were made from rubber gasket o-rings that were used in watch manufacturing. The micro-calcifications were small cut offs from wires with the required diameters. The metallic balls used for MTF calculation were the balls from ball point pens.

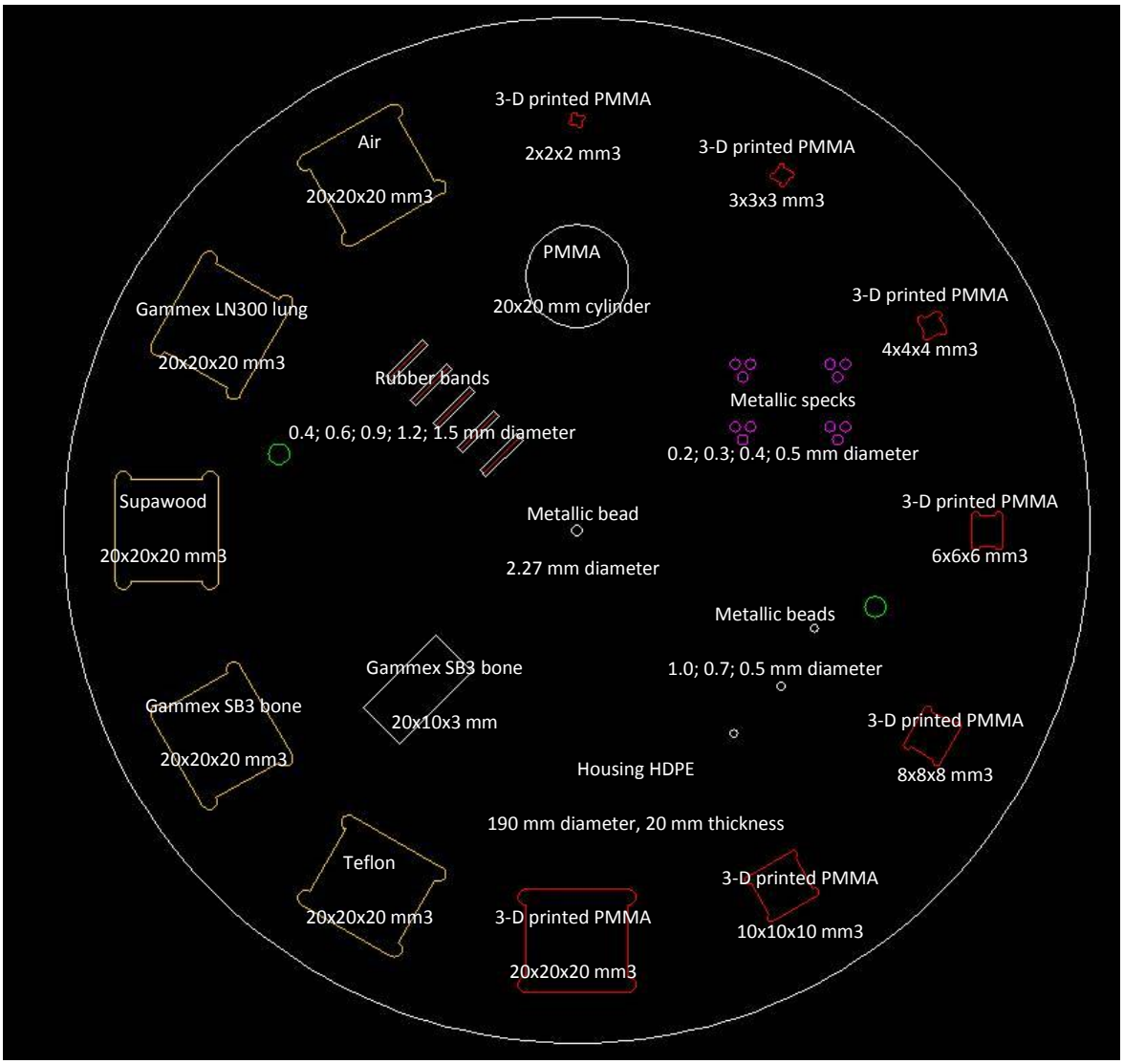

Figure 4.6: Prototype insert materials and layout. (created by Gebrateq Advanced Engineering)

Table 4.4: Prototype insert materials.

Insert	Material	Density (gcm^{-3})
Housing	High density polyethylene (HDPE)	0.95 [75]
Sensitometry	Polymethyl methacrylate (PMMA)	1.18 [74]
Contrast resolution	Teflon	2.20 [74]
	Gammex SB3 bone	1.82 [77]
	Supawood	0.74 *
	Gammex LN300 lung	0.30 [77]
	Air	0.00
Fibres	Rubber	1.26 *
Slice thickness ramp	Gammex SB3 bone	1.82 [77]
Circular geometry cylinder	Polymethyl methacrylate (PMMA)	1.18 [74]
Micro-calcifications	Metal	Not known
MTF beads	Metal	Not known

* As calculated in Appendix C

4.2.2 Prototype machining and manufacturing

The machining of the two halves of the phantom housing is illustrated in Figure 4.7.

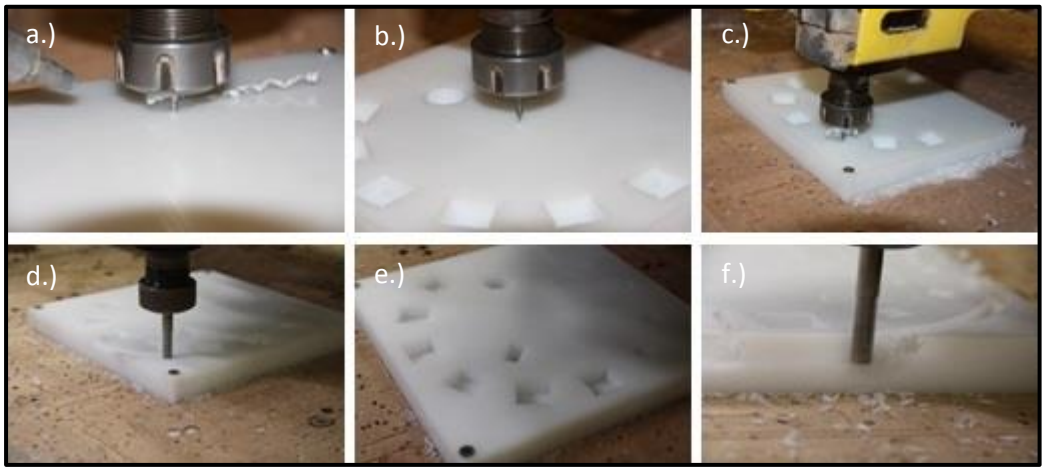

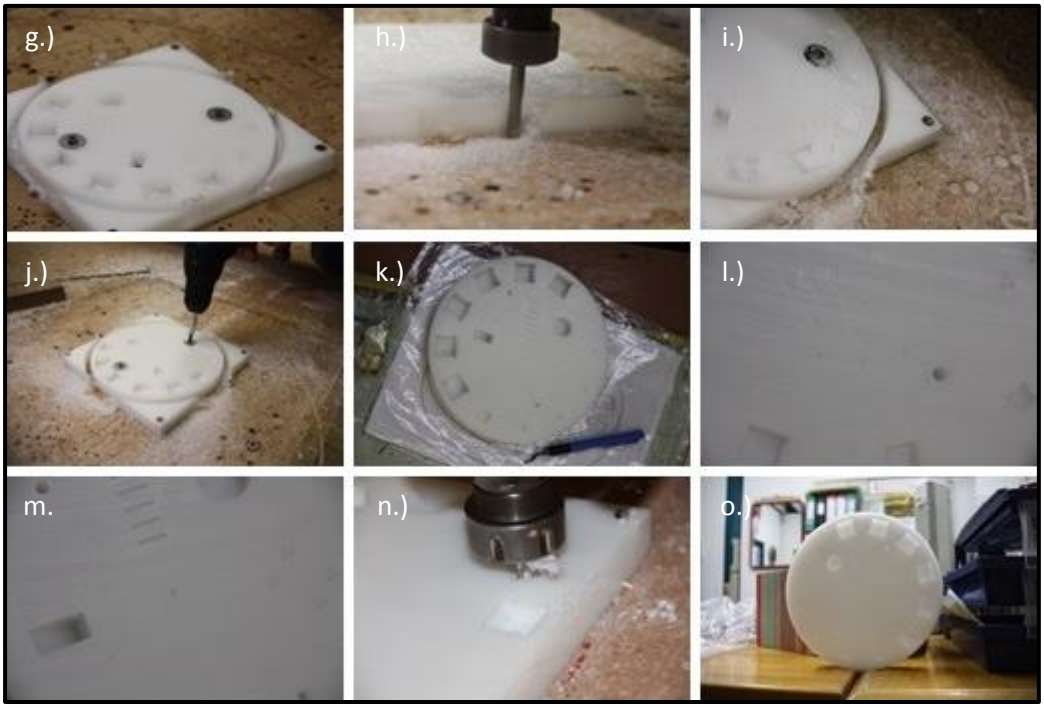

Figure 4.7: Machining of the phantom housing. a.) The cutter is kept cool using high pressure air. b-d.) The voids are machined in the bottom half of the phantom housing. e.) The bottom half of the phantom housing. f-j.) The circular housing was cut from the square HDPE slab. k.) The finished bottom half of the phantom housing. l-m.) Close-up views of the machined voids. n.) Machining the top half of the phantom housing. o.) The finished phantom housing top half.

The prototype housing was constructed from solid slabs of HDPE material. Voids were machined into these slabs at the required depths, with the required dimensions. The machining procedure was programmed using SolidWorks 2015 Premium CAD software. Machining was done on a Multicam 3000 series router machine. This was done with assistance from Johan Braasch of Gebrateq Advanced Engineering. The top half of the prototype was a mirror image of the bottom half, excluding the voids for fibres and micro-calcification simulation, the MTF balls and the slice thickness ramp.

During construction of the prototype it was found difficult to accurately machine a 20 cm diameter phantom housing disk from a 200x200x20 mm^3 HDPE slab. It was decided to use 220x220x20 mm^3 slabs for manufacturing of the final phantom, unless the overall size of the phantom could be reduced. HDPE was also a very soft material, and thus the machining was not completely perfect. Although a logic concept, thought

was not given to fitting size to size before prototype manufacturing. The 3-D printed inserts were measured to be accurate with ± 0.5 mm. All the inserts thus did not fit into exact size voids cut in the housing, e.g. 20.05 mm did not fit into 20.0 mm. The programming for the machining of the voids in the housing was adjusted to be cut 0.1 mm larger with a 2 mm cutter. However, when the 10 mm and 8 mm cubes were fitted it was found that +0.1 mm was too big for the smaller inserts. The programming was adjusted again to +0.05 mm for the remainder of the voids smaller than 20 mm in the bottom half and for the entire top half. However, when the 6 mm cube was fitted at +0.05 mm it was a loose fit. It was decided to adjust the programming to +0.1 mm for all 20x20x20 mm^3, 10x10x10 mm^3 and 8x8x8 mm^3 cubes and to leave it at size-to-size for all the smaller inserts.

The central ball was measured with a vernier calliper to be 2.27 mm in diameter and the programming for machining the hole for the ball in the housing halves was adjusted for this, i.e. 2.36 mm diameter hole. For micro-calcification simulation, the design was adapted to have 3 small voids per metallic speck size to allow a speck to be placed in every hole, instead of three specks per hole which would be difficult to place accurately. Once all the voids were machined the circular housing had to be cut from the square block, as in Figure 4.7 f-j.). For this the circular housing was held down in a secure manner to prevent movement during machining, which would lead to a non-circular finish. Two drill holes, 4 mm in diameter, were added at 60 mm from the central bead to screw the HDPE plate into position.

The rate of machining was very important. Cutting too fast or too deep would damage the cutter and cutting too slow would melt the plastic. Machining was therefore done in a layer by layer manner, as shown in Figure 4.7 f). It was also important to keep the cutter cool with high pressure air during machining, as shown in Figure 4.7 a).

The different inserts were then fitted in the phantom housing bottom half as shown in Figure 4.8. Cartel super glue was used to secure the inserts in place.

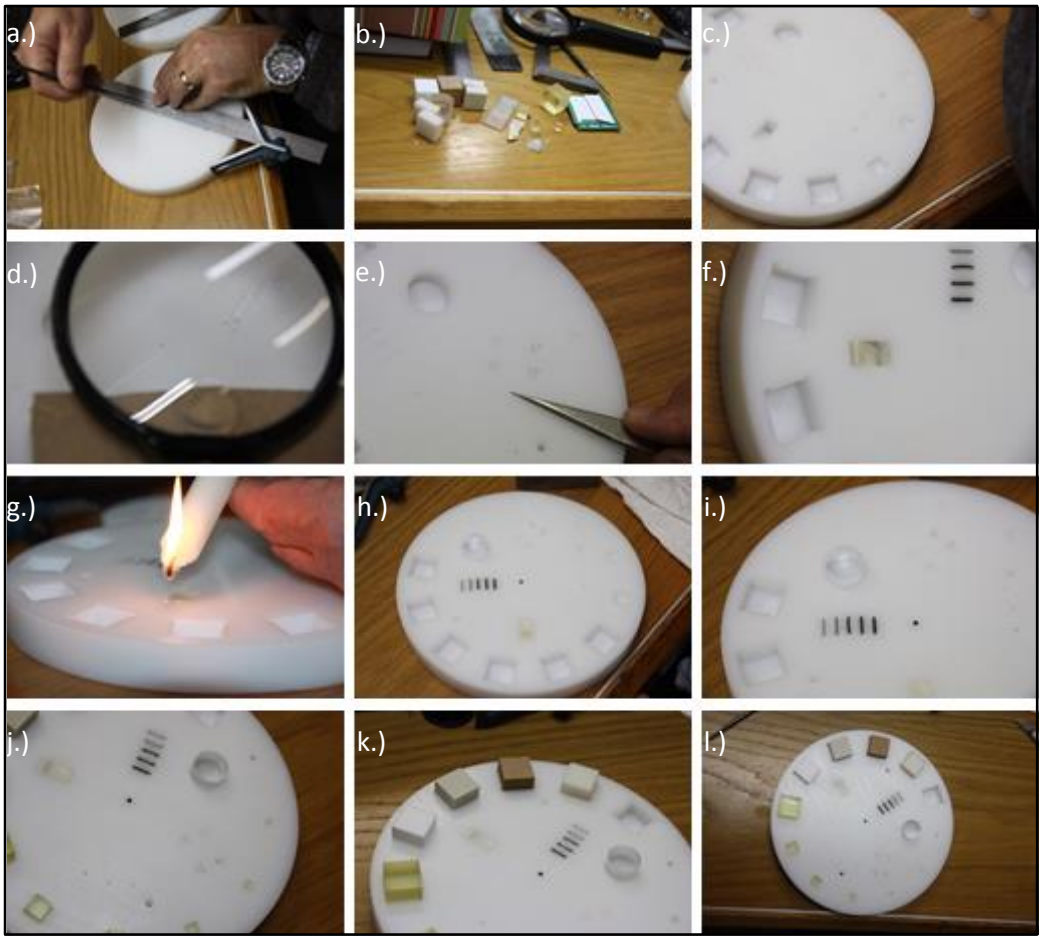

Figure 4.8: Positioning the inserts in the phantom housing. a.) Adding the scribe lines. b.) The different inserts to be used. c-e.) Placing the micro-calcification specks. f.) Slice thickness ramp in position. g.) Filling the slice thickness ramp void with wax. h-k.) Placing the other inserts. l.) The completed bottom half of the prototype.

The cubic inserts in Figure 4.8 l.) have semi-circle cut outs on the corners. This resulted as round cutters were used to machine cubic holes. These holes were left open, i.e. air filled, but could be filled with wax, with density of 0.93 gcm^{-3}, a density comparable to that of the HDPE housing material. The effect of these gaps filled with air will be investigated with imaging validation of the prototype.

When the two halves were fitted together, a slight rotation of the halves with respect to each other was observed. This misfit was due to inaccurate positioning of the small cubes. Nylon screws were added to the existing screw holes to pull the two halves tightly together. The holes were enlarged to 5 mm diameter and 6 mm diameter screws were used. The position of these holes should be changed in future to be

closer to the small cubic inserts, as the largest misfit effect was seen in that position. Countersunk screws were also recommended. Future machining should also be done void-by-void, fitting each insert before progressing to the next void. For small inserts, the voids should initially be machined marginally smaller than the insert, extending the size incrementally as needed. Scribe lines were made on the prototype using a centre finder, as in Figure 4.8 a.). It was recommended that scribe lines should be machined in future.

The completed first prototype is shown in Figure 4.9. The prototype weighed 1.14 kg.

Figure 4.9: First prototype of the universal image quality assurance phantom.

4.2.3 Initial prototype imaging and evaluation

The first prototype, in Figure 4.9 above, was imaged at Winelands Radiology, Vergelegen Medi Clinic, Somerset West, South Africa. Figure 4.10 shows the obtained images.

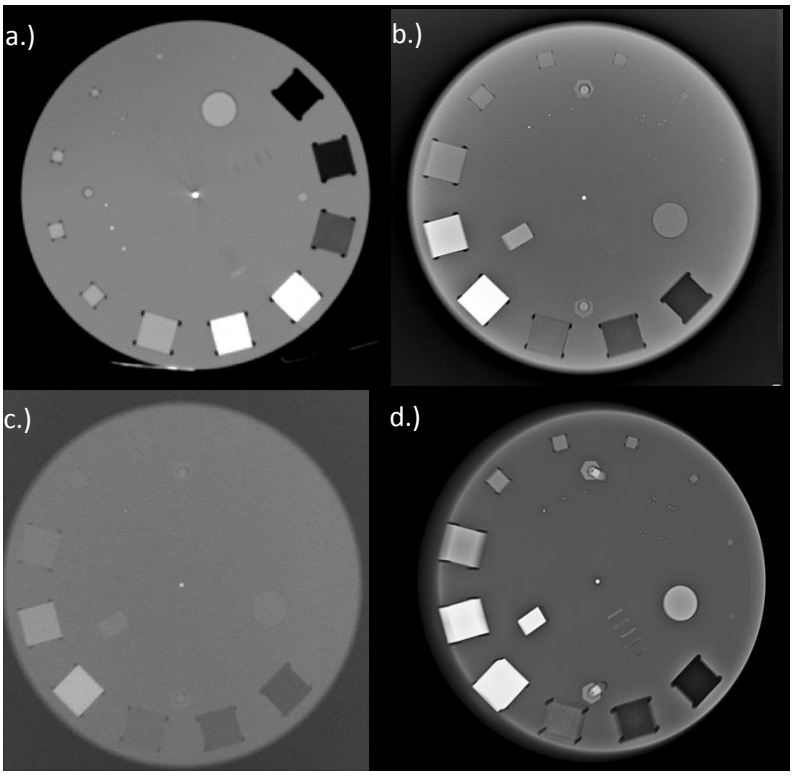

Figure 4.10: First images of the first universal image quality assurance phantom prototype. a.) CT scan. b.) General x-ray. c.) Fluoroscopic image. d.) Mammogram.

The parameters used for obtaining the images in Figure 4.10 are tabulated in Table 4.5.

Table 4.5: First prototype imaging parameters.

Modality	Unit	kV	mAs	Additional
CT scan	Siemens Somatom Definition Edge scanner	120 kV	298 mAs	5 mm slices, 235 cm FOV, J30s median smooth filter and pitch of 0.8
General x-ray	Siemens Ysio DR unit	40 kVp	2 mAs	100 cm SID, large focus outside of bucky
Fluoroscopy image	Siemens Axiom Luminos DRF unit	62.5 kV	10.2 mA and 0.01 ms	
Mammogram	Siemens Mammomat Inspiration unit	28 kV	62.1 mAs	AEC (the standard for image quality assurance in the department)

From these initial images, future development and changes were recognised. These were confirmed with validation of the prototype, as discussed in section 4.3 below. With the CT scan the artefact from the central bead can be lessened if a smaller bead was used, which would still be acceptable for the other imaging modalities too, as seen in Figure 4.10 a-d.). A 1 mm diameter bead was proposed. A smaller diameter fibre group, 0.3 mm diameter, should be added for mammography. A smaller speck group was also proposed, i.e. cuttings from a 0.1 mm diameter wire. The cuttings should also be made smaller as to represent specks better. The overall size of the phantom could be reduced. From Figure 4.10 d.) above it was seen that the peripheral low contrast resolution or mammography mass cubes could be positioned closer to each other, hence reducing the diameter of the phantom. This will make the phantom more manageable, easier to handle, lighter (for transport or courier cost purposes) and slightly cheaper to manufacture. A 1x1x1 mm^3 3-D printed PMMA cube should be added to the phantom for low contrast detectability in all imaging modalities and as additional mass for mammography. In all images the effect of the air filled semi-

circular voids at the corners of the cubic inserts was negligible and hence wax filling was not necessary.

The orientation of the slice thickness ramp needed further investigation. Slice thickness can be calculated with Equation 4.3, as explained in Figure 4.11, using trigonometry.

$$Slice\ thickness = \frac{Ramp\ measurement}{\tan\theta} \qquad \text{[Equation 4.3]}$$

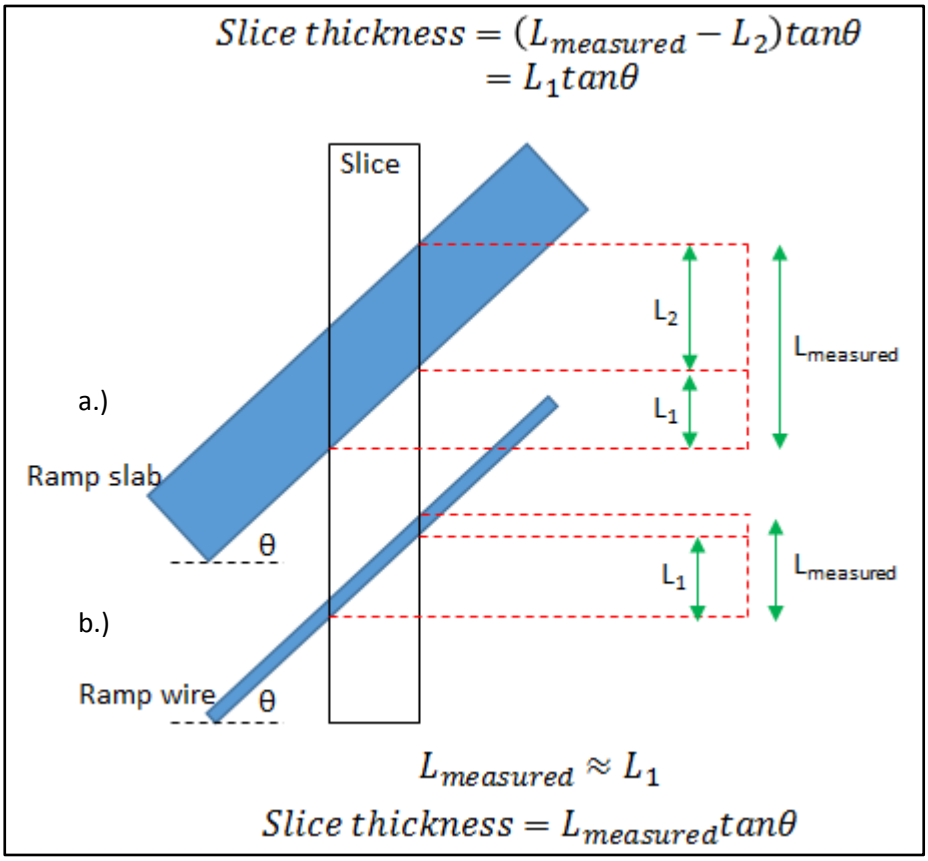

Figure 4.11: Slice thickness calculation for a.) a ramp made of a slab (as in the universal image quality assurance phantom) and b.) a wire ramp.

In the prototype a slice thickness slab, 20x10x3 mm^3, was used instead of a wire, with 3 mm the thickness of the slab. It was inserted in the phantom at an angle of 38°. Due to the finite thickness of the ramp, a correction is needed for the thickness in the calculation in Equation 4.3 above. This is illustrated in Figure 4.11. For a ramp with a significantly small thickness, as in Figure 4.11 b.), such a correction is not needed and the reconstructed image measured can be used directly in the calculation of slice thickness with good approximation. With the universal image quality assurance phantom it was found that slice thickness does not have to be calculated, it can be measured directly from the obtained image, as in Figure 4.12. This was due to two errors cancelling out, i.e. the tan of 38 degrees and the thickness, L_2, of the ramp.

Ideally the ramp should be constructed of a gold sheet with micro-meter thickness at an angle of 45° (where $\tan 45 = 1$). For such an ideal ramp, the reconstructed displayed image would represent an almost exact measurement of the slice thickness without any required correction for slab thickness or angle. However, the thickness of 3 mm was a machining limitation. For a thinner slab the manufacturing costs will increase significantly. As cost reduction was one of the main aims of this study, and the current slice thickness assessment slab performed its function satisfactory, the design was not adjusted to include a thinner ramp.

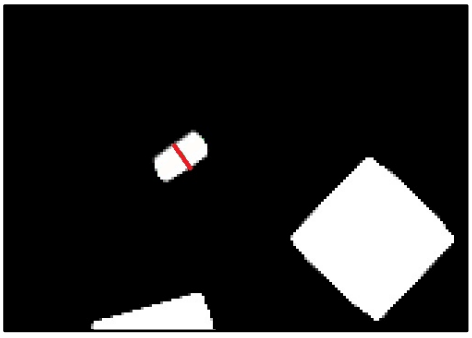

Figure 4.12: Slice thickness is measured in the red line direction in the universal image quality assurance phantom and prototype.

It was necessary to determine what exactly was measured by the slice thickness parameter in the prototype, i.e. the actual scan slice thickness or the reconstructed slice thickness. After a scan has been performed, the scanner software allows the user to reconstruct the actual scan into slices of a thickness selected by the user. This is referred to as the reconstructed slice thickness. It is therefore possible to reconstruct a scan performed with 3 mm slices into a data set consisting of 5 mm slices. Scans were done by scanning in 3 mm and 5 mm slices. The 3 mm scan was also reconstructed to 5 mm slice thickness. The obtained images were analysed in ImageJ software. The window width (WW) was set as low as possible and the window level (WL) was adjusted until the slice thickness ramp just disappeared. This WL value was recorded as the maximum value. Background was measured in a ROI next to the ramp and was subtracted from the maximum WL value. The WL value at 50 % of the background corrected peak value, background was added to the result and the WL was adjusted to this setting. This method is proposed in the Catphan® manual.[78] The slice thickness was measured in the direction indicated in Figure 4.12, with the obtained results in Table 4.6.

Table 4.6: Prototype slice thickness measurements.

Scanning slice thickness	Reconstructed slice thickness	Measured slice thickness
3 mm	3 mm	2.997 mm
3 mm	5 mm	5.713 mm
5 mm	5 mm	5.062 mm

It is suggested that the slice thickness measurement will be performed by the semi-automatic data analysis software.

4.3 Validation of the first prototype of the universal phantom

The prototype was compared to commercially available phantoms that were used for routine quality assurance in x-ray diagnostic radiology. The phantoms selected for this comparison are commonly used in diagnostic radiology quality assurance in South Africa. Included were the NORMI® 13 for general x-rays, NORMI® Rad/Flu for

fluoroscopy, NORMI® PAS for mammography and Catphan® 600 for CT scanning. The phantoms were supplied by Netcare and are shown, with the universal image quality assurance phantom prototype, in Figure 4.13.

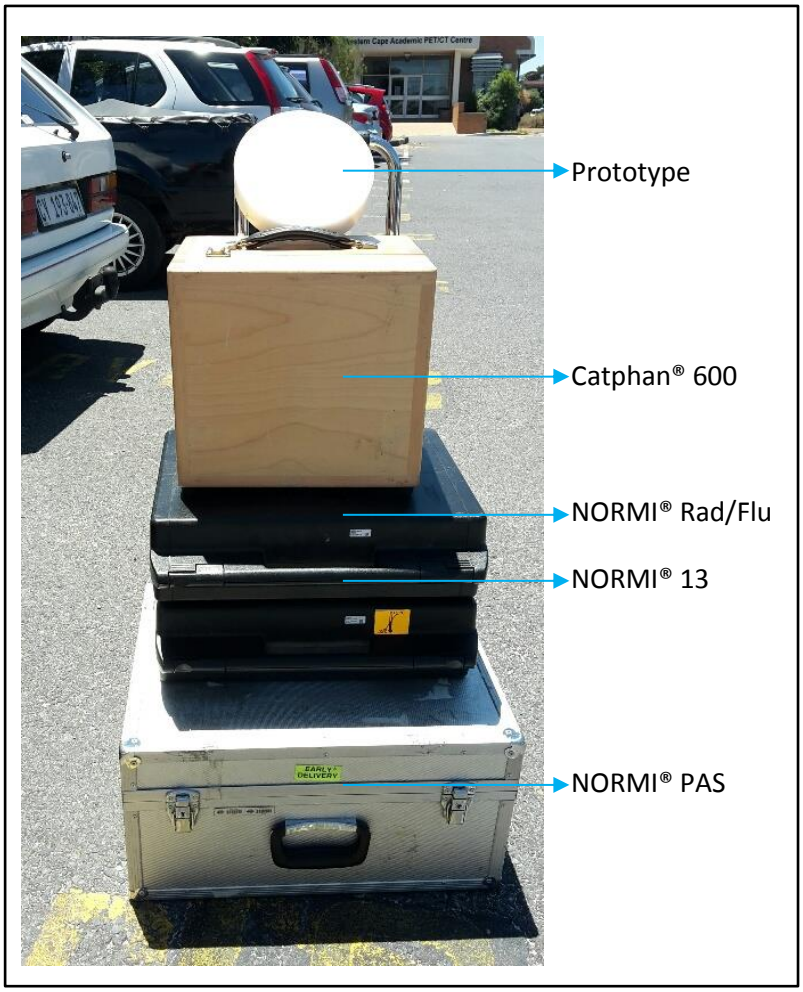

Figure 4.13: The universal image quality assurance phantom prototype with the commercial phantoms used for prototype validation.

The aim of this pilot study was to determine if the prototype was acceptable for routine image quality assurance, i.e. would the phantom be able to measure the image quality parameters assessed with commercial phantoms, and to derive the changes and improvements required for construction of the final phantom.

4.3.1 General x-ray imaging validation

For general x-ray imaging, the prototype was compared to the NORMI® 13 phantom. This phantom was described in Chapter 3 section 3.1.3. Two Philips Bucky Diagnost units were used with Fujifilm FCR IP Cassette Type CC. Exposures were made with manual and AEC settings, as in Table 4.7 and the obtained images are shown in Figure 4.14.

Table 4.7: General x-ray exposure parameters.

Unit	Technique	kV	mAs	FFD	Focus	Figure 4.14
1	Manual	70	40	100 cm	Large	a.) NORMI b.) Prototype
	AEC	70	8.06 NORMI 0.78 Prototype	100 cm	Large	c.) NORMI d.) Prototype
2	Manual	70	40	100 cm	Large	e.) NORMI f.) Prototype
	AEC	70	6.26 NORMI 0.85 Prototype	100 cm	Large	g.) NORMI h.) Prototype

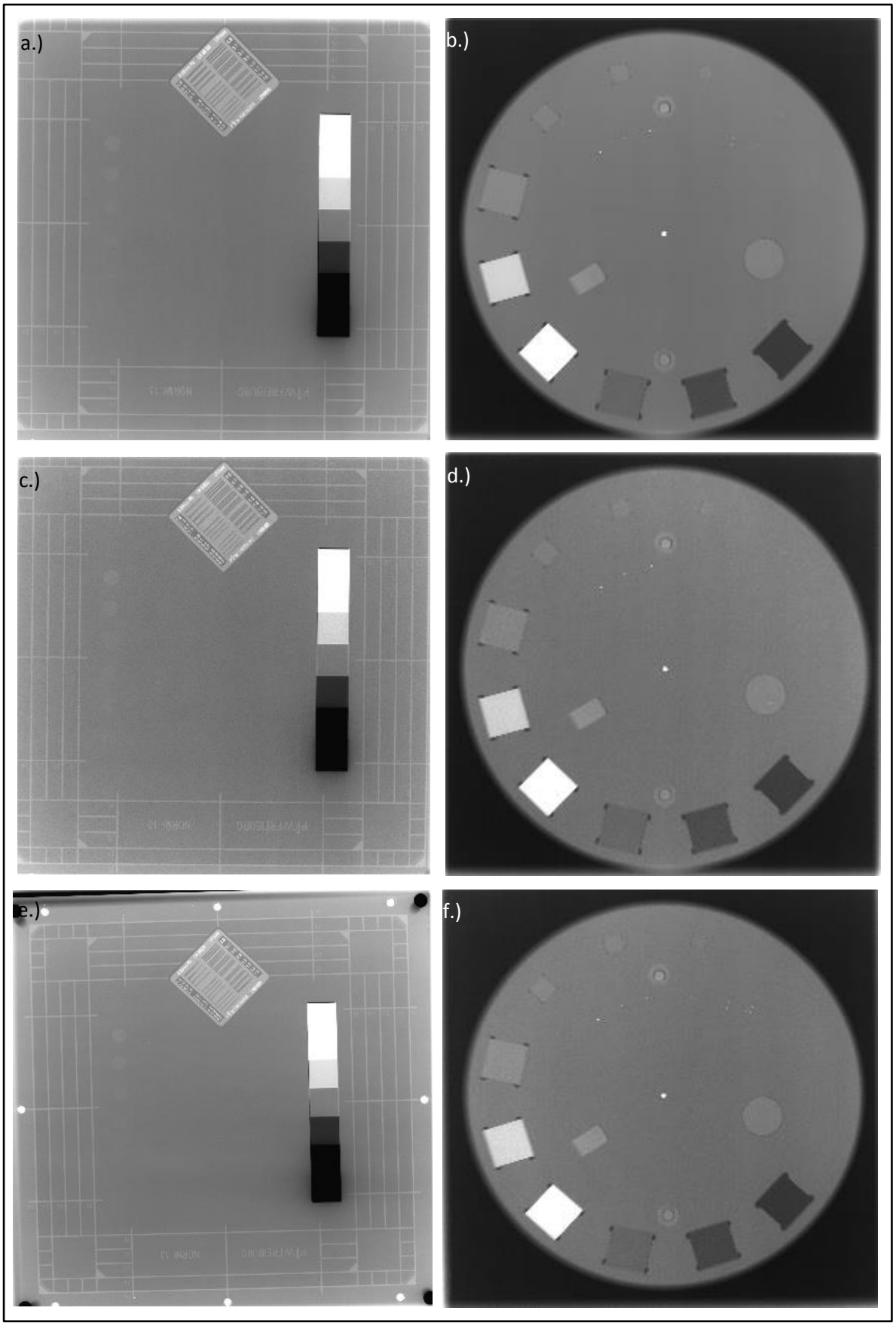

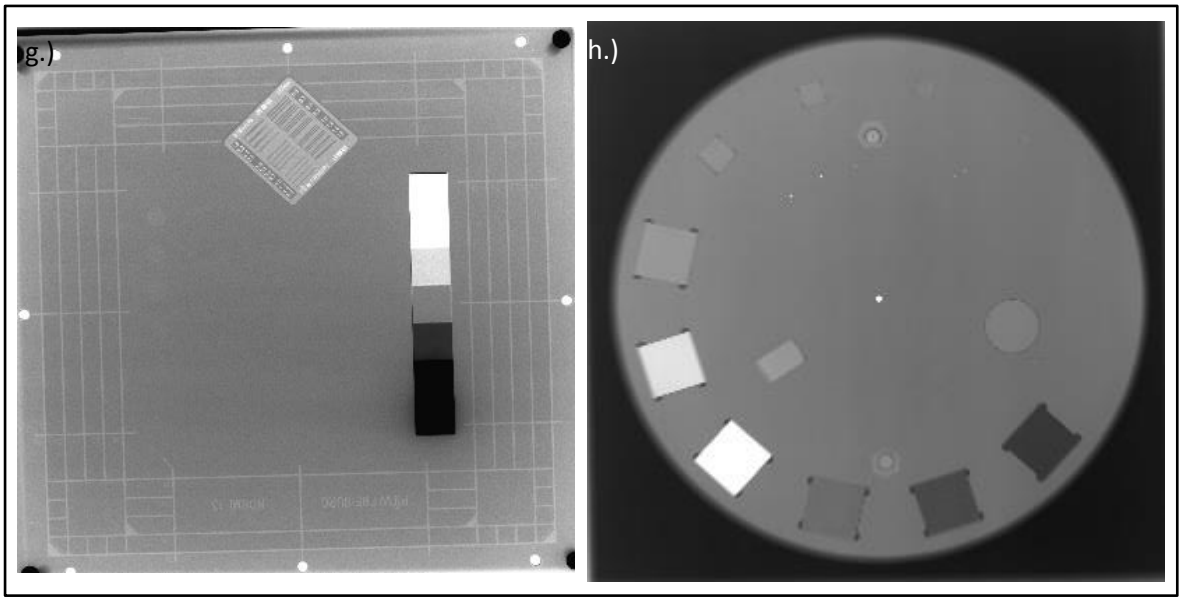

Figure 4.14: Comparison of prototype to NORMI® 13 phantom with general x-ray imaging parameters as in Table 4.7. a,e.) Manual exposures of NORMI® 13 phantom. b,f.) Manual exposures of prototype. c,g.) AEC exposures of NORMI® 13 phantom. d,h.) AEC exposures of prototype.

The mAs values in Table 4.7 were low for the prototype as the prototype was only 4 cm in thickness and not representative of patient thickness. For this additional 4 cm attenuation plates will be included. From Figure 4.14 the conclusions in Chapter 4 section 4.2 were confirmed. A smaller 1x1x1 mm^3 low contrast detectability insert should be added in the final design to make the proposed phantom more sensitive. The central bead should be made smaller, 1 mm diameter, for a neater appearance. The prototype performed all the required image quality assurance tests verified with the NORMI® 13 phantom, as seen from Chapter 3 Table 3.1 also. The prototype in addition measured sensitometry, noise and position and alignment. For general x-ray imaging the prototype was hence an acceptable solution for comprehensive image quality assurance.

4.3.2 Fluoroscopy imaging validation

The NORMI® Rad/Flu phantom, as discussed in Chapter 3 section 3.2.3, was used for comparison in fluoroscopy. A Superix 164 Tecmed 3000 unit was used with an AEC exposure. The resultant parameters are shown in Table 4.8 and the obtained images in Figure 4.15.

Table 4.8: Fluoroscopy exposure parameters.

Technique	kV	mA	s	Figure 4.15
AEC	74 NORMI	50	2	a.) NORMI
	45 Prototype	50	2	b.) Prototype

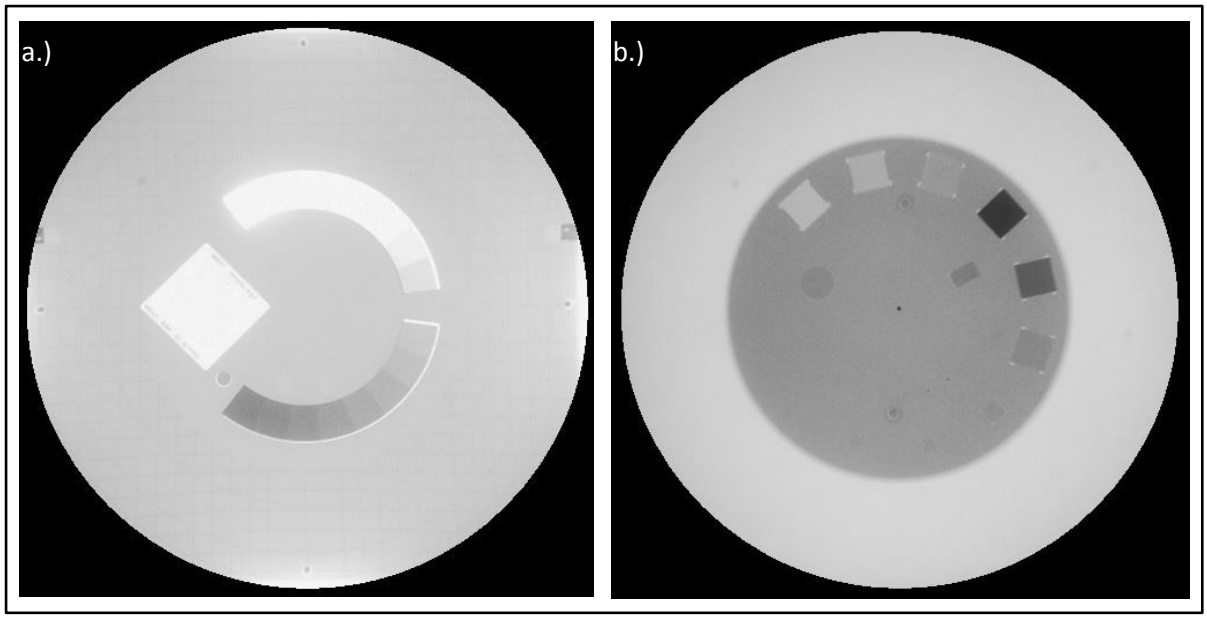

Figure 4.15: Comparison of prototype to NORMI® Rad/Flu phantom with fluoroscopy imaging parameters as in Table 4.7. a.) AEC exposure of NORMI® Rad/Flu phantom. b.) AEC exposure of prototype.

From Figure 4.15 no special additions or changes to the prototype were derived for fluoroscopic imaging and it was concluded that the prototype was an acceptable solution for fluoroscopic image quality assurance. The biggest disadvantage of the NORMI® Rad/Flu phantom was that the insert used for investigation of resolution was separate and needs to be fitted into the phantom prior to exposure. The prototype was a ready-assembled phantom, with all inserts included. From Figure 4.15 and Table 3.2 in Chapter 3 section 3.2.3, it was seen that the prototype assessed at least the same parameters as the NORMI® Rad/Flu phantom.

4.3.3 Mammography imaging validation

The universal image quality assurance phantom prototype was compared to the NORMI® PAS phantom in mammography. The images were acquired with a Siemens Mammomat Inspiration unit with exposure technique factors as in Table 4.9. Figure 4.16 shows the obtained images.

Table 4.9: Mammography exposure parameters.

Technique	kV	mAs	Target/Filter	Focus	Figure 4.16
AEC	28	131.1 NORMI 19.3 Prototype	Mo/Rh	Large	a.) NORMI b.) Prototype
Manual	28	62.9 NORMI 63.1 Prototype	Mo/Rh	Large	c.) NORMI d.) Prototype

The NORMI® PAS phantom is described in Chapter 3 section 3.3.3. The disadvantage of the NORMI® PAS phantom was that different test elements had to be fitted into the structure plate cut out and several exposures were needed for comprehensive image quality assurance. All the inserts of the prototype were contained in the phantom and only one exposure was needed for overall image quality analysis. Although the universal image quality assurance phantom prototype assessed all the parameters measured with the NORMI® PAS phantom, as well as image uniformity and geometry and measurement tools (as in Chapter 3 Table 3.3), certain improvements were derived for final phantom design, as commented in section 4.2.

Suggested improvements included addressing the geometric distortion seen in Figure 4.16. Geometric distortion resulted from the depth dimension of the inserts. This could be addressed by orientating the phantom such that the larger inserts were more perpendicular to the x-ray beam, i.e. at the chest wall side. Proper scribe lines, orientation markers and detailed explanation in the user's manual (Appendix A) would achieve this set-up. The depth dimension of the 20x20x20 mm^3 inserts could be changed to 10 mm, reducing the geometric distortion artefact. For the fibres, scribe lines were made with a 1 mm diameter cutter. This resulted in air trapped around the rubber bands. With construction of the final phantom wax, with density of 0.93 g/cm^3, will be used to fill the air gaps. A smaller diameter rubber band, 0.3 mm, will also be

added. The specks of the different speck groups will be cut more accurately and a smaller group, made from 0.1 mm diameter wire, will also be added. As previously recommended, a 1x1x1 mm^3 low contrast detectability and mammography mass cube should be added. In Table 4.9 the mAs for AEC exposure of the prototype was again low comparted to the NORMI® PAS phantom, as explained in section 4.3.1 due to the prototype not being patient thickness representative. Additional attenuator plates will address this.

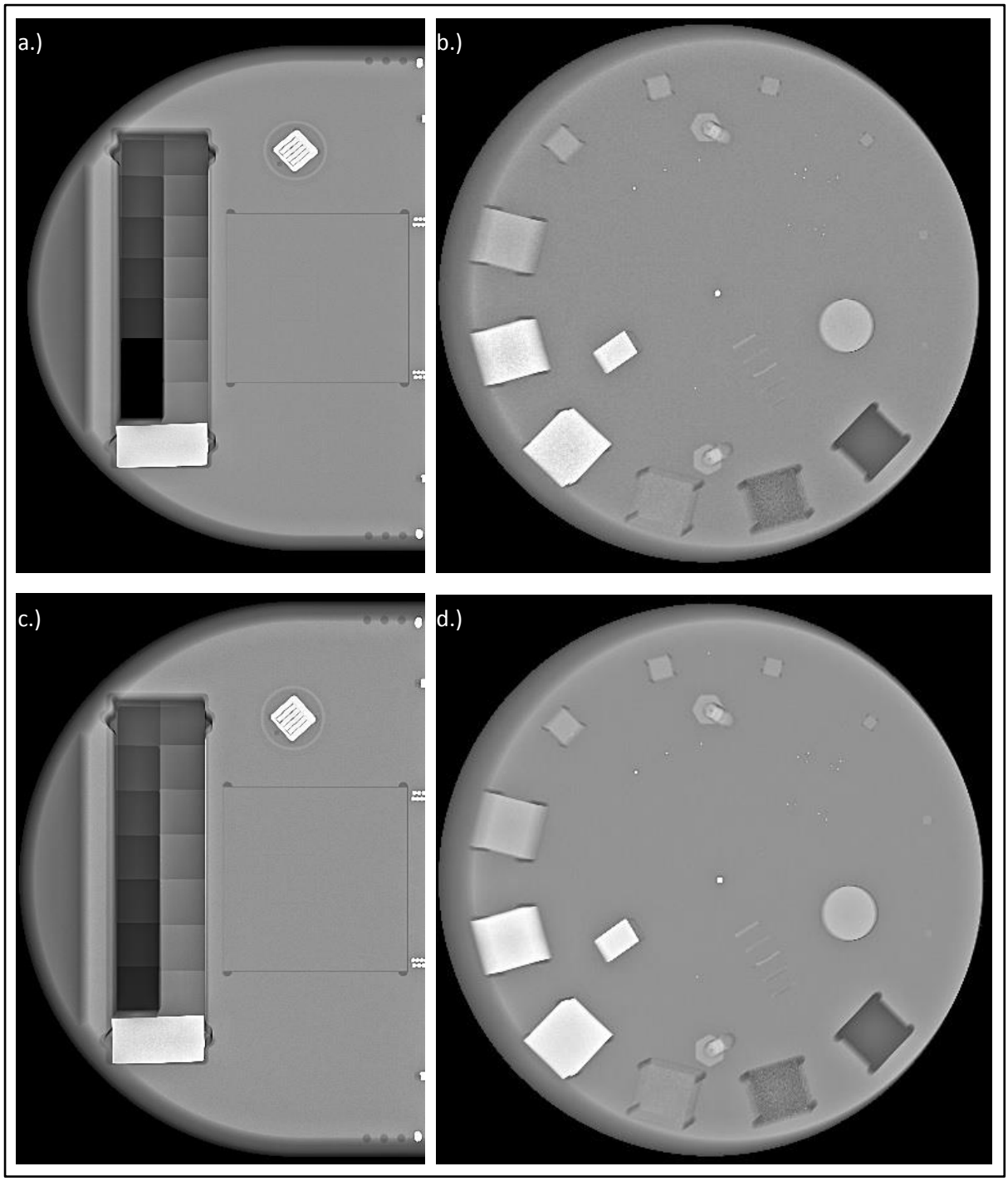

Figure 4.16: Comparison of prototype to NORMI® PAS phantom with mammography imaging parameters as in Table 4.8. a.) AEC and c.) manual exposure of the NORMI® PAS phantom. b.) AEC and d.) manual exposure of the prototype. (created by author)

4.3.4 Computed tomography scanning validation

For CT scanning the universal phantom prototype was compared to the Catphan® 600 phantom. This phantom was described in Chapter 3 section 3.4.3. Scan parameters as in Table 4.10 were used to obtain CT scan study sets of the Catphan® 600 and prototype phantoms, with selected slices included in Figure 4.17. A Toshiba Aquillion 1 helical CT scanner was used.

Table 4.10: CT scanning exposure parameters.

kV	mA	s	FOV	Pitch	Slice thickness	Filter	Figure 4.17
120	300	13.0 Catphan 4.5 Prototype	240	3	5 mm	FC30/ORG	a-e.) Catphan f.) Prototype

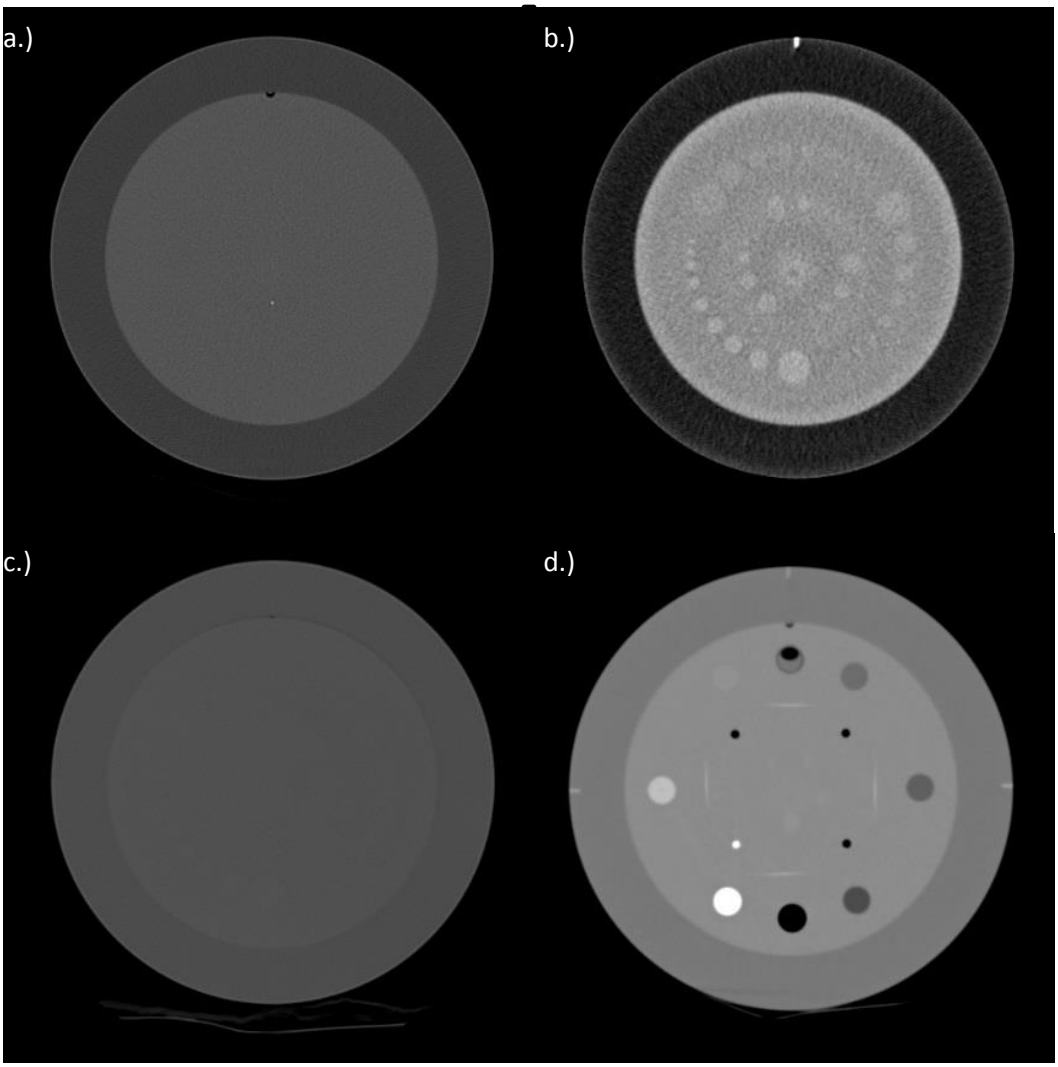

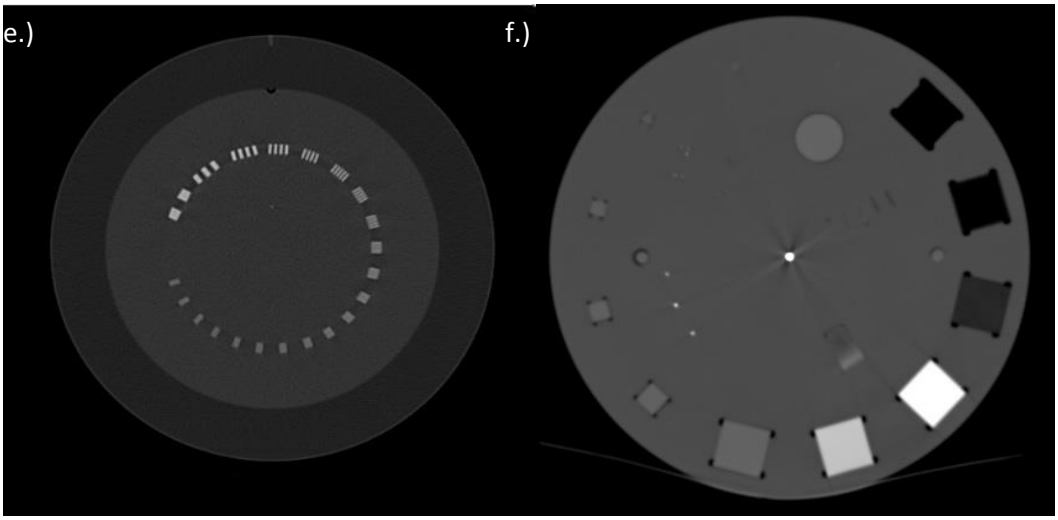

Figure 4.17: Comparison of prototype to Catphan® 600 phantom with CT scanning parameters as in Table 4.9. a.) Bead for MTF calculation. b.) Low contrast supra- and sub-slice inserts. c.) Uniformity module. d.) Slice thickness ramps, sensitometry, distance accuracy and patient alignment check slice. e.) Resolution module. f.) Single slice of prototype with all required inserts.

From Table 3.5 in Chapter 3 section 3.4.3 and from Figure 4.17 it was clear that the Catphan® 600 phantom and the universal image quality assurance phantom prototype could measure all the parameters required for CT image QC. The universal phantom has multi-modality applicability, i.e. not limited to CT scanning only as Catphan® 600 is. In addition, all of the required parameters can be evaluated from a single slice of the universal image quality assurance phantom, where several slices have to be considered for Catphan® 600 as seen from Figure 4.17.

From Figure 4.17 it was concluded that the central bead's diameter should be decreased to reduce streaking metal artefacts. This was in accordance with the recommendations for the planar imaging modalities. As with general x-ray imaging and mammography, also for CT scanning a smaller 1x1x1 mm^3 low contrast resolution insert should be included.

Consideration was now given to the stand for upright CT set-up. It was decided that the easiest, smallest and cheapest solution would be the first design of the initial concept, i.e. making a flat side on the phantom. A plate of HDPE material, 10 mm

thick, 500 mm in length and 50 mm wide, will be supplied as stand, to be fitted across the CT couch, with the phantom placed flat side down on the plate. This is shown in Figure 4.18.

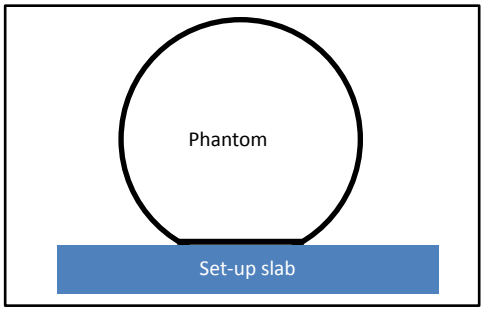

Figure 4.18: CT scanning set-up plate.

Having a flat side on the phantom makes orientation for set-up for CT scanning and for mammography easier, as the flat side is positioned on the chest wall side.

The recommendations derived from Figures 4.14 to 4.17 were implemented in the design of the final universal image quality assurance phantom, as described in section 4.4.

4.4 Final phantom

A descriptive user's manual will be supplied with the phantom, as included in Appendix A. The manual explains in detail how to set up and use the universal phantom for setting baseline values and for routine image quality control. It explains comparing the routine results to the baseline values for the same phantom, states accepted tolerance values and describes the use of the data analysis software.

The user will be required to position and image the phantom, as explained in detail with illustrations and examples in the user's manual, to enable the user to evaluate all images visually and to load images into the data analysis software. The data analysis software will use ROI analysis to measure the mean and standard deviation values for sensitometry, SNR, CNR and uniformity calculations. It will also measure known distances for geometry and scaling evaluation and display the loaded image for the

visual image quality analysis tests, e.g. low contrast detectability. If tests fail, the user should perform further tests or call in a technician or medical physicist, as described in the user's manual. The functioning of the data analysis software is described in Chapter 5 and Appendix B. The user will also have to record these results, as explained in the manual.

The user's manual and data analysis software is used with the final universal image quality assurance phantom for comprehensive routine diagnostic radiology x-ray image quality control. The phantom composition and assembly is described in this section.

4.4.1 Phantom inserts and materials

The changes as derived in section 4.3 were used to improve the design of the phantom. A 1x1x1 mm^3 low contrast resolution cube was suggested from the findings of section 4.3. Accurate 3-D printing at such small scale was only available from the Department of Mechanical and Mechatronic Engineering at Stellenbosch University, using a Stratasys Objet 30 Scholar micro-medical printer and RGD 240 photopolymer material. The low contrast resolution inserts were reprinted and the density of the material was calculated as in Appendix C. Although a 1 mm diameter central bead was suggested, it was not possible to accurately position such a small bead exactly centrally in the phantom in three dimensions. A 2 mm diameter bead was therefore used. The geometrical distortion from the 20 mm thick inserts (sensitometry blocks and circular geometry cylinder) seen in mammography imaging, as in section 4.3.3, was addressed by decreasing the thickness dimension to 10 mm. Also from this section, wax filling of the mammography fiber scribe lines, the addition of a 0.3 mm diameter rubber band as thinnest mammography fiber simulator and adding a 0.1 mm diameter mammography micro-calcification speck group was done in the phantom. Scribe lines were accurately machined onto the phantom top surface and sides and a flat phantom surface was introduced for upright set-up on a CT scanning stand, as in Figure 4.18 above. The materials of the inserts for the phantom are shown in Figure 4.19 and Table 4.11.

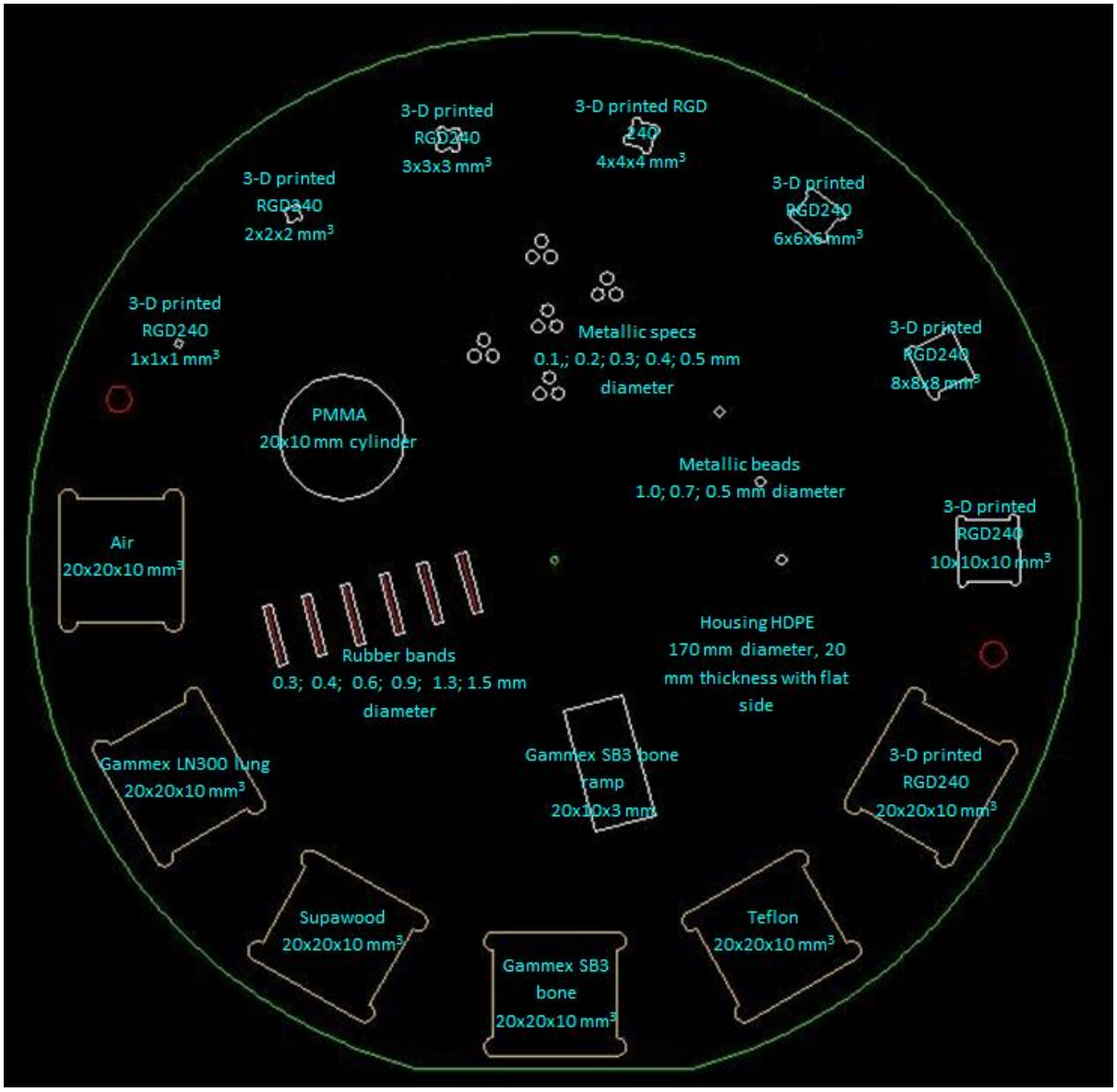

Figure 4.19: Universal phantom insert materials and dimensions. (created by Gebrateq Advanced Engineering)

Table 4.11: Prototype insert materials.

Insert	Material	Density (gcm^{-3})
Housing	High density polyethylene (HDPE)	0.95 [75]
Sensitometry	Objet RGD240	1.17 *
Contrast resolution	Teflon	2.20 [74]
	Gammex SB3 bone	1.82 [77]
	Supawood	0.74 *
	Gammex LN300 lung	0.30 [77]
	Air	0.00
Fibres	Rubber	1.26 *
Slice thickness ramp	Gammex SB3 bone	1.82 [77]
Circular geometry cylinder	Polymethyl methacrylate (PMMA)	1.18 [74]
Micro-calcifications	Metal	Not known
MTF beads	Metal	Not known

* As calculated in Appendix C

4.4.2 Phantom machining and manufacturing

The inserts and phantom housing was machined from the plastics in Table 4.11. A similar process to that described in section 4.2.2 was followed. It is illustrated in Figure 4.20.

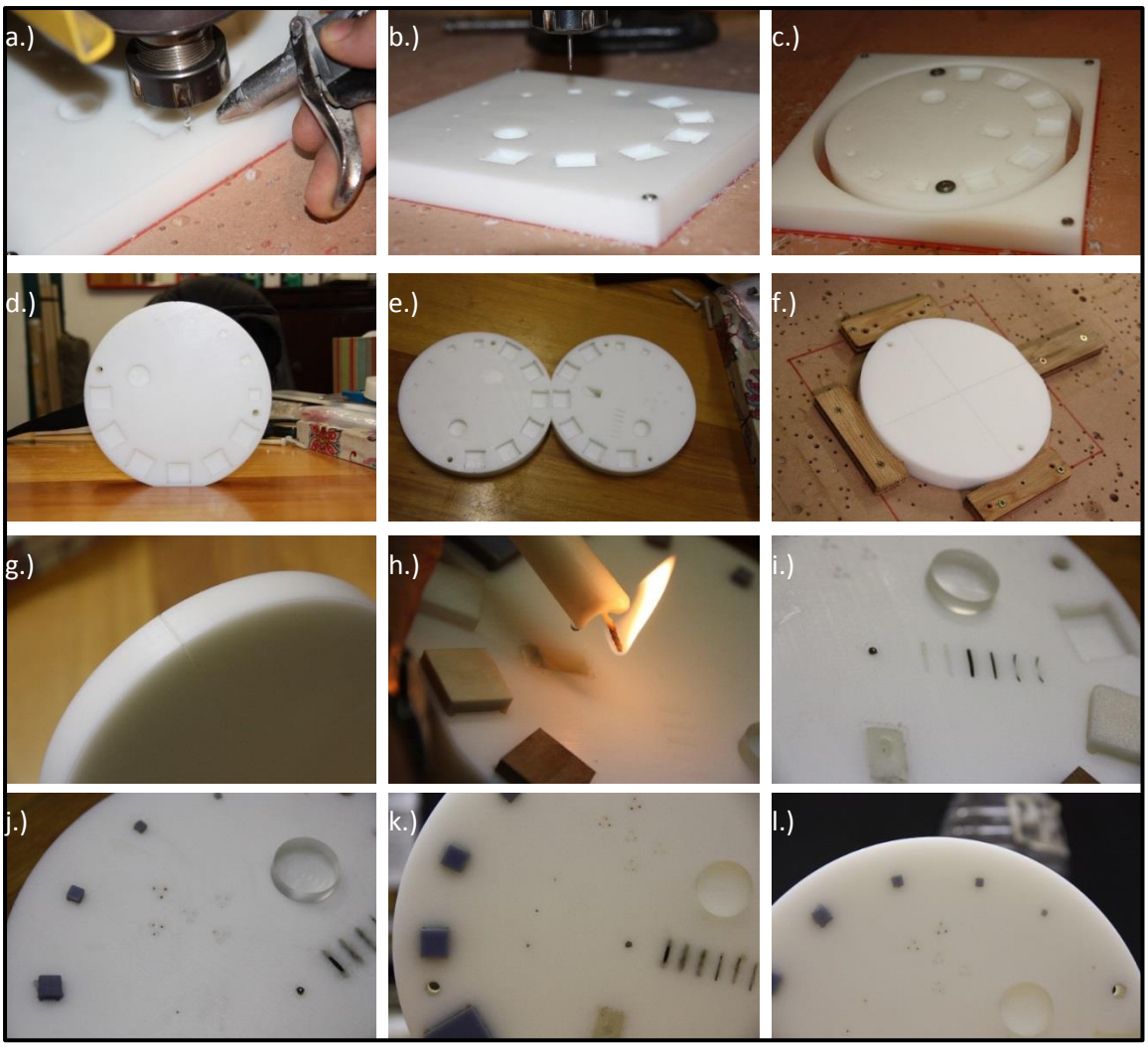

Figure 4.20: Making the universal phantom. a.) Cutter is kept cool with high pressure air. b.) Voids are machined in HDPE slab. c.) Phantom housing is cut from the slab once all voids are machined. d.) The process is repeated for the top half. e.) Completed top and bottom half phantom housings. f.) Using a jig, the top half is turned over to machine scribe lines. g.) Scribe lines on phantom side and top half. h.) Wax is used to fill the ramp void. i.) Rubber fibers are placed. j.) Micro-calcification specks are placed. k.) MTF balls are placed. l.) The small inserts, i.e. 1x1x1 mm^3 low contrast detectability cube, micro-calcifications and MTF balls.

The machining procedure was programmed using SolidWorks 2015 Premium CAD software. Machining was done on a Multicam 3000 series router machine. This was done with assistance from Johan Braasch of Gebrateq Advanced Engineering. Machining was done on a layer-by-layer manner, cutting voids from a slab of HDPE housing material. One void was machined at a time, its insert was fitted and only if

the fit was correct was the next void cut. The 20 mm voids were machined with a 3 mm diameter cutter at 0.1 mm bigger than the insert, i.e. 20.1 mm voids were cut. For the 4, 6, 8 and 10 mm voids a 1.5 mm diameter cutter was used at 0.1 mm bigger and for 1, 2 and 3 mm voids a 1 mm diameter cutter was used with size-to-size machining. In the prototype the small voids were slightly large. By machining the small voids size-to-size compared to the actual insert, a tighter fit was achieved in the phantom.

In the bottom half, the mammography fiber slots were cut with a 1 mm diameter cutter at 1 mm depth for the 0.3, 0.4 and 0.6 mm diameter rubbers and 2 mm diameter cutter and 2 mm depth for the 0.9, 1.3 and 1.5 mm diameter rubbers. The voids were filled with wax once the rubbers were fitted. The central bead was a 2 mm diameter ball bearing and a 2 mm diameter cutter was used to machine a 2 mm diameter and 1 mm deep void. For the MTF balls and micro-calcification speck groups, a 1 mm diameter cutter was used to make 1 mm deep and 2 mm diameter holes. The inserts were secured in place with Cartel super glue. The completed bottom half is shown in Figure 4.21.

The top half was fitted over the bottom half containing the inserts and he nylon screws were put in to keep the two halves together. The completed phantom is included in Figure 4.22.

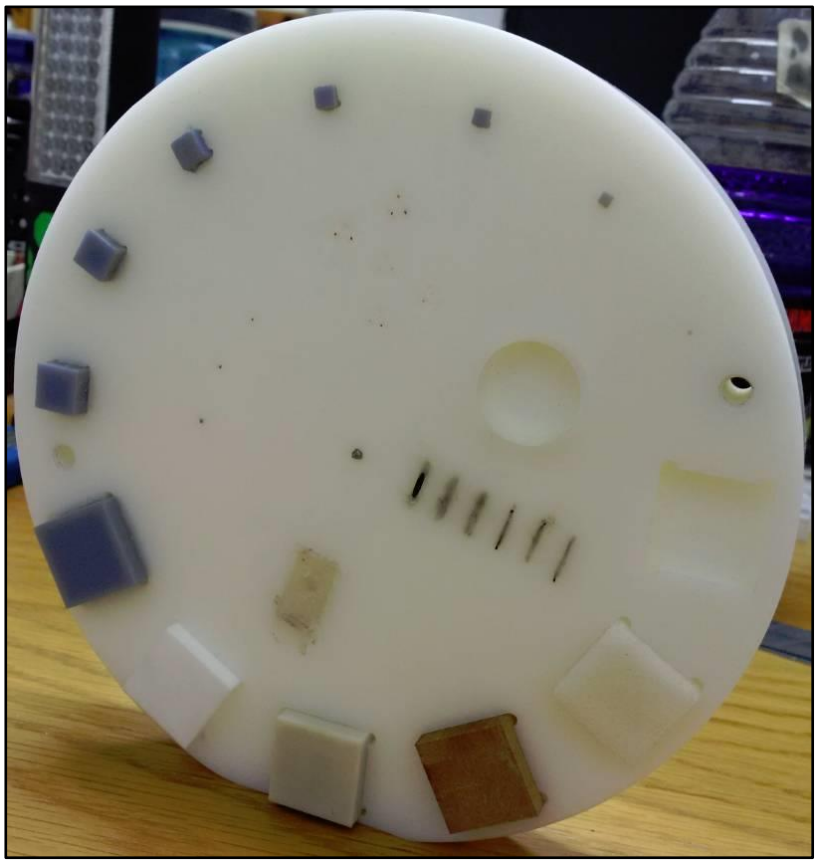

Figure 4.21: The completed phantom bottom half with inserts in place.

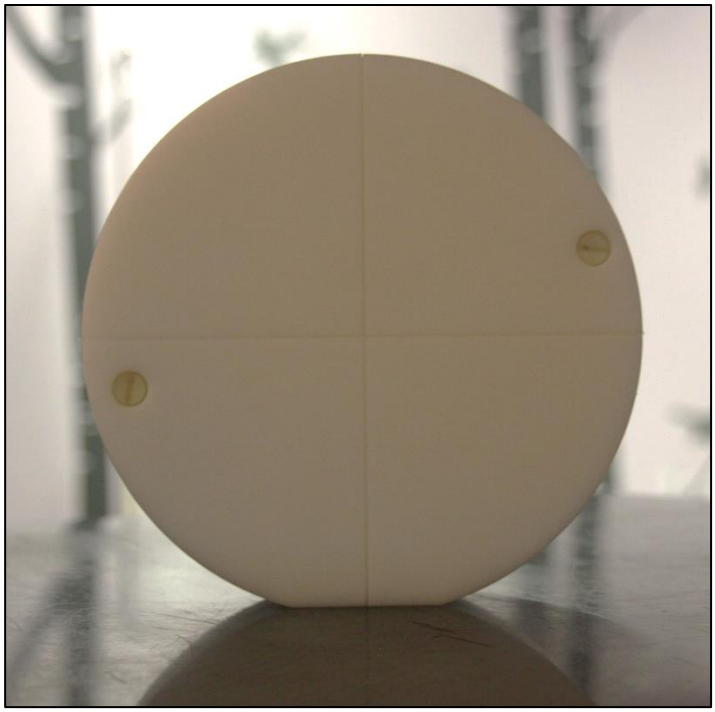

Figure 4.22: The universal image quality assurance phantom.

The phantom weighs 0.87 kg and is substantially smaller than the prototype, as shown in Figure 4.23.

Figure 4.23: Comparison of the prototype phantom and final phantom with the prototype below the final phantom in the images.

This method of phantom manufacturing is crude and introduces some inaccuracies in insert locations and sizes. This is the main identified draw back of the universal image quality assurance phantom. Improvement in phantom manufacturing accuracy would greatly improve accuracy of the obtained results and is necessary when several phantoms will be produced, i.e. all phantoms should be nearly identical.

4.4.3 Initial phantom imaging and evaluation

The phantom was imaged at Winelands Radiology, Vergelegen Medi Clinic, in Somerset West with imaging parameters as tabulated in Table 4.12 and the obtained images shown in Figure 4.24.

Table 4.12: Phantom imaging parameters.

Modality	Unit	kV	mAs	Additional
General x-ray	Siemens Ysio DR unit	40 kV	2 mAs	100 cm FFD, large focus, outside of bucky
Fluoroscopy image	Siemens Axiom Luminos DRF unit	50 kV	2.5 mAs	115 cm FFD, outside of bucky
Mammogram	Siemens Mammomat Inspiration unit	28 kV	105.4 mAs	AEC (the standard for image quality assurance in the department)
CT scan	Siemens Somatom Definition Edge scanner	120 kV	278 mAs	3 mm slices, pitch of 0.8

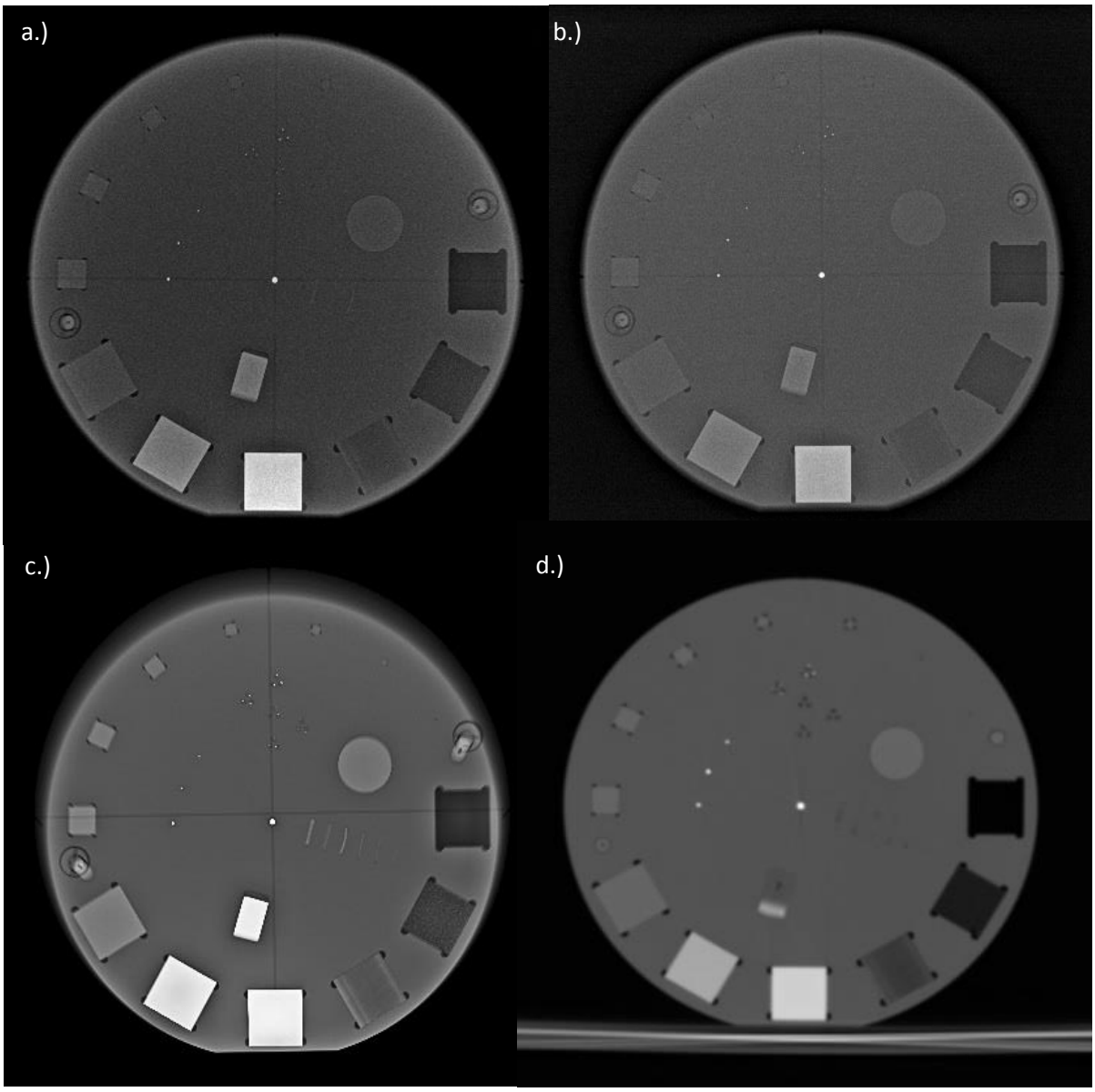

Figure 4.24: Initial images of the universal image quality assurance phantom. a.) General x-ray. b.) Fluoroscopy image. c.) Mammogram. d.) CT scan slice.

Considering the phantom in Figure 4.24, and comparing it to the images of the prototype in Figure 4.10 in section 4.2.3, the improvements in the phantom are clear. The recommendations as derived in section 4.3 were all incorporated and the resultant phantom is a comprehensive diagnostic radiology x-ray image quality assurance tool. The phantom, user's manual and data analysis software must be validated individually, and as a complete package, and this is discussed in Chapters 5 and 6.

Chapter 5

The universal phantom as image quality assurance solution

In this chapter, the routine image quality control parameters that can be assessed with the universal phantom are described. The inserts in the universal image quality assurance phantom are used with the data analysis software for comprehensive routine image quality control in general x-rays, fluoroscopy, mammography and CT scanning, i.e. the phantom is not modality specific. A complete user's manual and description of the data analysis software is included as Appendices A and B, however a summary of these are given in conclusion to this chapter. The universal image quality assurance phantom is intended to simplify routine x-ray image quality control, making it available in resource limited institutions at reduced cost, as an additional image QC tool for diagnostic radiology.

5.1 Image quality assurance using the universal phantom

The universal phantom and accompanying data analysis software can be used for commissioning, i.e. setting baseline values, and routine image QC, as required in diagnostic radiology x-ray equipment licence conditions. Refer to Table 2.1 in Chapter 2 for the image quality control tests required by the Directorate Radiation Control of the South African DoH.

5.1.1 Image quality tests applicable to general x-rays, fluoroscopy, mammography and CT scanning

The universal image quality assurance phantom assesses the following image quality parameters for all projection radiography modalities as well as for CT scanning. The stated limits are derived from the DoH recommendations, as described in Chapter 2.

1.) Sensitometry, grey scale linearity or CT number reproducibility

Using the 20x20x10 mm^3 cubic inserts including air, Gammex LN300 Lung tissue equivalent plastic, Supawood, Gammex SB3 Bone equivalent plastic, Teflon and RGD240, a ROI is drawn in each cube. The ROI is approximately half the diameter of the insert and must not be close to or extend beyond the cube edge. The mean value and standard deviation in each ROI are displayed and recorded. The locations of these ROIs are illustrated in red in Figure 5.1. The quantitative value obtained in routine quality control is compared to the baseline value for each insert. The accepted limit is baseline grey scale value ± 0.2 for projection radiography and ± 10 HU for CT scanning.

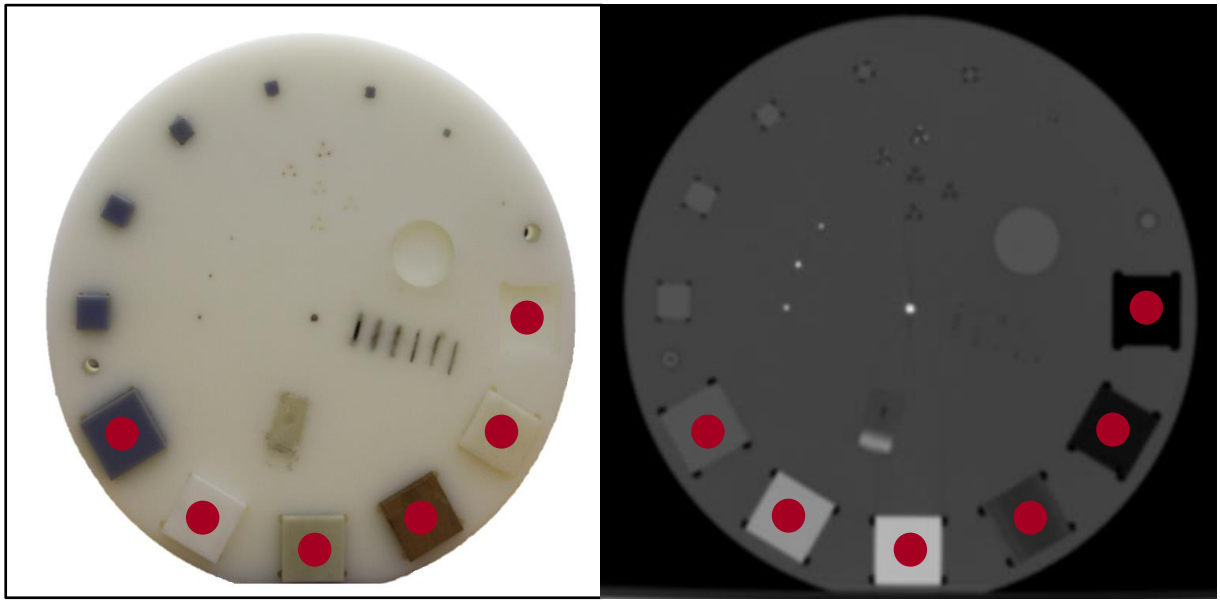

Figure 5.1: ROI location for sensitometry assessment, indicated in red.

2.) Low contrast detectability

RGD 240 cubes of 20, 10, 8, 6, 4, 3, 2 and 1 mm^3, as in Figure 5.2, are visually inspected, i.e. subjective analysis, by the observer to determine the smallest cube that is visible. The size of this cube is recorded. This must remain reproducible over time.

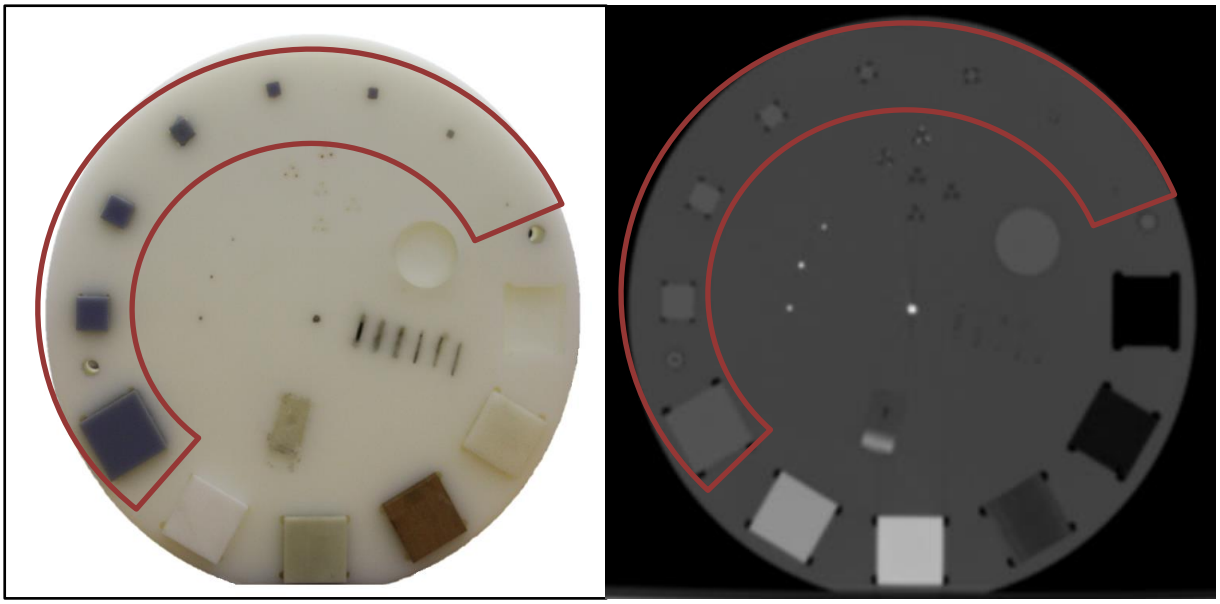

Figure 5.2: ROI location for low contrast detectability assessment. Cubes are pointed out in red.

3.) Image uniformity

The data analysis software quantitatively calculates uniformity using ROIs of similar size at four different locations in the HDPE phantom housing area. The ROIs are drawn as shown in red in Figure 5.3. The obtained value is compared to the set baseline value. A tolerance of baseline ± 5 % for DR and ± 10 % for CR, film-screen and CT scanning is accepted.

4.) Resolution

The data analysis software quantitatively calculates the MTF from a PSF produced from different sized metallic balls, using a ball with diameter smaller than a pixel size. From the graph the software also reports the limiting spatial resolution as the frequency (cycles/mm) at which the MTF has 10 % value. The tolerance used is baseline - 25 %. Figure 5.4 shows the location of the metallic balls in red.

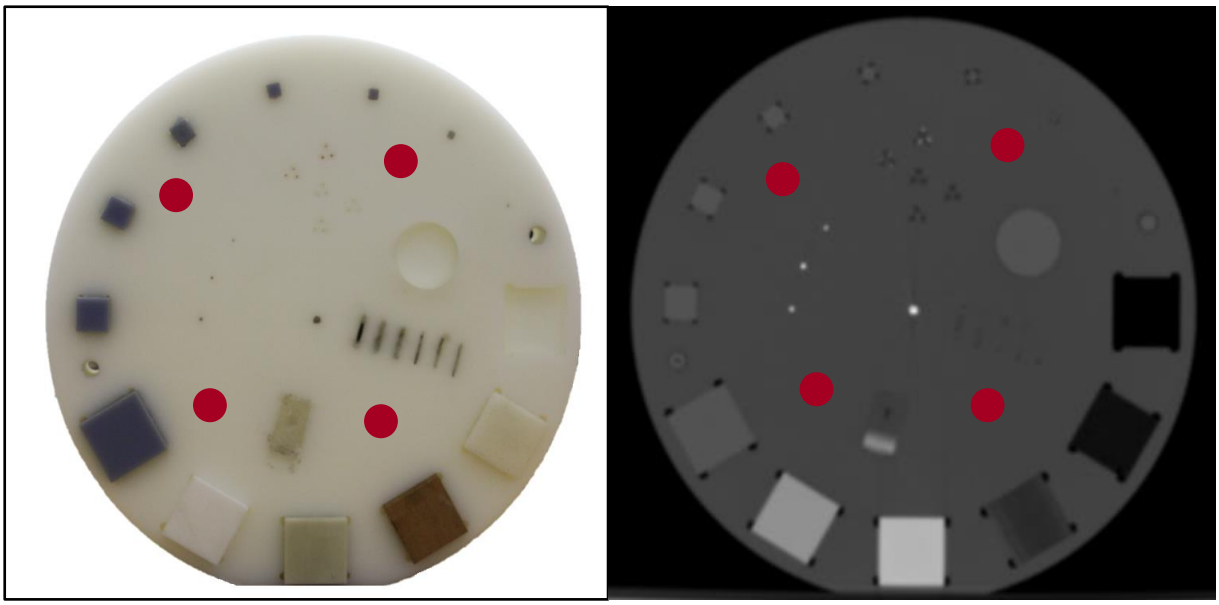

Figure 5.3: ROI location illustrated in red used for uniformity assessment.

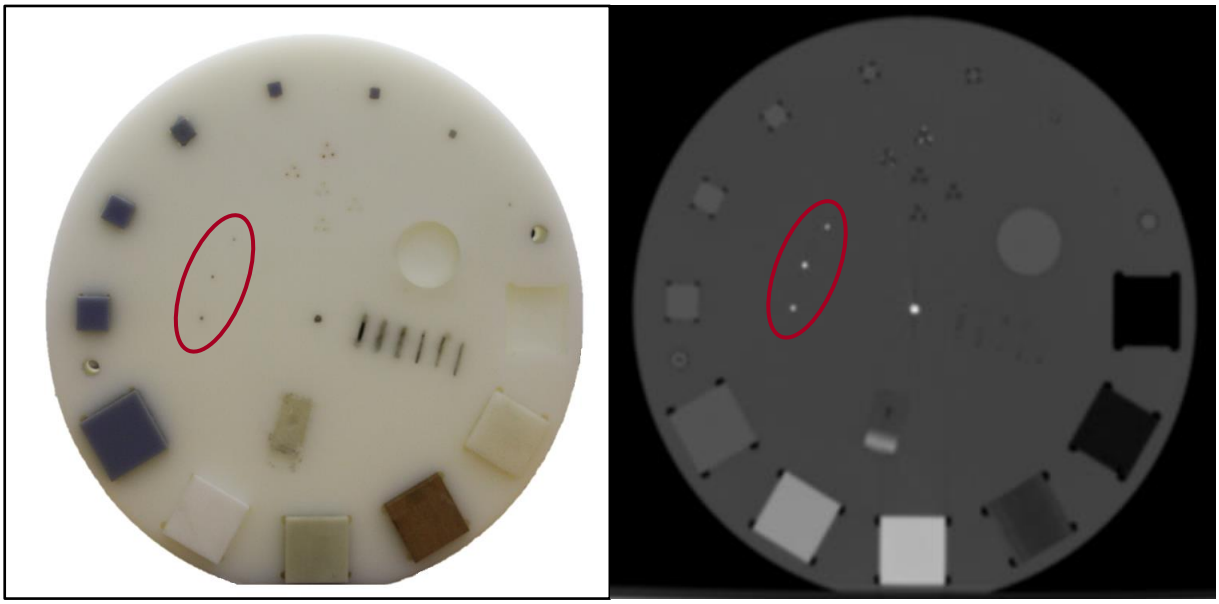

Figure 5.4: Metallic ball location for resolution MTF assessment, as shown in red.

5.) Noise

Image noise is quantitatively calculated by the data analysis software using ROI analyses and Equations 5.1 and 5.2. The location of the ROIs is shown in red in Figure 5.5. The noise is expressed as the SNR and CNR. A tolerance of baseline value ± 10 % is used.

$$SNR = \frac{mean}{standard\ deviation} \qquad \text{[Equation 5.1]}$$

$$CNR = \frac{mean(a) - mean(b)}{standard\ deviation(b)}$$ [Equation 5.2]

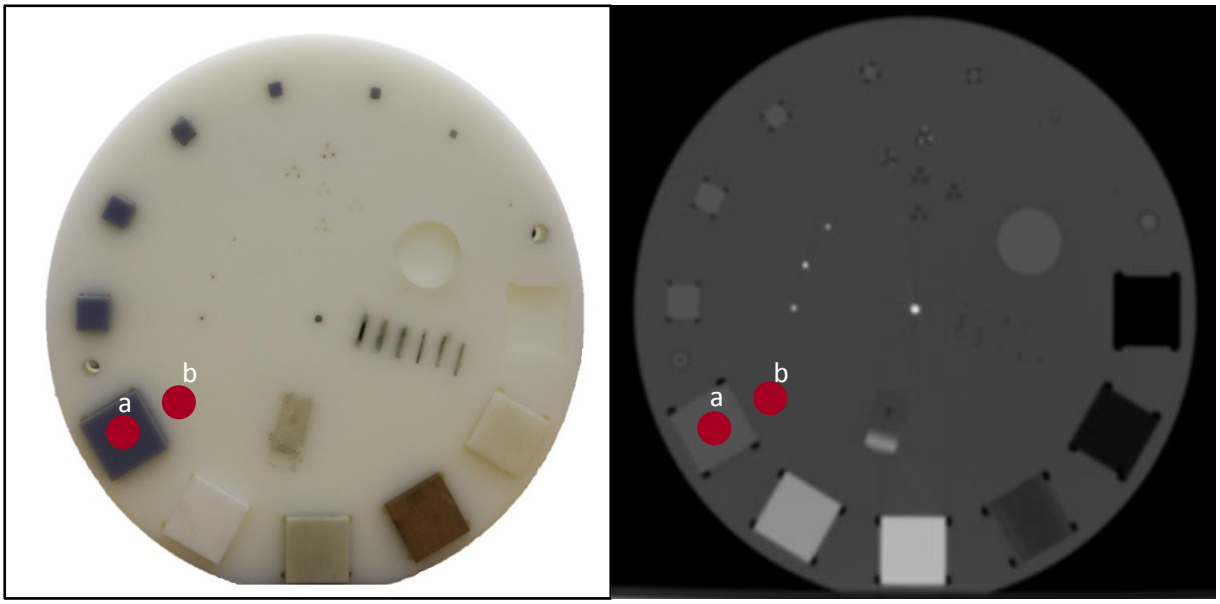

Figure 5.5: ROI location, in red, for SNR and CNR assessment as in Equations 5.1 and 5.2.

6.) Positioning and alignment

This refers to zero slice position or scan plane localisation for CT scanning and x-ray to light beam centring for planar imaging. Scribe lines on the phantom surface are used to position the phantom on the bed for imaging using the displayed cross wires or lasers. If set-up correctly, the centrally placed metallic ball will appear in the middle of the image or on the CT slice that was given the 0-coordinate position. The user evaluates the obtained image, thus subjective analysis, which was acquired with collimation to just enclose the entire phantom. Deviations, for example in Figure 5.6, are noted as results. The accepted tolerance is ± 2 % of source-to-image distance (SID) for planar imaging and 2 mm for CT scanning.

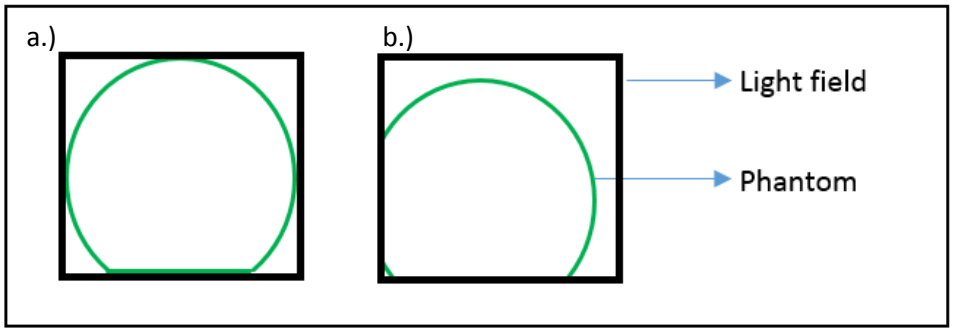

Figure 5.6: a.) Correct x-ray to light field coincidence. b.) The light field is smaller than the x-ray field to the left and bottom.

7.) Geometry and measurement tools

This assesses distance accuracy, scaling errors and circular geometry. The dimensions of the PMMA cylinder insert, as in Figure 5.7 in red, are measured by the software, from lines drawn by the user, and compared to their actual sizes of 2 cm diameter. The tolerance from actual value is ± 5 mm or ≤ 2 % for general x-rays, fluoroscopy and CT scanning. For mammography no deviation should be seen.

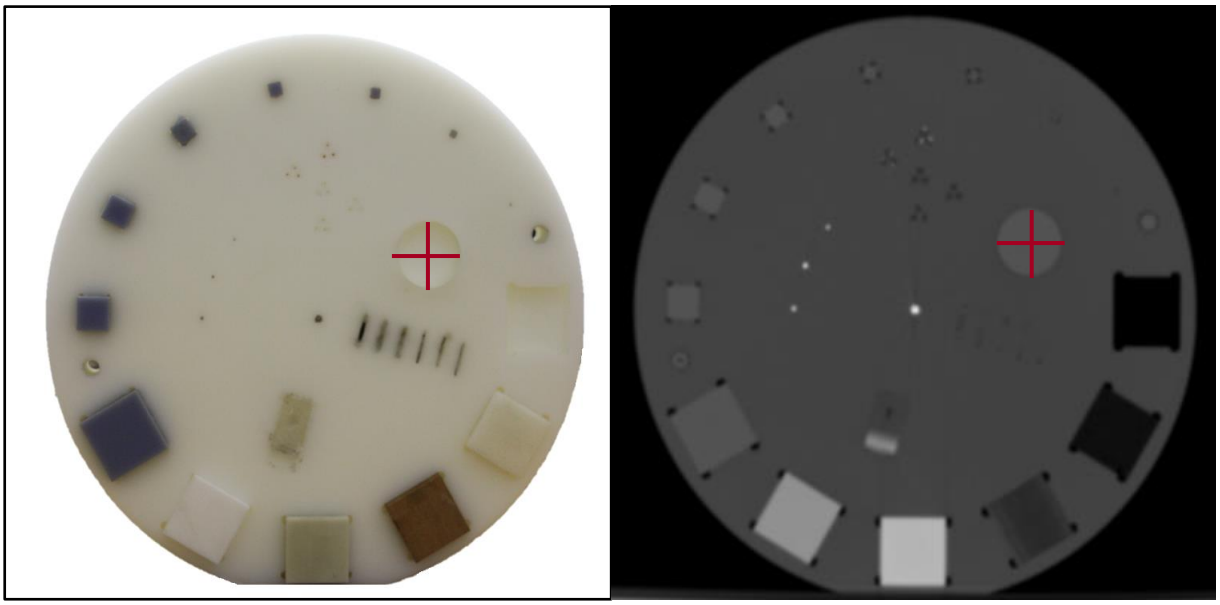

Figure 5.7: Measurements for distance accuracy and scaling assessment, indicated with red lines.

8.) Artefacts

In this subjective analysis, the image is visually inspected by the user for the presence of artefacts under normally used clinical WW and WL settings. The image should be free of dots, lines, streaks, ghost images or any other disturbance.

9.) Image quality visual inspection

The obtained images are visually inspected by the user at clinically used WW and WL settings, noting the inserts seen, any artefacts and any changes from the previously obtained or baseline images. An overall impression of the image is recorded as result and this should remain reproducible over time. The results from this test are therefore subjective.

10.) Standard signal

The data analysis software quantitatively measures the mean and standard deviation in a ROI, consistently positioned in the HDPE housing of the phantom. This is shown in Figure 5.8 with a red circle. This value should remain constant over time, compared to the baseline value, with a tolerance of ± 0.2 for planar imaging or ± 10 HU for CT scanning.

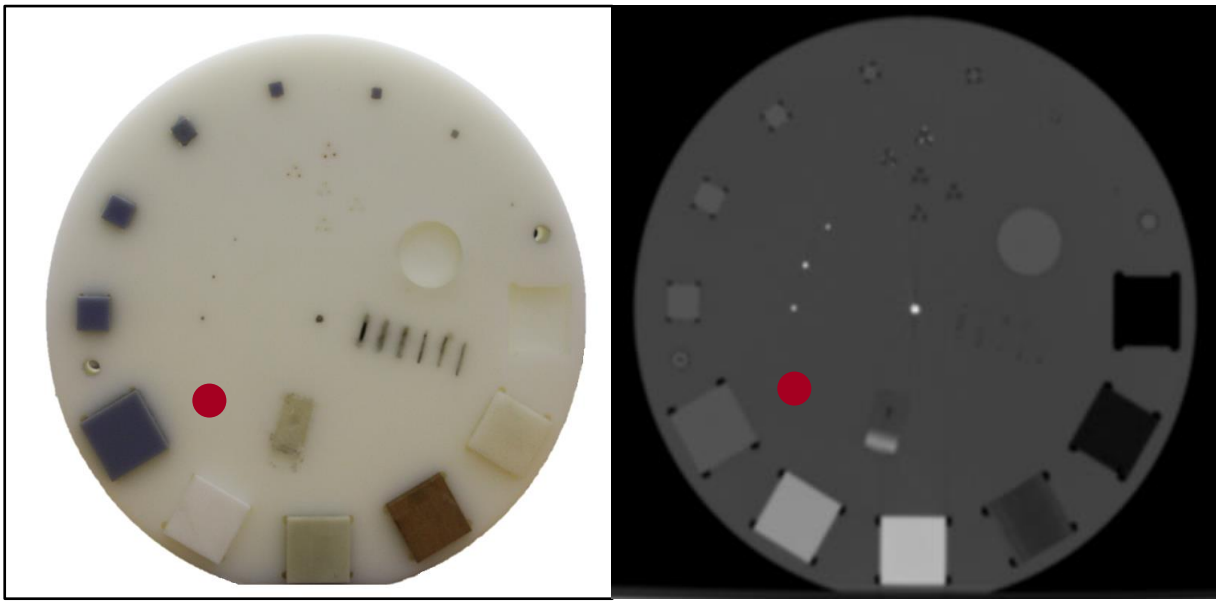

Figure 5.8: ROI location for standard signal assessment, as shown in red.

5.1.2 Automatic exposure control image quality tests applicable to general x-rays, fluoroscopy and mammography

These tests are performed in addition to those discussed in section 5.1 for general x-rays, fluoroscopy and mammography. They are designed to assess the effectiveness of AEC to produce acceptable image quality.

1.) AEC performance

The image quality should be maintained at an acceptable level for different thicknesses of phantom. AEC exposures should compensate for phantom thickness. The user makes an AEC exposure with no additional attenuator HDPE, i.e. 0 cm, and then also with 2 cm and 4 cm additional HDPE added on top of the phantom and repeats the tests in sections 5.1.1 and 5.1.3. The obtained results will be quantitative and subjective, as mentioned in sections 5.1.1 and 5.1.3.

2.) AEC repeatability

Image quality should remain constant with repeat exposures of the same phantom thickness using AEC. The user makes three AEC exposures with the same phantom thickness and compares the quantitative and subjective results of the tests in sections 5.1.1 and 5.1.3. Image quality should vary within 5 %.

5.1.3 Image quality tests applicable to mammography

In addition to the tests described in sections 5.1 and 5.2, there are three additional parameters to be assessed in mammography, i.e. fibres, masses and micro-calcifications. The universal image quality assurance phantom houses inserts for this application.

1.) Fibres

The user must subjectively identify the number of fibre simulating inserts that can be seen and note the size of the smallest seen insert. The location of these inserts in the universal phantom is shown in red in Figure 5.9. All the fibres in the phantom should be visible and remain so over time.

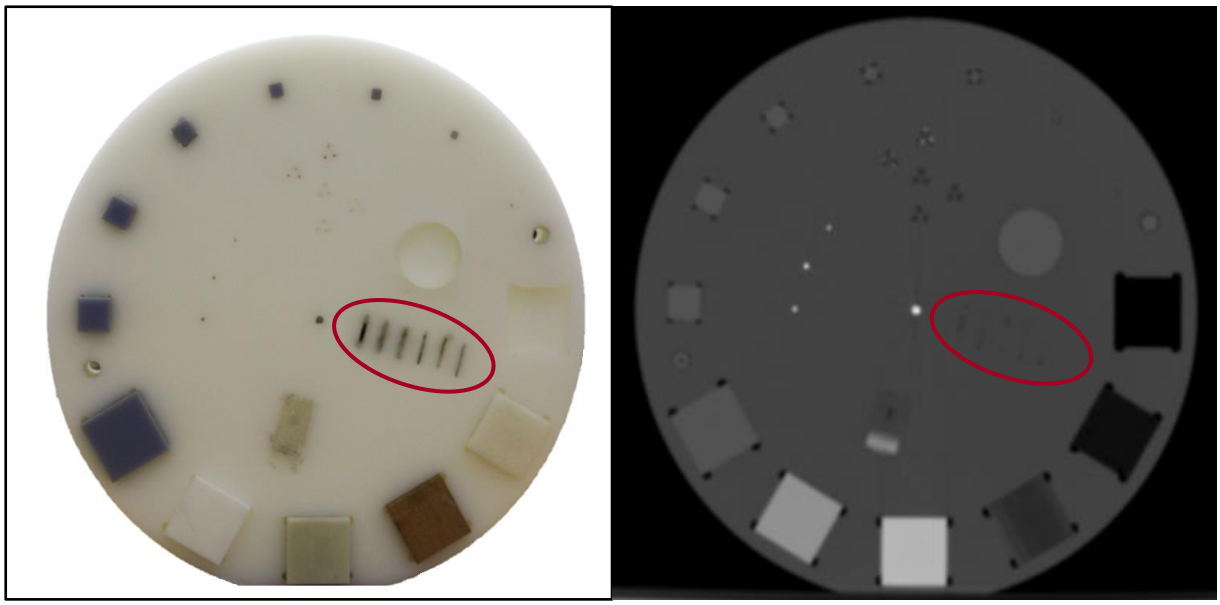

Figure 5.9: Location of fibre simulating inserts, included in red outline.

2.) Masses

The low contrast detectability inserts, as in Figure 5.2, are used to simulate mass like structures in mammography. The user must visually determine the smallest mass that can be seen, i.e. subjective analysis. Ideally all the inserts should be visible and the results must remain constant with periodic testing.

3.) Micro-calcifications

Metallic specs are included in five different clusters, with three specs of a size in each cluster, as indicated by the red circle in Figure 5.10. These simulate micro-calcifications in mammography. The user visually determines if all the specs in each of the five clusters can be seen and the obtained subjective result should be reproducible over time.

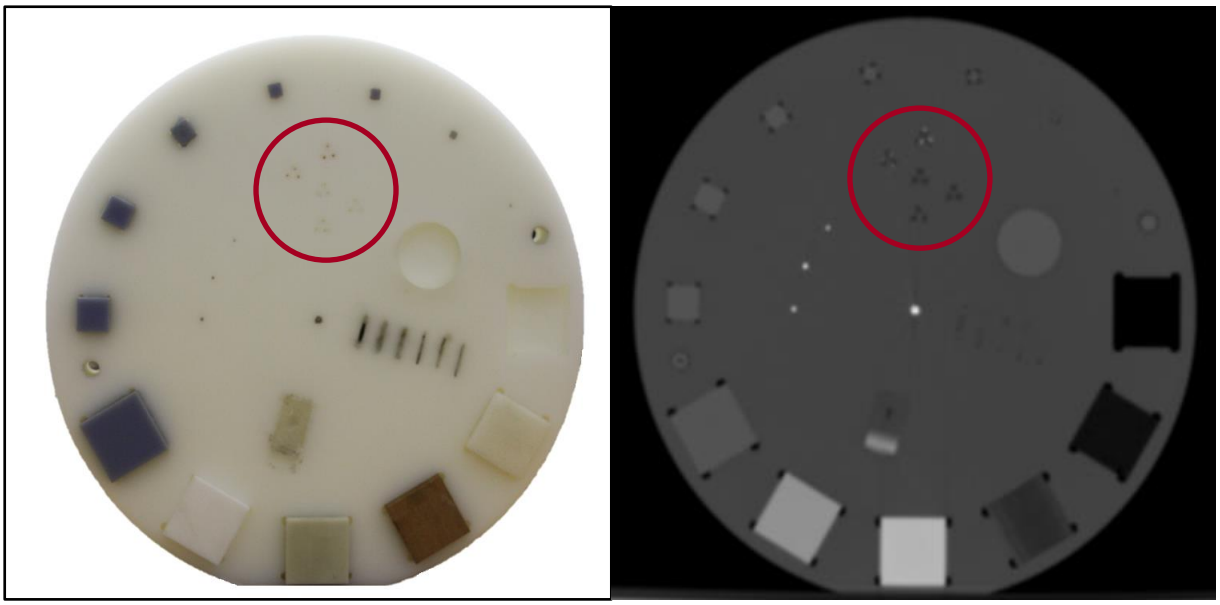

Figure 5.10: Location of micro-calcification simulating inserts in the red circle outline.

5.1.4 Image quality tests applicable to CT scanning

In addition to the tests described in section 5.1, slice thickness must also be investigated for CT scanning.

1.) Slice thickness

A Gammex SB3 bone equivalent ramp inserted in the phantom at an angle is used to measure slice thickness with user input into the data analysis software. The ramp is shown in Figure 5.11, in the red outline.

The data analysis software uses the FWHM to measure the slice thickness from the ramp. By adjusting the WW and WL, correcting for background, finding the 50% background corrected peak WL value and setting the image grey scales to this value, the data analysis software then measures the actual scanned slice thickness from a subjective line drawn by the user. This is compared to the slice thickness selected for the scan. The difference between the selected and actual slice thicknesses has a tolerance of ± 20 % or 1 mm, whichever is smaller.

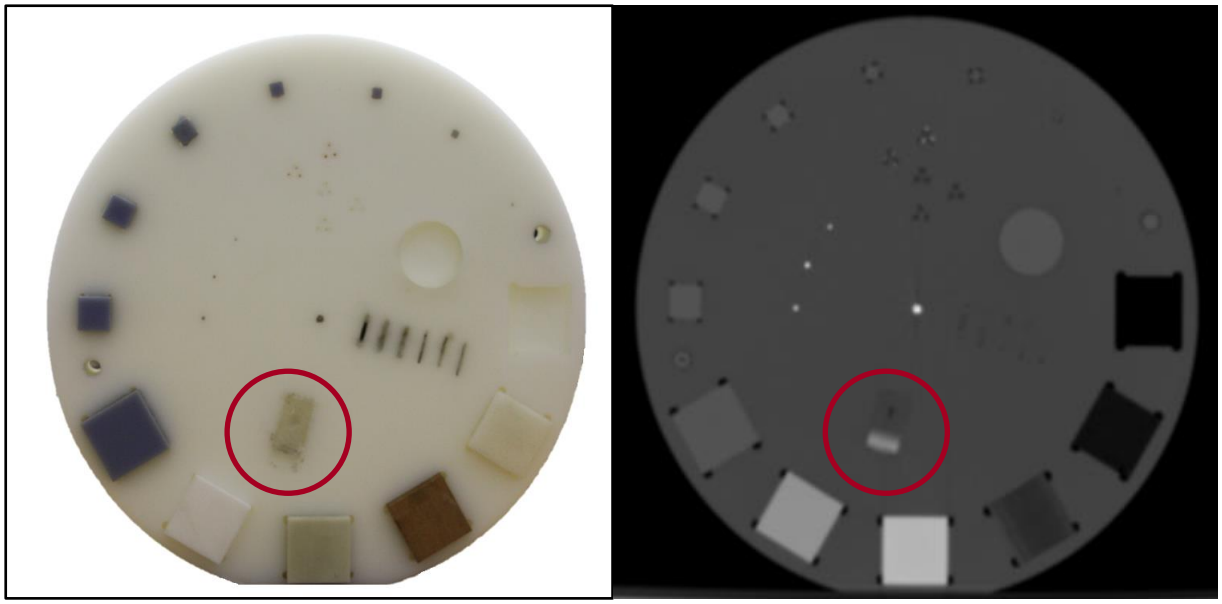

Figure 5.11: The red circle shows the location of ramp for CT slice thickness measurement.

5.2 Overview of the universal phantom user's manual and data analysis software

A complete user's manual is presented in Appendix A. The manual discusses the operation and use of the phantom and software, analysis of the results and contains result recording example pages. The manual includes general information about the universal image quality assurance phantom and the manual, its intended use and safety information for using the phantom. The manual aims to simplify the image quality assurance process, explaining data analysis software installation, phantom set-up, exposure and image quality evaluation in a step-by-step manner. It also includes recommendations of actions required when obtained results are out of tolerance. The manual is divided into sub sections for general x-rays and fluoroscopy imaging, mammography imaging and CT scanning. In each section the visual and data analysis software tests and the recording of results are described. It also contains the complete technical specifications of the phantom and instructions for cleaning, preventative maintenance and disposing of the phantom. Sample result data recording sheets are included for all the imaging modalities.

The data analysis software is a Microsoft .NET application written in C# by Ernst Uys and is licensed to the developer. The software provides a simple interface, that is

easy to understand and use, in accordance with the aim of the study. The software is described in Appendix B. The source code can be obtained from the developer.

The user's manual and data analysis software are included with the universal image quality assurance phantom to form a complete user friendly image quality assurance package.

Chapter 6

Reproducibility testing of the universal phantom

To be scientifically useful, the results obtained with the universal image quality assurance phantom and data analysis software must be reproducible and accurate. This means that consistent results are obtained using the same equipment and exposure parameters. To test this, ten exposures of the phantom were made using the same general x-ray, fluoroscopy and mammography unit and CT scanner, with exposure technique factors as tabulated in Tables 6.1, 6.4, 6.7 and 6.10. For each exposure the set-up of the phantom was repeated, i.e. the phantom was completely repositioned for every exposure. Variability in x-ray output between identical exposures exist, inherent to the equipment used, and could account for some of the variation seen in the results. This was mentioned in Chapter 2. In an attempt to minimise this, all exposures were acquired on the same day, directly after each other.

6.1 General x-ray reproducibility testing

The exposure parameters used for general x-ray imaging are included in Table 6.1 with the obtained results in Tables 6.2 and 6.3 and Figures 6.1 to 6.9.

Table 6.1: Reproducibility testing exposure technique factors for general x-ray imaging.

Modality	General x-rays
Unit	Siemens Ysio
kV	40
mAs	2
FFD	100 cm
Slice thickness	-
Other	Outside bucky

Table 6.2: General x-ray reproducibility testing visual inspection results. (Appendix A, A.2.3.4)

Image number	Low contrast detectability	Positioning and alignment	Artefacts	Image quality visual inspection
1	2	X-ray field too small	None	Acceptable
2	3	X-ray field too large	None	Acceptable
3	2	X-ray field too small	None	Acceptable
4	3	X-ray field too large	None	Acceptable
5	3	X-ray field too large	None	Acceptable
6	3	X-ray field too large	None	Acceptable
7	3	X-ray field too large	None	Acceptable
8	3	X-ray field too large	None	Acceptable
9	3	X-ray field too large	None	Acceptable
10	3	X-ray field too large	None	Acceptable

Table 6.3: General x-ray reproducibility testing data analysis software results. (Appendix A, A.2.3.5)

Image number	Sensitometry values as measured with software (arb. units)					
	Air		Lung		Supawood	
	Mean	Std dev	Mean	Std dev	Mean	Std dev
1	1606.4	36.5	1674.4	43.1	1742.8	38.8
2	1640.7	36.5	1701.5	43.6	1764.8	38.4
3	1646.5	36.5	1710.4	42.6	1773.5	38.4
4	1611.3	36.5	1676.3	42.4	1729.3	36.8
5	1625.9	36.7	1693.5	45.2	1752.8	38.6
6	1623.4	36.9	1687.0	43.0	1743.5	38.2
7	1620.2	37.4	1690.5	42.8	1746.3	38.3
8	1620.3	36.0	1684.2	42.7	1741.4	38.7
9	1616.0	36.1	1681.6	43.4	1736.8	39.0
10	1611.5	36.5	1674.8	43.6	1733.3	37.8
Average calculated	1622.2 ± 12.2		1687.4 ± 11.3		1746.5 ± 13.1	

Image number	Sensitometry values as measured with software (arb. units)					
	Bone		Teflon		RGD240	
	Mean	Std dev	Mean	Std dev	Mean	Std dev
1	2492.4	80.0	2007.9	50.0	1768.2	39.9
2	2499.0	77.2	2039.9	52.7	1796.4	40.3
3	2515.2	79.0	2046.7	51.7	1802.6	40.2
4	2465.2	77.0	2000.3	50.3	1764.1	39.1
5	2483.5	80.5	2021.7	52.6	1780.4	39.7
6	2491.9	80.8	2020.5	52.2	1776.3	39.2
7	2484.3	79.7	2014.8	52.6	1775.9	40.2
8	2458.9	76.8	2008.7	51.0	1769.8	39.7
9	2476.2	79.5	2007.9	51.8	1772.0	40.3
10	2474.0	79.4	2007.8	53.0	1767.6	39.9
Average calculated	2484.1 ± 15.7		2017.6 ± 14.3		1777.3 ± 12.1	

Image number	Uniformity (arb. units)	Limiting resolution (cycles/cm)	Image noise (arb. units)		Geometry and measurement tools (mm)		Standard signal (arb. units)	
			SNR	CNR	Horizontal value	Vertical value	Mean	Std dev
1	31.9	11.1	44.5	2.1	20.3	20.0	1687.1	36.1
2	34.7	11.1	45.4	2.1	19.6	19.9	1716.2	35.7
3	35.3	11.1	44.6	2.1	19.9	19.6	1723.9	36.4
4	37.1	11.1	44.7	2.1	19.9	19.9	1687.8	35.9
5	34.1	11.2	45.2	2.2	19.9	19.6	1703.6	37.1
6	36.1	11.2	44.1	2.4	20.3	19.6	1703.3	36.8
7	33.3	11.2	44.9	2.0	19.9	19.9	1697.4	37.3
8	31.3	11.1	45.5	2.0	19.9	19.5	1706.2	38.8
9	32.7	11.2	43.9	2.1	19.9	19.9	1694.1	37.7
10	37.2	11.1	43.4	2.2	19.9	20.3	1691.3	36.5
Average calculated	34.4±2.0	11.1±0.1	44.6±0.6	2.1±0.1	20.0±0.2	20.0±0.2	1701.1±11.5	

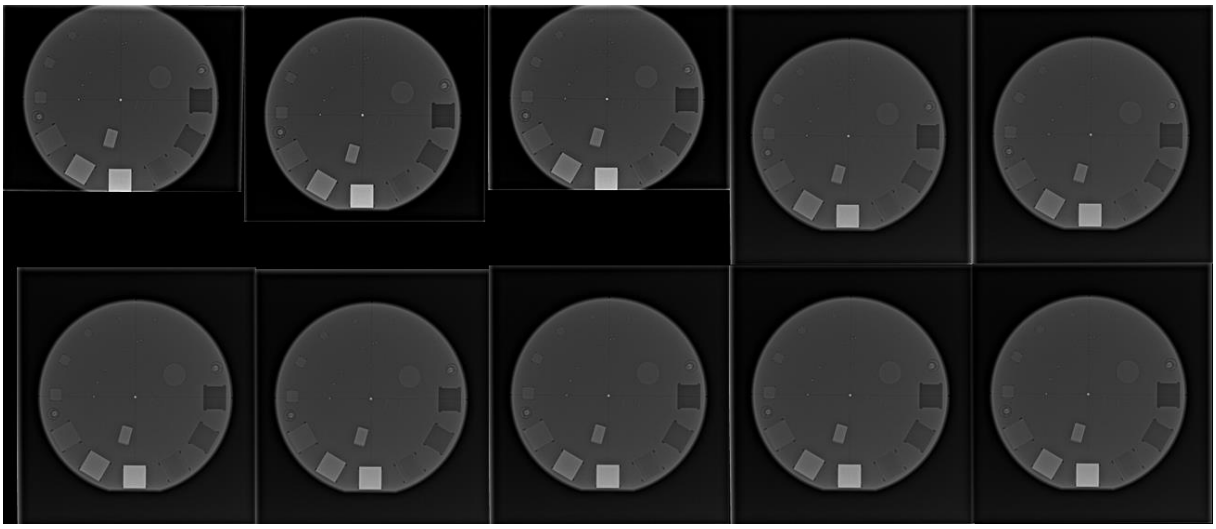

Figure 6.1: General x-ray reproducibility images.

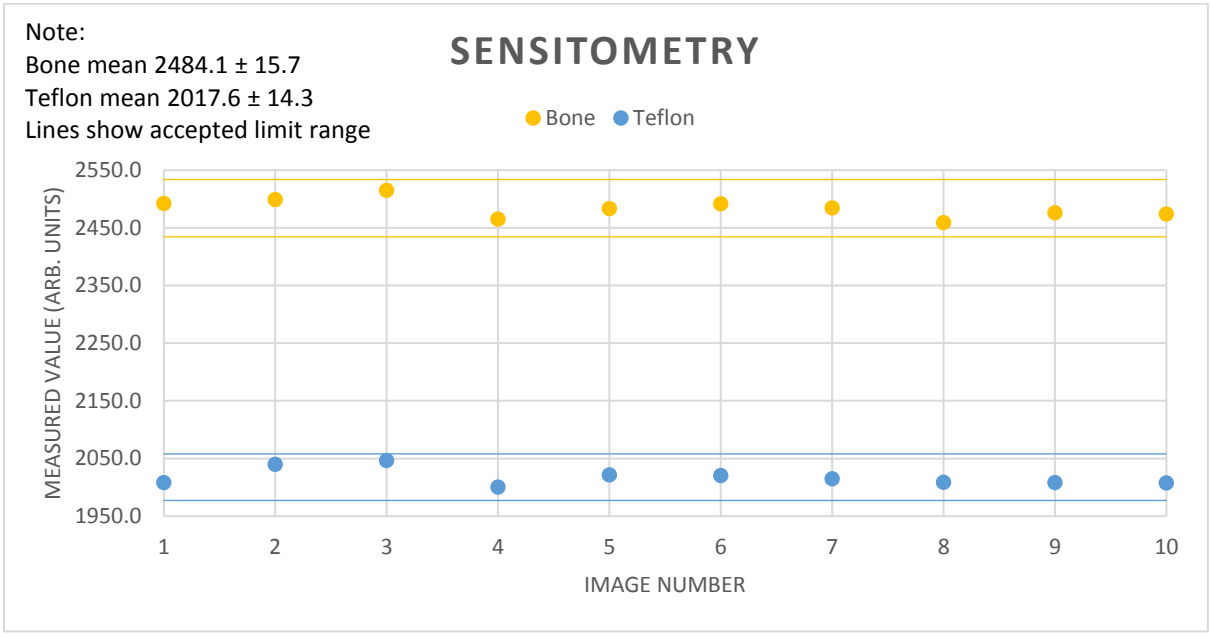

Figure 6.2: General x-rays data analysis software reproducibility results for sensitometry for bone and Teflon with tolerance limits of ± 2 %.

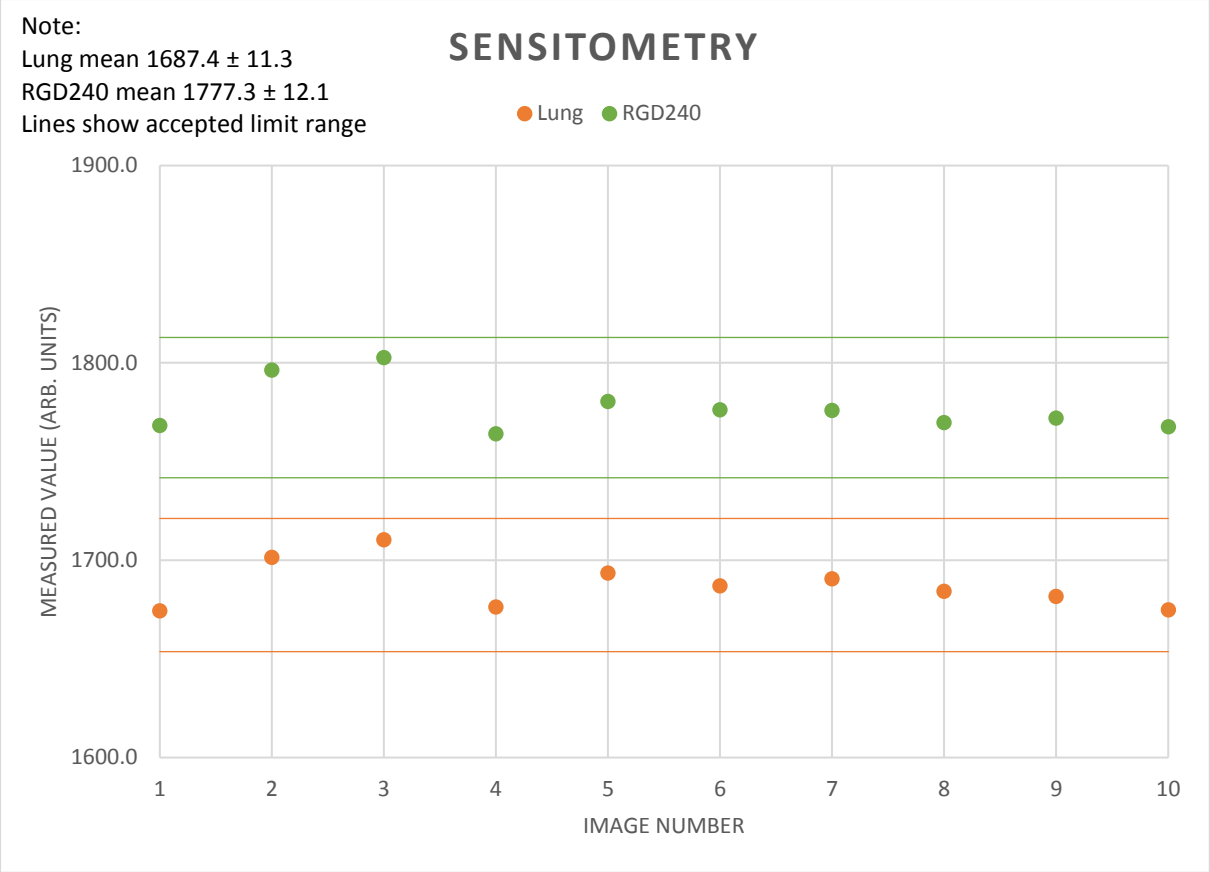

Figure 6.3: General x-rays data analysis software reproducibility results. for sensitometry for lung and RGD240 with tolerance limits of ± 2 %.

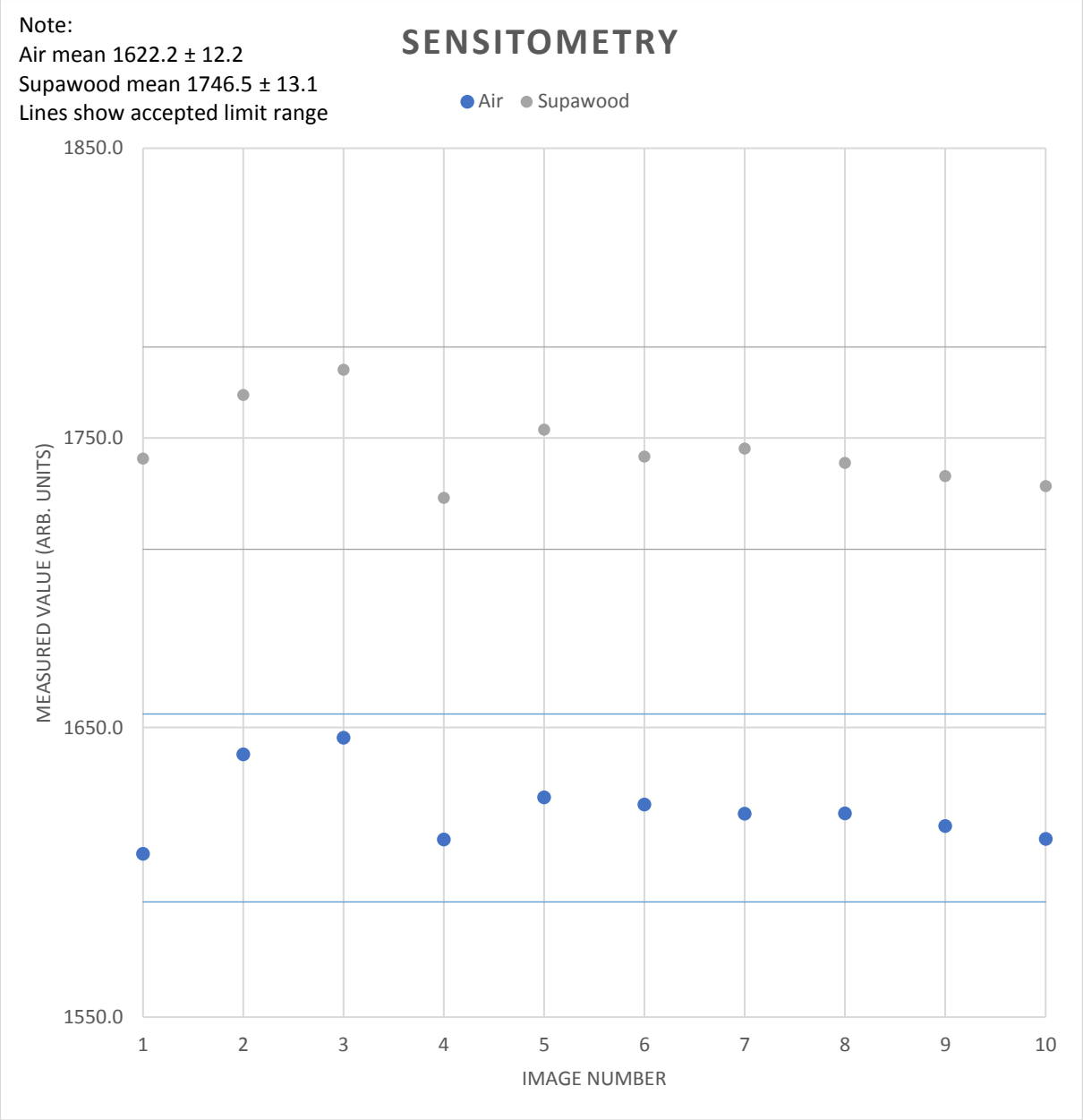

Figure 6.4: General x-rays data analysis software reproducibility results for sensitometry for air and Supawood with tolerance limits of ± 2 %.

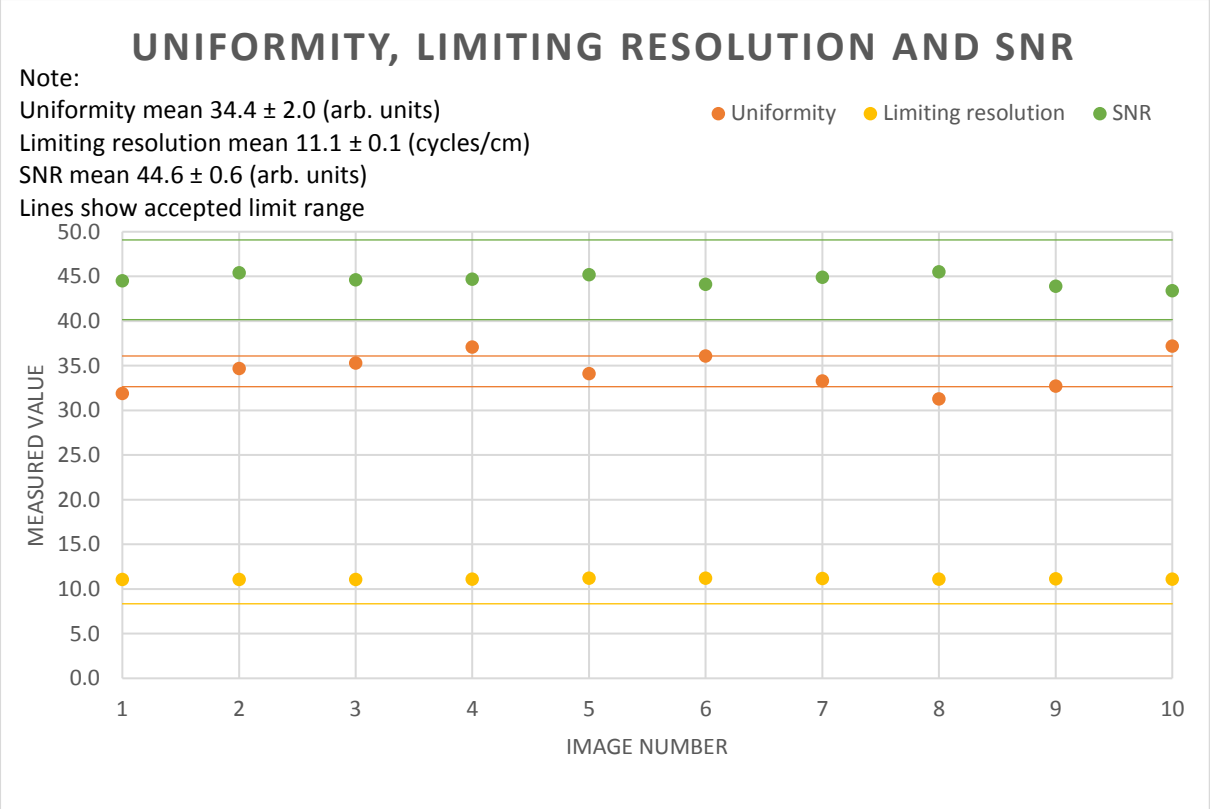

Figure 6.5: General x-rays data analysis software reproducibility results for uniformity with tolerance limits of ± 5 %, limiting resolution results with tolerance limits of – 25 % and SNR results with tolerance limits of ± 10 %.

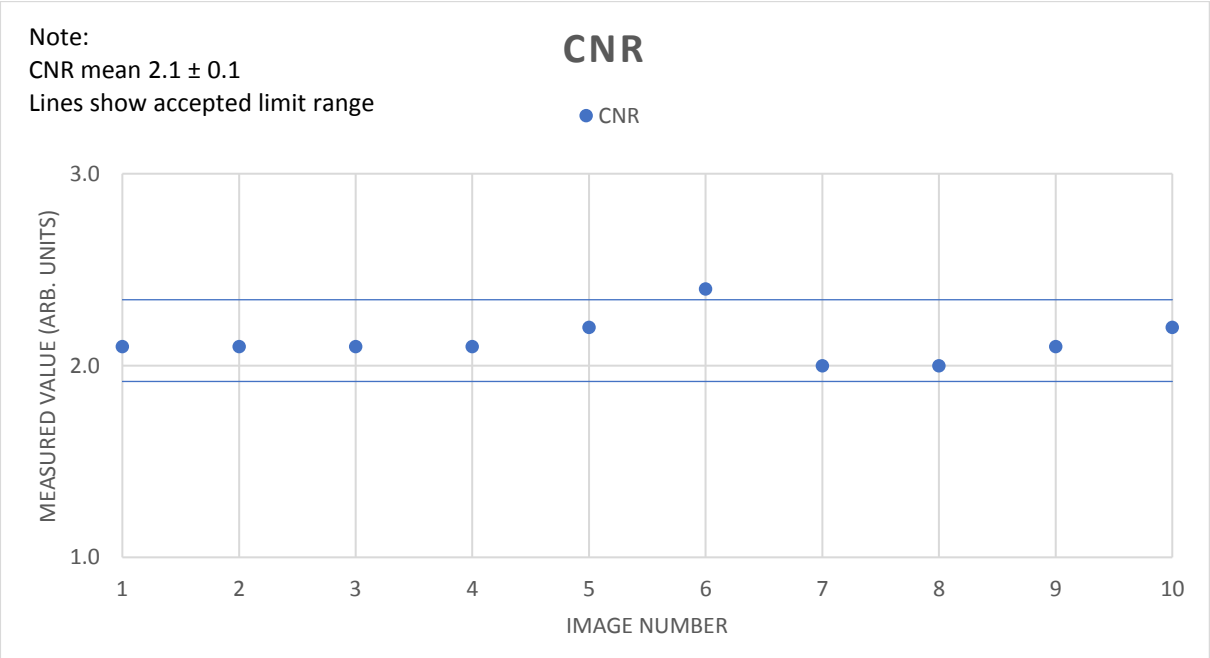

Figure 6.6: General x-rays data analysis software reproducibility results for CNR with tolerance limits of ± 10 %.

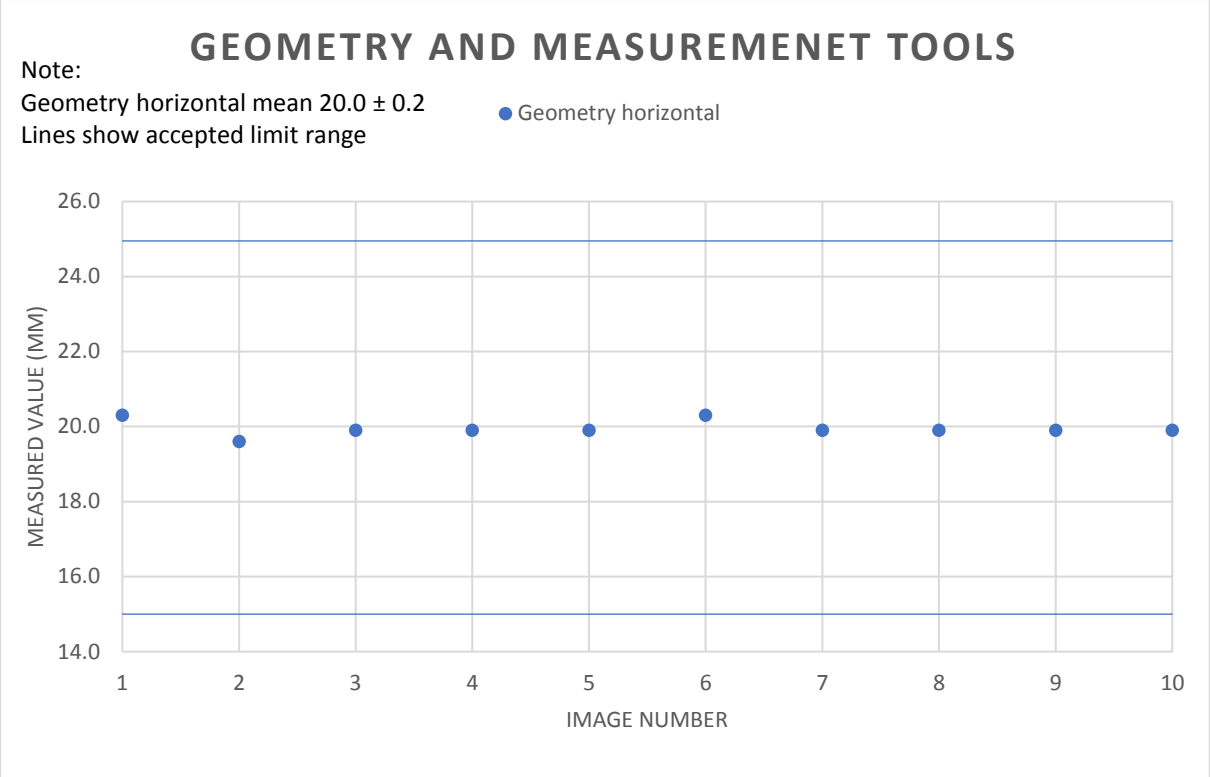

Figure 6.7: General x-rays data analysis software reproducibility results for geometry and measurement tools for horizontal measurement with tolerance limits of ± 5 mm.

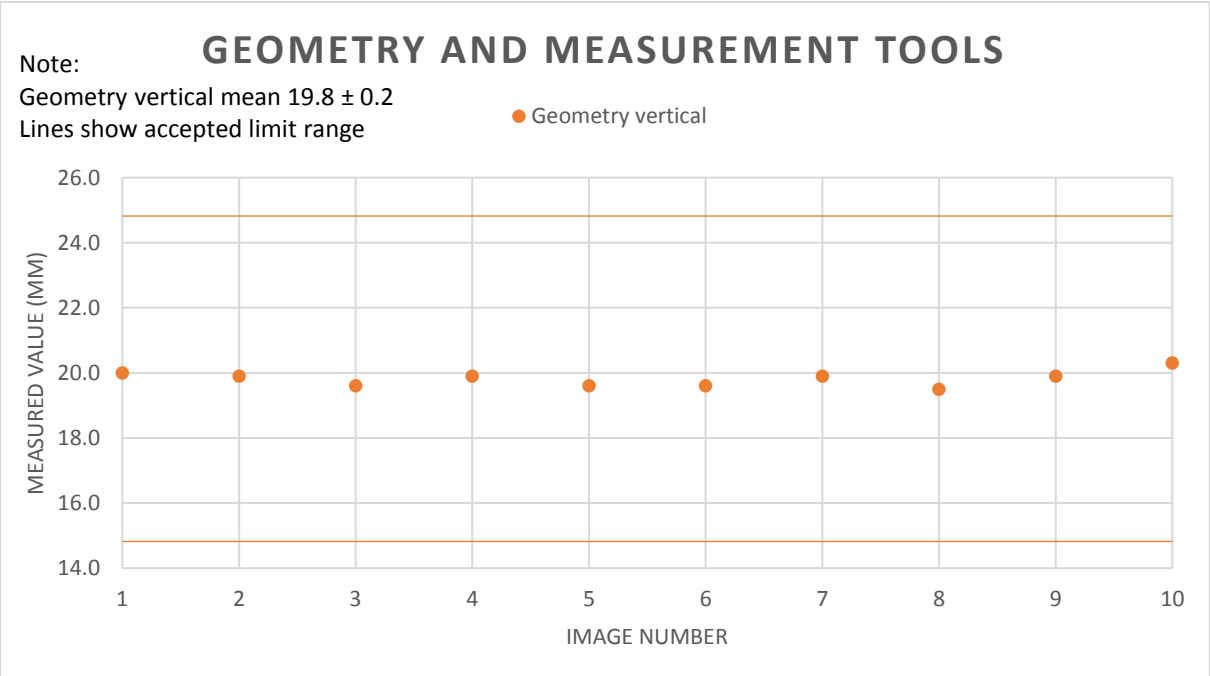

Figure 6.8: General x-rays data analysis software reproducibility results for geometry and measurement tools for vertical measurement with tolerance limits of ± 5 mm.

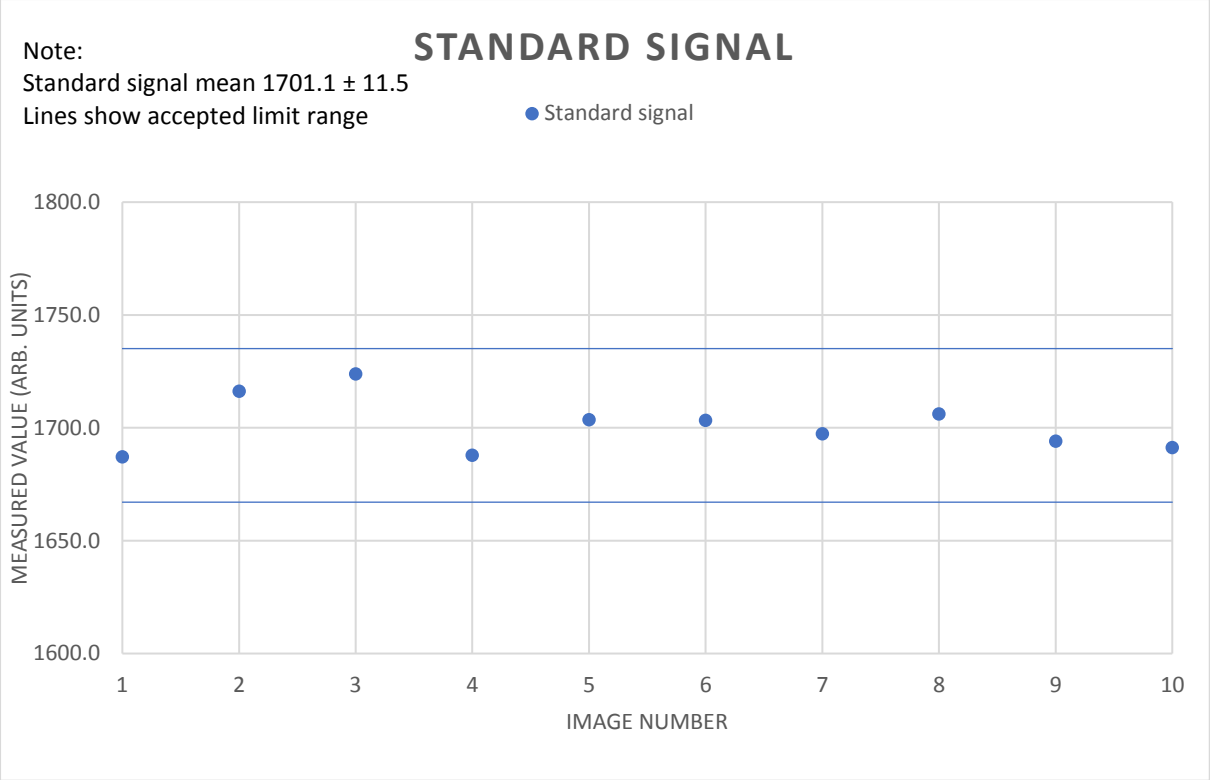

Figure 6.9: General x-rays data analysis software reproducibility results for standard signal with tolerance limits of ± 2 %.

Table 6.2 for the visual inspection of the obtained images refers. For low contrast detectability the tolerance from DoH is baseline ± 1 insert size. From Table 6.2 the baseline value would be 3, thus all results are within limits. A variation of ± 1 cm at 100 cm SID is accepted for positioning and alignment. With collimation of the light field to phantom edges, the phantom was cut off in images 1 and 3, so the x-ray field was smaller than the light field. The collimation was adjusted to extend beyond the phantom edges to have the whole phantom in the image, which resulted in the x-ray field being large enough to include the entire phantom. The inconsistency in the field size was attributed to the fact that the phantom was repositioned, with collimation readjusted, for every exposure. The set up was thus slightly different each time. There should not be any visible artefacts in images according to DoH recommendations, and none of the images contained any artefacts. Overall, the visual image quality should remain reproducible over time, and this was the case for images 1 to 10.

For sensitometry and standard signal the recommended tolerance from DoH is baseline grey scale ± 0.2. However, as a densitometer is not used to measure the

actual grey scale value, a tolerance of ± 2 % is suggested for the universal image quality assurance phantom and data analysis software. From Figures 6.2 to 6.4 for sensitometry and Figure 6.9 for standard signal, the obtained values are reproducible within this range. For uniformity, a tolerance of mean value ± 10 % is recommended for film/screen and CR systems and a mean value ± 5 % for DR. As a DR unit was used for the reproducibility exposures, the ± 5 % tolerance was applied to the mean value from the ten exposures. Except for images 4,8 and 10, with results within ± 10 %, all values fall within this range as seen in Figure 6.5. The limiting resolution should not vary by more than – 25 % according to the DoH accepted limits. Figure 6.5 shows the largest deviation being for image 6 of 0.9 %. For image noise, i.e. SNR and CNR, the limit is baseline ± 10 %. Figure 6.5 shows all results for SNR are within these limits, with image 8 having the largest deviation of 2.0 %. For CNR in Figure 6.6 image 6 has a deviation of 13.2%. This is outside of tolerance, and would require the test to be repeated, and for images 7 to 10 the results were within tolerance. The quoted tolerance for geometry and measurement tools are ± 0.5 cm or ± 2 %. Figures 6.7 and 6.8 shows all results within the ± 0.5 cm limit.

From Tables 6.2 and 6.3 and Figures 6.1 to 6.9 it is concluded that the results from the universal image quality assurance phantom and data analysis software are indeed reproducible and hence acceptable for routine image QC consistency testing in general x-ray imaging.

6.2 Fluoroscopy reproducibility testing

For fluoroscopy the results for the reproducibility testing are included in Tables 6.5 and 6.6 and in Figures 6.10 to 6.19. The exposure technique factors are shown in Table 6.4. For each exposure the phantom was repositioned completely.

Table 6.4: Reproducibility testing exposure technique factors for fluoroscopy imaging.

Modality	Fluoroscopy
Unit	Siemens Axiom Luminos DRF
kV	AEC (hand protocol)
mAs	AEC (hand protocol)
FFD	115 cm
Slice thickness	-
Other	Outside bucky

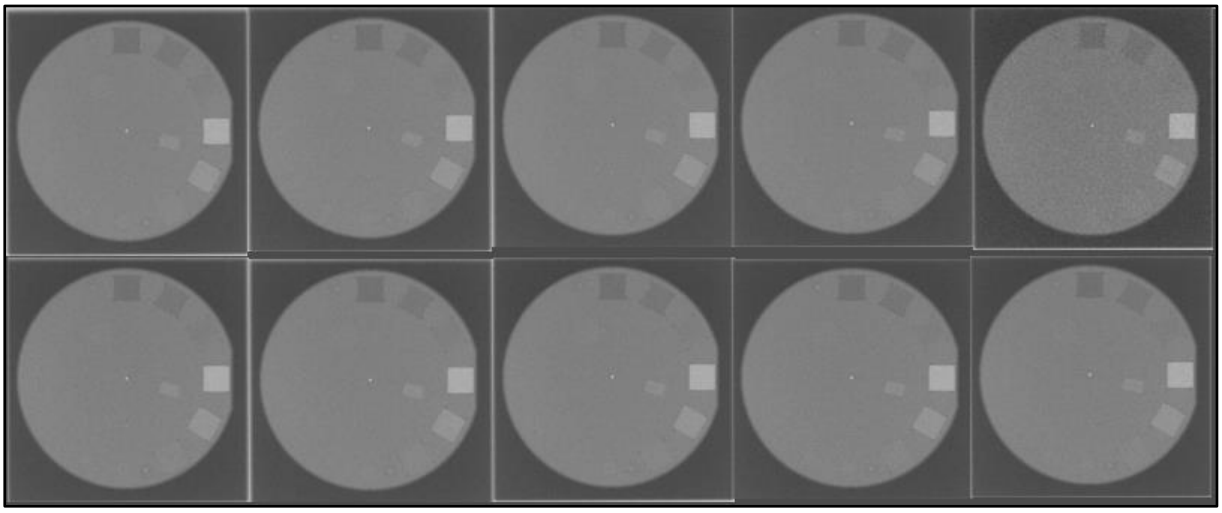

Figure 6.10: Fluoroscopy reproducibility images.

Table 6.5: Fluoroscopy x-ray reproducibility testing visual inspection results. (Appendix A, A.2.3.4)

Image number	Low contrast detectability	Positioning and alignment	Artefacts	Image quality visual inspection
1	8	Correct	None	Grainy low contrast, other projection radiography inserts not visible
2	8	Correct	None	Grainy low contrast, other projection radiography inserts not visible
3	10	Correct	None	Grainy low contrast, other projection radiography inserts not visible
4	10	Correct	None	Grainy low contrast, other projection radiography inserts not visible
5	20	Correct	None	Noisy, only 20 mm insert and central bead visible
6	8	Correct	None	Grainy low contrast, other projection radiography inserts not visible
7	8	Correct	None	Grainy low contrast, other projection radiography inserts not visible
8	8	Correct	None	Grainy low contrast, other projection radiography inserts not visible
9	10	Correct	None	Grainy low contrast, other projection radiography inserts not visible
10	10	Correct	None	Grainy low contrast, other projection radiography inserts not visible

Table 6.6: Fluoroscopy x-ray reproducibility testing data analysis software results. (Appendix A, A.2.3.5)

Image number	Sensitometry values as measured with software (arb. units)					
	Air		Lung		Supawood	
	Mean	Std dev	Mean	Std dev	Mean	Std dev
1	2816.5	54.2	2857.5	50.9	2928.1	57.4
2	2809.9	54.2	2857.2	63.3	2925.5	60.7
3	2816.1	57.6	2860.5	54.5	2926.6	62.1
4	2755.4	119.4	2813.2	131.2	2890.1	143.2
5	2798.8	118.6	2844.9	124.8	2924.4	137.1
6	2796.1	59.0	2845.8	59.6	2913.2	62.5
7	2802.0	55.6	2855.9	56.3	2926.6	59.7
8	2802.4	58.2	2847.6	59.5	2919.1	63.6
9	2790.5	56.1	2842.9	57.6	2911.8	60.8
10	2791.9	55.6	2842.5	56.7	2910.1	59.7
Average calculated	2798.0 ± 16.6		2846.8 ± 12.9		2917.6 ± 11.2	
Image number	Sensitometry values as measured with software (arb. units)					
	Bone		Teflon		RGD240	
	Mean	Std dev	Mean	Std dev	Mean	Std dev
1	3380.5	77.7	3150.3	64.5	3009.5	64.2
2	3384.4	88.7	3153.4	70.2	3011.8	65.8
3	3385.1	74.5	3148.0	65.1	3015.1	63.0
4	3409.4	197.2	3129.5	164.8	2976.1	135.3
5	3441.0	196.3	3170.6	164.7	3001.7	129.9
6	3380.3	83.5	3140.2	72.4	3001.3	67.6
7	3379.2	81.0	3148.9	68.9	3012.1	63.4
8	3384.2	77.1	3143.3	73.0	3005.1	64.5
9	3373.2	83.2	3139.1	69.1	3001.0	65.7
10	3377.6	82.3	3139.1	69.4	3004.3	66.2
Average calculated	3389.5 ± 19.5		3146.2 ± 10.5		3003.8 ± 10.4	

Image number		Limiting resolution (cycles/cm)	Image noise (arb. units)		Geometry and measurement tools (mm)		Standard signal (arb. units)	
			SNR	CNR	Horizontal value	Vertical value	Mean	Std dev
1	22.9	4.9	47.5	0.7	20.9	20.4	2966.4	61.9
2	23.3	4.9	46.0	0.6	19.5	20.9	2966.7	63.3
3	25.5	4.4	48.3	0.7	20.0	20.9	2967.9	62.0
4	22.4	4.7	42.1	0.6	20.0	20.0	2931.3	147.3
5	29.9	4.9	42.4	0.3	18.6	18.2	2968.0	139.2
6	28.7	4.3	45.1	0.6	20.8	20.5	2959.4	64.6
7	28.7	4.6	47.9	0.7	20.4	20.9	2964.8	60.3
8	22.0	4.3	46.6	0.7	20.0	20.4	2960.9	61.4
9	29.7	4.3	46.0	0.7	20.0	20.4	2957.5	63.6
10	22.1	4.3	46.5	0.7	19.3	20.3	2956.8	62.4
Average calculated	25.5±3.2	4.6±0.3	45.8±2.0	0.6±0.1	20.0±0.7	20.3±0.8	2960.0±10.4	

The limits from DoH for fluoroscopy and general x-rays are the same. Low contrast detectability baseline from Table 6.5 was 8 mm. A tolerance of +1 insert size is allowed, thus image 5 is out of tolerance. When results are out of tolerance, the recommendation, according to Figure A.2 in Appendix A, is to repeat the test. For images 6 to 10 the result was in tolerance. For positioning and alignment, a tolerance of ± 1 cm at 100 cm SID is allowed according to DoH regulations. The SID used was 115 cm and the agreement between the set light field (set to edges of phantom) and the obtained x-ray image was within tolerance. No artefacts were seen in the images, as is recommended by DoH. However, the overall visual image quality of the images was poor. All images were of low contrast, as is seen from Figure 6.10 with very small CNR, and most other planar imaging inserts were very unclear or not visible. The recommendation for visual image quality inspection from DoH is that the results must be reproducible, and although the image quality was poor, it was reproducible over the ten images.

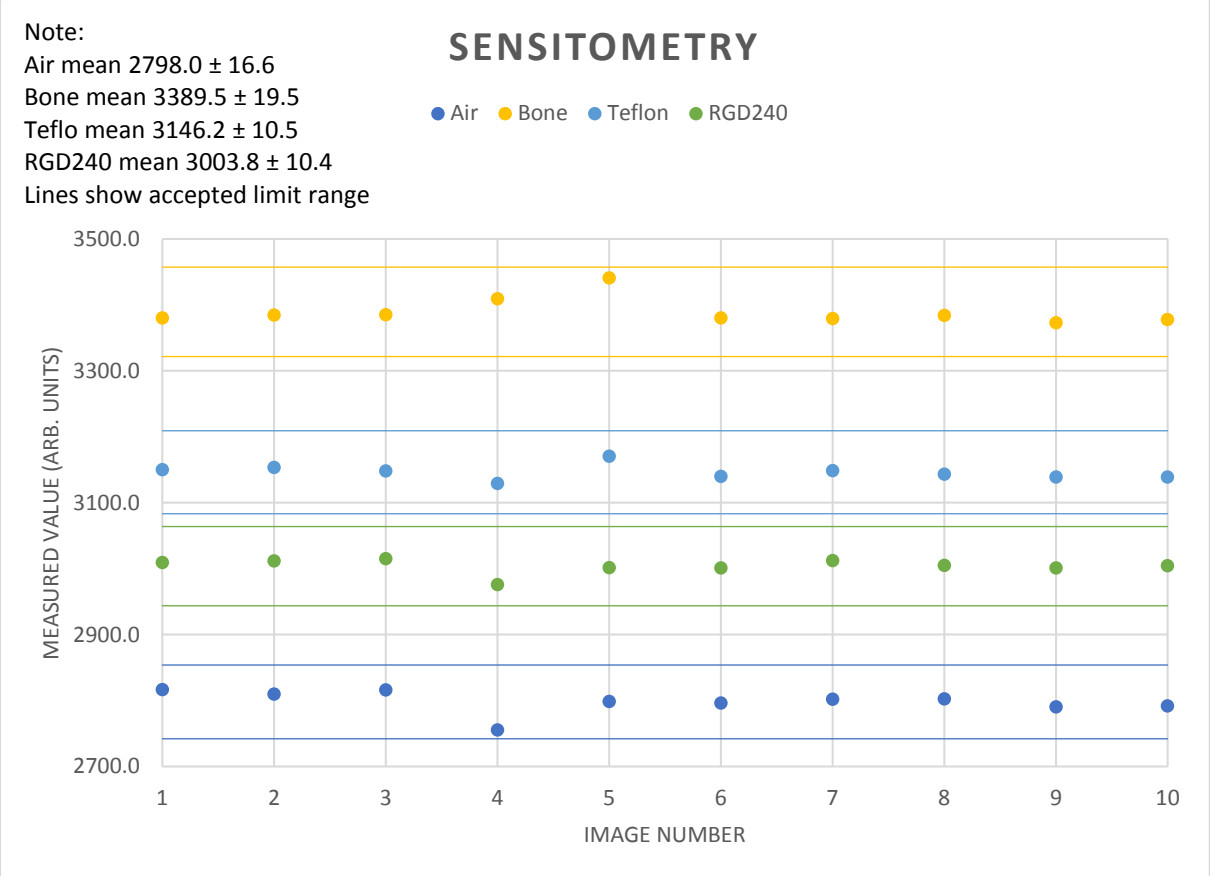

Figure 6.11: Fluoroscopy data analysis software reproducibility results for sensitometry for air, bone, Teflon and RGD240 with tolerance limits of ± 2 %.

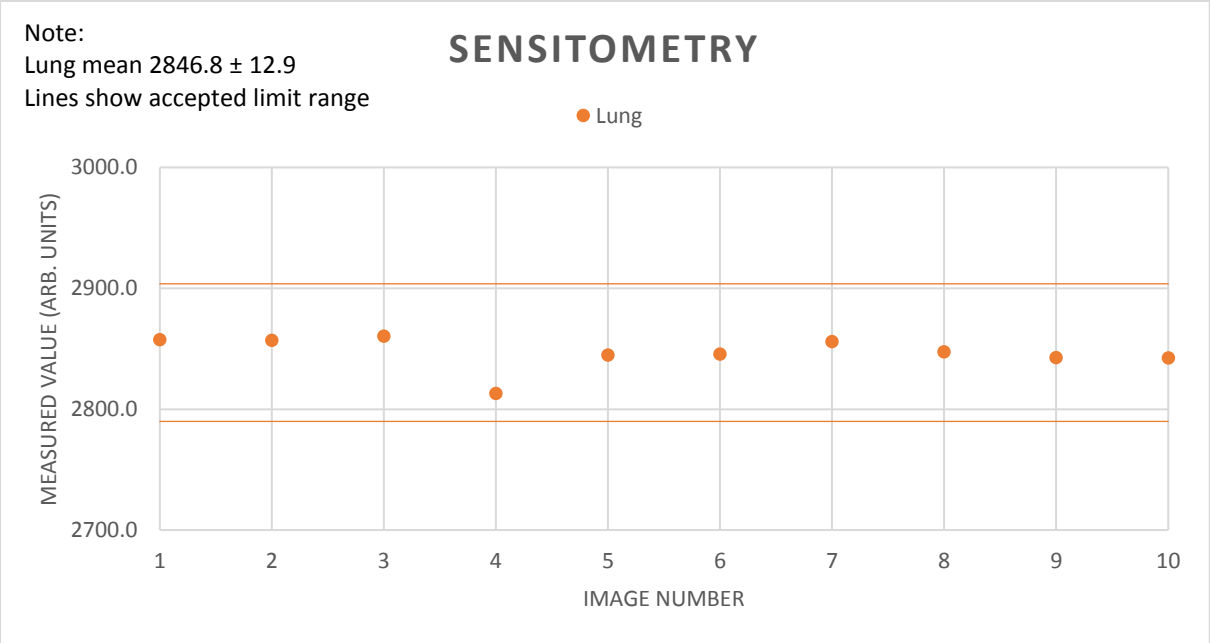

Figure 6.12: Fluoroscopy data analysis software reproducibility results for sensitometry for lung with tolerance limits of ± 2 %.

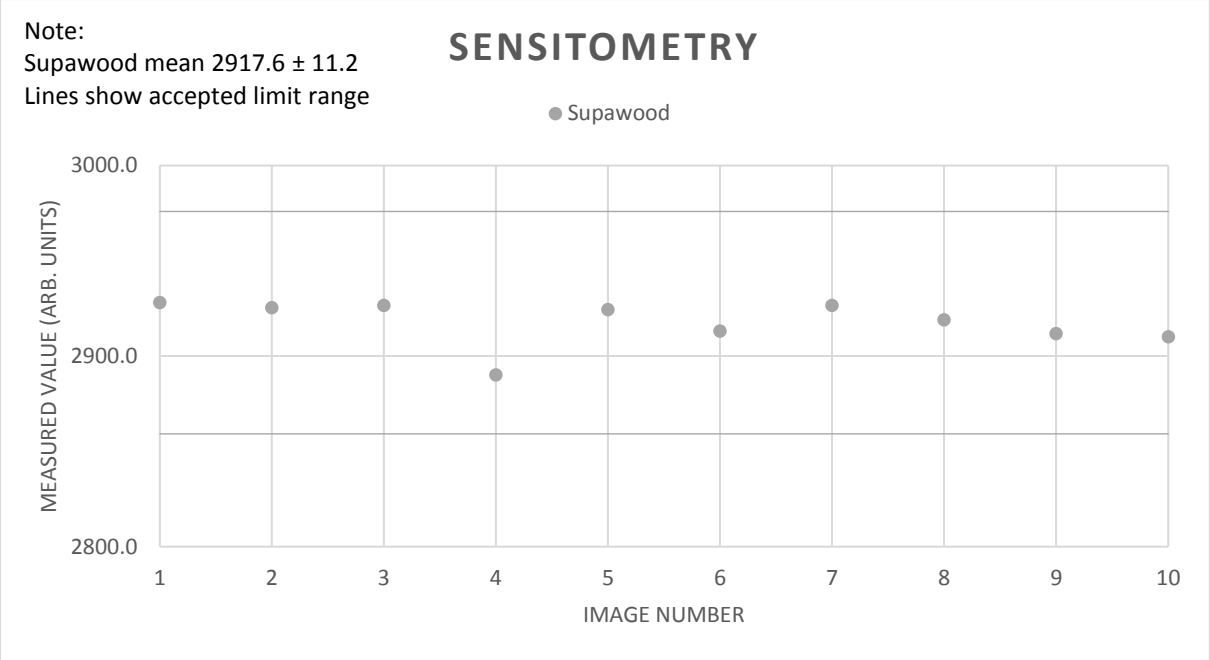

Figure 6.13: Fluoroscopy data analysis software reproducibility results for sensitometry for supawood with tolerance limits of ± 2 %.

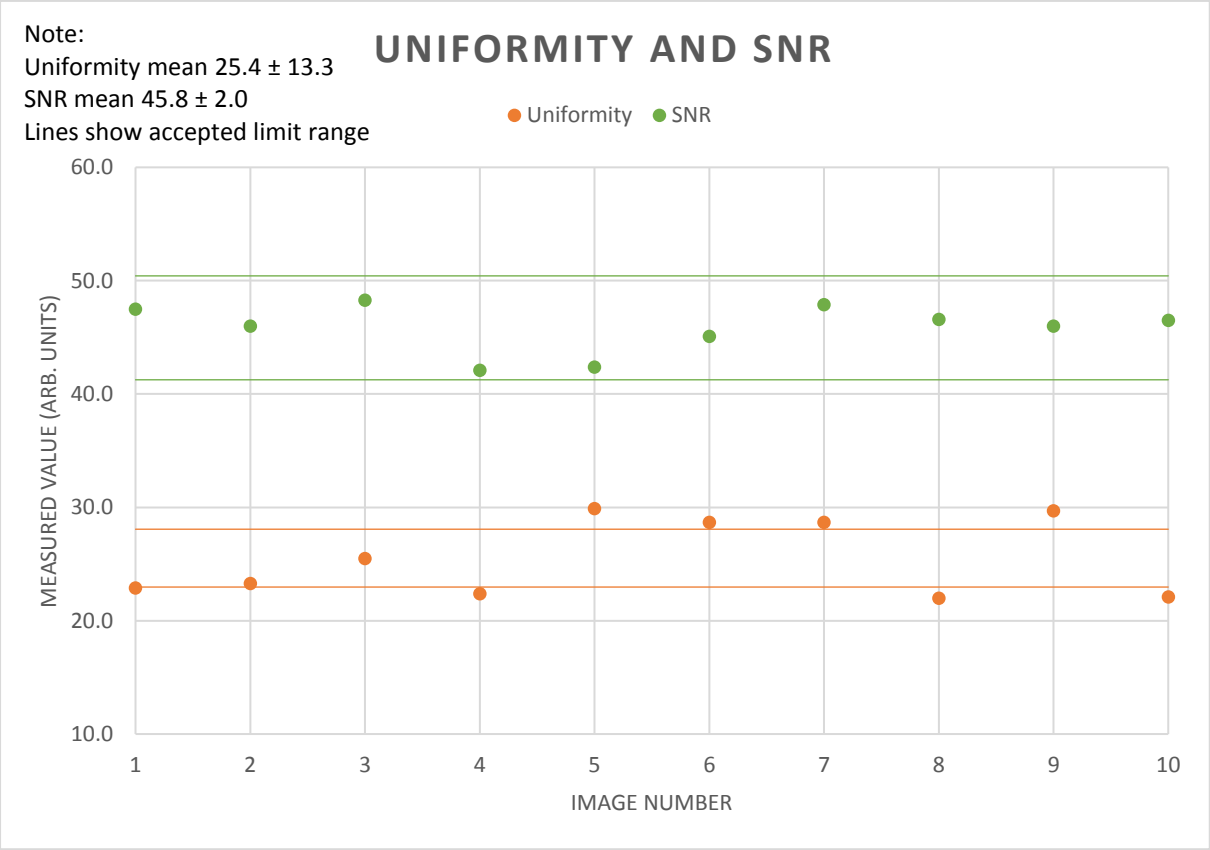

Figure 6.14: Fluoroscopy data analysis software reproducibility results for uniformity and SNR with tolerance limits of ± 10 %.

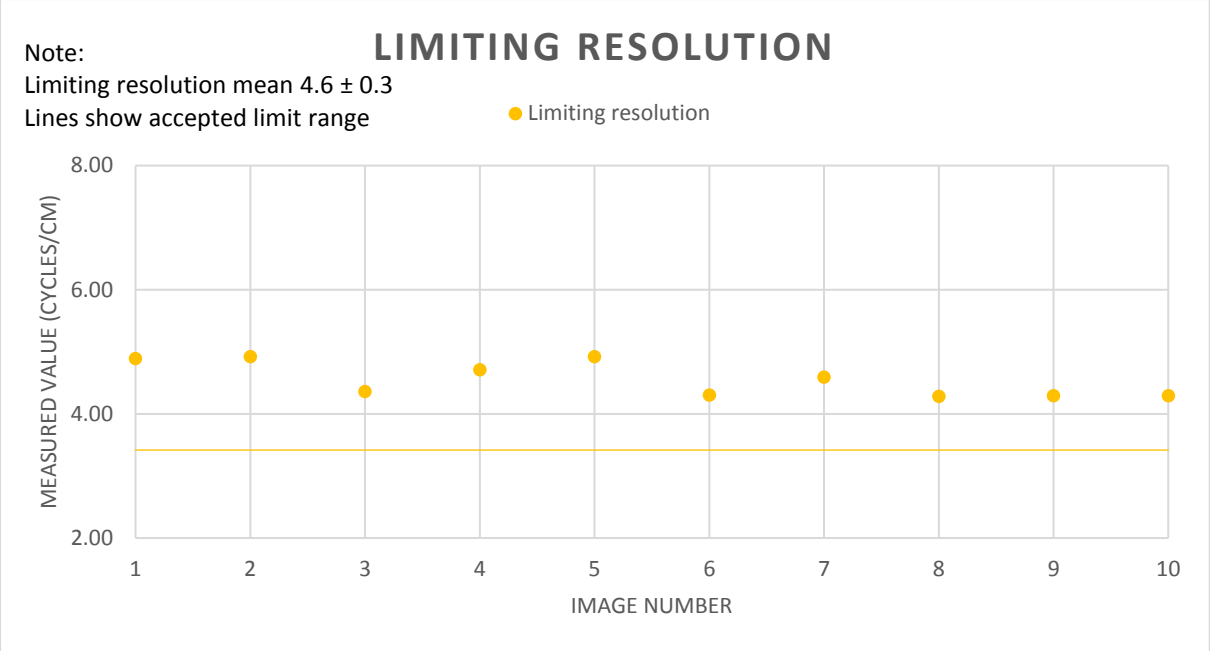

Figure 6.15: Fluoroscopy data analysis software reproducibility results for limiting resolution results with tolerance limits of – 25 %.

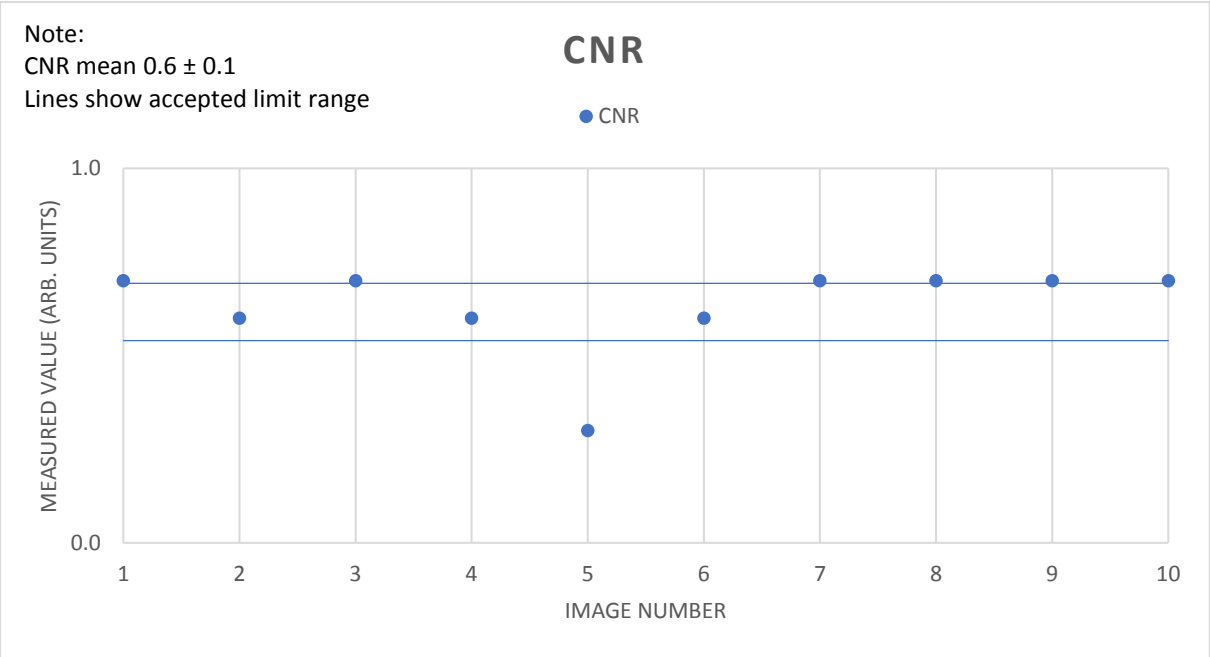

Figure 6.16: Fluoroscopy data analysis software reproducibility results for CNR with tolerance limits of ± 10 %.

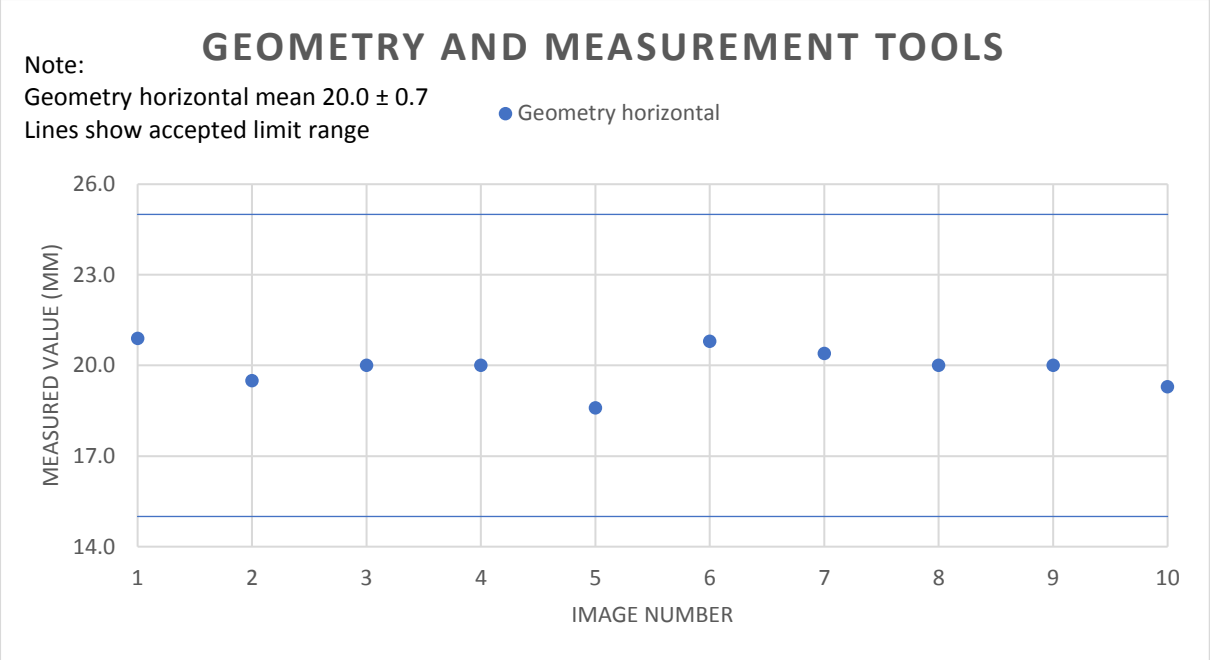

Figure 6.17: Fluoroscopy data analysis software reproducibility results for geometry and measurement tools results for horizontal measurement with tolerance limits of ± 5 mm.

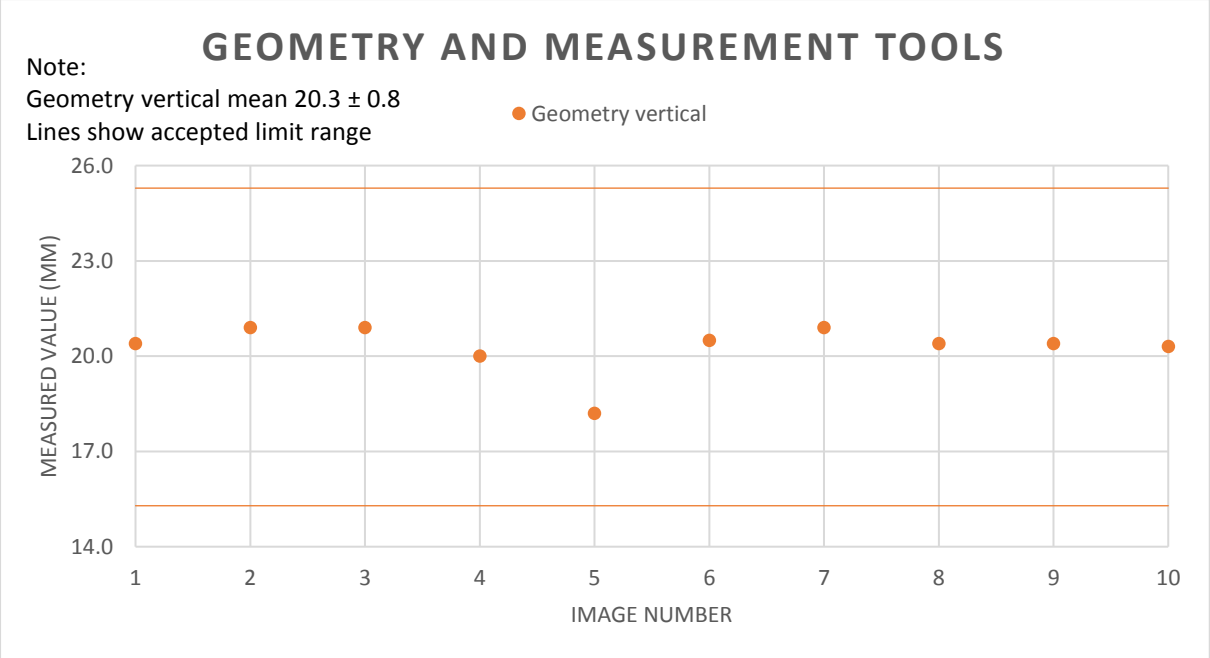

Figure 6.18: Fluoroscopy data analysis software reproducibility results for geometry and measurement tools for vertical measurement with tolerance limits of ± 5 mm.

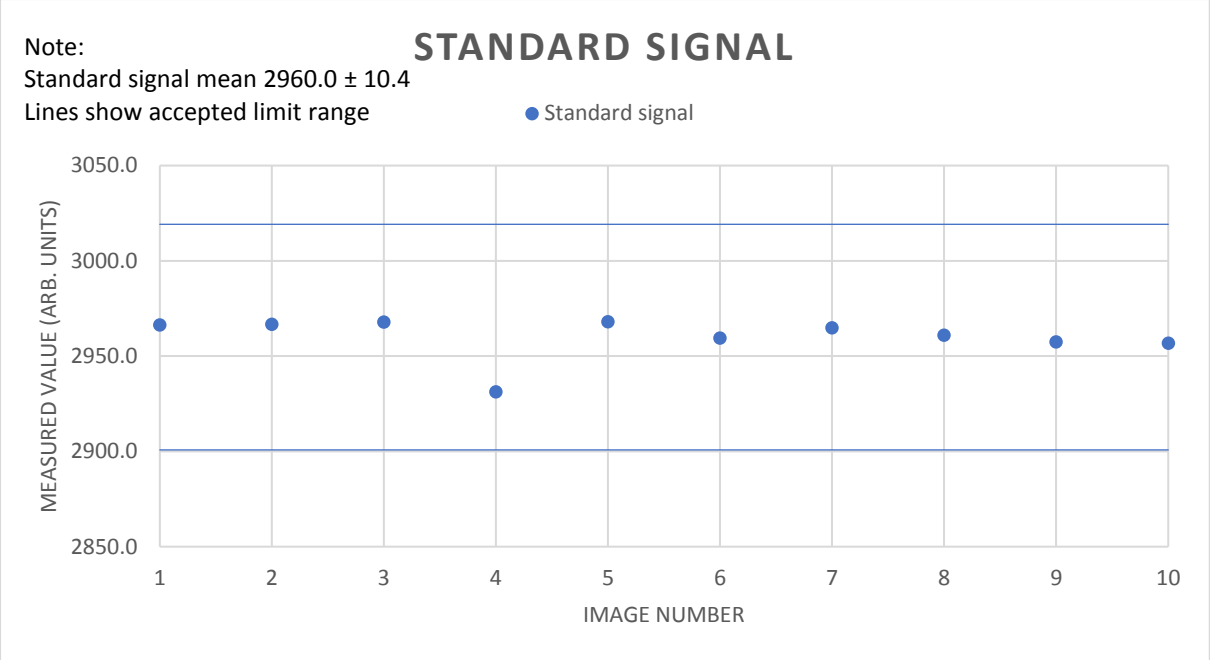

Figure 6.19: Fluoroscopy data analysis software reproducibility results for standard signal results with tolerance limits of ± 2 %.

For sensitometry and standard signal the recommended tolerance from DoH is baseline grey scale ± 0.2. As discussed in section 6.1, as a densitometer is not used to measure the actual grey scale value, a tolerance of ± 2 % is suggested for the universal image quality assurance phantom and data analysis software. From Figures 6.11 to 6.13 for sensitometry and Figure 6.19 for standard signal, it is clear that the obtained values are reproducible within this range. Figure 6.14 shows the results for uniformity and SNR, both with a DoH recommended tolerance of ± 10 %. All SNR results were within tolerance. The uniformity of image 5 is 17.7 % above the mean value, the largest deviation seen in the ten obtained images. However, from Table 6.5 it is seen that the image quality of image 5 was the poorest, with a noisy and grainy image. Such a deviation is therefore expected. Repetition of the test produced images with better image quality and results within tolerance. A similar trend is seen with the CNR results in Figure 6.16. The percentage difference for image 5 is 50 %, however as the CNR values are such small values, a small change will reflect a large percentage variation. The limiting resolution should not vary by more than – 25 % according to the DoH accepted limits. Figure 6.15 shows the values for images 1, 2 and 5 to be better than the mean value. For this calculation the MTF balls, as marked in Figure 5.4 were not used. In some images the balls were not visible. In those

images where the largest of the three balls, i.e. 1 mm diameter, was visible, the data analysis software could not produce an acceptable MTF using the ball, due to the graininess of the images. The limiting resolution calculations for fluoroscopy were thus done using the central 2 mm diameter ball. The quoted tolerance for geometry and measurement tools are ± 0.5 cm or ± 2 %. Figure 6.17 for horizontal and Figure 6.18 for vertical shows the geometry and measurement tools results. The accepted tolerance is ± 0.5 cm. For the horizontal measurements, images 1, 6 and 5 measured values higher than the average value from the ten images, with image 5 having the largest deviation of 7.0 %. Image 5 also measured 10.3 % lower than the average horizontal value. As the PMMA cylinder, shown in Figure 5.7 was very unclear in the fluoroscopy images, and almost invisible in image 5 with the poor image quality as from Table 6.5, these differences were expected.

The results in Tables 6.5 and 6.6 and Figures 6.10 to 6.19 show that the universal image quality assurance phantom and data analysis software can be used reproducibly in routine fluoroscopy image quality control.

6.3 Mammography reproducibility testing

Reproducibility tests with the universal image quality assurance phantom and data analysis software was also done for mammography, with exposure technique factors as shown in Table 6.7. The results are tabulated in Tables 6.8 and 6.9 and shown in Figures 6.20 to 6.27.

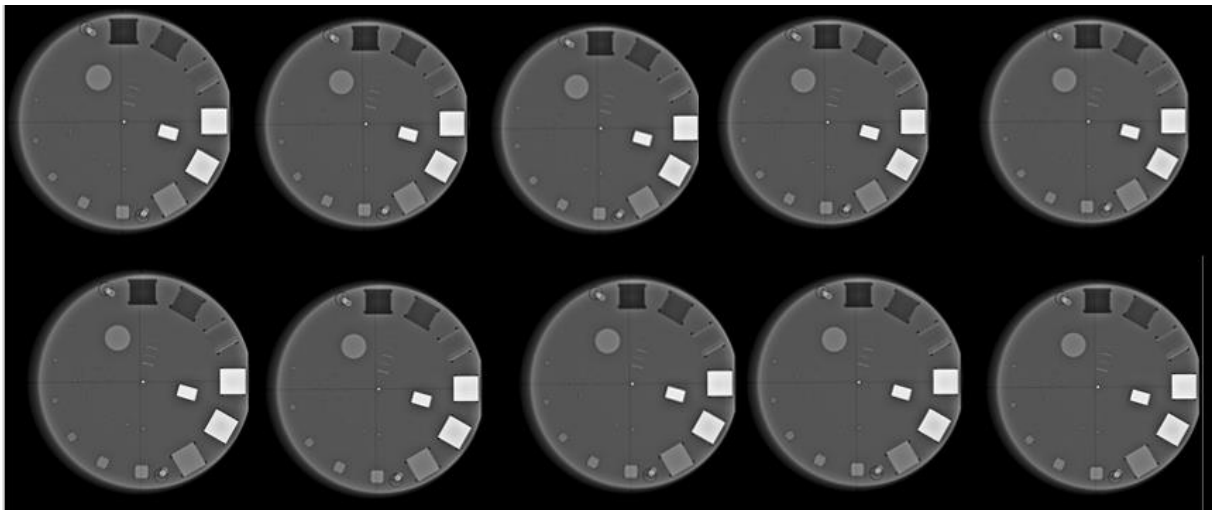

Figure 6.20: Mammography reproducibility images.

Table 6.7: Reproducibility testing exposure technique factors for mammography imaging.

Modality	Mammography
Unit	Siemens Mammomat Inspiration
kV	28
mAs	63
FFD	-
Slice thickness	-
Other	Large focus, Mo/Rh

Table 6.8: Mammography reproducibility testing visual inspection results. (Appendix A, A.2.4.4)

Image number	Low contrast detectability	Positioning and alignment	Artefacts	Image quality visual inspection
1	1	Correct	Slight geometrical distortion	Acceptable
2	1	Correct	Slight geometrical distortion	Acceptable
3	1	Correct	Slight geometrical distortion	Acceptable
4	1	Correct	Slight geometrical distortion	Acceptable
5	1	Correct	Slight geometrical distortion	Acceptable
6	1	Correct	Slight geometrical distortion	Acceptable
7	1	Correct	Slight geometrical distortion	Acceptable
8	1	Correct	Slight geometrical distortion	Acceptable
9	1	Correct	Slight geometrical distortion	Acceptable
10	1	Correct	Slight geometrical distortion	Acceptable

Image number	Fibres	Masses	Micro-calcifications
1	6	8	5
2	6	8	5
3	6	8	5
4	6	8	5
5	6	8	5
6	6	8	5
7	6	8	5
8	6	8	5
9	6	8	5
10	6	8	5

Table 6.9: Mammography reproducibility testing data analysis software results. (Appendix A, A.2.4.5)

Image number	Sensitometry values as measured with software (arb. units)					
	Air		Lung		Supawood	
	Mean	Std dev	Mean	Std dev	Mean	Std dev
1	785.7	62.9	1035.3	141.5	1317.2	43.9
2	796.5	62.8	1033.5	139.5	1315.1	43.5
3	782.5	63.5	1042.5	142.3	1315.7	43.1
4	784.8	66.3	1042.7	143.0	1321.0	44.8
5	803.6	61.9	1042.5	143.0	1322.1	43.0
6	792.6	60.7	1042.1	143.1	1326.7	50.0
7	809.8	64.4	1045.6	142.8	1323.0	46.3
8	792.2	60.9	1044.6	141.2	1320.8	44.3
9	790.6	61.5	1039.6	142.2	1324.5	45.1
10	790.7	63.4	1045.5	142.9	1326.1	45.2
Average calculated	792.9 ± 8.1		1041.4 ± 3.9		1321.2 ± 9.9	
Image number	Sensitometry values as measured with software (arb. units)					
	Bone		Teflon		RGD240	
	Mean	Std dev	Mean	Std dev	Mean	Std dev
1	3583.2	37.9	3390.9	63.5	1943.3	36.5
2	3594.7	45.1	3375.7	64.4	1928.9	31.7
3	3606.8	52.0	3360.9	49.6	1928.7	30.6
4	3622.0	57.0	3389.7	64.0	1931.2	31.4
5	3597.9	48.3	3390.7	64.2	1940.2	35.8
6	3604.5	49.3	3418.4	85.7	1984.1	41.1
7	3611.5	53.8	3400.7	77.5	1932.8	33.1
8	3606.7	47.3	3405.7	71.3	1944.5	36.7
9	3598.0	44.2	3401.9	77.6	1934.2	32.9
10	3601.8	48.8	3374.7	58.0	1944.4	35.5
Average calculated	3602.7 ± 9.9		3390.9 ± 16.1		1941.2 ± 15.5	

Image number	Uniformity (arb. units)	Limiting resolution (cycles/cm)	Image noise (arb. units)		Geometry and measurement tools (mm)		Standard signal (arb. units)	
			SNR	CNR	Horizontal value	Vertical value	Mean	Std dev
1	10.7	17.9	49.4	27.9	20.1	20.1	1379.3	20.2
2	11.7	18.1	52.5	27.6	20.1	20.3	1378.1	20.2
3	10.1	17.9	54.3	27.7	19.6	20.3	1379.8	20.0
4	11.6	17.9	56.5	27.8	20.1	20.1	1380.7	20.1
5	11.9	18.1	58.1	26.8	19.6	20.1	1382.7	20.2
6	13.5	18.0	52.7	27.5	20.1	20.1	1380.8	20.8
7	13.8	18.1	58.4	25.7	20.1	20.1	1382.0	20.3
8	14.5	18.1	57.9	25.8	19.6	20.1	1381.0	20.3
9	14.1	18.0	51.6	26.2	20.1	19.7	1382.1	20.3
10	15.4	17.9	57.1	26.3	19.6	20.1	1383.5	20.7
Average calculated	12.7±1.7	18.0±0.1	54.9±3.0	26.9±0.8	19.9±0.2	20.1±0.2	1381.0±1.6	

According to the DoH recommendations, all low contrast detectability, masses, fibres and micro-calcifications should be visible. From Table 6.8 above this was the case for the ten reproducibility images. The flat side of the phantom was aligned with the chest wall side of the bucky, and the alignment was correct and within the specified ± 2 % of SID. According to DoH no artefacts should be visible in the image. However, slight geometric distortion, as discussed in section 4.3.3, was still evident. This however remained reproducible over the ten acquired images and did not interfere with further image quality assessment. It is therefore recommended that for the universal image quality assurance phantom and data analysis software, such geometric distortion will be accepted as normal and that only artefacts other than this should be noted. The image quality should remain reproducible with visual inspection test, and this was confirmed in Table 6.8.

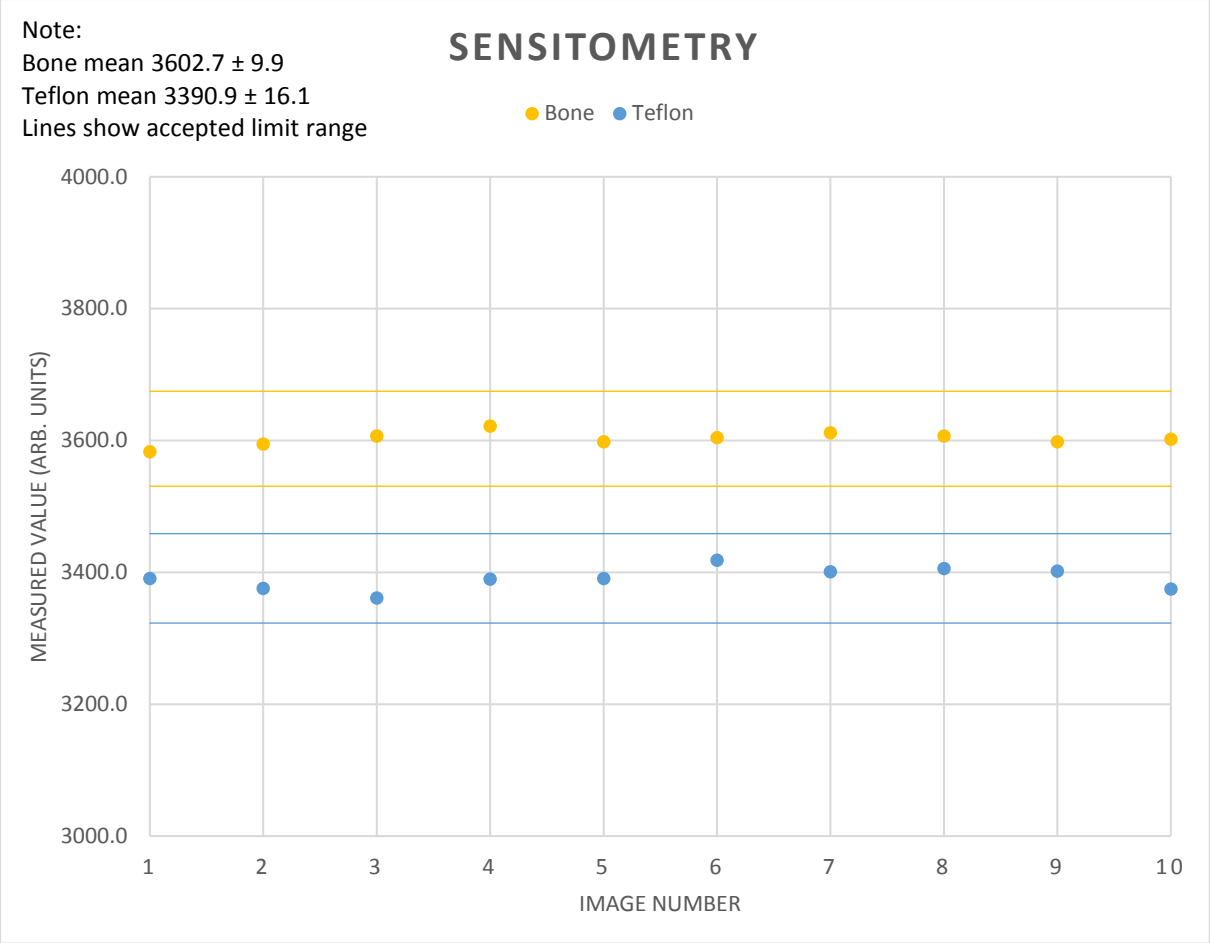

Figure 6.21: Mammography data analysis software reproducibility results for sensitometry for bone and Teflon with tolerance limits of ± 2 %.

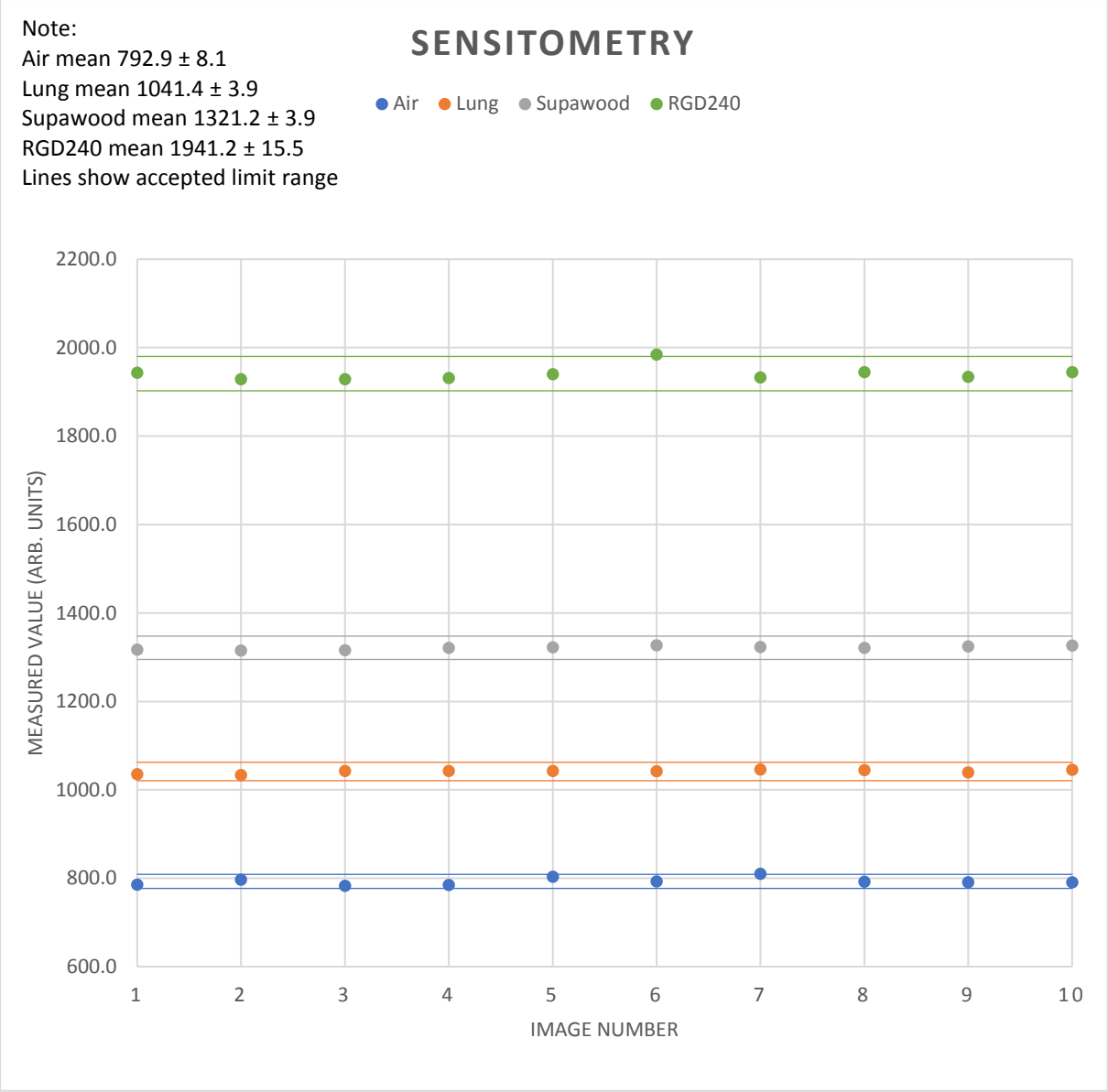

Figure 6.22: Mammography data analysis software reproducibility results for sensitometry results for air, lung, Supawood and RGD240 with tolerance limits of ± 2 %.

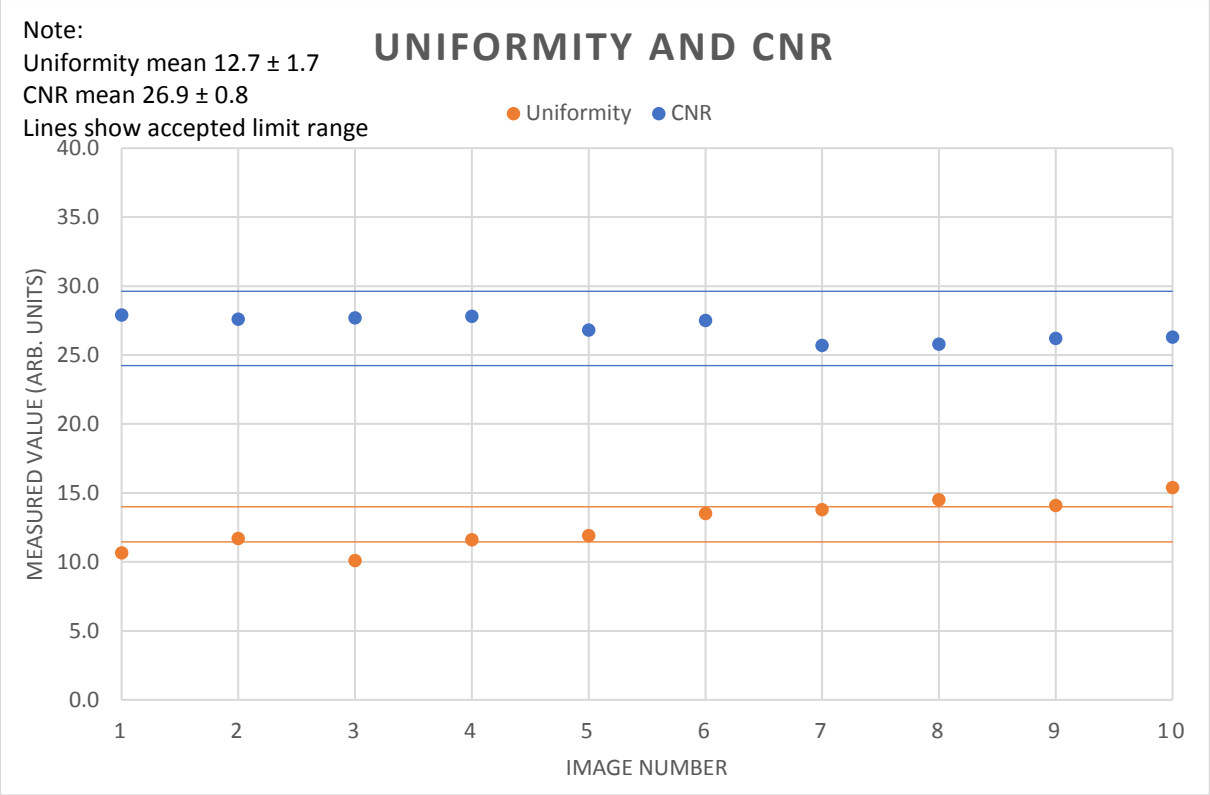

Figure 6.23: Mammography data analysis software reproducibility results for uniformity and CNR with tolerance limits of ± 10 %.

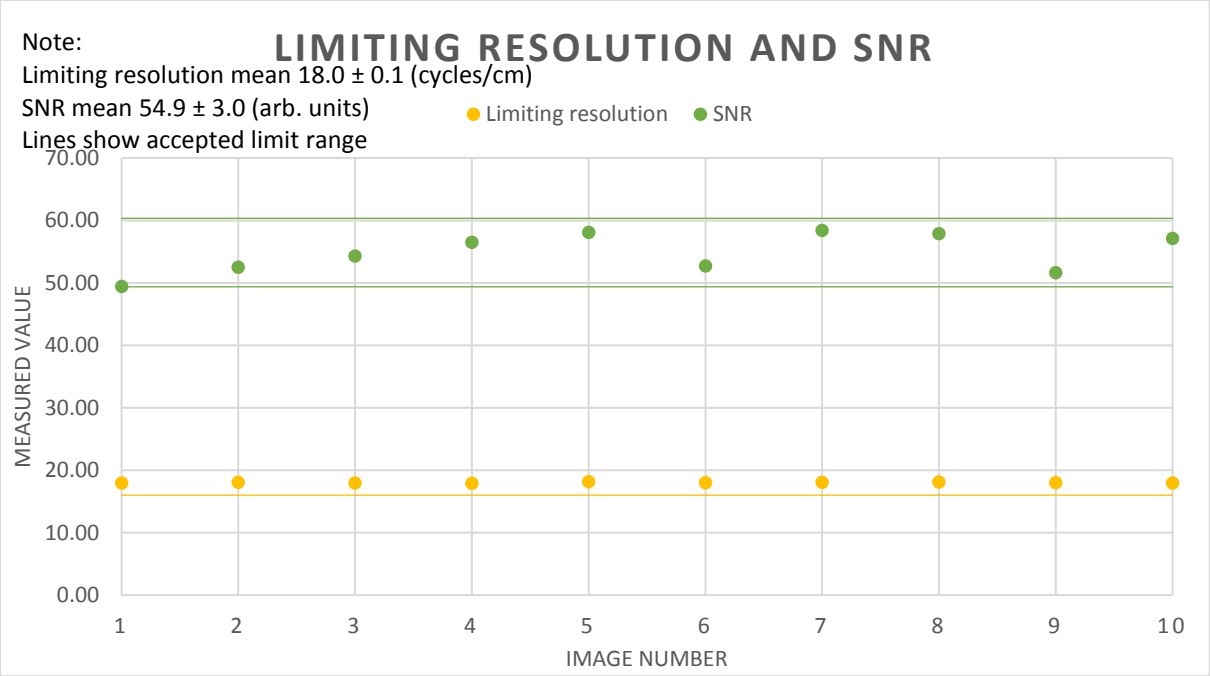

Figure 6.24: Mammography data analysis software reproducibility results for limiting resolution and SNR with tolerance limits of – 2 for limiting resolution and ± 10 % for SNR.

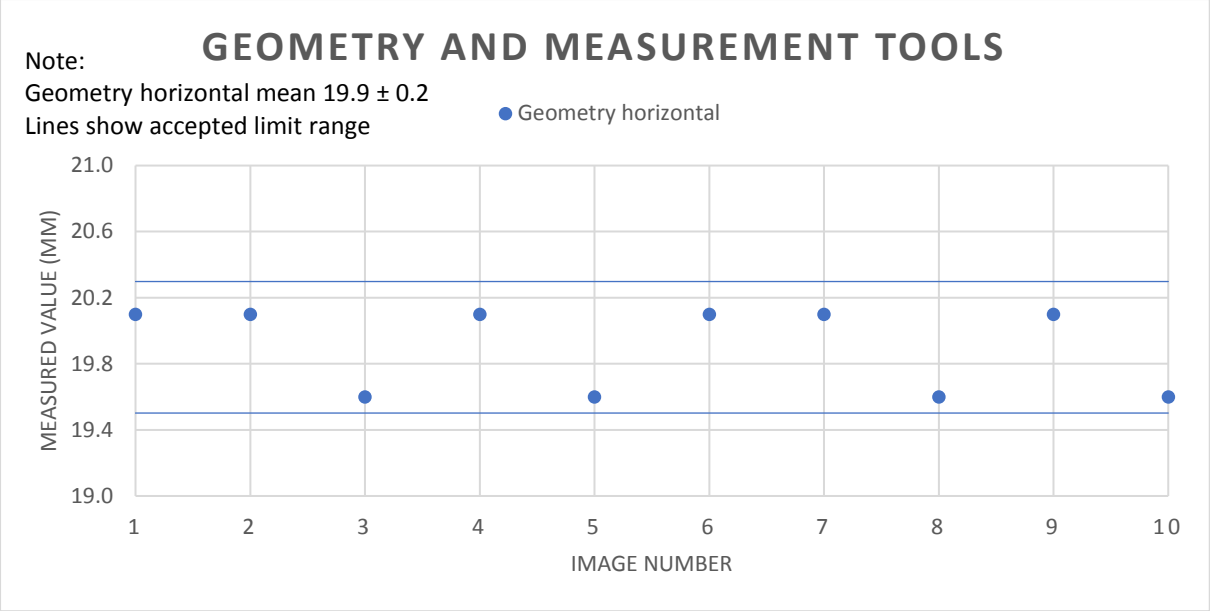

Figure 6.25: Mammography data analysis software reproducibility results for geometry and measurement tools results for horizontal measurement with tolerance limits of ± 2 %.

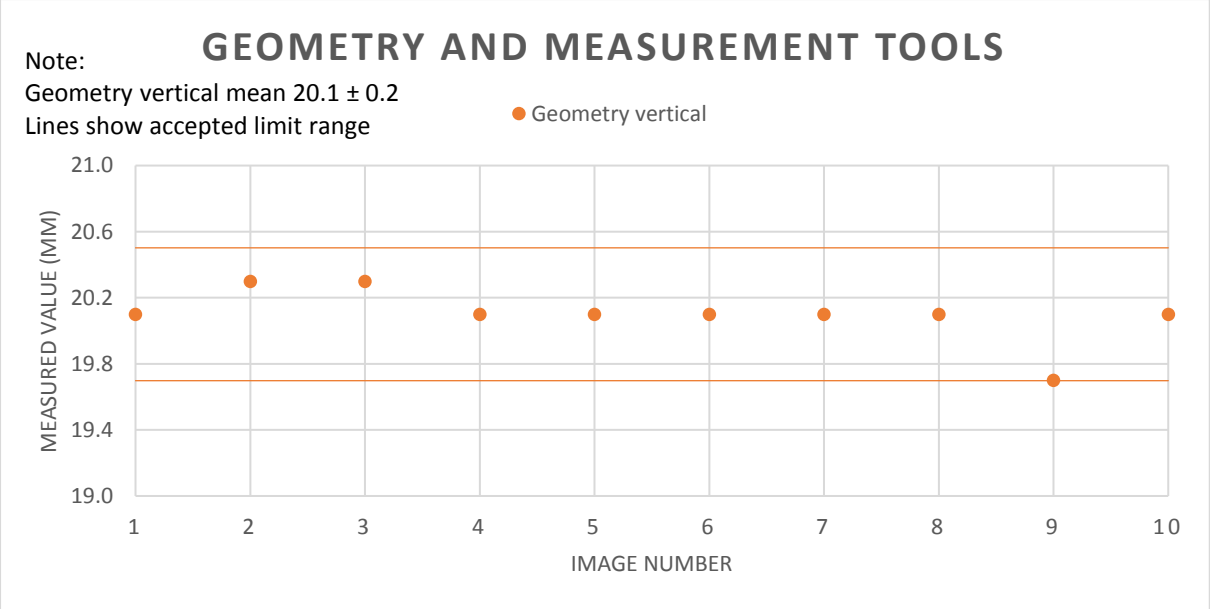

Figure 6.26: Mammography data analysis software reproducibility results for geometry and measurement tools for vertical measurement with tolerance limits of ± 2 %.

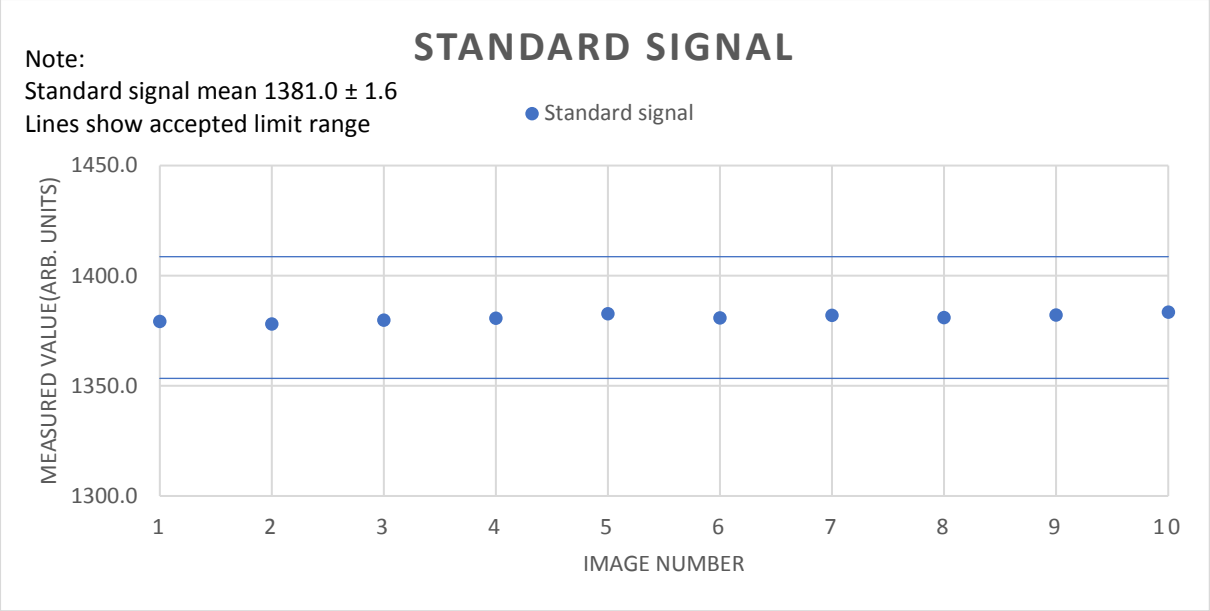

Figure 6.27: Mammography data analysis software reproducibility results for standard signal with tolerance limits of ± 2 %.

For sensitometry and standard signal the recommended tolerance from DoH is baseline grey scale ± 0.2. Again, a tolerance of ± 2 % is suggested for the universal image quality assurance phantom and data analysis software as previously discussed. From Figures 6.21 and 6.22 for sensitometry and Figure 6.27 for standard signal, it is clear that the obtained values are reproducible within this range. Figure 6.23 shows the results for uniformity and CNR, with a DoH recommended tolerance of ± 10 %. With uniformity, image 1 was 15.7 % below average and image 10 21.3 % above the average value for the ten images. According to the user's manual in Appendix A, Figure A.2, in the event of a value being out of tolerance the test should be repeated. For the other eight images the results were in tolerance. The results for CNR were within limits. The limiting resolution is quoted as 11 – 13 lp/mm by DoH, i.e. a variation of 2. In Figure 6.24 tolerance limits of – 2 were used and the obtained results were within, i.e. above, this limit. SNR also has an accepted ± 10 % limit by DoH, and the obtained results were within this limit in Figure 6.24. In mammography, the limit for geometry and measurement tools is ± 0.5 cm or ± 2 %. As ± 2 % resulted in a smaller actual value, this was used as the limit in Figures 6.25 and 6.26. All results were within these limits.

The universal image quality assurance phantom and the data analysis software are acceptable routine QC tools in mammography also, giving reproducible results as deduced from Figures 6.20 to 6.27 and Tables 6.8 and 6.9.

6.4 CT scanning reproducibility testing

Reproducibility testing was also done for CT scanning with exposure parameters as shown in Table 6.10. The results are recorded in Tables 6.11 and 6.12 and in Figures 6.28 to 6.36.

Table 6.10: Reproducibility testing exposure technique factors for CT scanning.

Modality	CT scanning
Unit	Siemens Somatom Definition Edge
kV	120
mAs	385
FFD	-
Slice thickness	5 mm
Other	190 cm FOV, CareDose 4D, Pitch 0.8

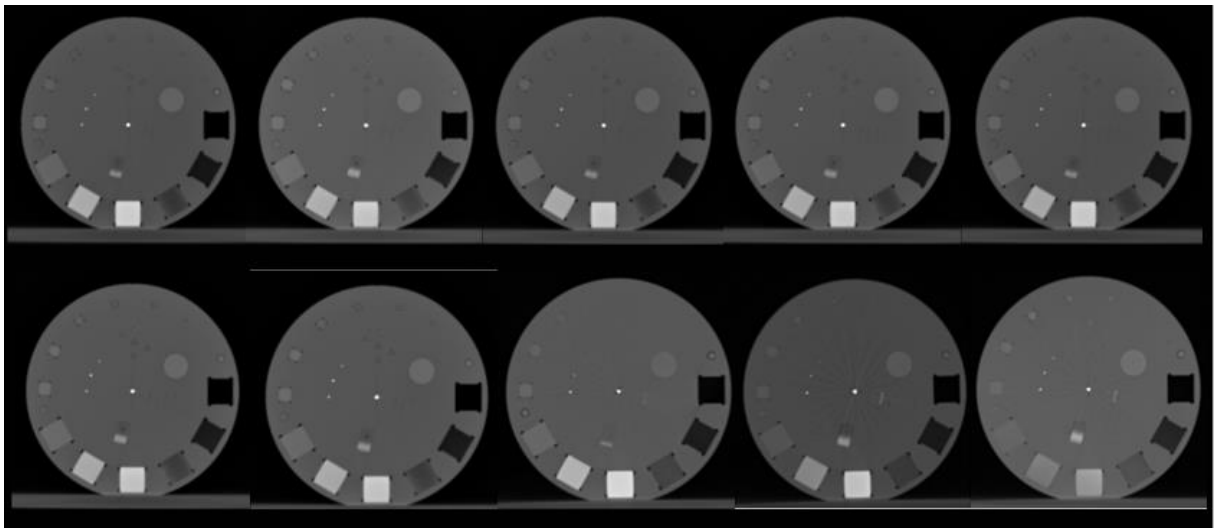

Figure 6.28: CT scanning reproducibility images.

Table 6.11: CT scanning reproducibility testing visual inspection results. (Appendix A, A.2.5.4)

Image number	Low contrast detectability	Positioning and alignment	Artefacts	Image quality visual inspection
1	1	Correct	Streaks from central bead	Acceptable
2	1	Correct	Streaks from central bead	Acceptable
3	1	Correct	Streaks from central bead	Acceptable
4	1	Correct	Streaks from central bead	Acceptable
5	1	Correct	Streaks from central bead	Acceptable
6	1	Correct	Streaks from central bead	Acceptable
7	1	Correct	Streaks from central bead	Acceptable
8	1	Correct	Streaks from central bead	Acceptable
9	1	Correct	Streaks from central bead	Acceptable
10	1	Correct	Streaks from central bead	Acceptable

The recommendation from DoH is that the low contrast detectability should not vary by more than + 1 insert size from baseline value. Table 6.11 shows the baseline value for the CT scanner used is 1 mm^3 insert, and the same result was obtained for all ten images. For positioning and alignment, the central bead should appear on the central slice, i.e. the slice assigned the zero-position after set-up with lasers and scribe lines. The accepted tolerance is ± 0.2 cm, however all ten reproducibility images were at the zero-position. DoH recommends that no artefacts should be visible. However, with the universal image quality assurance phantom, streak artefact from the central bead will always exist. This could be lessened if a smaller ball was used. This was not possible, as explained in section 4.4.1. Streak artefacts from the central bead will therefore be accepted as normal with the universal image quality assurance phantom. For image quality visual inspection, the results should remain reproducible. This was achieved with the ten images.

Table 6.12: CT scanning reproducibility testing data analysis software results. (Appendix A, A.2.5.5)

Image number	Sensitometry values as measured with software (arb. units)					
	Air		Lung		Supawood	
	Mean	Std dev	Mean	Std dev	Mean	Std dev
1	-1023.7	0.5	-759.3	7.2	-376.4	20.1
2	-1012.7	3.5	-687.6	12.5	-313.8	14.2
3	-1023.8	0.5	-752.9	9.2	-371.3	10.5
4	-1023.8	0.4	-747.2	8.9	-365.1	15.3
5	-1023.8	0.4	-756.6	7.8	-372.5	14.7
6	-1023.7	0.5	-754.6	7.1	-374.0	13.7
7	-1021.7	0.7	-722.1	9.5	-331.5	15.0
8	-1023.4	0.5	-761.4	6.2	-385.5	12.0
9	-1021.4	1.1	-730.0	10.5	-340.5	16.5
10	-1021.6	0.9	-723.6	10.0	-332.8	16.9
Average calculated	-1022.0 ± 3.2		-739.5 ± 22.3		-356.3 ± 23.1	

Image number	Sensitometry values as measured with software (arb. units)					
	Bone		Teflon		RGD240	
	Mean	Std dev	Mean	Std dev	Mean	Std dev
1	1417.0	17.8	1000.3	11.4	161.1	7.9
2	1192.3	34.1	914.6	11.6	156.8	6.8
3	1316.7	12.4	955.8	6.2	158.5	6.7
4	1300.8	18.2	942.9	8.4	153.9	5.8
5	1358.5	13.3	984.9	9.8	157.0	6.8
6	1395.5	13.7	986.2	6.7	158.3	6.3
7	1188.5	16.6	869.8	13.6	155.8	6.4
8	1352.9	8.4	1009.3	10.4	157.9	7.0
9	1172.1	25.0	874.8	12.5	161.0	9.9
10	1174.8	23.6	879.6	14.0	158.3	7.0
Average calculated	1286.9 ± 91.5		941.8 ± 51.3		157.9 ± 2.1	

Image number	Uniformity (arb. units)	Limiting resolution (cycles/cm)	Image noise (arb. units)		Geometry and measurement tools (mm)		Standard signal (arb. units)	
			SNR	CNR	Horizontal value	Vertical value	Mean	Std dev
1	28.3	3.3	22.8	67.8	20.0	20.0	-71.2	3.8
2	28.3	4.8	22.6	69.1	19.7	20.0	-68.1	3.9
3	27.3	4.8	25.3	59.6	20.4	20.0	-74.2	4.7
4	24.8	4.9	21.2	63.9	20.0	20.4	-69.7	4.4
5	26.8	4.6	23.0	57.1	20.0	20.4	-70.2	4.3
6	29.6	4.6	24.8	66.2	20.4	20.0	-75.9	4.5
7	26.0	4.8	26.6	59.1	19.7	19.7	-70.5	3.7
8	26.8	5.0	26.8	54.5	20.0	20.4	-75.0	4.9
9	27.7	4.8	22.0	61.9	19.7	20.4	-69.0	3.7
10	25.2	5.0	22.7	63.5	19.7	19.7	-67.4	3.6
Average calculated	27.1±1.4	4.7±0.5	23.8±1.9	62.3±4.5	20.0±0.3	20.1±0.3	-71.1±2.8	

Image number	Slice thickness (mm)
1	5.3
2	5.3
3	4.8
4	4.8
5	5.2
6	5.2
7	5.2
8	5.0
9	5.2
10	5.2
Average calculated	5.1±0.2

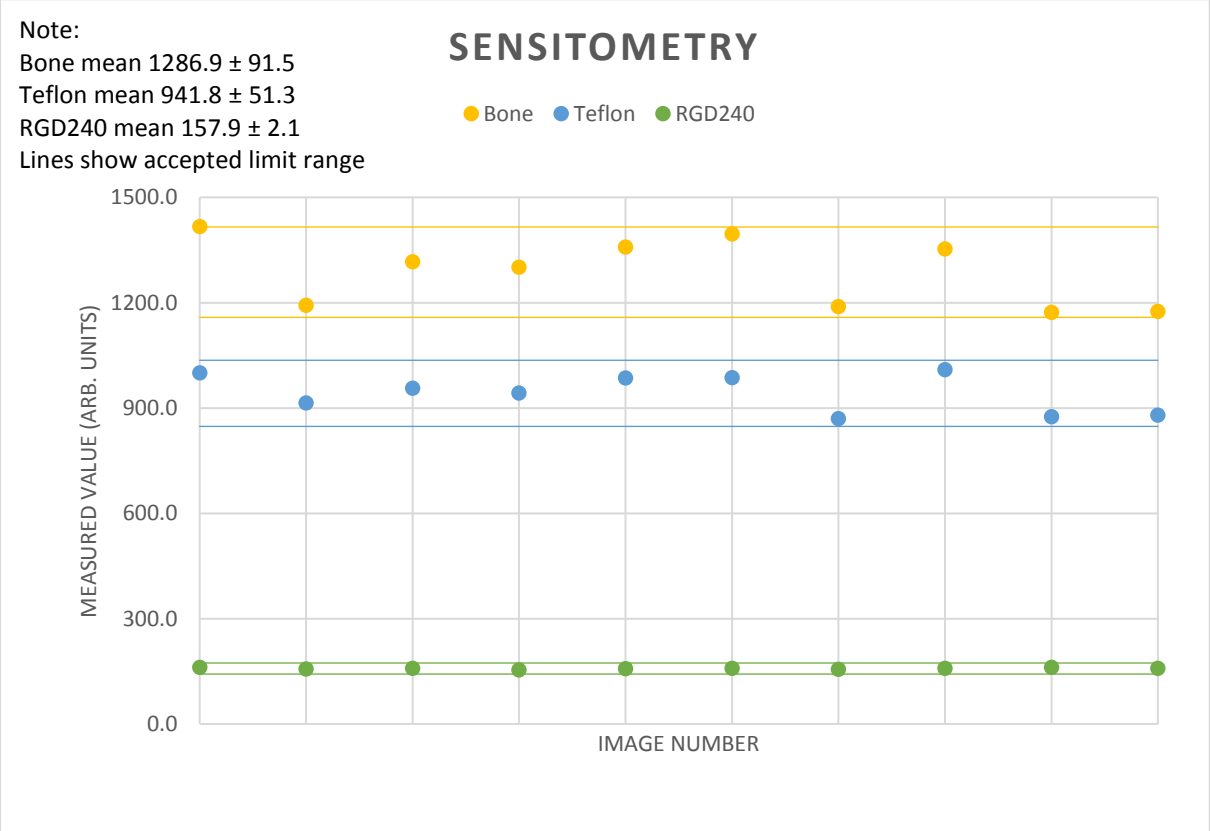

Figure 6.29: CT scanning data analysis software reproducibility results for sensitometry results for bone, Teflon and RGD240 with tolerance limits of ± 10 %.

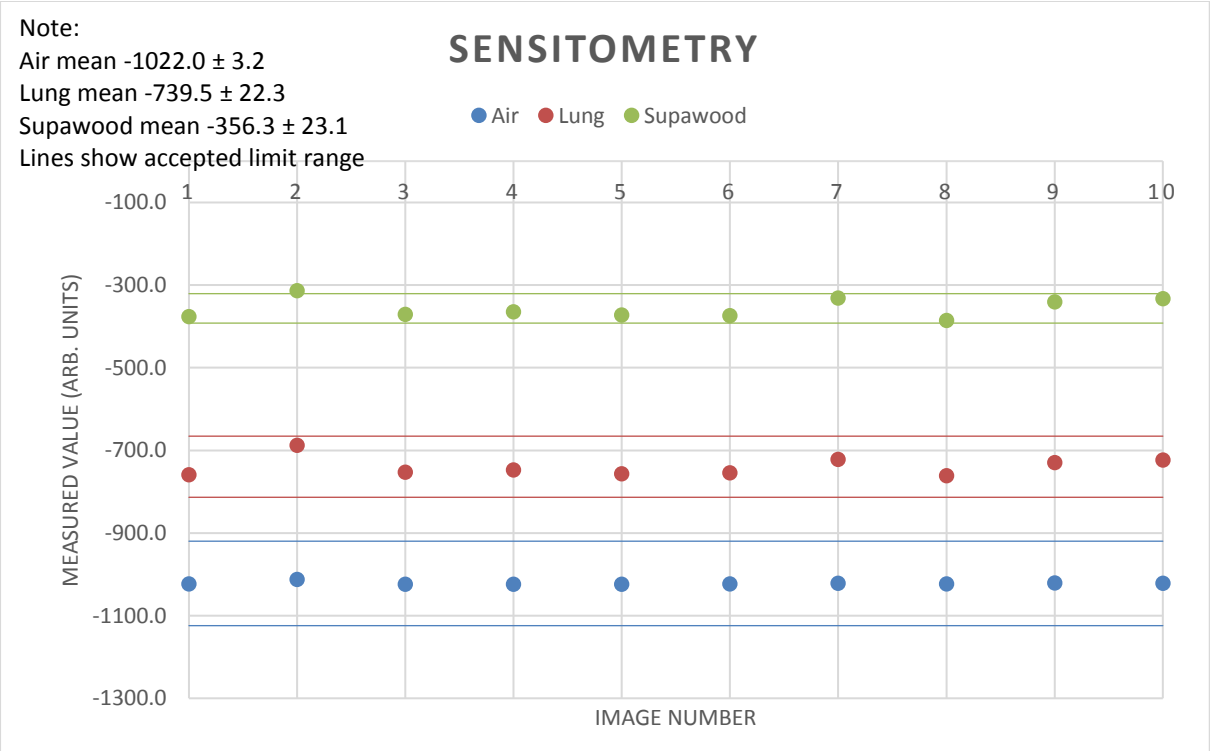

Figure 6.30: CT scanning data analysis software reproducibility results for sensitometry for air, lung and supawood with tolerance limits of ± 10 %.

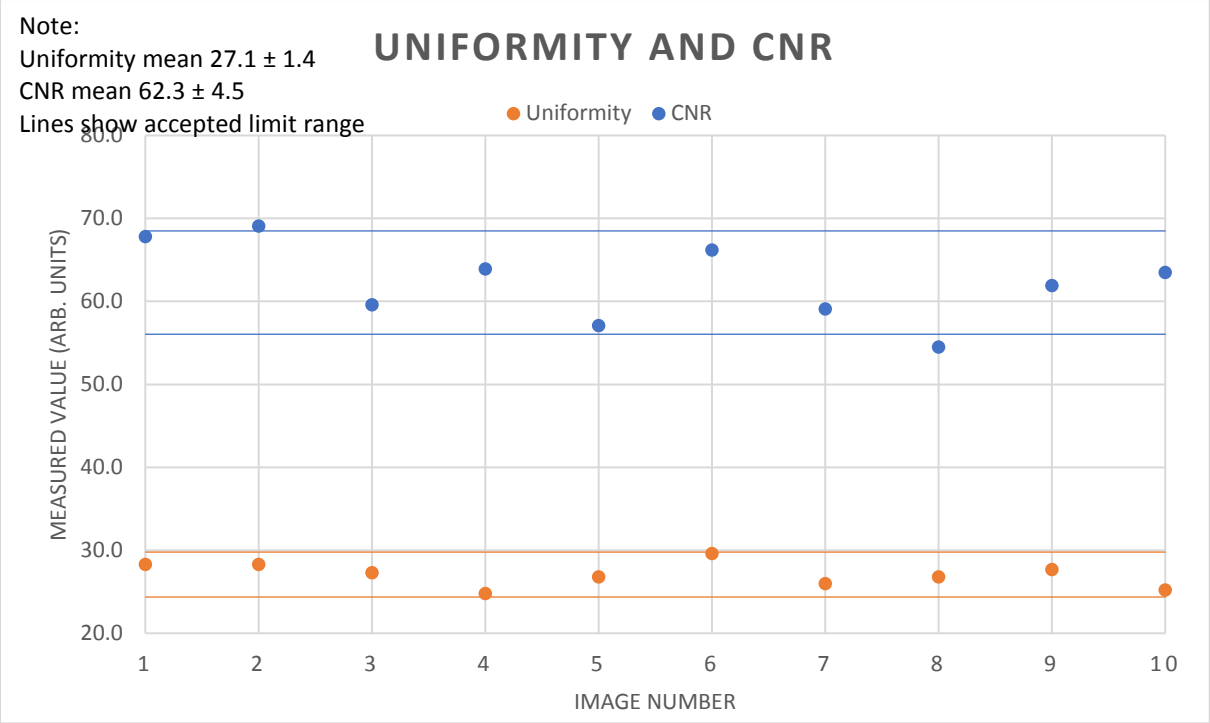

Figure 6.31: CT scanning data analysis software reproducibility results for uniformity and CNR results with tolerance limits of ± 10 %.

Figure 6.32: CT scanning data analysis software reproducibility results for limiting resolution with tolerance limits of – 25 % and SNR results with tolerance limits of ± 10 %.

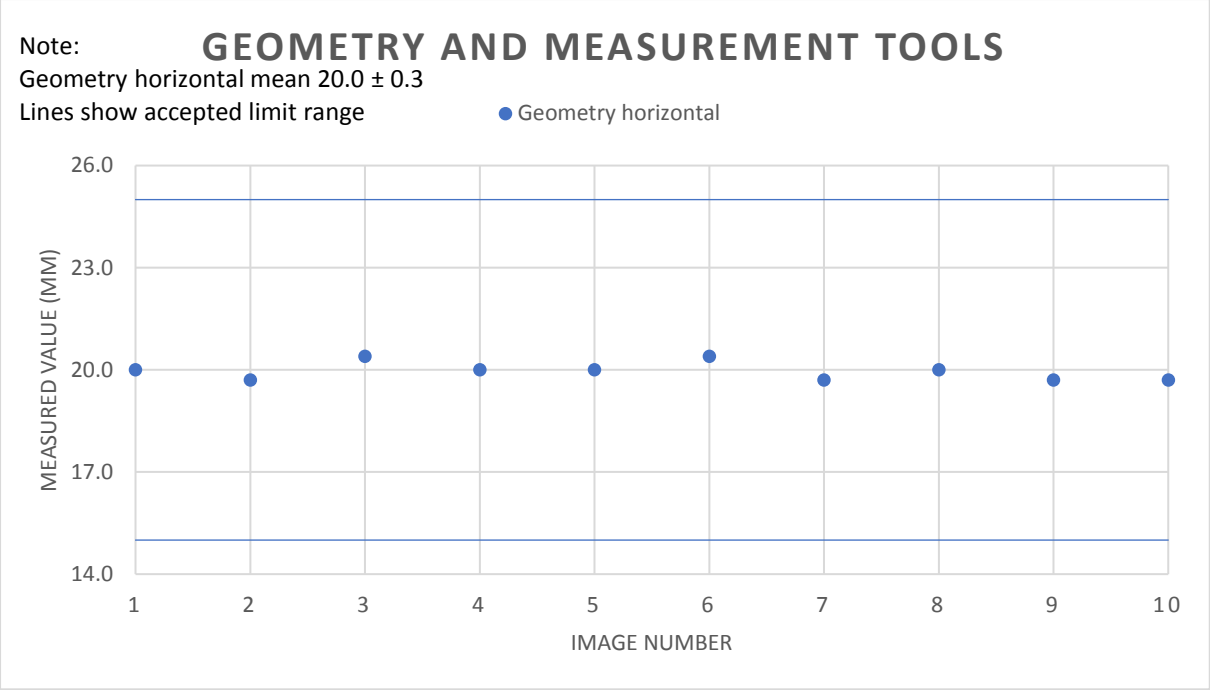

Figure 6.33: CT scanning data analysis software reproducibility results for geometry and measurement tools for horizontal measurement with tolerance limits of ± 5 mm.

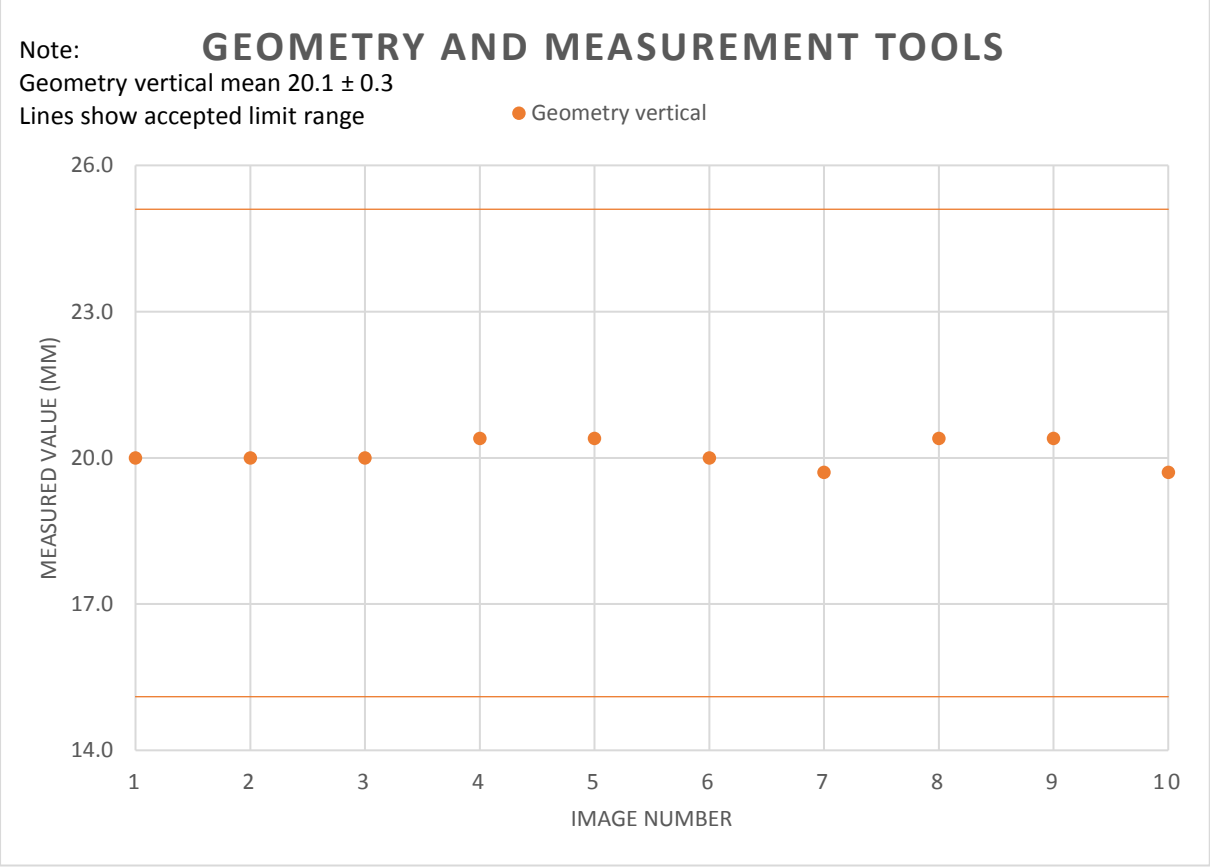

Figure 6.34: CT scanning data analysis software reproducibility results for geometry and measurement tools for vertical measurement with tolerance limits of ± 5 mm.

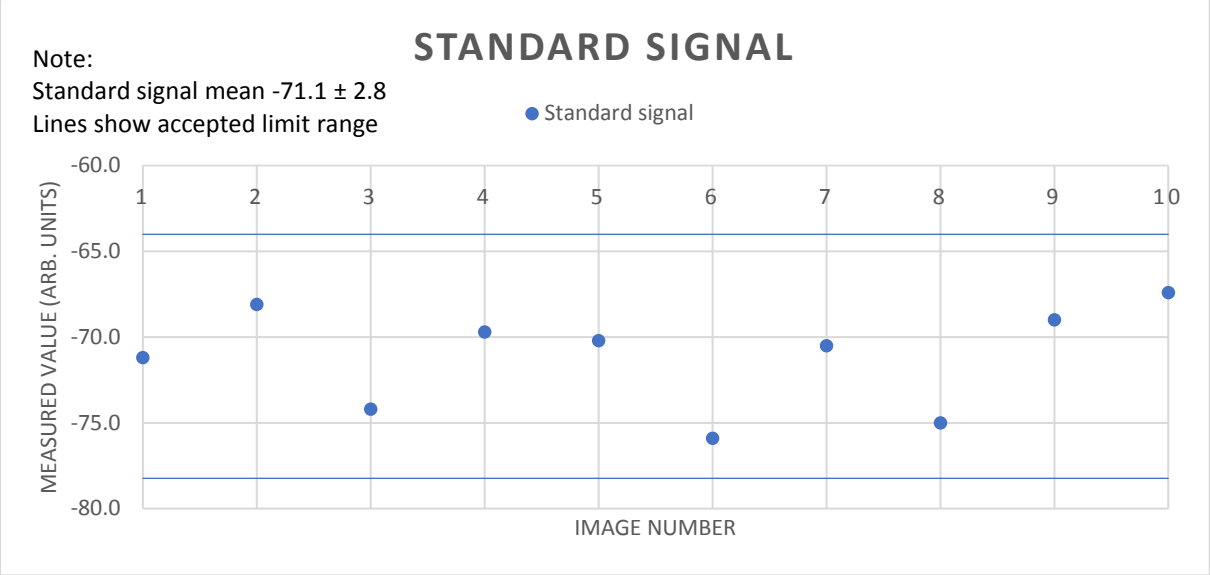

Figure 6.35: CT scanning data analysis software reproducibility results for standard signal with tolerance limits of ± 10 %.

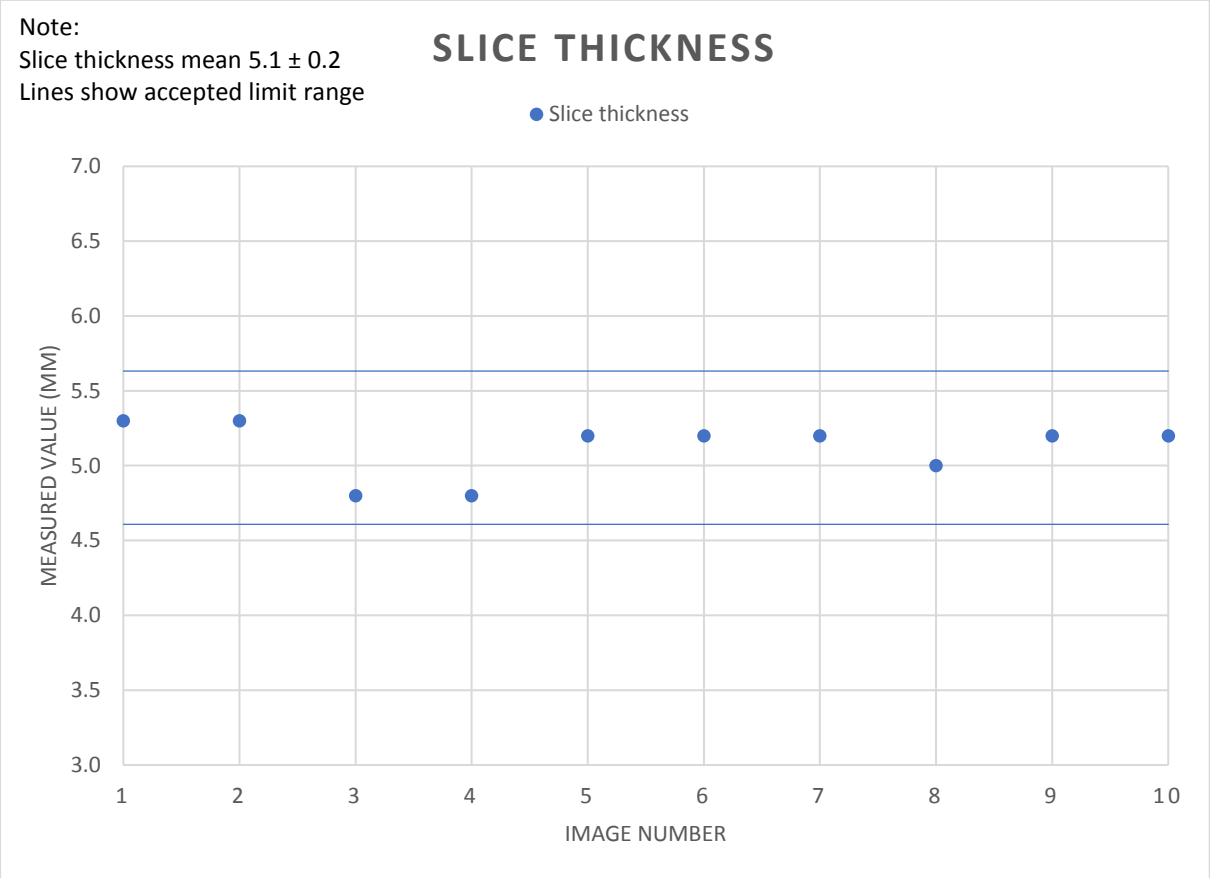

Figure 6.36: CT scanning data analysis software reproducibility results for slice thickness with tolerance limits of ± 10 %.

With reference to Figures 6.29 and 6.30 all the sensitometry (or HU linearity) results were within the ± 10 % limit. A limit of ± 10 % is suggested, although DoH recommends ± 10 HU, as the data analysis software does not measure actual Hounsfield units but only relative image grey scale values. Figure 6.31 shows that the uniformity results were reproducible in the allowed ± 10 % limits. For image 8 the CNR was 12.5 % low. Again, this would mean repetition of the test, according to Figure A.2 in the user's manual, and for images 9 and 10 the results were within limits. The limiting resolution should not decrease by more than 25 % according to DoH. In Figure 6.32 for image 1 the variation was 29.8 %. However the results for all the subsequent images were within tolerance. For SNR images 4, 7 and 8 fell outside the recommended ± 10 % limits, with the greatest deviation 12.6 % for image 8. The results for all ten images were within the accepted limits for geometry and measurement tools for both horizontal and vertical measurements, as seen in Figures 6.33 and 6.34. For standard signal, Figure 6.35 and slice thickness, Figure 6.36, the results were within ± 10 % of the average value, although the accepted tolerance for slice thickness is baseline value ± 20 %.

From Tables 6.11 and 6.12 and Figures 6.28 to 6.36 it was concluded that the universal image quality assurance phantom and the data analysis software produced reproducible results for CT scanning. This implied that the phantom is suitable for routine CT image quality control.

Chapter 7

Independent validation of the universal phantom package

The universal image quality assurance phantom, user's manual and data analysis software were made available to independent medical physicists to evaluate. The participating institutions were Groote Schuur Hospital (GSH) (Cape Town, South Africa), Inkosi Albert Luthuli Central Hospital (IALCH) (Durban, South Africa) and Charlotte Maxeke Johannesburg Academic Hospital (CMJAH) (Johannesburg, South Africa). Three phantoms were manufactured and CT scanned by the primary investigator to compare their similarity. As the evaluation of image quality is primarily dependent on insert density, and the same materials from the same manufacturers and slabs of plastic as for the primary phantom was used, the phantoms were sufficiently similar. This was done to save time as a six week period was given to each institution to work with the package and complete the evaluation sheets. This was done in addition to their routine work as a favour to the primary investigator. The participating institutions were completely independent of the primary investigator, and the medical physicists that performed the analysis and evaluation were unknown. No bias is therefore expected in the results.

Evaluation was done as per the criteria in Figure 7.2 in general x-rays, fluoroscopy, mammography and CT scanning. The results from this validation are discussed in this chapter. Figure 7.1 shows the package that was send to the participating institutions.

Figure 7.1: The universal image quality assurance phantom package, including the phantom, additional attenuator plates, printed user's manual, data analysis software on compact disk and a stand for set-up at CT scanning, packed into a durable aluminium case.

Figure 7.2 shows examples of the evaluation forms that the independent evaluators were asked to complete. These compared the universal phantom to the phantoms routinely used in these institutions. The evaluators were instructed to be honest in their responses, even if the comments were negative. The phantom, manual and software were individually scored and the package as a whole was also evaluated. A simple scoring system of 1 – 5 were used, where 1 indicated that the evaluator strongly disagreed with the statement and 5 indicated strong agreement with the statement. This simple scoring technique is often used in comparative evaluations and as it is easy to follow it also contributes to the aim of the study of making image quality assurance more accessible, easier and quicker in resource limited institutions. In addition, participants were asked to include comments and recommendations. Sections 7.1 to 7.4 discusses the results for general x-rays, fluoroscopy, mammography and CT scanning and section 7.5 the overall evaluation of the complete package.

a.) **Evaluation of the universal phantom package in general x-ray imaging**

Phantom(s) usually used for general x-ray QC:	1	
	2	
	3	
	4	

Objectives - Compared to currently available phantoms and/or packages:	**Score**				
	1	**2**	**3**	**4**	**5**
The universal phantom is easy to set-up and image					
Image acquisition time is reduced					
Data analysis is simplified with the software					
Data analysis time is reduced					
Decision making is simplified with the software					
Decision making time is reduced					
The extend to which the universal phantom covers the required image quality assurance needs					

Evaluation of the universal phantom package in fluoroscopy imaging

b.)

Phantom(s) usually used for fluoroscopy QC:	1	
	2	
	3	
	4	

Objectives - Compared to currently available phantoms and/or packages:	**Score**				
	1	**2**	**3**	**4**	**5**
The universal phantom is easy to set-up and image					
Image acquisition time is reduced					
Data analysis is simplified with the software					
Data analysis time is reduced					
Decision making is simplified with the software					
Decision making time is reduced					
The extend to which the universal phantom covers the required image quality assurance needs					

c.) Evaluation of the universal phantom package in mammography imaging

Phantom(s) usually used for mammography QC:	1	
	2	
	3	
	4	

Objectives - Compared to currently available phantoms and/or packages:	Score 1	2	3	4	5
The universal phantom is easy to set-up and image					
Image acquisition time is reduced					
Data analysis is simplified with the software					
Data analysis time is reduced					
Decision making is simplified with the software					
Decision making time is reduced					
The extend to which the universal phantom covers the required image quality assurance needs					

d.) Evaluation of the universal phantom package in CT scanning

Phantom(s) usually used for CT scanning QC:	1	
	2	
	3	
	4	

Objectives - Compared to currently available phantoms and/or packages:	Score 1	2	3	4	5
The universal phantom is easy to set-up and image					
Image acquisition time is reduced					
Data analysis is simplified with the software					
Data analysis time is reduced					
Decision making is simplified with the software					
Decision making time is reduced					
The extend to which the universal phantom covers the required image quality assurance needs					

e.) **General evaluation of the universal phantom package**

Objectives - Compared to currently available phantoms and/or packages:	**Score** 1	2	3	4	5
The universal phantom is easy to transport					
The universal phantom is light to handle					
The universal phantom is compact					
The universal phantom is simple to use					
The universal phantom is versatile					
The user's manual is easy to follow and understand					
The data analysis software is easy to install					
The data analysis software is easy to use					
Using the universal phantom saves time in data acquisition					
Using the software saves time in data analysis and decision making					
Results form the universal phantom package are reliable					
Results form the universal phantom package are accurate					
Results form the universal phantom package are reproducible					
The level of competence required to use the phantom					
The universal phantom package is a cost effectivesolution					

Limitations of the universal phantom package (please comment below)
The following limitations were noted when using the universal phantom package
The universal image quality assurance phantom:
The universal image quality assurance phantom user's manual:
The universal image quality assurance phantom data analysis software:

Other comments or recommendations (please comment below)

Figure 7.2: Evaluation sheets used by the independent evaluators to assess the universal image quality assurance phantom package and compare it to commercially available options. a.) Evaluation of the package for general x-ray imaging. b.) Evaluation of the package for fluoroscopy imaging. c.) Evaluation of the package for mammography imaging. d.) Evaluation of the package for CT scanning. e.) Overall evaluation of the package.

In Chapter 1 it was indicated that problems identified in resource limited institutions were cost, man power and expertise and time constraints. For the phantom to be successfully filling an identified gap in the existing commercial market, it had to address these problems. The evaluation criteria in Figure 7.2 a.) to d.) were based on these identified problems. The limitation of cost is addressed by the last criterion, evaluating the extent to which the phantom covers the QC required in each imaging modality, i.e. whether the universal image quality assurance phantom was sufficient as a single phantom solution for comprehensive image QC in each imaging modality. The criteria addressing ease of phantom set-up, data analysis and decision making simplification addressed the problem of man power and expertise. The universal image quality assurance phantom must be easy and simple enough to be successfully used by equipment operators, like radiographers, in institutions where medical physicists are not available. For time constraints, the criteria of ease of phantom set-up, acquisition, data analysis and decision making time reduction and simplification of data analysis and decision making were included. In addition, allowance was made for comparison of the universal image quality assurance phantom to the commercially available phantoms routinely used by the investigators.

To enable overall evaluation of the total package, i.e. the universal image quality assurance phantom, data analysis software and user's manual, the criteria in Figure 7.2 e.) were also based on the limitations identified in Chapter 1. The criteria of easy transport, light to handle, compact and cost effective solution address the cost limitation. If the phantom package, as shown in Figure 7.1, was robust enough, it means that one package can be acquired and shared with cheap transport (as it is compact and lightweight) between different institutions, further reducing costs for resource limited institutions. For the problem of limited man power and expertise, the criteria of simple to use, versatile, easy to follow user's manual, easy to install and user friendly data analysis software, reliable, reproducible and accurate results and a direct question on the required level of competence needed to use the phantom were included. Phantom package versatility and saving of time on data analysis and decision making were the criteria included to determine if the phantom package addressed the problem of time constraints.

7.1 General x-ray imaging validation

In general x-ray imaging the universal image quality assurance phantom was compared to the NORMI 13 and RMI phantoms.

7.1.1 Response from CMJAH

The universal image quality assurance phantom was compared to the Normi 13 phantom by CMJAH for general x-ray imaging, as shown in Figure 7.3.

Evaluation of the universal phantom package in general x-ray imaging

Phantom(s) usually used for general x-ray QC:	1	Normi 13 Phantom
	2	
	3	
	4	

Objectives - Compared to currently available phantoms and/or packages:	**Score**				
	1	**2**	**3**	**4**	**5**
The universal phantom is easy to set-up and image				x	
Image acquisition time is reduced					x
Data analysis is simplified with the software					x
Data analysis time is reduced				x	
Decision making is simplified with the software				x	
Decision making time is reduced				x	
The extend to which the universal phantom covers the required image quality assurance needs					x

Figure 7.3: Independent evaluation results from CMJAH for general x-ray imaging.

From Figure 7.3 it is seen that the universal phantom reduces the image acquisition time, simplifies data analysis and covers all the required image quality assurance tests needed for general x-rays, as shown by the 5 scores at these criteria. The evaluator still agreed with the other statements, scoring them at 4. Here a total score of 31 out of possible 35 indicates that the phantom package is a suitable solution for general x-ray image quality control.

7.1.2 Response from GSH

The results from GSH are shown in Figure 7.4, where the RMI phantom was used for comparison. Compared to the RMI phantom, the universal phantom package was still scored 29 out of 35, although a poorer score than with the Normi 13 phantom in Figure 7.3 above, it is still a suitable image quality assurance solution. This evaluator found the phantom very easy to set up compared to the CMJAH evaluator.

Evaluation of the universal phantom package in general x-ray imaging

Phantom(s) usually used for general x-ray QC:	1	RMI phantom
	2	
	3	
	4	

Objectives - Compared to currently available phantoms and/or packages:	**Score**				
	1	**2**	**3**	**4**	**5**
The universal phantom is easy to set-up and image					5
Image acquisition time is reduced				4	
Data analysis is simplified with the software				4	
Data analysis time is reduced				4	
Decision making is simplified with the software				4	
Decision making time is reduced				4	
The extend to which the universal phantom covers the required image quality assurance needs				4	

Figure 7.4: Independent evaluation results from GSH for general x-ray imaging.

7.1.3 Response from IALCH

The results from IALCH are shown in Figure 7.5. The evaluator compared the universal phantom to the Normi 13 phantom for general x-ray imaging. A total score of 31 out of possible 35 was given. The evaluator strongly agrees that the phantom is easy to set up, that data analysis is simplified with the software and that the package covers all the image QC required for general x-rays. It is also agreed that time is reduced, for image acquisition, data analysis and decision making and that the

decision making process is simplified. From this it is determined that the phantom package is a suitable image QC solution for general x-ray imaging.

Evaluation of the universal phantom package in general x-ray imaging

Phantom(s) usually used for general x-ray QC:	1	Normi 13 Phantom
	2	
	3	
	4	

Objectives - Compared to currently available phantoms and/or packages:	**Score**				
	1	**2**	**3**	**4**	**5**
The universal phantom is easy to set-up and image					x
Image acquisition time is reduced				x	
Data analysis is simplified with the software					x
Data analysis time is reduced				x	
Decision making is simplified with the software				x	
Decision making time is reduced				x	
The extend to which the universal phantom covers the required image quality assurance needs					x

Figure 7.5: Independent evaluation results from IALCH for general x-ray imaging.

From the three sets of results two evaluators strongly agreed that the phantom is easy to set up, the software simplified data analysis and that the package covered all the required QC for general x-ray imaging. One also strongly agreed that image acquisition time was reduced. All other criteria were scored 4 by the evaluators, implying that they still agreed with the criteria statements. It is thus clear that the universal image quality assurance phantom, user's manual and data analysis software is an acceptable, easy to use, cost effective and time saving QC solution for general x-ray image QC according to the limited evaluation sample.

7.2 Fluoroscopy imaging validation

In fluoroscopy, the universal image quality assurance phantom was compared to the NORMI 13 and NORMI 4 FLU phantoms by the evaluators.

7.2.1 Response from CMJAH

Figure 7.6 shows the results from CMJAH for fluoroscopy, comparing the universal image quality assurance phantom to the Normi 13 phantom for fluoroscopy. A total score of 32 out of 35 was allocated, with the phantom being easy to set up and data analysis and decision making time simplified and reduced. The evaluator again felt that the package was a suitable solution for image quality control in fluoroscopy.

Evaluation of the universal phantom package in fluoroscopy imaging

Phantom(s) usually used for fluoroscopy QC:	1	Normi 13 Phantom
	2	
	3	
	4	

Objectives - Compared to currently available phantoms and/or packages:	Score 1	2	3	4	5
The universal phantom is easy to set-up and image					x
Image acquisition time is reduced				x	
Data analysis is simplified with the software					x
Data analysis time is reduced				x	
Decision making is simplified with the software				x	
Decision making time is reduced					x
The extend to which the universal phantom covers the required image quality assurance needs					x

Figure 7.6: Independent evaluation results from CMJAH for fluoroscopy imaging.

7.2.2 Response from GSH

In comparison with the Normi 4 Flu phantom in GSH, the universal image quality assurance package scored lower that at CMJAH. The results are included in Figure 7.7. The evaluator felt that the phantom was not easier to set up and that image acquisition time was not significantly influenced using the universal phantom compared to the Normi 4 Flu phantom, scoring 3 (i.e. not agreeing and not disagreeing with the statements). The total score here was 27 out of 35. As with general x-rays in Figure 7.4, a score of 4 was given to the last statement, implying that the evaluator

still thinks that the phantom does cover the image quality assurance needs, but that improvements are needed.

Evaluation of the universal phantom package in fluoroscopy imaging

Phantom(s) usually used for fluoroscopy QC:	1	Normi 4 FLU Phantom
	2	
	3	
	4	

Objectives - Compared to currently available phantoms and/or packages:	Score				
	1	2	3	4	5
The universal phantom is easy to set-up and image			3		
Image acquisition time is reduced			3		
Data analysis is simplified with the software				4	
Data analysis time is reduced				4	
Decision making is simplified with the software					5
Decision making time is reduced				4	
The extend to which the universal phantom covers the required image quality assurance needs				4	

Figure 7.7: Independent evaluation results from GSH for fluoroscopy imaging.

7.2.3 Response from IALCH

At IALCH the universal phantom package was compared to the Normi 13 phantom for fluoroscopy imaging. The results shown in Figure 6.8 are exactly the same as those in Figure 7.5 for general x-ray imaging. The evaluator agreed with all the criteria, with a total score of 31 out of 35. The evaluator feels that the phantom is easy to set up, saves time and simplifies the QC process.

Evaluation of the universal phantom package in fluoroscopy imaging

Phantom(s) usually used for fluoroscopy QC:	1	Normi 13 Phantom
	2	
	3	
	4	

Objectives - Compared to currently available phantoms and/or packages:	Score				
	1	2	3	4	5
The universal phantom is easy to set-up and image					x
Image acquisition time is reduced				x	
Data analysis is simplified with the software					x
Data analysis time is reduced				x	
Decision making is simplified with the software				x	
Decision making time is reduced				x	
The extend to which the universal phantom covers the required image quality assurance needs					x

Figure 7.8: Independent evaluation results from IALCH for fluoroscopy imaging.

Two of the three evaluators strongly agreed that the phantom is easy to set up, the software simplifies data analysis and that the package covers all the required QC for fluoroscopy imaging. The third evaluator scored these criteria 4, which means they still agreed with the statements. One also strongly agreed that decision making is simplified with the software and that it saves decision making time also. As scores of 4 were given to these criteria by the other evaluators, also with these statements all the evaluators agreed. All the evaluators agreed with all the other statements, except for the GSH evaluator who scored 3 for phantom set-up and image acquisition time, in contrast to the overall scores from the evaluator of 5 for the criteria that the phantom is easy to use and saves time with data acquisition. According to these results the universal image quality assurance phantom package is suitable for image QC in fluoroscopy as it is user friendly and cost and time effective.

7.3 Mammography imaging validation

In mammography, the ACR and SIB phantoms were routinely used by the evaluators and they compared the universal image quality assurance phantom to these. Due to

logistical reasons IALCH was unable to evaluate the phantom package in mammography. The evaluator could not get access to a mammography unit.

7.3.1 Response from CMJAH

For mammography, CMJAH compared the universal phantom package to the ACR and SIB phantoms, as shown in Figure 7.9. A total score of 33 out of 35 was allocated by the evaluator, with the areas of improvement being the saving of time and simplification of the result analysis with the data analysis software. In section 7.5, Figure 7.15, it is seen that drawing accurate same sized ROIs is the reason for this. The universal phantom is however still a definite image quality solution for mammography.

Evaluation of the universal phantom package in mammography imaging

Phantom(s) usually used for mammography QC:	1	ACR Phantom
	2	SIB Phantom
	3	
	4	

Objectives - Compared to currently available phantoms and/or packages:	Score				
	1	2	3	4	5
The universal phantom is easy to set-up and image					x
Image acquisition time is reduced					x
Data analysis is simplified with the software				x	
Data analysis time is reduced				x	
Decision making is simplified with the software					x
Decision making time is reduced					x
The extend to which the universal phantom covers the required image quality assurance needs					x

Figure 7.9: Independent evaluation results from CMJAH for mammography imaging.

7.3.2 Response from GSH

At GSH the universal phantom package was also compared to the ACR phantom, however this evaluator scored the phantom lower overall, a total of 26 out of 35. The evaluator does not agree or disagree with the statement that the phantom is easy to set up and that image acquisition time is reduced, i.e. a score of 3. Even though not strongly, the evaluator does agree that data analysis and decision making is simplified and that data analysis time is reduced, and again that some improvements can make the phantom an even better solution to cover the required image quality assurance tests. The results are included in Figure 7.10.

Evaluation of the universal phantom package in mammography imaging

Phantom(s) usually used for mammography QC:	1	ACR Mammography accreditation phantom
	2	
	3	
	4	

Objectives - Compared to currently available phantoms and/or packages:	Score				
	1	2	3	4	5
The universal phantom is easy to set-up and image			3		
Image acquisition time is reduced			3		
Data analysis is simplified with the software				4	
Data analysis time is reduced				4	
Decision making is simplified with the software				4	
Decision making time is reduced				4	
The extend to which the universal phantom covers the required image quality assurance needs				4	

Figure 7.10: Independent evaluation results from GSH for mammography imaging.

Both GSH and CMJAH evaluators agreed that the software simplified data analysis and decision making and reduced data analysis and decision making time. They also felt that the phantom package covered all the required tests for mammography image QC. The GSH evaluator scored ease of phantom set up and image acquisition time reduction at 3, in contradiction to the overall scores for the whole phantom package

where these criteria were scored 5, however the CMJAH evaluator scored them 5. This was a contradiction in results from this evaluator. It was derived that the universal image quality assurance phantom, user's manual and data analysis software form a complete mammography image QC solution which is cheaper, easier and quicker than existing commercial phantom QC packages.

7.4 Computed Tomography scanning validation

In CT scanning the universal image quality assurance phantom was compared to the GE, Phillips and Catphan phantoms.

7.4.1 Response from CMJAH

Figure 7.11 shows the results from CMJAH. The comparative phantoms were the GE and Phillips phantoms. With a total score of 34 out of 35, it can be concluded that the universal image quality assurance phantom is a suitable solution for routine image QC in CT scanning, making set-up, data analysis and decision making easier. Image acquisition time might be slightly reduced, as the evaluator scored this criterion 4.

Evaluation of the universal phantom package in CT scanning

Phantom(s) usually used for CT scanning QC:	1	GE phantom
	2	Philips Phantom
	3	
	4	

Objectives - Compared to currently available phantoms and/or packages:	Score				
	1	2	3	4	5
The universal phantom is easy to set-up and image					x
Image acquisition time is reduced				x	
Data analysis is simplified with the software					x
Data analysis time is reduced					x
Decision making is simplified with the software					x
Decision making time is reduced					x
The extend to which the universal phantom covers the required image quality assurance needs					x

Figure 7.11: Independent evaluation results from CMJAH for CT scanning.

7.4.2 Response from GSH

Less favourable results were again obtained from GSH, as shown in Figure 7.12. Comparison was made to the Catphan 700 phantom. The universal phantom scored 5 for set-up ease and reduction in image acquisition time, but the evaluator was undecided on if the phantom addressed all the required QC in CT scanning, scoring this criterion 3, i.e. not agreeing neither disagreeing with the statement. A total of 29 out of 35 was obtained, with the evaluator agreeing that data analysis and decision making is simplified and time reduced.

Evaluation of the universal phantom package in CT scanning

Phantom(s) usually used for CT scanning QC:	1	Catphan 700 phantom
	2	
	3	
	4	

Objectives - Compared to currently available phantoms and/or packages:	Score				
	1	2	3	4	5
The universal phantom is easy to set-up and image					5
Image acquisition time is reduced					5
Data analysis is simplified with the software				4	
Data analysis time is reduced				4	
Decision making is simplified with the software				4	
Decision making time is reduced				4	
The extend to which the universal phantom covers the required image quality assurance needs			3		

Figure 7.12: Independent evaluation results from GSH for CT scanning.

7.4.3 Response from IALCH

At IALCH comparison was made to the Catphan phantom, as shown in Figure 6.13. As with general x-rays and fluoroscopy, the evaluator strongly agreed that the phantom was easy to set up, the software simplifies data analysis and that the phantoms covered all the required image QC tests required for CT scanning. The evaluator also felt that data analysis and decision making time was reduced using the phantom and that the decision making process was simplified. A score of 3 was given to the criterion that image acquisition time is reduced, which meant the evaluator neither agrees nor disagrees with this statement. A total score of 30 out of 35 was allocated. From this it was clear that the universal image quality assurance package would be suitable for routine image QC in CT scanning.

Evaluation of the universal phantom package in CT scanning

Phantom(s) usually used for CT scanning QC:	1	Catphan Phantom
	2	
	3	
	4	

Objectives - Compared to currently available phantoms and/or packages:	**Score**				
	1	**2**	**3**	**4**	**5**
The universal phantom is easy to set-up and image					x
Image acquisition time is reduced			x		
Data analysis is simplified with the software					x
Data analysis time is reduced				x	
Decision making is simplified with the software				x	
Decision making time is reduced				x	
The extend to which the universal phantom covers the required image quality assurance needs					x

Figure 7.13: Independent evaluation results from IALCH for CT scanning.

According to the CMJAH evaluator the universal image quality assurance phantom package is a great solution for CT image QC, as all criteria were strongly agreed with, except reduction in acquisition time, with which the evaluator still agreed. The GSH evaluator strongly agreed that image acquisition time was reduced, but the IALCH evaluator scored this criterion only 3. All evaluators felt the phantom was easy to set up, that data analysis and decision making time was reduced and these processes were simplified using the software. From these results it was expected that for CT scanning the universal image quality assurance phantom package would be a comprehensive image QC solution, saving time and cost and being easy to use.

7.5 Evaluation of the complete package

The independent evaluators were also asked to evaluate the complete package, as seen in Figure 7.2 e.), adding their comments and recommendations for improvements here.

7.5.1 Response from CMJAH

Figure 7.14 shows the results received from CMJAH. The evaluator strongly agreed that the phantom was easy to transport, simple to use and versatile, that the user's manual was easy to understand and follow and that the software was easy to install and user friendly. The evaluator also agreed with the statements that the phantom was light and compact and that time was saved, for image acquisition and for data analysis and decision making. The results obtained were reproducible and the package was a cost-effective image quality control solution. A score of 3 was allocated to the level of competence needed to perform the QC, however in the comments the evaluator does mention that radiographers will be able to successfully use the phantom package. No score was allocated to whether the results from the phantom are reliable or accurate. This could be attributed to the fact that the evaluator had very little time for the evaluation and hence limited experience with the phantom package. A total score of 57 out of possible 75 was obtained, with two criteria not evaluated. This implies that the three identified problems from Chapter 1 are addressed by the phantom package according to this evaluator, i.e. it is cost effective, it saves time and radiographers can perform the QC in institutions that do not have medical physicists on staff.

The evaluator also recommended improvements in the software. Indicating the size of a drawn ROI will ensure same sized ROIs are used in evaluation, giving better and more reproducible results. Mention of displaying ROI size is also made by the GSH evaluator, as seen in Figure 7.15. A guide can also be included for drawing the slice thickness line, as recommended in Figure 7.14. These recommendations will be incorporated in the final version of the software.

General evaluation of the universal phantom package

Objectives - Compared to currently available phantoms and/or packages:	Score 1	2	3	4	5
The universal phantom is easy to transport					x
The universal phantom is light to handle				x	
The universal phantom is compact				x	
The universal phantom is simple to use					x
The universal phantom is versatile					x
The user's manual is easy to follow and understand					x
The data analysis software is easy to install					x
The data analysis software is easy to use					x
Using the universal phantom saves time in data acquisition				x	
Using the software saves time in data analysis and decision making				x	
Results form the universal phantom package are reliable					
Results form the universal phantom package are accurate					
Results form the universal phantom package are reproducible				x	
The level of competence required to use the phantom			x		
The universal phantom package is a cost effective solution				x	

Limitations of the universal phantom package (please comment below)
The following limitations were noted when using the universal phantom package
The universal image quality assurance phantom:
The universal image quality assurance phantom user's manual:
The universal image quality assurance phantom data analysis software: The softwear doesn't show the size of the ROIs, so it is pretty easy to draw ROIs of different sizes and obtain inconsistant values. When measuring slice thickness, drawing a straight line across the ramp is quite a subjective procedure. when two people measuring the slice thickness of the same image tend to get different values.

Other comments or recommendations (please comment below)
Both the softwear and the Phantom are quite user friendly I believe that even radiographers can be able to perform the Qc successfully.

Figure 7.14: Independent evaluation results from CMJAH for overall evaluation of the package.

7.5.2 Response from GSH

Figure 7.15 shows the results received from GSH. The evaluator strongly agreed with the statements that the phantom was easy to transport, light, compact and the

phantom and software were simple to use. Scores of 5 were also given to the criteria that time was saved on data acquisition. This was in contradiction with the scores of 4 for general x-rays and 3 for fluoroscopy and mammography as seen in Figures 7.4, 7.7 and 7.10. All the other criteria were scored 4 by this evaluator. A total of 66 out of 75 was allocated to the complete package. From these results it is concluded that according to the GSH evaluator, the universal image quality assurance phantom package is a compact, versatile, user friendly, cost effective option which does not require a high level of expertise for successful use, i.e. the aims of the study set in Chapter 1 were met.

General evaluation of the universal phantom package

	Score				
Objectives - Compared to currently available phantoms and/or packages:	**1**	**2**	**3**	**4**	**5**
The universal phantom is easy to transport					5
The universal phantom is light to handle					5
The universal phantom is compact					5
The universal phantom is simple to use					5
The universal phantom is versatile				4	
The user's manual is easy to follow and understand				4	
The data analysis software is easy to install				4	
The data analysis software is easy to use					5
Using the universal phantom saves time in data acquisition					5
Using the software saves time in data analysis and decision making				4	
Results form the universal phantom package are reliable				4	
Results form the universal phantom package are accurate				4	
Results form the universal phantom package are reproducible				4	
The level of competence required to use the phantom				4	
The universal phantom package is a cost effective solution				4	

Limitations of the universal phantom package (please comment below)
The following limitations were noted when using the universal phantom package
None
The universal image quality assurance phantom user's manual: None
The universal image quality assurance phantom data analysis software: The software doesn't display the size/ area of the ROI. If the area can be displayed; I think it would be easy to get similarly sized ROI when determining the mean and standard deviation of which this will allow some form of reproducibility/repeatability of the results.

Other comments or recommendations (please comment below)

Figure 7.15: Independent evaluation results from GSH for overall evaluation of the package.

7.5.3 Response from IALCH

Figure 7.16 shows the overall evaluation results received from IALCH. Strong agreement was found with the criteria that the phantom was easy to transport, versatile and the software was easy to install. The evaluator also agreed that the phantom was light to handle, compact, simple to use, the user's manual and software were easy to use, decision making and acquisition time was reduced and the package was a cost effective image QC solution. This was in contrast with the score of 3 given to the criterion of saving on acquisition time with CT scanning in Figure 7.13. A score of 3 was given to the criteria that the results were reproducible and the level of competence required to use the phantom package. The criteria of reliable results and accuracy of results were not scored, as the evaluator had no experience with the phantom package and did not know what typical results are. These would be established with baseline testing for each x-ray unit evaluated, and this was not part of the independent validation request. The comments for improvements in the user's manual have all been added to the manual. As with the evaluators from GSH and CMJAH the IALCH evaluator recommended that ROI size should be displayed in the software. This was added in the final version of the software. The IALCH evaluator also mentioned, as the evaluator from CMJAH, that the slice thickness measurement was difficult to perform objectively. This was also addressed in the final version of the data analysis software. Unfortunately the concern that the phantom was slippery to the touch cannot be changed, as this is the texture of the HDPE housing material, which, as explained in Chapter 4, was the most suitable material for manufacturing the phantom housing.

General evaluation of the universal phantom package

Objectives - Compared to currently available phantoms and/or packages:	Score 1	2	3	4	5
The universal phantom is easy to transport					x
The universal phantom is light to handle				x	
The universal phantom is compact				x	
The universal phantom is simple to use				x	
The universal phantom is versatile					x
The user's manual is easy to follow and understand				x	
The data analysis software is easy to install					x
The data analysis software is easy to use				x	
Using the universal phantom saves time in data acquisition				x	
Using the software saves time in data analysis and decision making				x	
Results form the universal phantom package are reliable					
Results form the universal phantom package are accurate					
Results form the universal phantom package are reproducible			x		
The level of competence required to use the phantom			x		
The universal phantom package is a cost effective solution				x	

Limitations of the universal phantom package (please comment below)

The following limitations were noted when using the universal phantom package

The universal image quality assurance phantom: Slippery to the touch when taking out of housing

The universal image quality assurance phantom user's manual: Is not clear on some instructions:1. Page 5…Fig A.1b The numbers are labelled 1-20 but 14 seems to have been omitted
2. Page 7…If baseline values are set every major service/repair will that not cause a deterioration in the QA results in the case where the values deviate from commissioning/acceptance values?
3. Page 14…A2.3.2.h…says a total of 4 exposures…but 0, 2 &4cm is a total of 3 exposures…then another 3 for flouro so it wasn't clear where the 4 came from
4. Page 15 (and all other parts where corrective action is called for)…no corrective action was taken since not sure if the phantom is patented to have its values used as a reference for correction
5. Page 16…Fig A10.b..
6. Page 52..typo….it should be CT not Mammo on item A2.5.3.a
7. Page 53..A2.5.4..which 4 images for CT?
8. Results spreadsheet..Geometry and measurement tools(distance/accuracy/scaling) expects results for a square but there are no instructions on which square to be used…so it was assumed the one next to the cylinder.

The software doesn't specify the size of the ROIs; different sizes give different values.
When measuring slice thickness, drawing a straight line across the ramp is quite a subjective procedure. when two people measuring the slice thickness of the same image tend to get different values.

Other comments or recommendations (please comment below)

Figure 7.16: Independent evaluation results from IALCH for overall evaluation of the package.

With the overall evaluation of the entire universal phantom package, two of the evaluators did not score the criteria stating that the results are accurate. One did not score the reproducible results criterion and one did not score the reliable results criterion. The IALCH evaluator scored the reproducible results 3. This was due to the evaluators using the phantom package for the first time, with no experience on what results to expect and without any baseline results set for the universal phantom for the units they evaluated. However, with reference to the reproducibility testing of the phantom as discussed in Chapter 5, it can be stated with certainty that the results from the phantom are reproducible within the DoH prescribed tolerance levels.

Overall scores of 3 were given by two observers to the level of competence required to use the phantom package, however the CMJAH then comments that the phantom package can be successfully used by radiographers as well, in contradiction to the score. All other criteria were scored 4 or 5 by the three evaluators, i.e. agreement or strong agreement with the statements. All evaluators recommended ROI size to be displayed in the software, and this was added to the final version of the software. Two of the evaluators also reported the subjective drawing of the line for CT slice thickness, which was also simplified in the final software version. All recommended user's manual comments were incorporated as well.

7.6 Conclusions from independent validation

Further corrections, modifications and improvements to the phantom package were identified from the major concerns highlighted by the evaluators. The software was updated to display ROI size as it is drawn, to ensure more accurate results. It would also assist with drawing the line for slice thickness, which was subjective according to the evaluators. The recommended improvements were incorporated in the final version of the user's manual, included as Appendix A.

The universal image quality assurance phantom, the user's manual and data analysis software were independently validated for comprehensive routine image QC in general x-rays, fluoroscopy, mammography and CT scanning. Although the evaluation sample size was small, due to logistic, time and financial limitations, which are the identified problems in resource limited institutions, certain expectations can be made from these

results. It was expected that the universal image quality assurance phantom, user's manual and data analysis software addressed the three problems identified in resource limited institutions, as discussed in Chapter 1. The phantom thus:

1. Reduces costs as it is versatile and universal, i.e. not modality specific.
2. Addresses time constraints as image acquisition, data analysis and decision making times are reduced.
3. In response to the man power and expertise constraints the universal image quality assurance phantom package may be successfully used in institutions where medical physicists are not available by personnel operating the imaging equipment. This can be achieved with limited training, by using the step-by-step user's manual and intuitive data analysis software. Obtained results may be send to remote medical physicists or technicians for analysis, especially if results were out of limits, as recommended in Figure A.2. Also with proper training, it is hoped that radiographers would find this tool sufficiently user friendly so that it can be implemented more widely.

It is recommended that a larger evaluation population should be nominated to draw concrete conclusions from these expectations, and that this population should include radiographers. The phantom package is currently (September 2017) being evaluated by South African National Accreditation System (SANAS) accredited inspection bodies (IBs), i.e. by Siemens and East Cape X-Ray IBs. These institutions will report to DoH on the applicability, cost effectiveness and universal nature of the phantom for routine image QC in South Africa, making it a commercially viable option, recognised by DoH, for resource limited institutions.

Chapter 8

Conclusion

In diagnostic radiology, image quality must be maintained at clinically acceptable levels to prevent repeated examinations, misdiagnosis and oversights. To ensure this, routine image quality control is performed. This aids in the identification of faulty equipment and identifies image quality degradation before patient care is affected. Image quality is quantified using suitable phantoms. However commercially available phantoms could in some cases be expensive, complicated and time consuming to use. These are the problems that were identified in this study, i.e. inadequate funds, manpower and expertise and time constraints, especially considering the number of different phantoms that might be required to cover the needs of a radiology department. These problems are especially amplified in resource limited institutions and countries, such as many in Africa and including South Africa. The aim of the study was to simplify routine image quality control by developing a universal image quality assurance phantom that is cheap to manufacture, easy to use and not modality specific. This phantom would enable the operator to do comprehensive routine constancy check image quality control in general x-rays, fluoroscopy and mammography imaging and computed tomography (CT) scanning, with acceptable accuracy using a single phantom. A user's manual and data analysis software would assist the operator to setup the phantom and analyse results. This research was privately funded by the principal investigator and through a Harry Crossley bursary awarded to the principal investigator by Stellenbosch University.

A literature review on the physics of image formation was done in Chapter 2. The different interaction mechanisms of x-rays with materials and their influence on image quality were discussed. Image quality was defined in terms of contrast, resolution and noise and the equations needed to calculate these were included. The South African situation was highlighted in Chapter 2, showing the lack of medical physicists employed in diagnostic radiology both in private and in government institutions,

emphasizing the importance of this research. The Department of Health (DoH) requirements for image quality control (QC) in South Africa were summarized and these were used for reproducibility testing tolerance levels in Chapter 5.

The physics involved in the formation of x-ray produced images was considered for the imaging modalities investigated and the image quality assurance parameters that should be assessed for each imaging modality were determined. An in-depth literature review was done into current* image quality assurance phantoms commercially available. The advantages, disadvantages and design of these phantoms were considered. This knowledge, together with the physics of x-ray interactions in the diagnostic radiology energy range, was used to design a prototype phantom.

A prototype phantom design, based on conclusions from literature, was practically discussed with an engineer, machining limitations were identified and the design had to be adapted. For example, spherical inserts which would take advantage of spherical symmetry in different set up orientations of the phantom for planar imaging and CT scanning, could not be used. Spheres would be difficult and very expensive to manufacture and would also need to be large due to differences in attenuation of the incident x-ray beam through the sphere. These limitations were considered and a prototype phantom was manufactured, as described in Chapter 4. The prototype was validated by comparing it to commercially available phantoms.

The shortcomings of the prototype were addressed and a redesigned universal image quality assurance phantom was developed. This phantom was smaller than the prototype and contained smaller inserts for mammography fibres, micro-calcifications and masses, low contrast detectability and thinner sensitometry inserts, to minimise geometrical distortion in mammography. It also had a flat side to aid in phantom orientation during set up and for easy set up on a flat stand for CT scanning.

Data analysis software was written by a software programmer and the principal investigator compiled a complete step-by-step user's manual for analysing the images obtained with this phantom.

* This is implied as at the time of writing in 2016.

The phantom passed rigorous reproducibility testing in all imaging modalities and it was concluded that the results from the phantom were reproducible to within the limits stipulated by DoH, as discussed in Chapter 6. In Chapter 7 the phantom package (phantom, software and manual) was validated by three independent evaluators. They compared the universal image quality assurance phantom package to commercially available phantom options. All agreed that the phantom package was easy to transport, simple to use, compact and light, versatile and a cost-effective image quality control solution. It also saves time in image acquisition, data analysis and decision making. It was also mentioned that it can be successfully used by radiographers in institutions where medical physicists are not employed. The limitations mentioned by the evaluators included improving the data analysis software to display region of interest (ROI) size, to minimise bias when drawing the slice thickness ramp and updating the user's manual. These changes have already been made.

According to the results from the independent evaluators, although a small sample size for evaluation, it was expected that the universal phantom, user's manual and data analysis software offered an acceptable solution for comprehensive routine image QC for diagnostic radiology x-ray imaging modalities, especially for consistency purposes. It was simple to use and implement, with clear instructions, ensuring suitability for the full spectrum of diagnostic radiology practices and clinics, including those with maximum workload using CT, mammography, general x-rays (including mobile x-ray units) and fluoroscopy, to small clinics using a single or only a few imaging units with fewer patients. The phantom was compact, robust, easy to use and cheaper to manufacture, addressing the above mentioned problems and answering the aims of the study.

The limitations of the universal image quality assurance phantom are:

a.) Encountered machining limitations. The method of manufacturing the phantom is human based, as the inserts are placed in the machined phantom housing by hand. This introduces some inaccuracies in placement and dimensions of the inserts. As the manufacturing equipment at Gebratech Advanced Engineering is not designed for optimal use at the small scales encountered in phantom manufacturing, the accuracy of the manufacturing of the phantom inserts can be improved, at an increased cost. However, it is important to note the image quality evaluation that the universal

phantom is intended for, i.e. consistency testing, depends primarily on the densities of the housing material and different inserts. As the same materials are used in each phantom, the variation between different phantoms will be minimal. It is advised that baseline values should be set for every individual phantom and that only that phantom should be used routinely, i.e. cross population of results is not recommended. As region of interest analysis is used in most image QC tests, small variations in insert size and position will not affect obtained results and are not a major concern. Most importantly, the density of the different materials should not vary noticeably. With cost one of the identified problems in resource limited institutions, improved accuracy and smaller machining tolerances must be weighed up against increased manufacturing costs to achieve these. For routine image QC, comparing the results from a certain phantom to its set baseline results, improving the manufacturing will increase the costs, contradicting one of the aims of the study, with no real gain in obtained results. However, for acceptance testing this does not apply.

b.) Another limitation is that the universal image quality assurance phantom is not suitable for acceptance testing, where accurate results are required to ensure equipment conforms to specifications, but it is a good tool for routine image QC consistency testing, comparing routine results to baseline values set at commissioning.

c.) The phantom can also not measure Hounsfield unit (HU) linearity in CT scanning, rather just an indication of CT number consistency for different inserts, as the linear attenuation coefficients of the insert materials are not known.

d.) As discussed in Chapter 4, the slice thickness in only applicable for 5 mm slice thickness or larger. A correction for the thickness dimension, i.e. 3 mm, of the ramp is needed, as well as a correction of the angle at which it is placed in the phantom, i.e. 38^{o}. These two corrections, in this setting, cancel out, which means the projected image is the actual slice thickness and can be measured. The ramp would not be able to assess slice thicknesses smaller than its thickness. More accurate results can be obtained, as discussed in Chapter 4, but again at a significant cost increase, and as the current design is quite suitable for routine image QC consistency testing, such increased expensed would defy the cost reduction purpose of the phantom.

e.) There is a limitation on the imageable area that can be assessed for non-uniformities due to the limited dimension, i.e. 170 mm of the phantom. Image quality is assessed only within this dimension. With tests like uniformity or the presence of

artefacts for example, errors could exist outside the phantom dimensions and these would be missed.

f.) The results from the phantom are not yet recognised by the DoH in South Africa, proving that it is an acceptable routine QC solution in our country, and with South African Bureau of Standards (SABS) endorsement the phantom package could address the problems in resource limited institutions internationally.

It is important to note that the phantom package does not substitute medical physics knowledge, and when problems in routine image QC are encountered a medical physicist and/or equipment technician should still be contacted. The phantom package is only intended to simplify routine image QC and to make QC available in institutions affected by the identified problems. Further improvements include refining of the phantom packaging case, to be even more compact with better internal design for holding the different components.

The universal image quality assurance phantom, user's manual and data analysis software will make comprehensive routine consistency checking x-ray image quality control in diagnostic radiology easier, quicker, cheaper (with a manufacturing cost of the phantom package of less than R 15 000 per unit) and available to resource limited institutions. It will fill an identified gap in the existing market, as an additional option to the current* commercially available phantoms, protected under the PCT International Patent Application No. PCT/IB2016/051165.

* This is implied as at the time of writing in 2016.

Bibliography

1. Dance, D.R., Christofides, S., Maidment, A.D.A., et al. 2014. *Diagnostic radiology physics - a handbook for teachers and students*. 1st ed. Ch 1. Austria: IAEA.
2. Dance, D.R., Christofides, S., Maidment, A.D.A., et al. 2014. *Diagnostic radiology physics - a handbook for teachers and students*. 1st ed. Ch 19. Austria: IAEA.
3. Reis, C., Pascoal, A., Sakellaris, T., Koutalonis M. 2013. Quality assurance and quality control in mammography: a review of available guidance worldwide. *Insights Imaging*, 4, p.539-553.
4. Task group no 7 - diagnostic x-ray imaging. 1990. Equipment requirements and quality control for mammography. *AAPM Report No 29*, p.32-69.
5. Diagnostic radiology committee task force on quality assurance protocol. 1977. Basic quality control in diagnostic radiology. *AAPM Report No 4*, p.1-51.
6. Report task group no 12 – diagnostic x-ray imaging committee. 2002. Quality control in diagnostic radiology. *AAPM Report No 74*, p.1-56.
7. Department of Health, directorate radiation control. 2014. Requirements for licence holders with respect to quality control tests for diagnostic radiology x-ray imaging systems. Code: Diagnostic QC, 8, p.4-26.
8. Dance, D.R., Christofides, S., Maidment, A.D.A., et al. 2014. *Diagnostic radiology physics - a handbook for teachers and students*. 1st ed. Ch 7. Austria: IAEA.
9. Bushberg, J.T., Deibert, J.A., Leidholdt, E.M., Boone, J.M. 2012. *The essential physics of medical imaging*. 3rd ed. Ch 1. Philadelphia: Lippincott Williams & Wilkens.
10. Bushberg, J.T., Deibert, J.A., Leidholdt, E.M., Boone, J.M. 2012. *The essential physics of medical imaging*. 3rd ed. Ch 6. Philadelphia: Lippincott Williams & Wilkens.

11. Dance, D.R., Christofides, S., Maidment, A.D.A., et al. 2014. *Diagnostic radiology physics - a handbook for teachers and students*. 1st ed. Ch 2. Austria: IAEA.
12. Bushberg, J.T., Deibert, J.A., Leidholdt, E.M., Boone, J.M. 2012. *The essential physics of medical imaging*. 3rd ed. Ch 3. Philadelphia: Lippincott Williams & Wilkens.
13. Dance, D.R., Christofides, S., Maidment, A.D.A., et al. 2014. *Diagnostic radiology physics - a handbook for teachers and students*. 1st ed. Ch 11. Austria: IAEA.
14. Bushberg, J.T., Deibert, J.A., Leidholdt, E.M., Boone, J.M. 2012. *The essential physics of medical imaging*. 3rd ed. Ch 4. Philadelphia: Lippincott Williams & Wilkens.
15. Dance, D.R., Christofides, S., Maidment, A.D.A., et al. 2014. *Diagnostic radiology physics - a handbook for teachers and students*. 1st ed. Ch 4. Austria: IAEA.
16. Bushberg, J.T., Deibert, J.A., Leidholdt, E.M., Boone, J.M. 2012. *The essential physics of medical imaging*. 3rd ed. Ch 6. Philadelphia: Lippincott Williams & Wilkens.
17. Bushberg, J.T., Deibert, J.A., Leidholdt, E.M., Boone, J.M. 2012. *The essential physics of medical imaging*. 3rd ed. Ch 10. Philadelphia: Lippincott Williams & Wilkens.
18. Bushberg, J.T., Deibert, J.A., Leidholdt, E.M., Boone, J.M. 2012. *The essential physics of medical imaging*. 3rd ed. App G4. Philadelphia: Lippincott Williams & Wilkens.
19. Department of Health, directorate radiation control. ECRI codes and X-ray totals per ECRI. [Email]. (Personal communication with Mr E Smit from Radiation Control, 17 March 2016) Available at: SmitE@health.gov.za
20. South African Association of Physicists in Medicine and Biology. SAAPMB members. [Email]. (Personal communication with Ms T du Plessis, secretary of SAAPMB, 15 February 2016) Available at: Tamarisk Du Plessis tduplessis@equrahealth.co.za
21. Bushberg, J.T., Deibert, J.A., Leidholdt, E.M., Boone, J.M. 2012. *The essential physics of medical imaging*. 3rd ed. Ch 11. Philadelphia: Lippincott Williams & Wilkens.

22. Guidelines and standards committee - medical physics. 2011. ACR technical standard for diagnostic medical physics performance monitoring of radiographic and fluoroscopic equipment. *ACR technical standard resolution 4*, p.1-4.
23. Committee on quality assurance in diagnostic x-ray. 2001. Quality control recommendations for diagnostic radiography volume 3: radiographic or fluoroscopy machines. *Conference of Radiation Control Program Directors, Inc*. p.1-61.
24. Leeds test objects. TOR CDR. 2017. [online]. Available at: http://www.leedstestobjects.com/index.php/phantom/tor-cdr/ [accessed 25 September 2013]
25. User manual Normi® 13. PTW Freiburg. Available from: wayne@flowbiomed.co.za [accessed 2 November 2015]
26. Dance, D.R., Christofides, S., Maidment, A.D.A., et al. 2014. *Diagnostic radiology physics - a handbook for teachers and students*. 1st ed. Ch 8. Austria: IAEA.
27. Bushberg, J.T., Deibert, J.A., Leidholdt, E.M., Boone, J.M. 2012. *The essential physics of medical imaging*. 3rd ed. Ch 9. Philadelphia: Lippincott Williams & Wilkens.
28. Leeds test objects. TOR 18FG. 2017. [online]. Available at: http://www.leedstestobjects.com/index.php/phantom/tor-18fg/ [accessed 25 September 2013]
29. CIRS tissue simulation & phantom technology. RD/FL contrast resolution test phantom. 2013. [online]. Available at: http://www.meditron.ch/industrial-and-research/downloads/L647_DS_120913.pdf [accessed 25 September 2013]
30. Universal Medical. CIRS L600 fluoroscopic alignment device. 2017. [online]. Available at: http://www.hnamedical.com/product/radiology/phantoms-cirs/fluoroscopic-alignment-device/ [accessed 25 September 2013]
31. JRT Associates. Pro-RF HighRes. 2015. [online]. Available at: http://jrtassociates.com/pro-rfhighres.aspx [accessed 2 February 2016]
32. JRT Associates. Fluoro-test resolution tool. 2015. [online]. Available at: http://jrtassociates.com/fluoro-testresolutiontool.aspx [accessed 26 March 2014]
33. Fluke Biomedical. Fluoro-test tool. 1995. [online]. Available at: http://www.flukebiomedical.com/biomedical/usen/diagnostic-imaging-

qa/radiography-fluoroscopy/07-645-fluoro-test-tool.htm?pid=54332 [accessed 26 March 2014]

34. Fluke Biomedical. CDRH fluoroscopic phantom. 1995. [online]. Available at: http://www.flukebiomedical.com/biomedical/usen/diagnostic-imaging-qa/radiography-fluoroscopy/07-649-cdrh-fluoroscopic-phantom.htm?pid=54334 [accessed 26 March 2014]
35. Radcal. SFS set. 2011. [online]. Available at: http://www.el-se.com/wp-content/uploads/2016/02/SFS-SET-product-specifications.pdf [accessed 26 March 2014]
36. JRT Associates. R/F QC phantom. [online]. Available at: http://jrtassociates.com/pdfs/07-647.pdf [accessed 25 September 2013]
37. Medical Device Depot Inc. Radiography fluoroscopy AQ phantom. 2015. [online]. Available at: http://www.medicaldevicedepot.com/Radiography-Fluoroscopy-QA-Phantom-p/903.htm [accessed 25 September 2013]
38. JRT Associates. Gammex radiographic/fluoroscopic kit. [online]. Available at: http://jrtassociates.com/pdfs/184d.pdf [accessed 26 March 2014]
39. Fluke Biomedical. Fluoroscopic imaging test phantom. 1995. [online]. Available at: http://www.flukebiomedical.com/biomedical/usen/diagnostic-imaging-qa/radiography-fluoroscopy/07-653-fluoroscopic-imaging-test-phantom.htm?pid=54337 [accessed 26 March 2014]
40. Rauch, P. Fluoroscopic imaging equipment guidelines for detector input dose settings and image optimization. Henry Ford Health Systems. 2009. [online]. Available at: http://www.aapm.org/meetings/amos2/pdf/42-11966-85041-390.pdf [accessed 25 September 2013]
41. PTW Freiburg. Normi® Rad/Flu. 2012. [online]. Available at: http://www.ptw.de/normi_rad-flu_test_object0.html?&cId=4194 [accessed 1 November 2015]
42. PTW Freiburg. Normi® Rad/Flu. 2012. [online]. Available at: http://ptw.de/2856.html [accessed 4 February 2016]
43. User manual Normi® 3 + 4. PTW Freiburg. 1987. Available from: wayne@flowbiomed.co.za [accessed 2 November 2015]
44. Dance, D.R., Christofides, S., Maidment, A.D.A., et al. 2014. *Diagnostic radiology physics - a handbook for teachers and students*. 1st ed. Ch 9. Austria: IAEA.

45. Task group no 7 - diagnostic x-ray imaging. 1990. Equipment requirements and quality control for mammography. *AAPM Report No 29*, p.1-31.
46. Bushberg, J.T., Deibert, J.A., Leidholdt, E.M., Boone, J.M. 2012. *The essential physics of medical imaging*. 3rd ed. Ch 8. Philadelphia: Lippincott Williams & Wilkens.
47. De las Heras, H., Schöfer, F., Tiller, B. et al. 2013. A phantom using titanium and Landolt rings for image quality evaluation in mammography*. Physics in Medicine and Biology*, 58, p.L17-L30.
48. JRT Associates. Mammographic accreditation phantom Gammex 156. 2015 [online]. Available at: http://jrtassociates.com/mammographicaccreditationphantom.aspx [accessed 25 September 2013]
49. JRT Associates. Stereotactic mammographic accreditation phantom Gammex 156D. [online]. Available at: http://jrtassociates.com/pdfs/156d.pdf [accessed 25 September 2013]
50. JRT Associates. Tissue equivalent phantom for mammography. [online]. Available at: http://jrtassociates.com/pdfs/011a.pdf [accessed 25 September 2013]
51. JRT Associates. Routine mammographic QC kit. [online]. Available at: http://jrtassociates.com/pdfs/183.pdf [accessed 25 September 2013]
52. JRT Associates. Mammography QA package. [online]. Available at: http://jrtassociates.com/pdfs/c_mammo_kit.pdf [accessed 25 September 2013]
53. JRT Associates. Special high contrast resolution phantom. [online]. Available at: http://jrtassociates.com/pdfs/c_016b.pdf [accessed 25 September 2013]
54. JRT Associates. Single exposure high contrast resolution phantom. 2011. [online]. Available at: http://jrtassociates.com/pdfs/016a.pdf [accessed 25 September 2013]
55. JRT Associates. Artifact identification phantom. 2015. [online]. Available at: http://jrtassociates.com/artifactidentificationphantom.aspx [accessed 25 September 2013]
56. JRT Associates. Contrast detail phantom for mammography. [online]. Available at: http://jrtassociates.com/pdfs/18-252.pdf [accessed 25 September 2013]
57. JRT Associates. Mammography BR3D phantom. [online]. Available at: http://jrtassociates.com/pdfs/c_020.pdf [accessed 25 September 2013]

58. JRT Associates. Mammography BR3D phantom. [online]. Available at: http://jrtassociates.com/pdfs/c_017_018.pdf [accessed 25 September 2013]
59. User manual Normi® PAS. PTW Freiburg. 2013. Available from: wayne@flowbiomed.co.za [accessed 2 November 2015]
60. Smith, S.W. 1997. *The scientist and engineer's guide to digital signal processing*. [e-book]. 1st ed. DSP: San Diego. Available at: http://www.dspguide.com/ [accessed 11 January 2016]
61. Diagnostic radiology committee task force on CT scanner phantoms. 1977. Phantoms for performance evaluation and quality assurance of CT scanners. *AAPM Report No 1*, p.1-23.
62. McCollough, C.H., Bruesewitz, M.R., McNitt-Gray, M.F. et al. 2004. The phantom portion of the American College of Radiology (ACR) Computed Tomography (CT) accreditation program: practica tips, artifact examples, and pitfalls to avoid. *Medical Physics*, 31 (9), p.2423-2442.
63. McCollough, C.H. CT accreditation program: image quality and dose measurements. 2003. [online]. Available at: https://www.aapm.org/meetings/03AM/pdf/9785-27333.pdf [accessed 11 January 2016]
64. Gammex. ACR CT accreditation phantom. 2015. [online]. Available at: https://www.sunnuclear.com/documents/datasheets/gammex/ct_acr_464_phantom.pdf [accessed 17 December 2013]
65. Gammex. Head/body CT phantom. 2017. [online]. Available at: http://test.gammex.netphoria.com/n-portfolio/productpage.asp?id=321&category=Diagnostic+Radiology&name=Head%2FBody+CT+Phantom%2C+Gammex+461A [accessed 17 December 2013]
66. CIRS tissue simulation & phantom technology. AAPM CT performance phantom. 2017. [online]. Available at: http://www.cirsinc.com/products/all/31/aapm-ct-performance-phantom/ [accessed 17 December 2013]
67. JRT Associates. Mammography BR3D phantom. [online]. Available at: http://jrtassociates.com/pdfs/c_610.pdf [accessed 17 December 2013]

68. Universal Medical. Spiral/Helical CT phantom. 2012. [online]. Available at: http://cspmedical.com/content/110-1063_061_spiral_ct_phantom.pdf [accessed 25 September 2013]
69. The phantom laboratory. Catphan® 600 CT phantom. [online]. Available at: https://www.phantomlab.com/catphan-600 [accessed 17 December 2013]
70. JRT Associates. Catphan® 500/600. [online]. Available at: http://jrtassociates.com/pdfs/Catphan.pdf [accessed 17 December 2013]
71. Chiarot, C.B., Siewerdsen, J.H., Haycocks, T. et al. 2005. An innovative phantom for quantitative and qualitative investigation of advanced x-ray imaging technologies. *Physics in Medicine and Biology*, 50, p.N287-N297.
72. Groenewald, A., Groenewald, WA. 2014. In-house development of a neonatal chest simulation phantom. *Journal of Applied Clinical Medical Physics*, 15 (3), p.282-296.
73. Groenewald, A., Groenewald, W.A. 2014. Cancer Induction to Neonates Receiving Anterior-Posterior Chest X-Rays. *Global Journal of Science Frontier Research*, 14 (3), p.32-39.
74. Gartech Engineering Plastics. Density of plastics. [Email]. (Personal communication with Mr C Vine-Soanes from Gartech Engineering Plastics, 18 March 2015) Available at: http://www.gartech.co.za / chris@gartech.co.za
75. Goodfellow Catalogue., 2012. Polyamide/imide sheet and Polyethylene – High density, [online]. Available at: http://www.goodfellowusa.com/A/Polyethylene-High-density.html [accessed 22 March 2012]
76. Protolink3D. Density specifications for ABS, PLA and Hips. [Email]. (Personal communication with local representative, Mr M Havinga from Protolink3D, 6 November 2014) Available at: http://www.prolink3d.co.za / info@prolink3d.co.za
77. Gammex RMI©. Specifications Gammex 457, 450, 452, 453, 454, 455, 456. [Email]. (Personal communication with local Gammex representative, Mr G Corazza from CM Nuclear Systems c.c., 8 December 2010)
78. The phantom laboratory. Catphan® 500 and 600 manual. 2006. [online]. Available at: http://www.uio.no/studier/emner/matnat/fys/FYS4760/v13/obligatorisk-oppgave-ct/catphan500-600manual.pdf [accessed 2 November 2015]

Appendix A

Universal image quality assurance phantom user's manual

This manual forms part of the research presented in partial fulfilment of the requirements for the degree of PhD (Medical Physics) in the Faculty of Medicine and Health Sciences at Stellenbosch University. The research proposal is the intellectual property of Stellenbosch University under the PCT International Patent Application No. PCT/IB2016/051165.

Table of contents

This page is intentionally left blank.

A.1 General information

The purpose of this document is to provide guidance on the design and implementation of a quality assurance program in a diagnostic radiology division for x-ray generating equipment using the universal image quality phantom and accompanying data analysis software. The phantom, user's manual and data analysis software can be used in any department, operating at any level of business. The user's manual describes the construction of the phantom, its set-up for exposure in the different imaging modalities and explains the image acquisition and result analysis process, with reference to the data analysis software. The figures included in the manual are for guidance only and do not necessarily represent desired or expected results.

In the general requirements for diagnostic radiology equipment licence holders, the Department of Health (DoH), states that the licence holder must obtain Quality Control (QC) manuals or develop in-house protocols, describing step by step the procedure for correctly performing QC tests. DoH also states that results have to be recorded and stored and must include the measurements, test date, results summary, identification of equipment tested, phantoms used and person performing the tests. The universal phantom's user's manual and example data collection sheets complies to this. In addition, the universal phantom assesses all the tests specified by DoH.

The universal image quality assurance phantom aims to simplify routine image quality control, reducing costs and giving resource limited institutions access to comprehensive routine image quality control with easy to follow user's manual and data analysis software. The phantom is intended for constancy testing, comparing routine results obtained with the phantom to those base line values set with the phantom.

A.1.1 Intended use

The universal image quality assurance phantom, user's manual and data analysis software are designed for image quality constancy testing of x-ray generating equipment in diagnostic radiology. This includes general x-ray machines, both fixed and mobile units, fluoroscopy devices, mammography units and computed tomography (CT) scanners.

Using the universal phantom fulfils the requirements from the South African regulatory body, the Directorate Radiation Control of the South African Department of Health, for comprehensive routine image quality control.

A.1.2 Safety information

- Do not handle the phantom hard-handedly. Impact can cause the phantom halves to separate and inserts to shift or fall out.
- Do not open the phantom. Small parts are contained, which can get lost and are a choking hazard.
- Store the phantom in a cool place (room temperature of maximum 28^{o}C). The phantom and insert plastics are heat sensitive.

A.2 Operating manual

This section explains the procedures for set-up and imaging of the phantom and analysis of the obtained images. The frequency of conducting the tests is based on the recommendations from the South African Department of Health and according to recommendations from literature.

The tests can be conducted by a radiographer, medical physicist, technician or any other suitably qualified personnel who is adequately trained on the operation of the different imaging units. The test frequency in Tables A.2 to A.4 is the recommended minimum standard and frequency of tests can be increased for best practice level, according to the man power and time constraints of each individual department.

The objective of image quality control by consistency testing in x-ray imaging is to ensure image quality is maintained at clinically acceptable levels to prevent misdiagnosis and oversights. It also decreases patient radiation exposure as retake exposures can be reduced if equipment failure is identified early, thus adhering to the As Low As Reasonably Achievable (ALARA) principle.

A schematic representation of the phantom is included in Figure A.1 a.) with a photo of the phantom bottom half in Figure A.1 b.). The densities of the different insert materials are included in Table A.1.

Table A.1: Phantom insert materials.

Insert	Material	Density (gcm^{-3})
Housing	High density polyethylene (HDPE)	0.95
Sensitometry	Objet RGD240	1.17
Contrast resolution	Teflon	2.20
	Gammex SB3 bone	1.82
	Supawood	0.74
	Gammex LN300 lung	0.30
	Air	0.00
Fibres	Rubber	1.26
Slice thickness ramp	Gammex SB3 bone	1.82
Circular geometry cylinder	Polymethyl methacrylate (PMMA)	1.18
Micro-calcifications	Metal	Not known
MTF beads	Metal	Not known

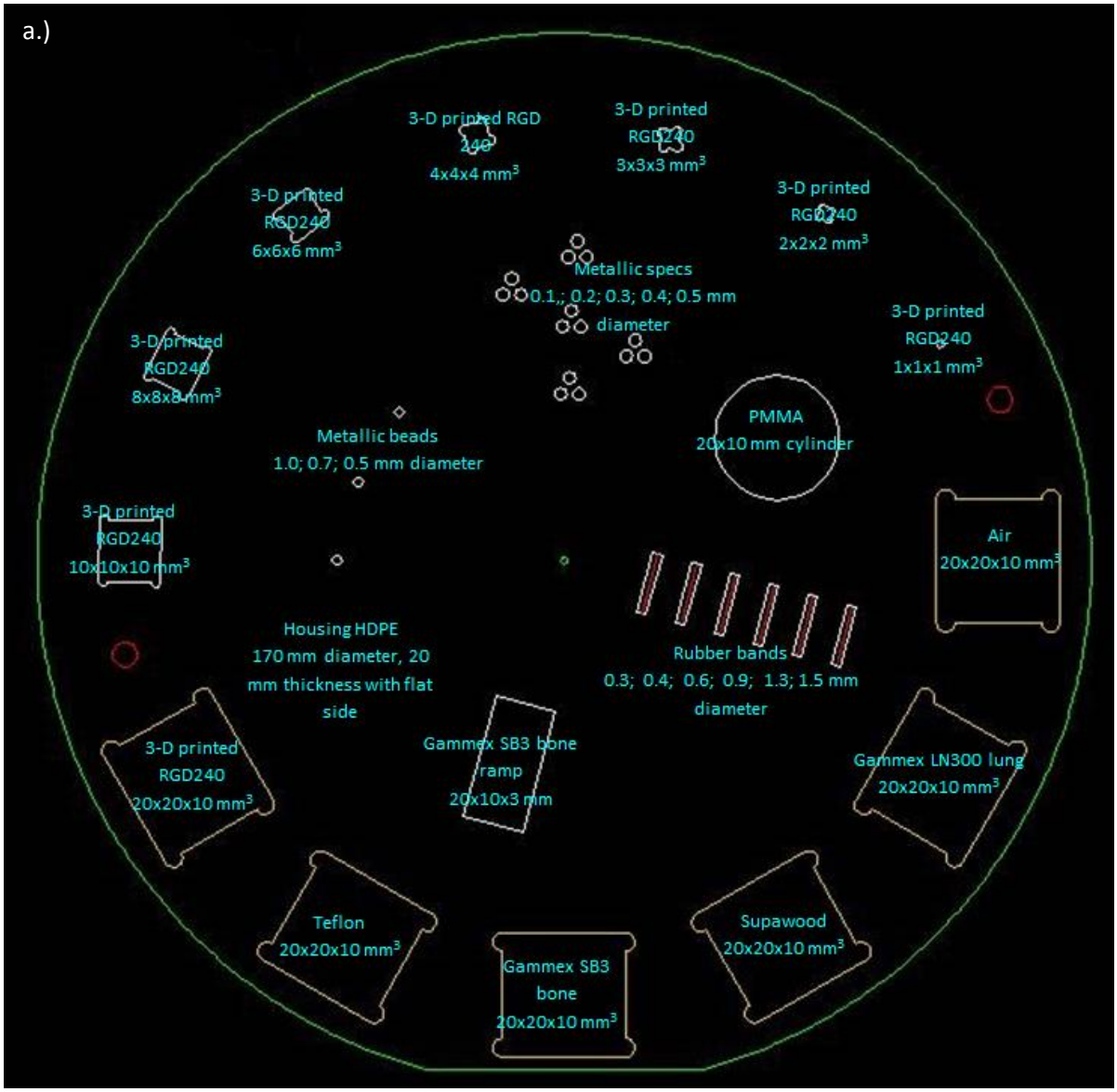

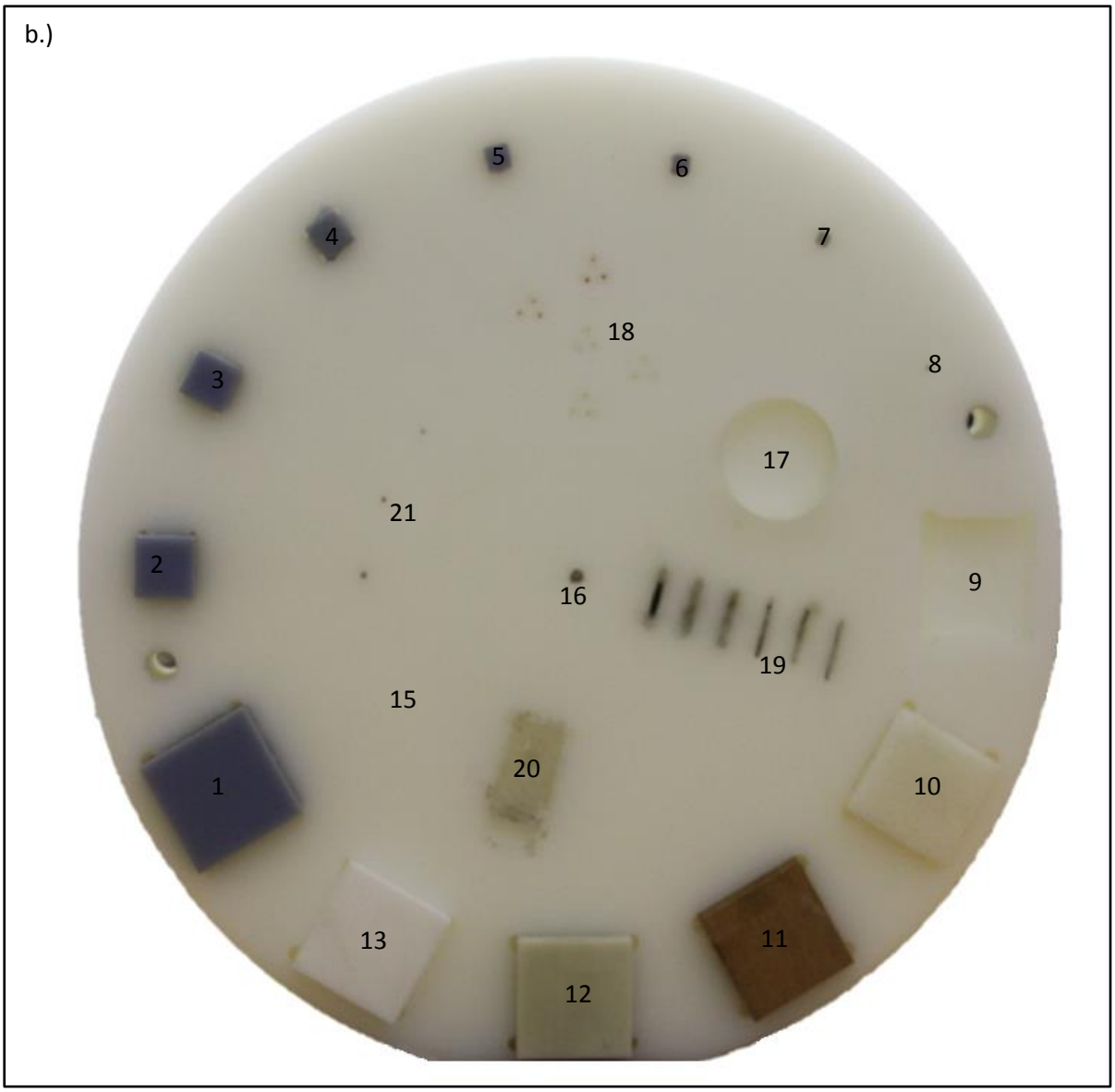

Figure A.1: a.) Schematic representation of the sizes and materials of the different inserts of the universal image quality assurance phantom. b.) A photo of the phantom showing the layout of the inserts in the phantom bottom half. The numbers in the figure are used in Tables A.2 to A.4.

Should the results be out of tolerance, i.e. the stated limits in Tables A.2 to A.4 are exceeded, the recommended corrective action procedure is shown in Figure A.2.

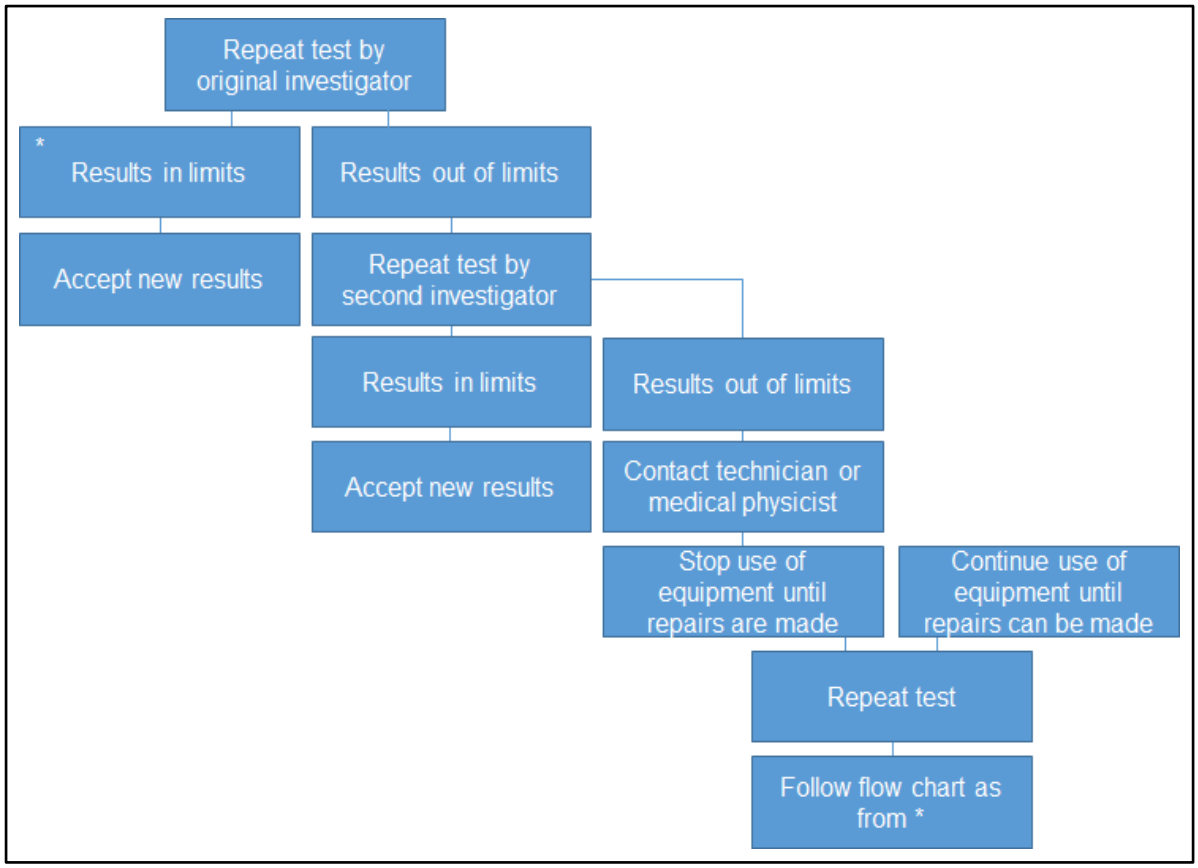

Figure A.2: Corrective action procedure for out of tolerance test results.

A.2.1 Acceptance testing versus routine QC

Acceptance testing is performed when equipment is first installed. It ensures that equipment specifications are met. For this very accurate results and values are required, which cannot be delivered by the current version of the universal image quality assurance phantom.

At commissioning, baseline values are set. The universal image quality assurance phantom can be used for this application. The baseline values, i.e. the initial performance of the equipment, are used for future comparison to routine QC results obtained with the universal image quality assurance phantom. Where baseline results are out of tolerance, the necessary steps have to be taken to correct these before the results are accepted as baseline. Routine QC results are then compared to these initial results to ensure equipment performance is maintained.

After major services or repairs, the commissioning tests should be repeated and new baseline values set.

The phantom is intended for constancy testing, comparing routine results obtained to those base line values set with the phantom during commissioning. As the universal image quality assurance phantom is unique, its results cannot be directly compared to those obtained with other commercially available phantoms, i.e. routine image QC results from the universal phantom should be compared to universal phantom set baseline values.

A.2.2 Installing the data analysis software on your computer

Data analysis software forms part of the universal image quality assurance phantom package and is included on a compact disk (CD).

To install the software on a computer that will be used for data analysis, the following system requirements are needed:

- At least Windows 7 Service Pack 1 (Apple is not supported)
- Minimum screen resolution of 1024 x 768
- CD drive
- 2 GB RAM memory

To install the software:

- Insert the CD into the CD drive.
- When prompted by the AutoPlay message, select Open folder to view files. This is shown in Figure A.3.

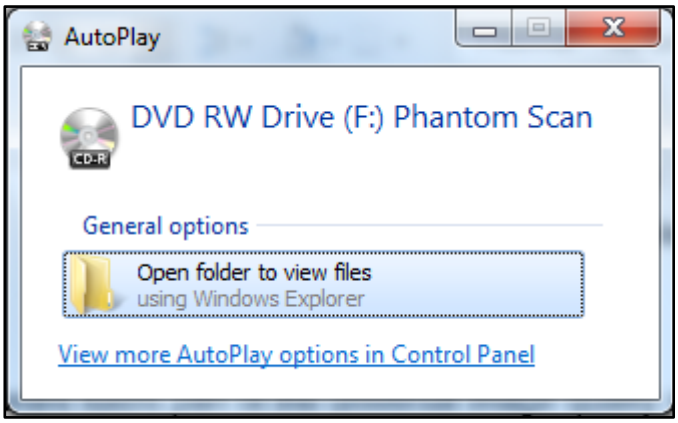

Figure A.3: AutoPlay prompt to open the CD.

- Under Files Currently on the Disk a Phantom Scan Data Analysis Software folder is available. Right click on the folder and select Copy. This is shown in Figure A.4.

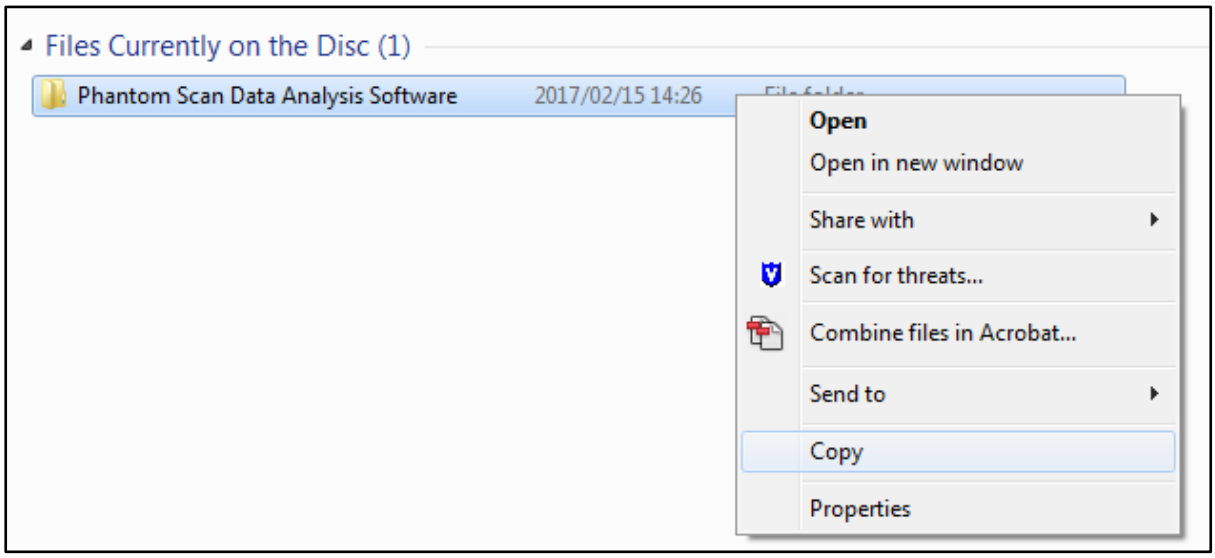

Figure A.4: Copying the software folder.

- Choose a location where the software will be stored, e.g. Desktop. At this location, right click and select Paste, as shown in Figure A.5. The Phantom Scan Data Analysis Software folder is now available at this location on your computer.

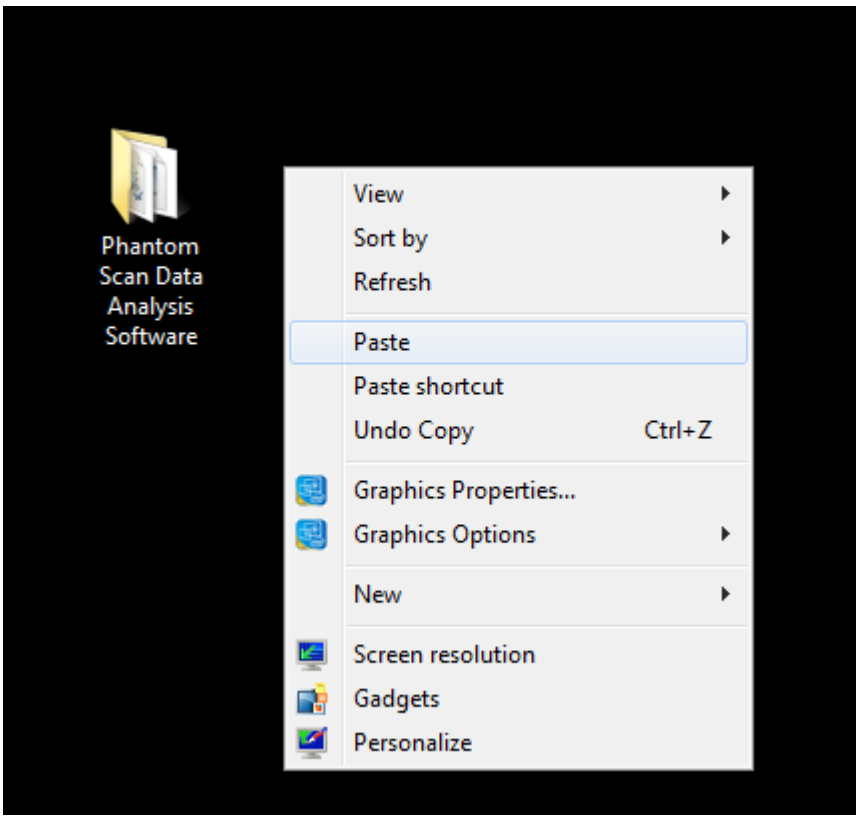

Figure A.5: Pasting the software folder.

- Double left click on the folder. A window showing the files in Figure A.6 will open.

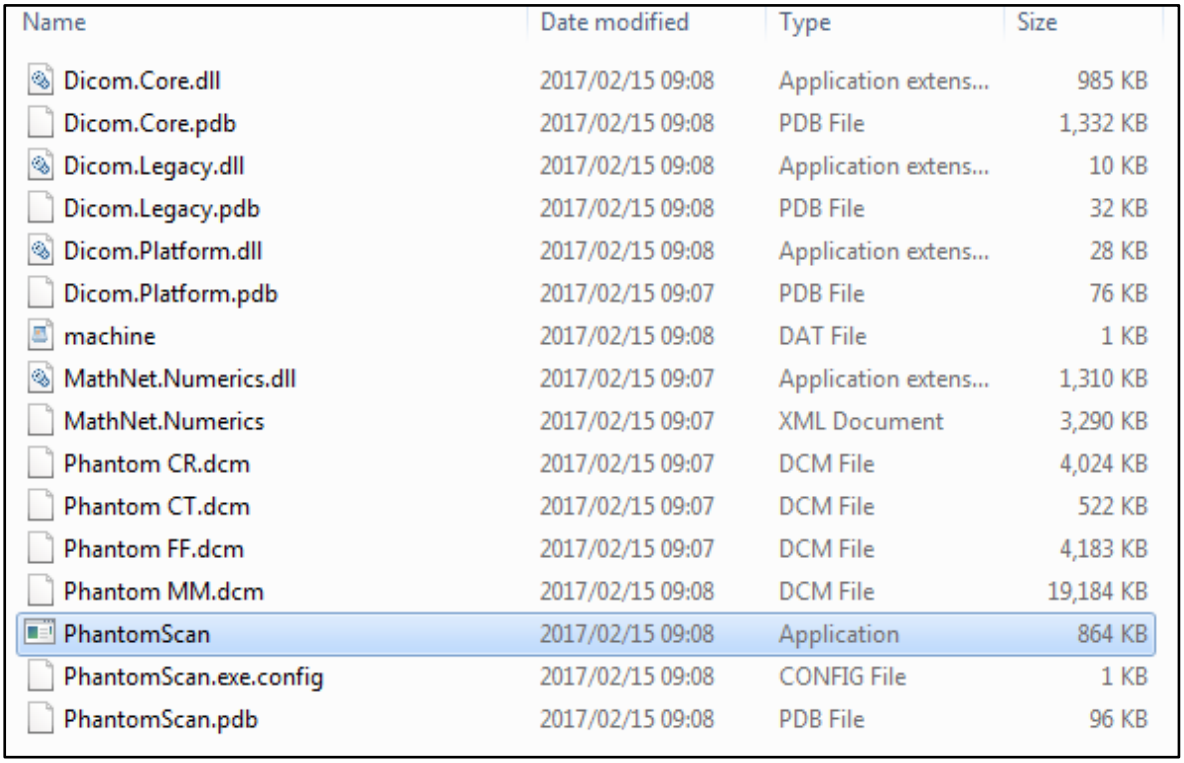

Name	Date modified	Type	Size
Dicom.Core.dll	2017/02/15 09:08	Application extens...	985 KB
Dicom.Core.pdb	2017/02/15 09:08	PDB File	1,332 KB
Dicom.Legacy.dll	2017/02/15 09:08	Application extens...	10 KB
Dicom.Legacy.pdb	2017/02/15 09:08	PDB File	32 KB
Dicom.Platform.dll	2017/02/15 09:08	Application extens...	28 KB
Dicom.Platform.pdb	2017/02/15 09:07	PDB File	76 KB
machine	2017/02/15 09:08	DAT File	1 KB
MathNet.Numerics.dll	2017/02/15 09:07	Application extens...	1,310 KB
MathNet.Numerics	2017/02/15 09:07	XML Document	3,290 KB
Phantom CR.dcm	2017/02/15 09:07	DCM File	4,024 KB
Phantom CT.dcm	2017/02/15 09:07	DCM File	522 KB
Phantom FF.dcm	2017/02/15 09:07	DCM File	4,183 KB
Phantom MM.dcm	2017/02/15 09:08	DCM File	19,184 KB
PhantomScan	2017/02/15 09:08	Application	864 KB
PhantomScan.exe.config	2017/02/15 09:08	CONFIG File	1 KB
PhantomScan.pdb	2017/02/15 09:08	PDB File	96 KB

Figure A.6: Files in the Phantom Scan Data Analysis Software folder.

- Double left click on the PhantomScan Application file, as highlighted in Figure A.6.
- The Phantom Scan application opens and is ready for use. This is shown in Figure A.7.

Figure A.7: Phantom Scan application open and ready for use.

A.2.3 General x-ray and fluoroscopy imaging

These tests are performed for both fixed and mobile x-ray units and for fluoroscopy devices. Table A.2 shows the tests required for comprehensive image quality assurance in general x-ray and fluoroscopy imaging.

Table A.2: Tests required for comprehensive general x-ray and fluoroscopy image quality assurance. (Insert numbers in table refer to Figure A.1 b.))

Test	Objective	Method	Frequency	Limits
Sensitometry & grey scale linearity (optical density consistency)	Maintain grey scale value for different object densities	ROI analysis with data analysis software using inserts 1, 9-13	Acceptance, 3 monthly	Baseline grey scale value ± 0.20 For universal phantom baseline grey scale value ± 2 %
Low contrast detectability	Distinguish objects of density similar to background as they become progressively smaller	Visual inspection of inserts 1-8 to determine smallest visible insert	Acceptance, 3 monthly	Baseline value + 1 insert size
Uniformity	Ensure grey scale values across the image remain constant for the same material	ROI analysis with data analysis software using phantom housing 15	Acceptance, 3 monthly	Mean value ± 10 % Mean value ± 5 % for DR
Resolution	Consistently distinguish objects as they become smaller and closer together	MTF analysis and plot with data analysis software using insert group 21	Acceptance, 3 monthly	Baseline value minus 25 %
Image noise	Quantum mottle is sufficiently low as to not degrade image quality unacceptably	ROI analysis with data analysis software using phantom housing 15 and Equations A.1 and A.2	Acceptance, 3 monthly	Baseline value ± 10 %
Positioning & alignment (X-ray / light beam centring)	Checks the coincidence of the light and x-ray fields	Visually check that the entire phantom is captured in the image	Acceptance, 3 monthly	Obtained value ± 1 cm for imaging at 100 cm SID

Geometry and measurement tools (distance accuracy / scaling errors)	To ensure geometrical distortion and scaling does not occur	Comparing distances measured with data analysis software to know distances	Acceptance, 3 monthly	Obtained value ± 0.5 cm or ± 2 %, whichever is smaller
Artefacts	Check that the image is free of artefacts	Visually inspect images for lines, spots, blur, marks, etc	Acceptance, 3 monthly	No visible artefacts
Image quality visual inspection	Consistently maintains visual image quality	Visually inspect images noting inserts and artefacts seen	Acceptance, 3 monthly	Reproducible results
Standard signal	Keep the grey scale value of a certain material (HDPE) constant over time	ROI analysis with data analysis software using phantom housing 15	Acceptance, 3 monthly	Baseline grey scale value ± 0.20 For universal phantom baseline grey scale value ± 2 %
AEC performance	Maintains image quality at acceptable level for different phantom thicknesses	Compare the results from AEC exposures with different phantom thicknesses	Acceptance, 3 monthly	Image quality variation within 10 % for 0, 20 and 40 mm phantom thickness
AEC repeatability	Ensures image quality is maintained using AEC	Compare the results from different AEC exposures of the same phantom thickness	Acceptance, yearly	Mean grey scale value ± 0.2 For universal phantom baseline value ± 2 % Image quality variation within 5 %

A.2.3.1 Phantom set-up

a. Place the phantom on the bed underneath the x-ray tube, with the scribe lines facing the x-ray tube.
b. Position the flat side towards the anode side of the x-ray tube.

c. Align the phantom scribe lines and x-ray tube cross hairs. This is shown in Figure A.7 a.).
d. Measure 100 cm source-to-surface distance (SSD) from x-ray tube to the surface of the phantom. Figure A.7 b-c.) illustrates this.
e. Collimate the light field so that the phantom is exactly covered by the light field, refer to Figure A.7 d.).

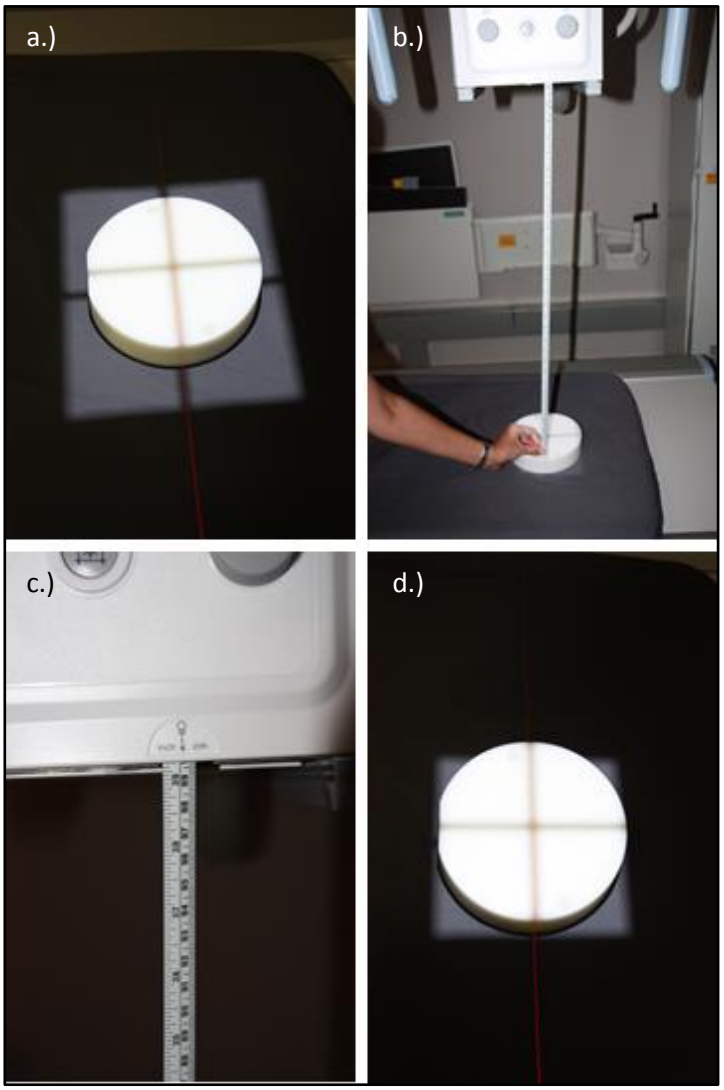

Figure A.7: a.) Align cross wires with scribe lines. b.) and c.) Set to 100 cm SSD. d.) Collimate light field to phantom edges.

A.2.3.2 Phantom exposure

a. For manual exposure, set up technique factors typical for extremity imaging in your department.
NOTE: This is done only for general x-ray imaging, not for fluoroscopy.
b. Make the exposure.
c. On the obtained image note the following details:

i. Unit name
ii. Test date
iii. Technique factors used
iv. Additional attenuator plates added
v. Operator

d. For automatic exposure control (AEC), make an exposure with the AEC option selected.
NOTE: Only AEC exposures are used for fluoroscopy.
e. On the obtained image note the following details:
i. Unit name
ii. Test date
iii. Technique factors used
iv. Additional attenuator plates added (0 cm in this example)
v. Operator
f. Now add 2 cm additional attenuator plates on top of the phantom and repeat points d – e. (refer to Figure A.26 a.) in Mammography section A.2.4 for illustration)
g. Add a total of 4 cm additional attenuator plates and repeat points d – e. (refer to Figure A.26 b.) in Mammography section A.2.4 for illustration)
h. A total of 3 exposures are therefore made.

A.2.3.3 Load images into data analysis software

a. Export the raw obtained images from the x-ray unit control console or computed tomography (CR) reader control computer in Digital Imaging and Communications in Medicine (DICOM) format. Contact a technician or medical physicist to write a standing operating procedure (SOP) for doing this for your unit or department.
b. In the Phantom Scan application, click on File and select Open Image as shown in Figure A.8.

Figure A.8: Opening an image for analysis.

c. Select the image you wish to evaluate and click on Open. The image will now be displayed in the application, as shown in Figure A.9.

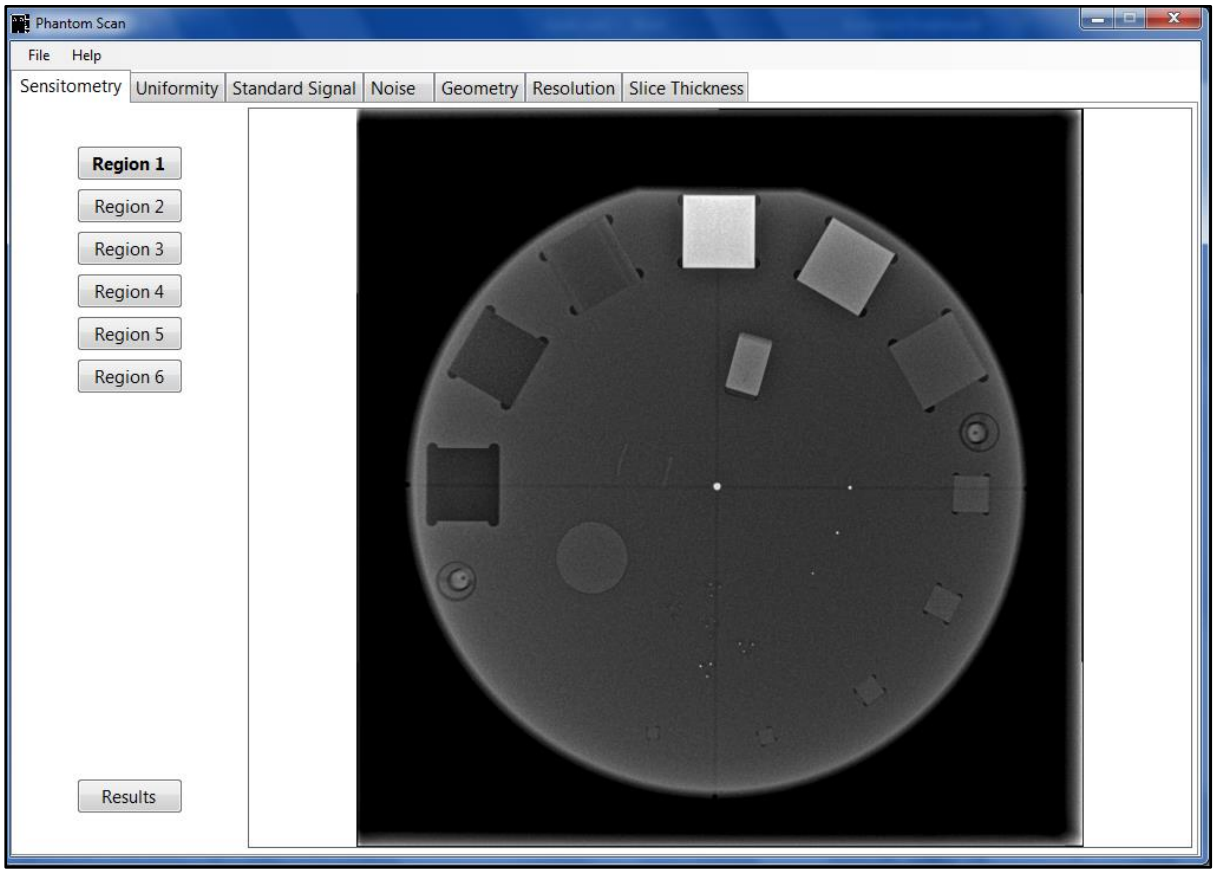

Figure A.9: Image opened in the application and ready for evaluation.

A.2.3.4 Visual inspection of the obtained images

Load the obtained images one by one into the data analysis software as explained in section A.2.3.3 above. In the software, view the loaded images and visually inspect each of the 4 obtained images to determine:

a. Low contrast detectability
   - Visually determine the smallest low contrast detectability insert that can be seen. Refer to Figure A.1 for the location of these blocks, labelled 1-8 in Figure A.1 b.).
   - Record the size of the smallest visible block in the QC result page (at the end of the manual).
   - If the result is out of tolerance, i.e. the limit in Table A.2 is exceeded, follow the steps in Figure A.2 for taking corrective action.

b. Positioning and alignment (x-ray / light beam centring)
   - For x-ray to light field coincidence, visually check that the entire phantom is captured in the image. The light field is collimated to the edges of the phantom. If the phantom is cut-off, the x-ray field is smaller than the light field.

If the image is larger than the phantom, then the light field is greater than the x-ray field. This is indicated in Figure A.10.

- Record the results in the QC result page (at the end of the manual) and note the direction in which the deviation was observed.
- If the result fails, i.e. the limit in Table A.2 is exceeded, follow the steps in Figure A.2 for taking corrective action.

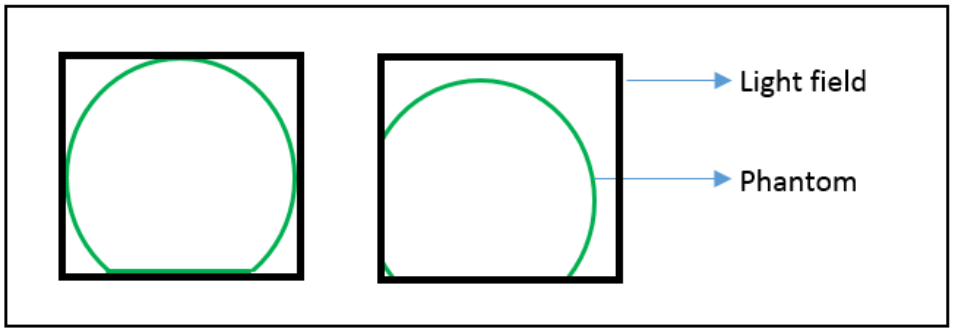

Figure A.10: a.) Correct x-ray to light field coincidence. b.) The light field is smaller than the x-ray field to the left and bottom.

c. Artefacts

- Visually inspect the image for the presence of any artefacts, for example ghost images, lines, streaks, marks, spots, blur or any other unexpected appearance.
- Record the artefact seen and where in the image it occurred in the QC result page (at the end of the manual).
- If the result is out of tolerance, i.e. the limit in Table A.2 is exceeded, follow the steps in Figure A.2 for taking corrective action.

d. Image quality visual inspection

- Visually inspect the image and note any visual obstructions, grey scale inversions, distortions or unexpected occurrences in the image.
- Record the manifestation seen and where in the image it occurred in the QC result page (at the end of the manual).
- If the result is out of tolerance, i.e. the limit in Table A.2 is exceeded, follow the steps in Figure A.2 for taking corrective action.

A.2.3.5 Data analysis software evaluation of the obtained images

Load the obtained images one by one into the data analysis software as explained in section A.2.3.3 above. Record the results obtained for the following tests.

a. Sensitometry and grey scale linearity (optical density consistency)

- In the Sensitometry tab in the application, click on the Region 1 button and draw a region of interest (ROI) in the insert numbered 9, i.e. air, of diameter approximately half the size of the insert, in Figure A.1 b.). The ROI should not extend beyond the insert or be close to insert edges.
- Click on the Region 2 button and draw a circular ROI, of diameter approximately half the size of the insert, in the insert numbered 10, i.e. lung, in Figure A.1 b.). The ROI should not extend beyond the insert or be close to insert edges.
- Repeat this for the Regions 3, 4, 5 and 6 buttons drawing ROIs in the inserts numbered 11, 12, 13 and 1 in Figure A.1 b.), i.e. supa wood, bone, Teflon and RGD. This is shown in Figure A.11.
  Note: First click on the Region button and then draw the ROI.

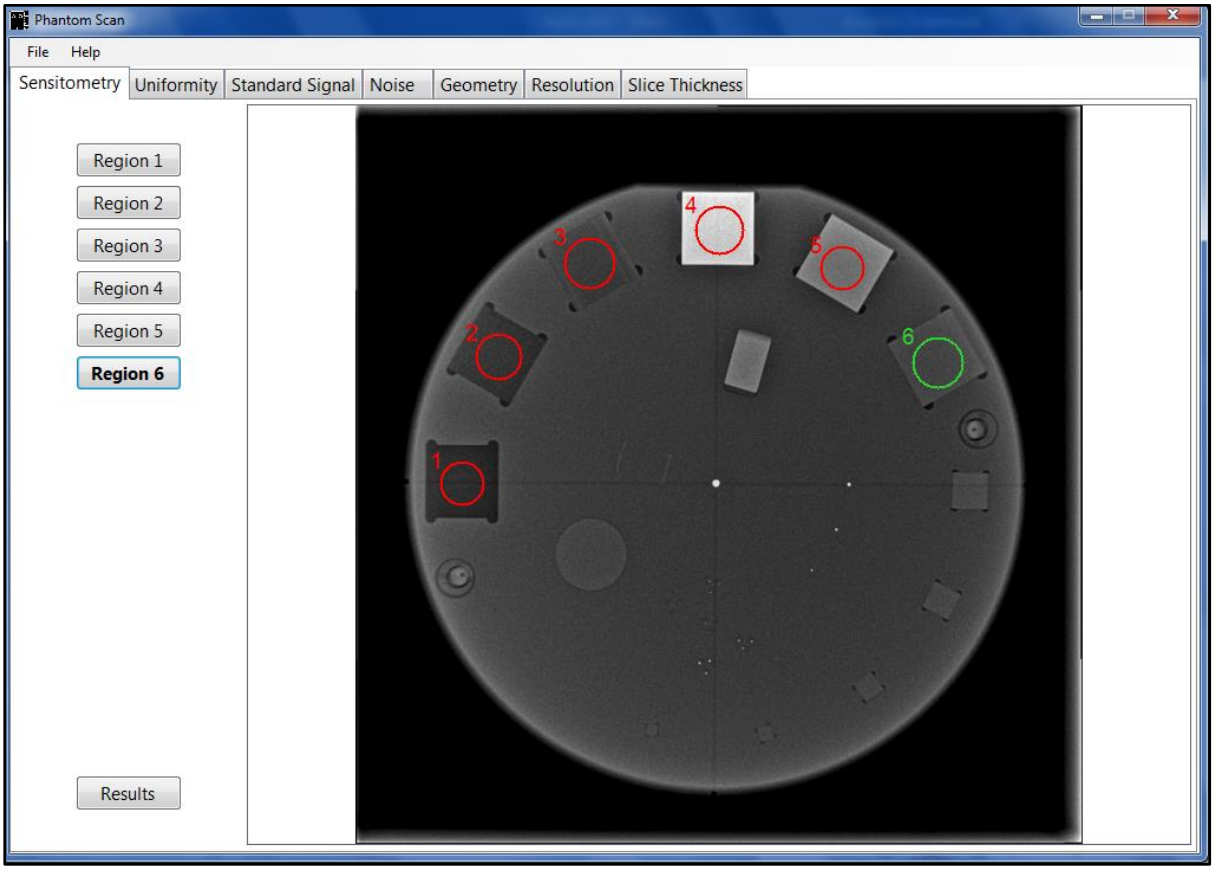

Figure A.11: Drawing the sensitometry ROIs.

- Click on the Results button.

- The mean and standard deviation in each ROI is measured and displayed as shown in Figure A.12.

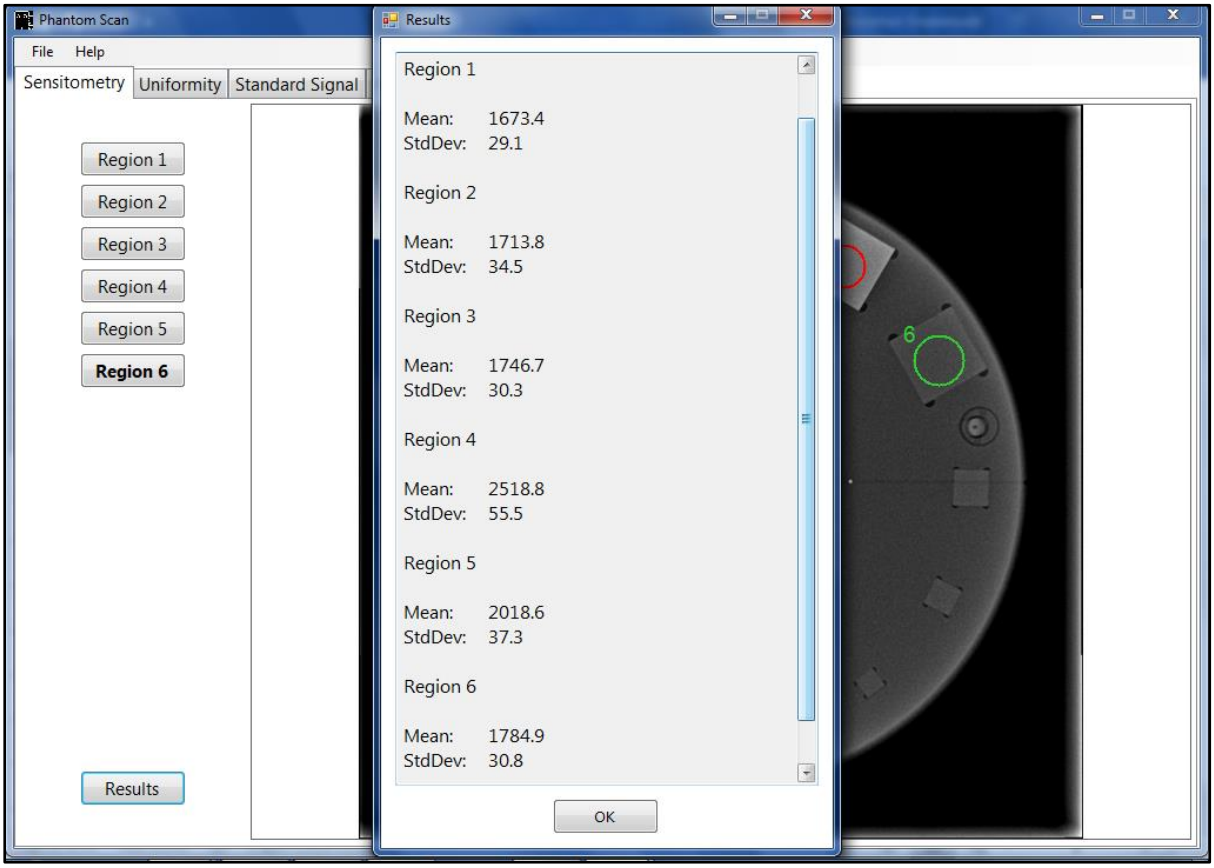

Figure A.12: Results for the sensitometry test.

- Record the results in the QC result page (at the end of the manual).
- If the result fails, i.e. the limit in Table A.2 is exceeded, follow the steps in Figure A.2 for taking corrective action.

b. Uniformity

- In the Uniformity tab in the application, click on the Region 1 button and draw a region of interest (ROI) in the HDPE housing material in a location that does not contain any other inserts.
- Click on the Region 2, 3 and 4 buttons and draw ROIs of similar size than in the first step in the remaining quadrants at locations with no other inserts. This is illustrated in Figure A.13.

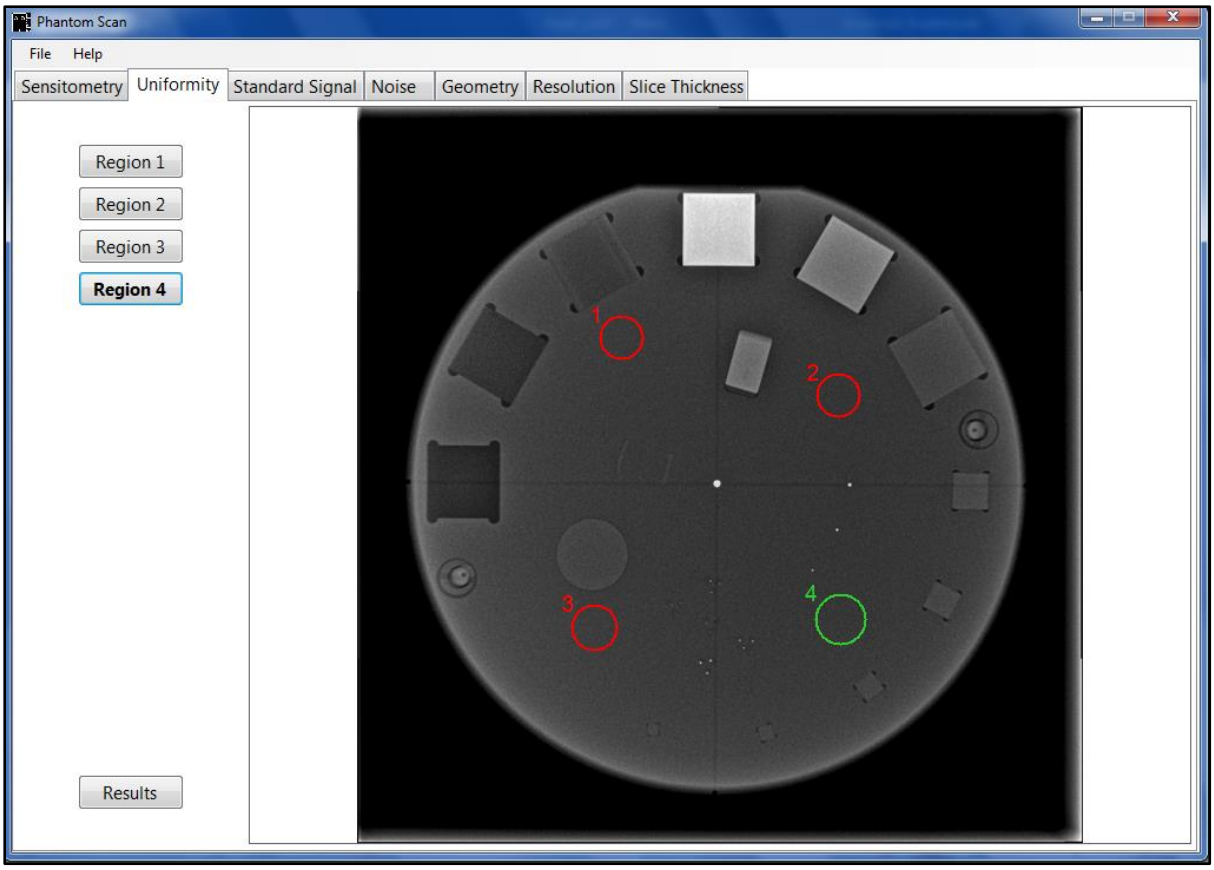

Figure A.13: Locations for ROIs for uniformity evaluation.

- Click on the Results button. The mean and standard deviation in each ROI is measured as shown in Figure A.14.
- Calculate the largest difference in the mean value and record the result in the QC result page (at the end of the manual).
- If the result fails, i.e. the limit in Table A.2 is exceeded, follow the steps in Figure A.2 for taking corrective action.

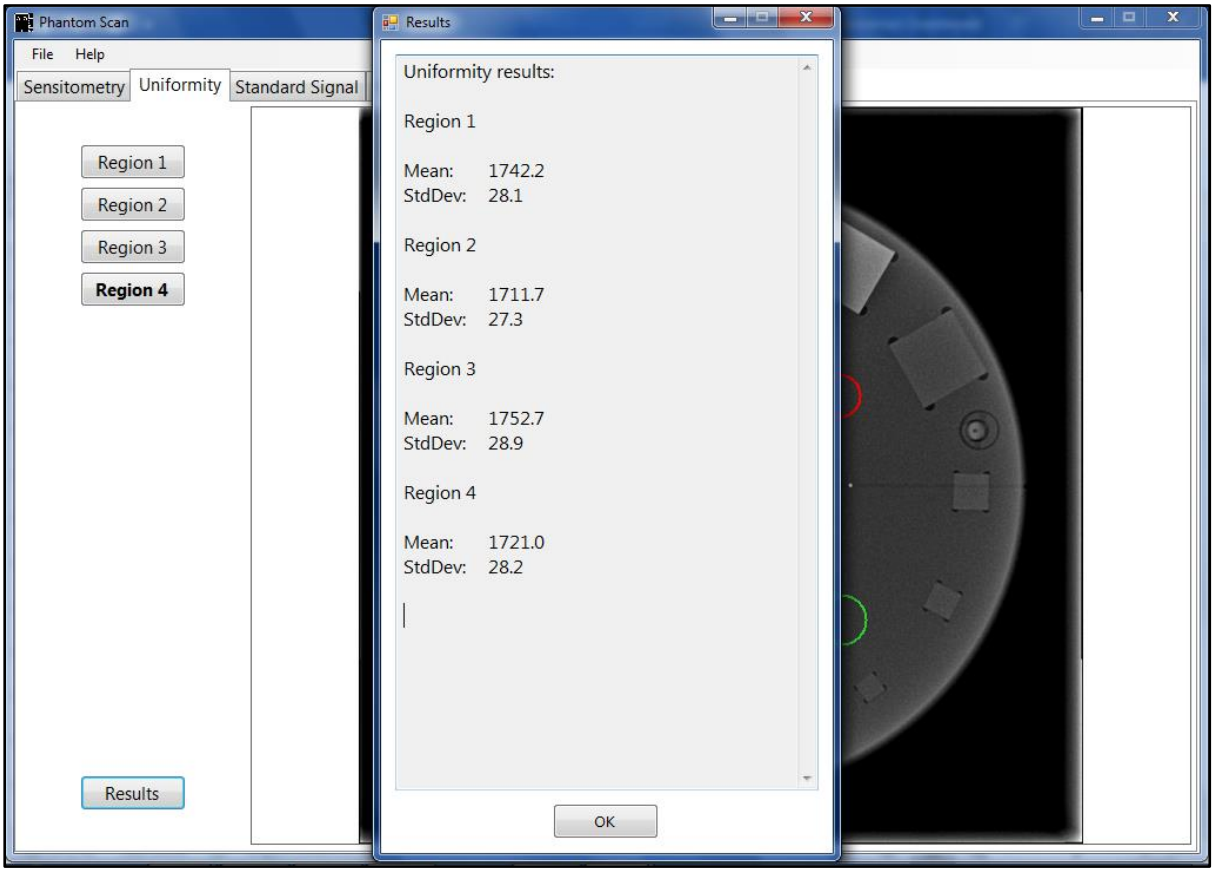

Figure A.14: Results for the uniformity test.

c. Resolution

- Determine the smallest ball visible from the inserts labelled number 21 in Figure A.1 b.).
- Click on the Point 1 button and draw a region of interest (ROI) around the ball. This is shown in Figure A.15.
- Click on the Results button. The data analysis software calculates the modulation transfer function (MTF) from the point spread function (PSF) of the ball. A MTF graph and the limiting spatial resolution are displayed. The limiting spatial resolution is the frequency where the MTF is at 10 %. This is indicated in Figure A.16.
- Record the results in the QC result page (at the end of the manual).
- If the result fails, i.e. the limit in Table A.2 is exceeded, follow the steps in Figure A.2 for taking corrective action.
- *NOTE: For fluoroscopy use the central bead.*

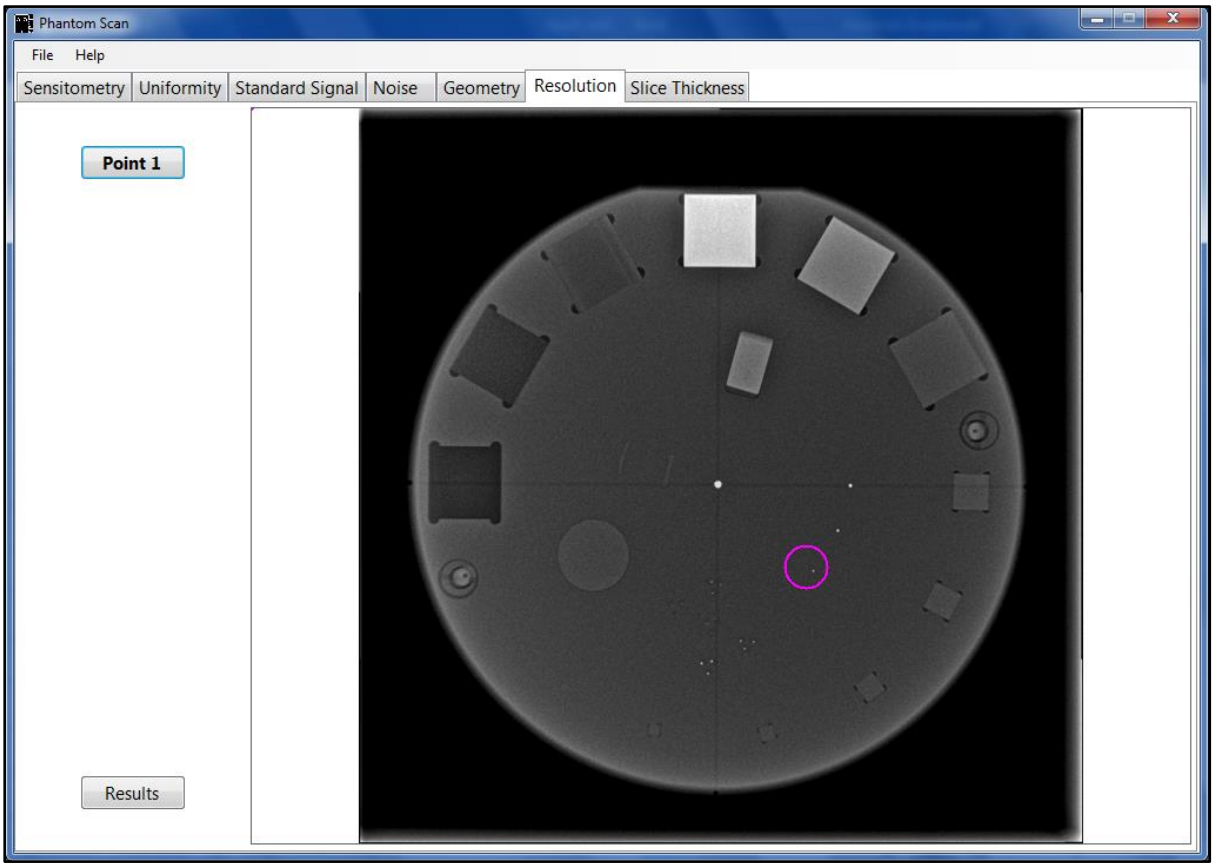

Figure A.15: Drawing a ROI around the smallest ball for resolution calculation.

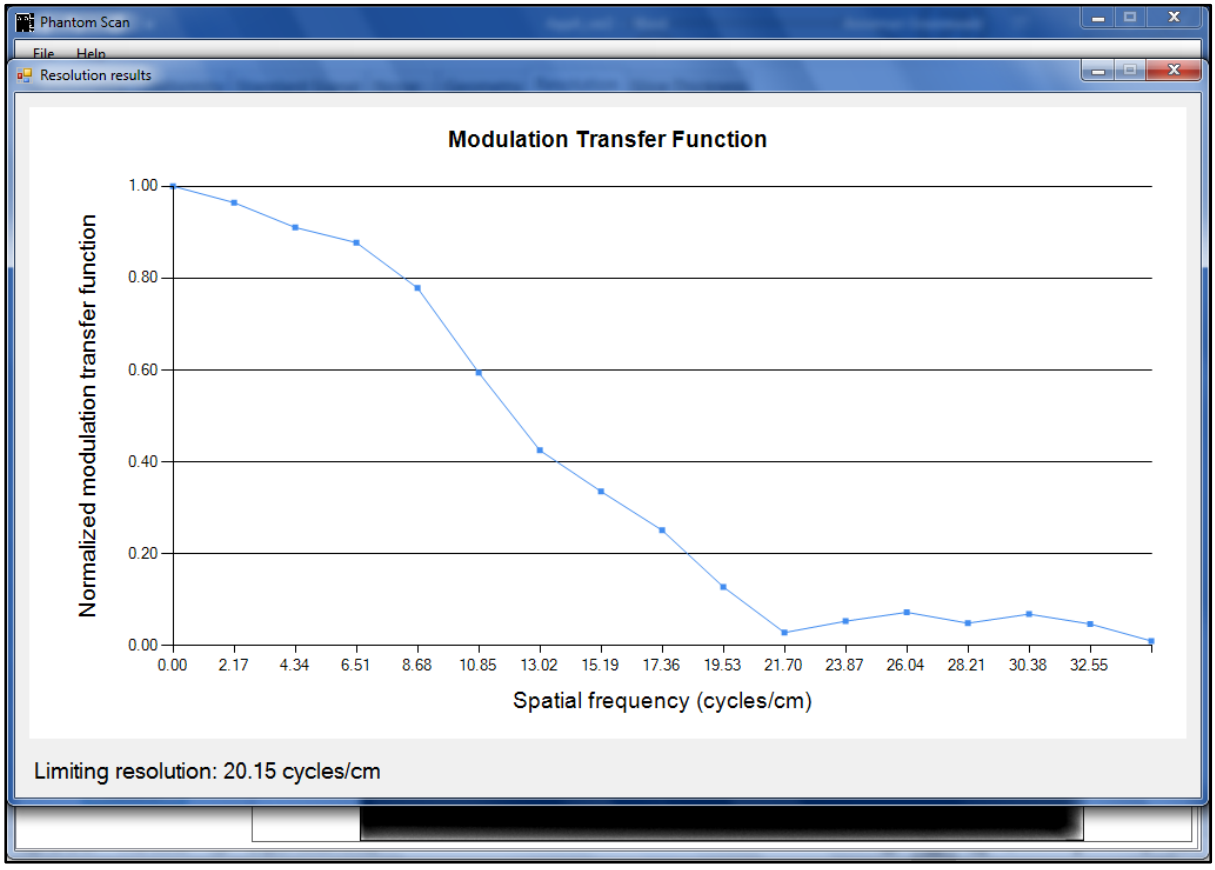

Figure A.16: Results for the resolution test.

d. Image noise

- In the Noise tab in the application, click on the Region 1 button and draw a region of interest (ROI) in the insert numbered 1 in Figure A.1 b.). The ROI should be of diameter approximately half the size of the insert and should not extend beyond the insert or be close to insert edges.
- Click on the Region 2 (background) button and draw a ROI of similar size to that of Region 1 next to the insert. This is shown in Figure A.17.
- Click on the Results button. The data analysis software shows the mean and standard deviations obtained in the ROIs and calculates the signal-to-noise ratio (SNR) and contrast-to-noise ratio (CNR) with Equations A.1 and A.2.

$$SNR = \frac{mean}{standard\ deviation} \quad \text{[Equation A.1]}$$

$$CNR = \frac{mean(a) - mean(b)}{standard\ deviation(b)} \quad \text{[Equation A.2]}$$

- Record the results, as shown in Figure A.18, in the QC result page (at the end of the manual).
- If the result fails, i.e. the limit in Table A.2 is exceeded, follow the steps in Figure A.2 for taking corrective action.

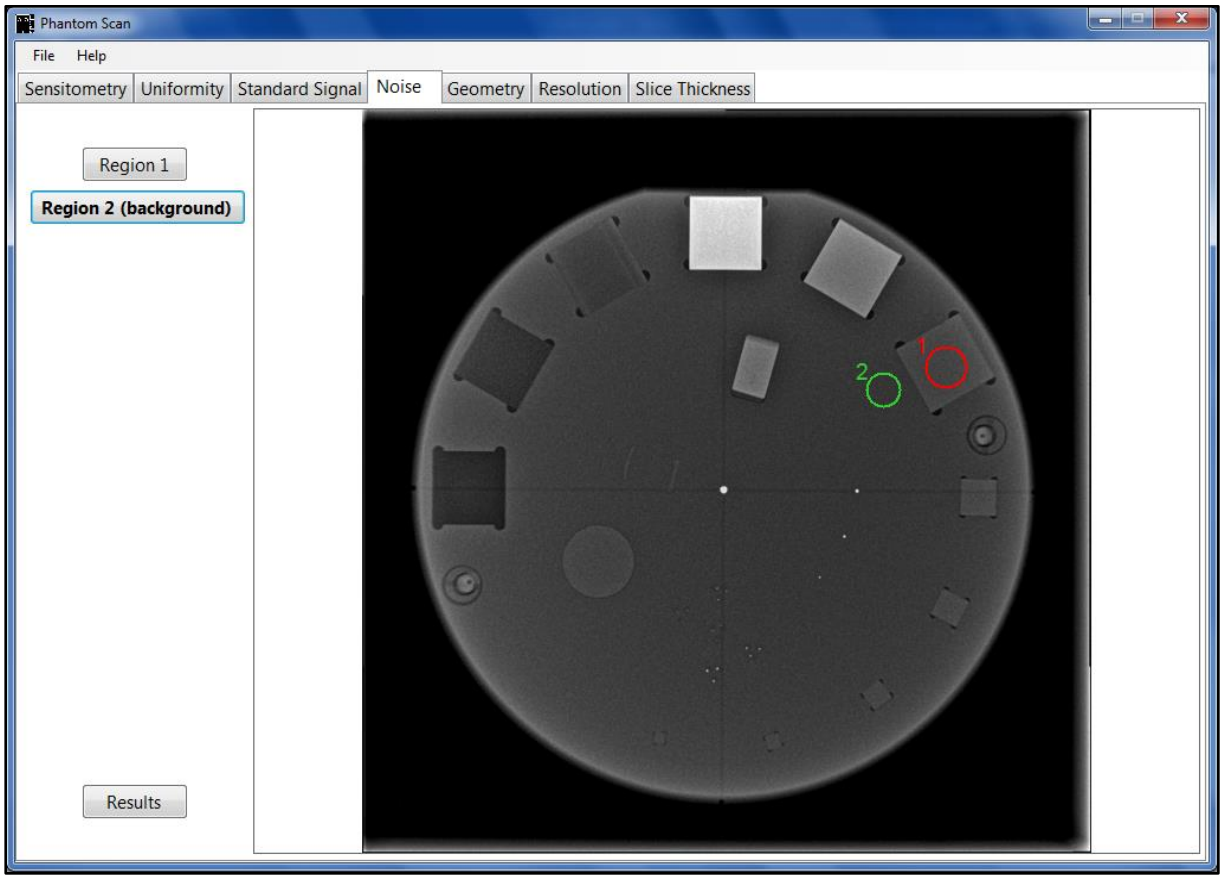

Figure A.17: Drawing ROIs for image noise analysis.

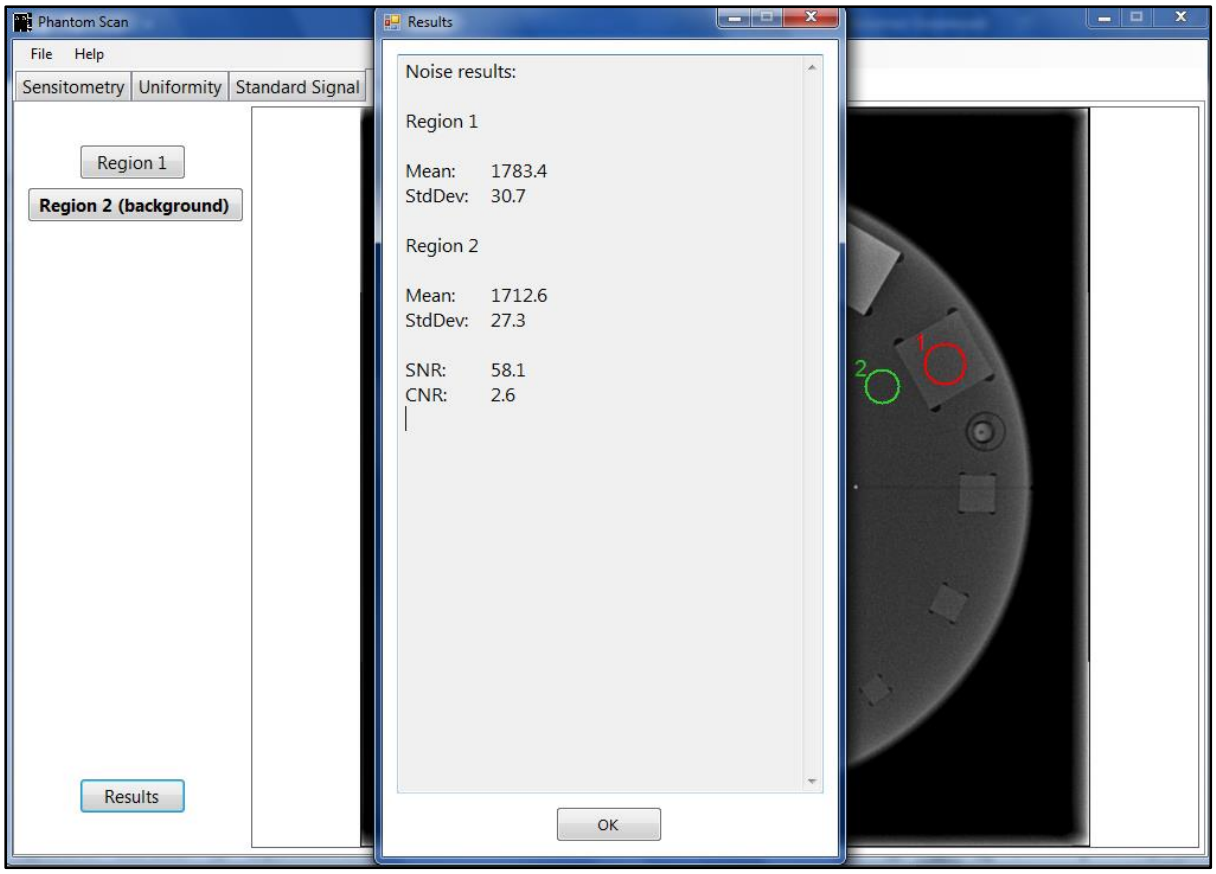

Figure A.18: Results for the noise test.

e. Geometry and measurement tools (distance accuracy / scaling errors)

- In the Geometry tab in the application, click on the Line 1 button and draw a vertical line from edge to edge in the insert numbered 17 in Figure A.1 b.).
- Click on the Line 2 button and draw a horizontal line from edge to edge in the same insert. This is shown in Figure A.19.
- Click on the Results button. The data analysis software measures the length of the drawn lines as indicated in Figure A.20.
- The actual size of the insert is 20 mm diameter. Compare the actual size of the insert to that measured with the software and calculate the difference.
- Record the results in the QC result page (at the end of the manual).
- If the result fails, i.e. the limit in Table A.2 is exceeded, follow the steps in Figure A.2 for taking corrective action.

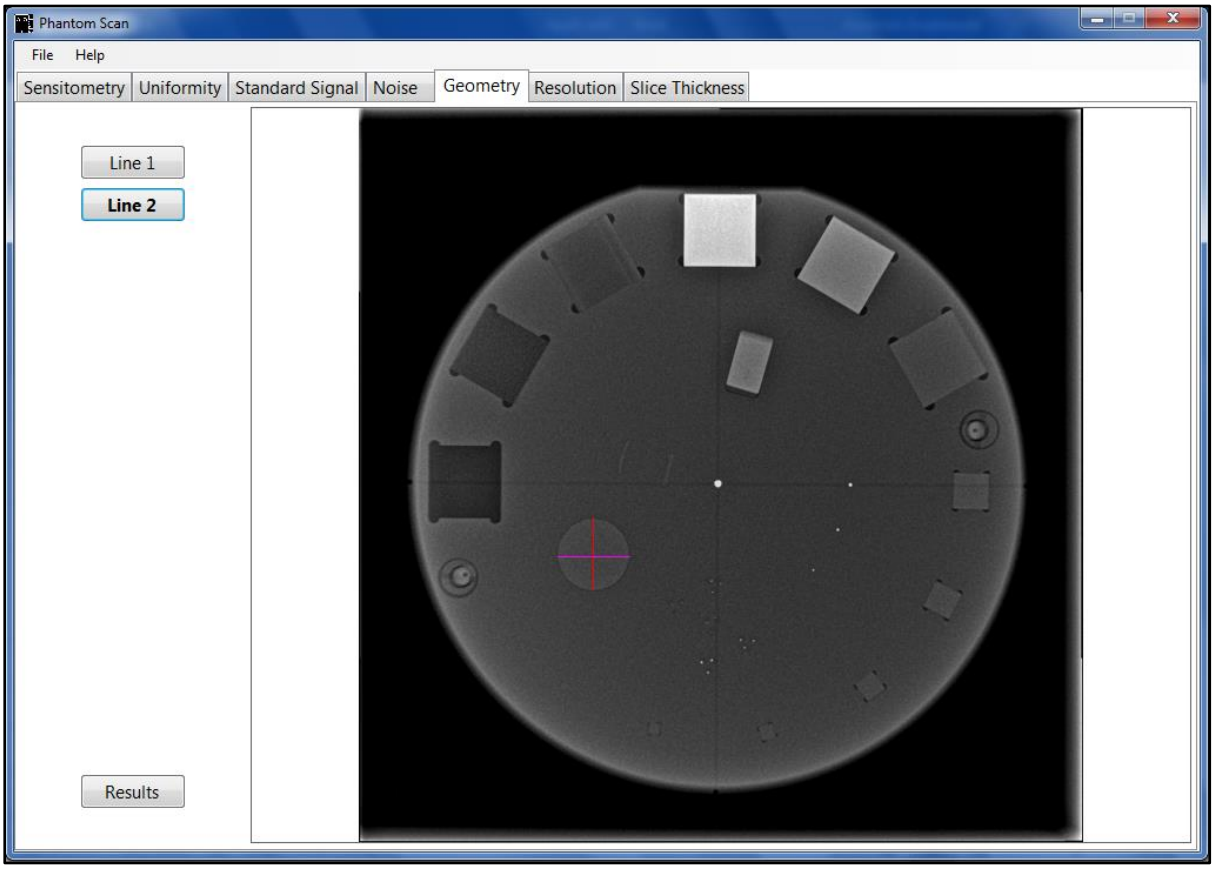

Figure A.19: Geometry measurement lines.

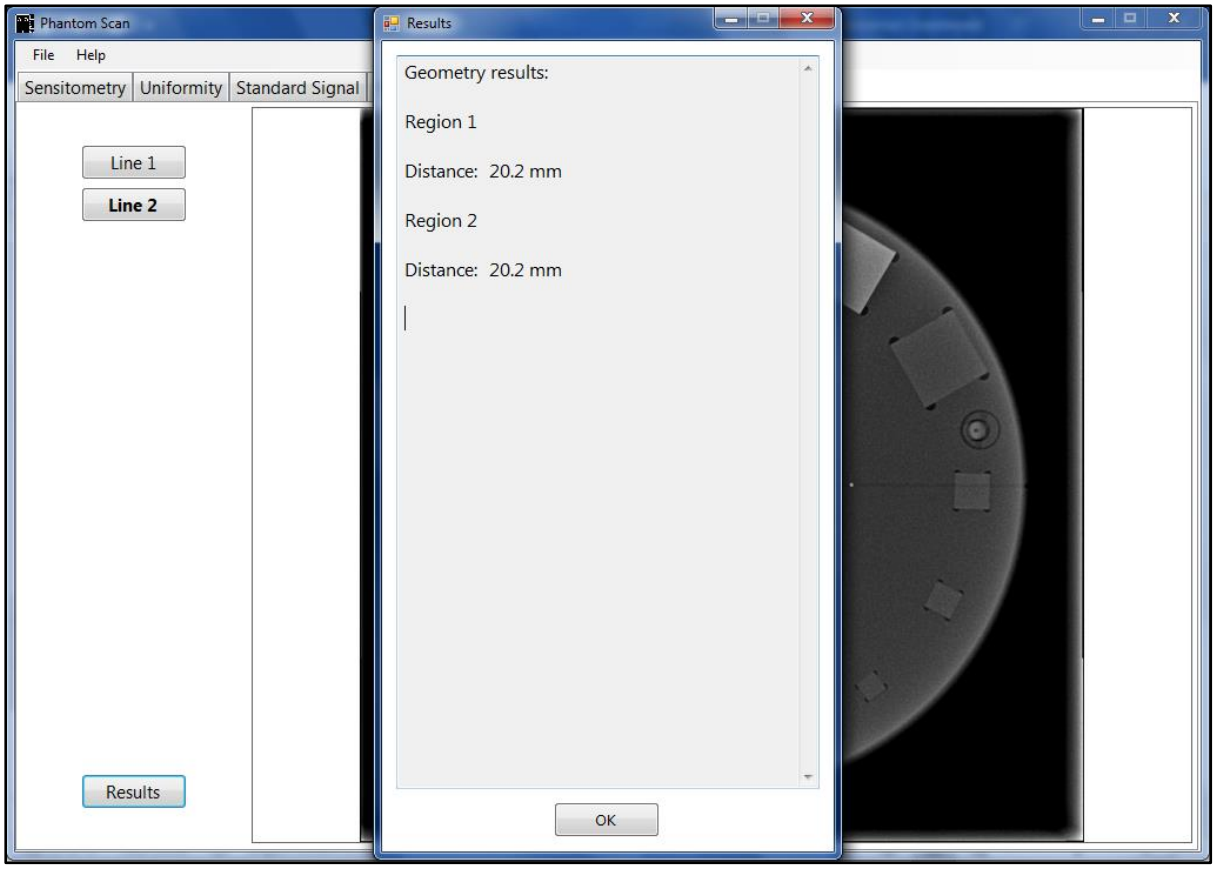

Figure A.20: Results for the geometry test.

f. Standard signal

- In the Standard Signal tab in the application, click on the Region 1 button and draw a region of interest (ROI) in the HDPE housing material at the location labelled 15 in Figure A.1 b.). This is shown in Figure A.21.

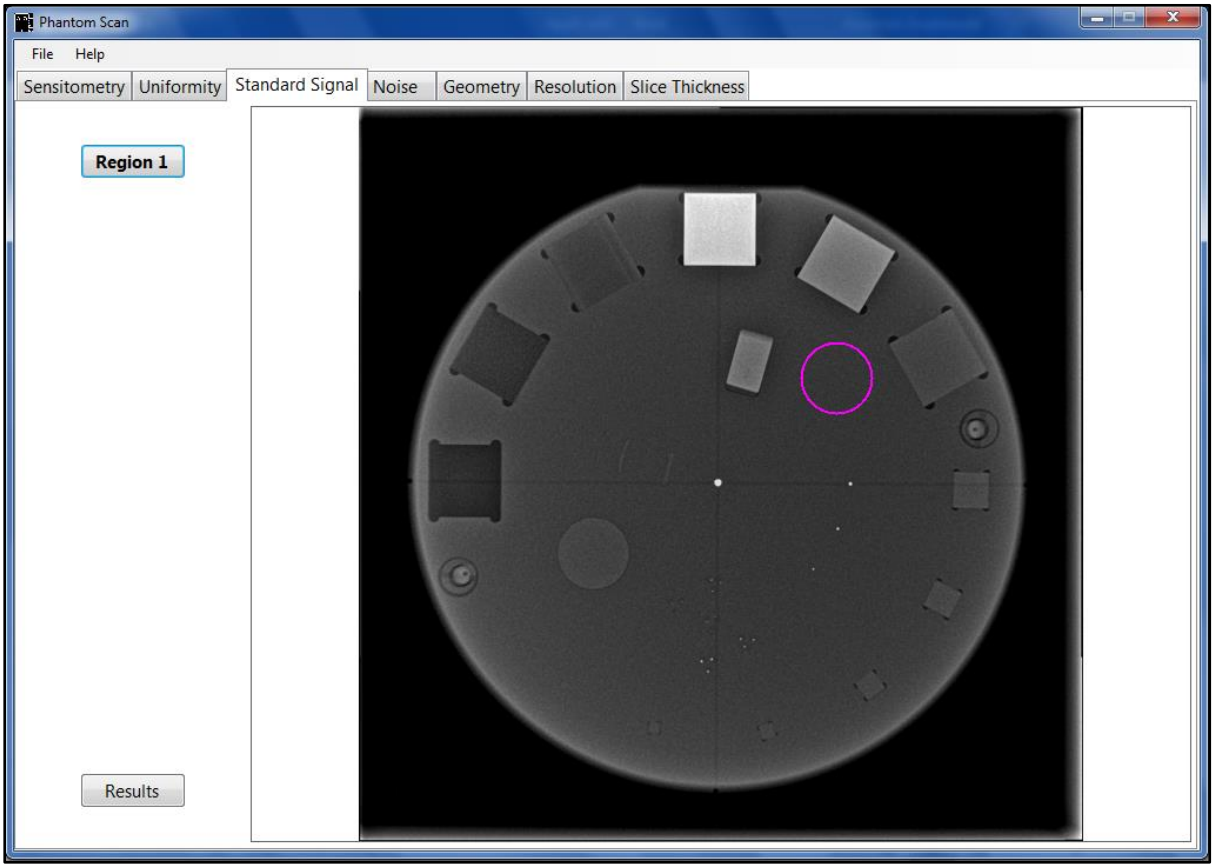

Figure A.21: Drawing a ROI for standard signal evaluation.

- Click on the Results button. The software measures and displays the mean and standard deviation in the ROI as shown in Figure A.22.
- Record the results in the QC result page (at the end of the manual).
- If the result fails, i.e. the limit in Table A.2 is exceeded, follow the steps in Figure A.2 for taking corrective action.

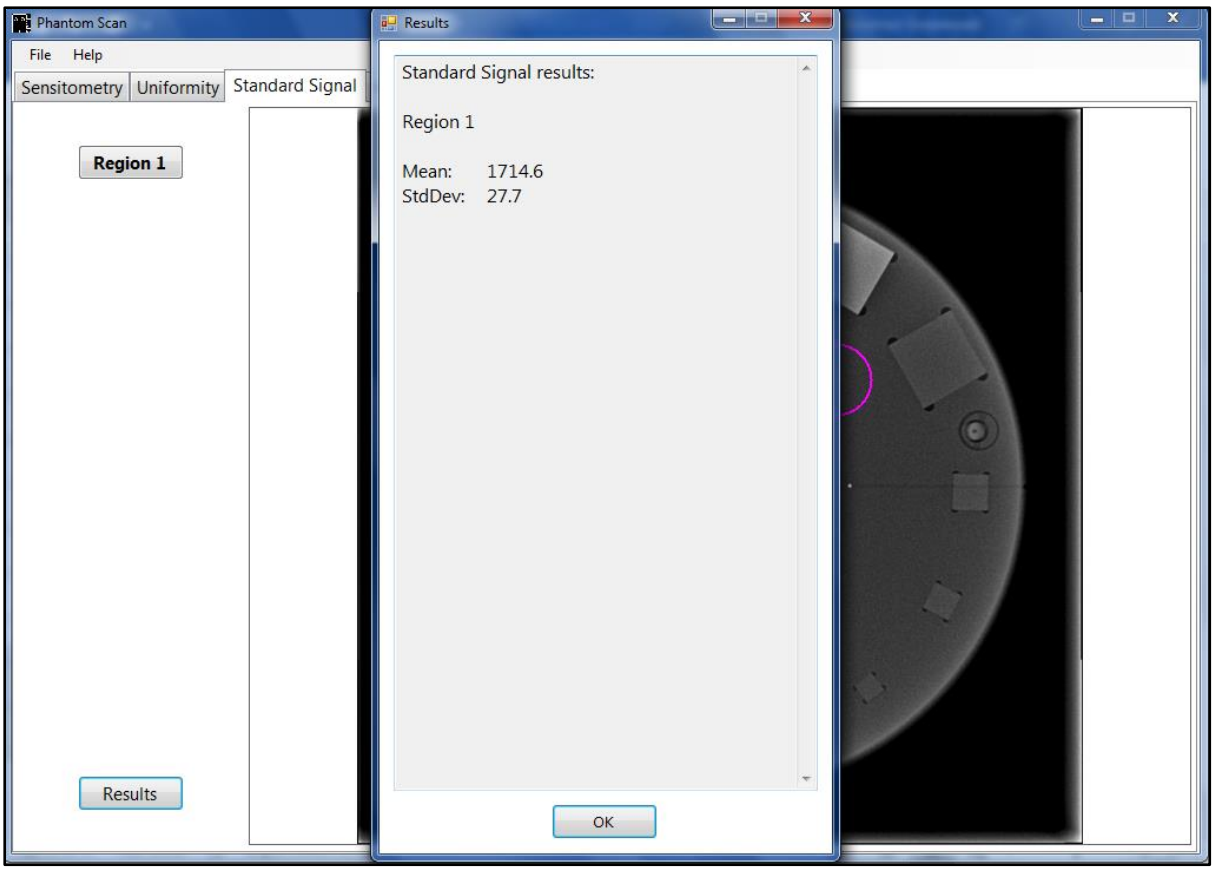

Figure A.22: Results for the standard signal test.

A.2.3.6 Automatic exposure control (AEC) results

a. AEC performance

- Repeat section A.2.3.4 a, c and d and A2.3.5 a, b, d and f for images obtained with AEC with 2 and 4 cm additional HDPE attenuator added.
- Compare the results for the different images.
- Record the results in the QC result page (at the end of the manual).
- If the result fails, i.e. the limit in Table A.2 is exceeded, follow the steps in Figure A.2 for taking corrective action.

b. AEC repeatability

- Repeat section A.2.3.4 a-d and A.2.3.5 a-f for three images obtained with AEC with the same thickness of additional HDPE attenuator added, e.g. perform 3 AEC exposures of the phantom only (0cm additional attenuator).
- Compare the results for the different images.
- Record the results in the QC result page (at the end of the manual).
- If the result fails, i.e. the limit in Table A.2 is exceeded, follow the steps in Figure A.2 for taking corrective action.

A.2.3.7 Saving and printing the results

- Click on File and select Save Results as shown in Figure A.23 a.).
- Enter a file name and choose the location where you want to save the results, as indicated in Figure A.23 b.).
- To print the results in hard copy, go to the selected save location, select the file name to be printed and double left click to open the file in Notepad.
- In Notepad, click on File and select Print. This is shown in Figure A.24 a.).
- Select the printer you want to use and click on Print, as shown in Figure A.24 b.).
- Sign and file the hard copy results.

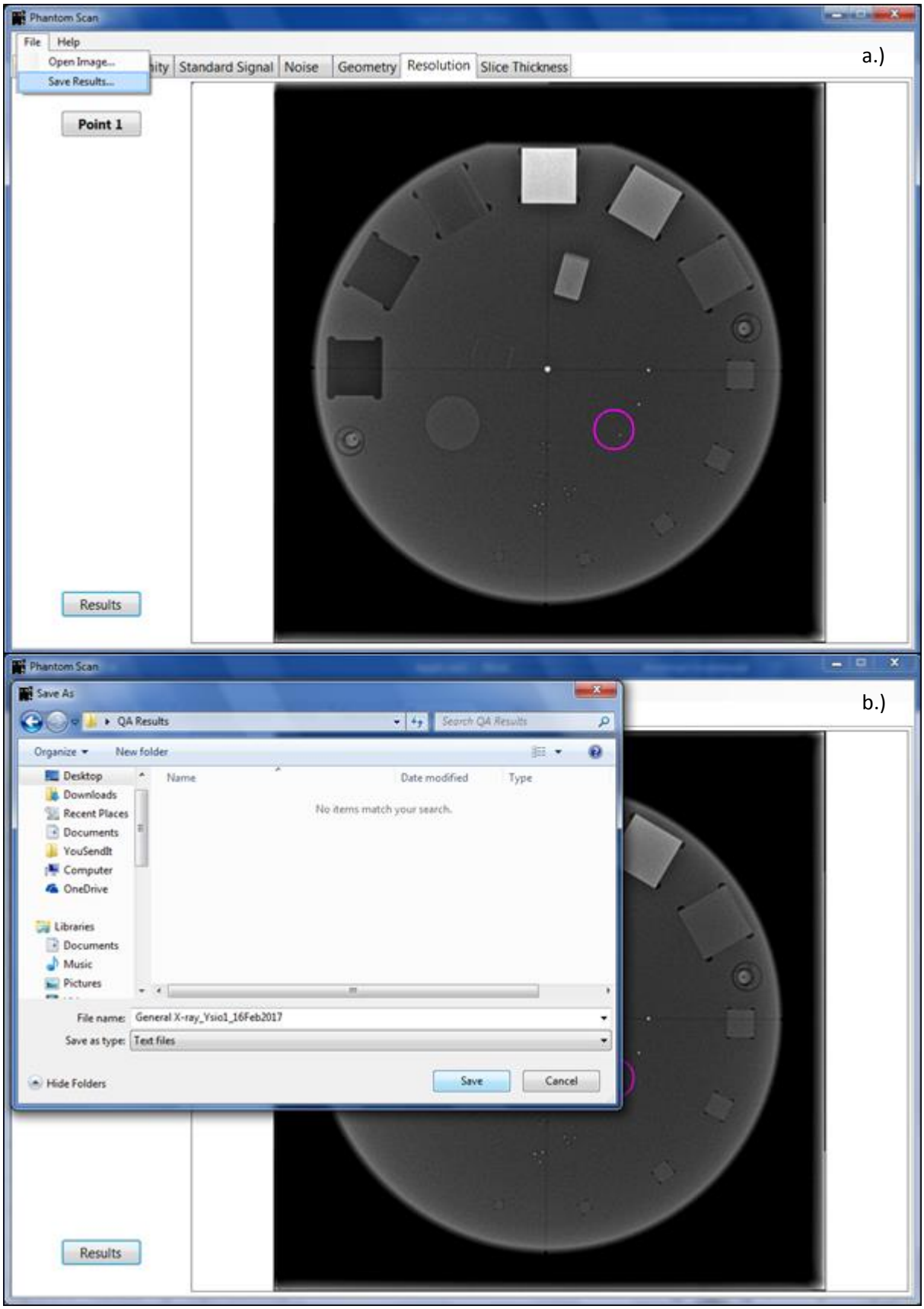

Figure A.23: Saving the obtained results. a.) Selecting the save option in the application. b.) Choosing the location to save to.

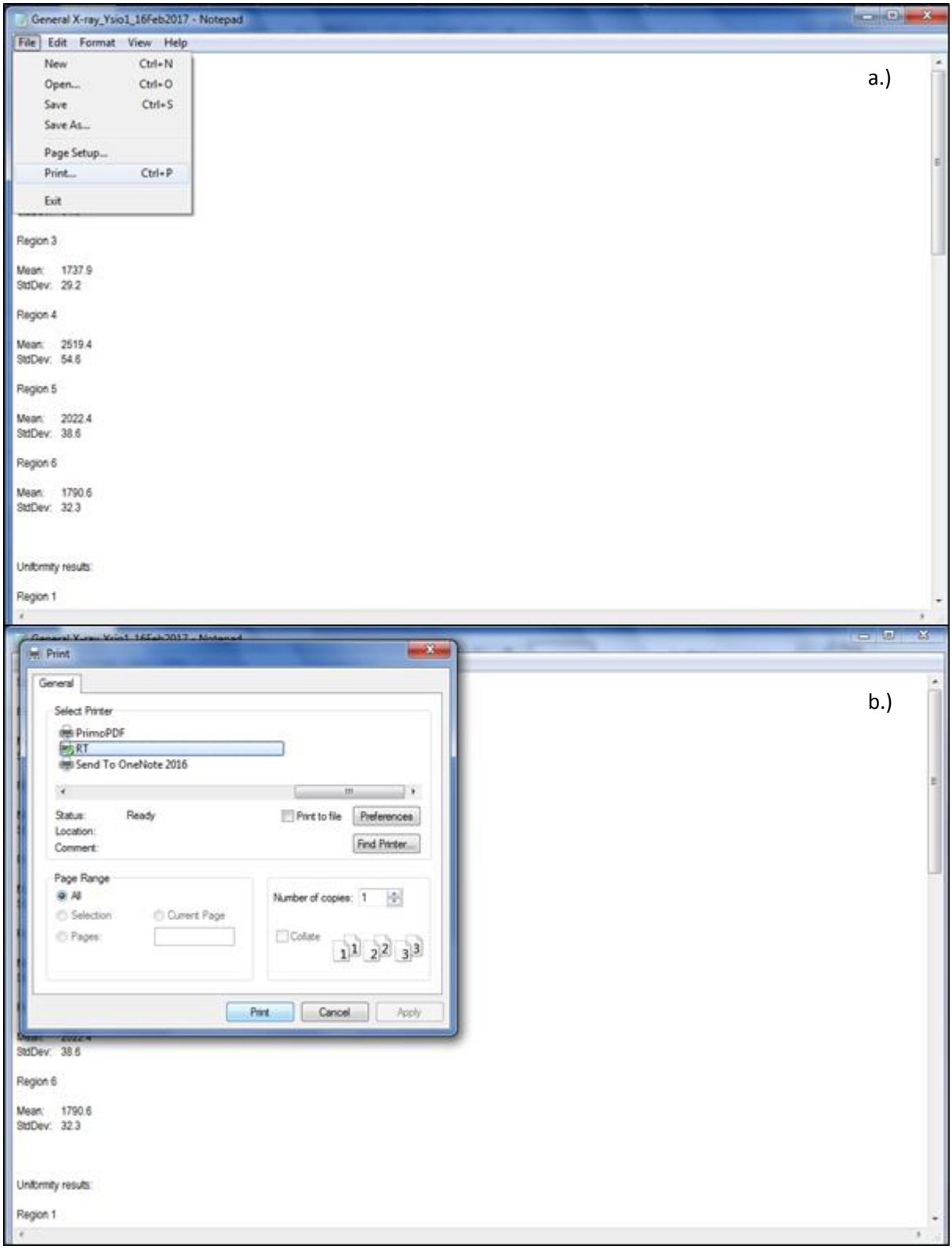

Figure A.24: Printing the results from Notepad. a.) Selecting the print option. b.) Selecting the printer.

A.2.4 Mammography imaging

These tests are performed for mammography units. Table A.3 shows the tests required for comprehensive image quality assurance in mammography imaging.

Table A.3: Tests required for comprehensive mammography image quality assurance. (Insert numbers in table refer to Figure A.1 b.))

Test	Objective	Method	Frequency	Limits
Sensitometry & grey scale linearity (optical density consistency)	Maintain grey scale value for different object densities	ROI analysis with data analysis software using inserts 1, 9-13	Acceptance, daily	Baseline grey scale value ± 0.20 For universal phantom baseline grey scale value ± 2 %
Low contrast detectability	Distinguish objects of density similar to background as they become progressively smaller	Visual inspection of inserts 1-8 to determine smallest visible insert	Acceptance, daily	All inserts are visible
Uniformity	Ensure grey scale values across the image remain constant for the same material	ROI analysis with data analysis software using phantom housing 15	Acceptance, weekly	Mean value ± 10 % Mean value ± 5 % for DR
Resolution	Consistently distinguish objects as they become smaller and closer together	MTF analysis and plot with data analysis software using insert group 21	Acceptance, yearly	11 - 13 lp/mm For universal phantom baseline limiting resolution value ± 2
Image noise	Quantum mottle is sufficiently low as to not degrade image quality unacceptably	ROI analysis with data analysis software using phantom housing 15 and Equations 1 and 2	Acceptance, weekly	Baseline value ± 10 %
Positioning & alignment (X-ray / light beam centring)	Checks the coincidence of the light and x-ray fields	Visually check that the entire phantom is captured in the image	Acceptance, 12 monthly	Obtained value ± 2 % of SID value

Geometry and measurement tools (distance accuracy / scaling errors)	To ensure geometrical distortion and scaling does not occur	Comparing distances measured with data analysis software to know distances	Acceptance, daily	Obtained value ± 0.5 cm or ± 2 %, whichever is smaller
Artefacts	Check that the image is free of artefacts	Visually inspect images for lines, spots, blur, marks, etc	Acceptance, daily	No visible artefacts or distortion For universal phantom geometric distortion will be present, no other artefacts or distortions to be visible
Image quality visual inspection	Consistently maintains visual image quality	Visually inspect images noting inserts and artefacts seen	Acceptance, 3 monthly	Reproducible results
Standard signal	Keep the grey scale value of a certain material (HDPE) constant over time	ROI analysis with data analysis software using phantom housing 15	Acceptance, 3 monthly	Baseline grey scale value ± 0.2 For universal phantom baseline grey scale value ± 2 %
AEC performance	Maintains image quality at acceptable level for different phantom thicknesses	Compare the results from AEC exposures with different phantom thicknesses	Acceptance, 3 monthly	Image quality variation within 10 % for 0, 20 and 40 mm phantom thickness
AEC repeatability	Ensures image quality is maintained using AEC	Compare the results from different AEC exposures of the same phantom thickness	Acceptance, yearly	Mean grey scale value ± 0.15 For universal phantom baseline vaue ± 2 % Image quality variation within 5 %.

Fibres	Evaluates mammography specific image quality assurance parameters	Visually determine the smallest fibre, from insert group 19, that is visible	Acceptance, weekly	All fibres arevisible
Masses	Evaluates mammography specific image quality assurance parameters	Visually determine the smallest mass, from inserts 1-8, that is visible	Acceptance, weekly	All masses are visible
Micro-calcifications	Evaluates mammography specific image quality assurance parameters	Visually determine the smallest calcification group, from insert group 18, that is visible	Acceptance, weekly	All micro-calcification groups are visible

A.2.4.1 Phantom set-up

a. Place the phantom on the bucky underneath the x-ray tube, with the scribe lines facing the x-ray tube.
b. Position the flat side towards the chest wall side as in Figure A.25.
c. Align the phantom scribe lines and x-ray tube cross hairs. This is shown in Figure A.25 a.).
d. Use the largest compression paddle, as shown in Figure A.25 b.).

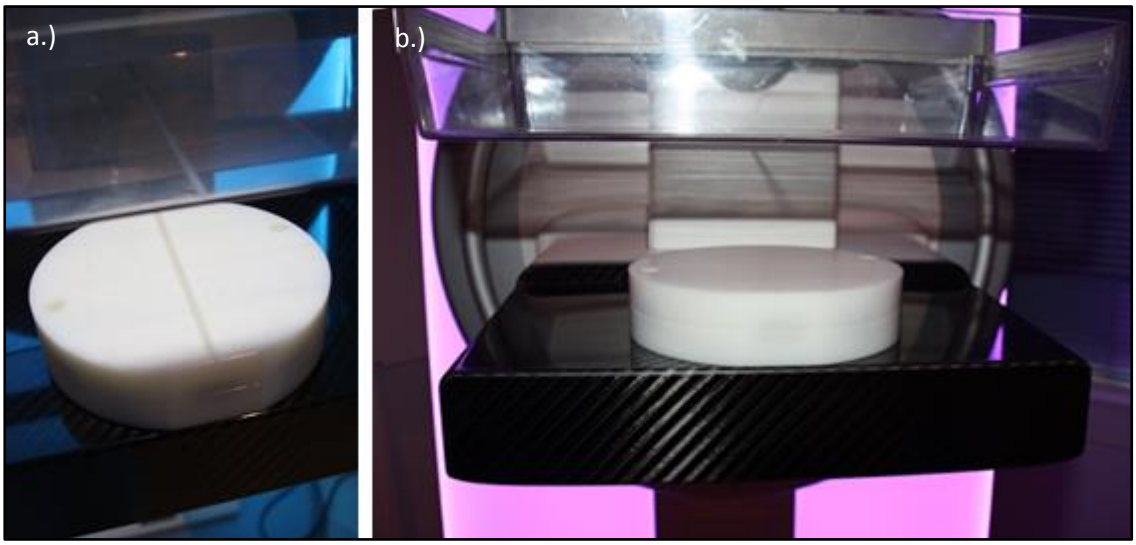

Figure A.25: a.) With phantom positioned flat side towards chest wall side, align cross hairs with scribe lines. b.) Use a large compression paddle.

A.2.4.2 Phantom exposure

a. For manual exposure, set up technique factors typical for craniocaudal (CC) mammogram imaging in your department.
b. Make the exposure.
c. On the obtained image note the following details:
    i. Unit name
    ii. Test date
    iii. Technique factors used
    iv. Additional attenuator plates added
    v. Operator
d. For AEC, make an exposure with the AEC option selected.
e. On the obtained image note the following details:
    i. Unit name
    ii. Test date
    iii. Technique factors used
    iv. Additional attenuator plates added (0 cm in this example)
    v. Operator
f. Now add 2 cm additional attenuator plates on top of the phantom and repeat points d – e. This is shown in Figure A.26 a.).
g. Add a total of 4 cm additional attenuator plates, as shown in Figure A.26 b.), and repeat points d – e.
h. A total of 3 exposures are therefore made.

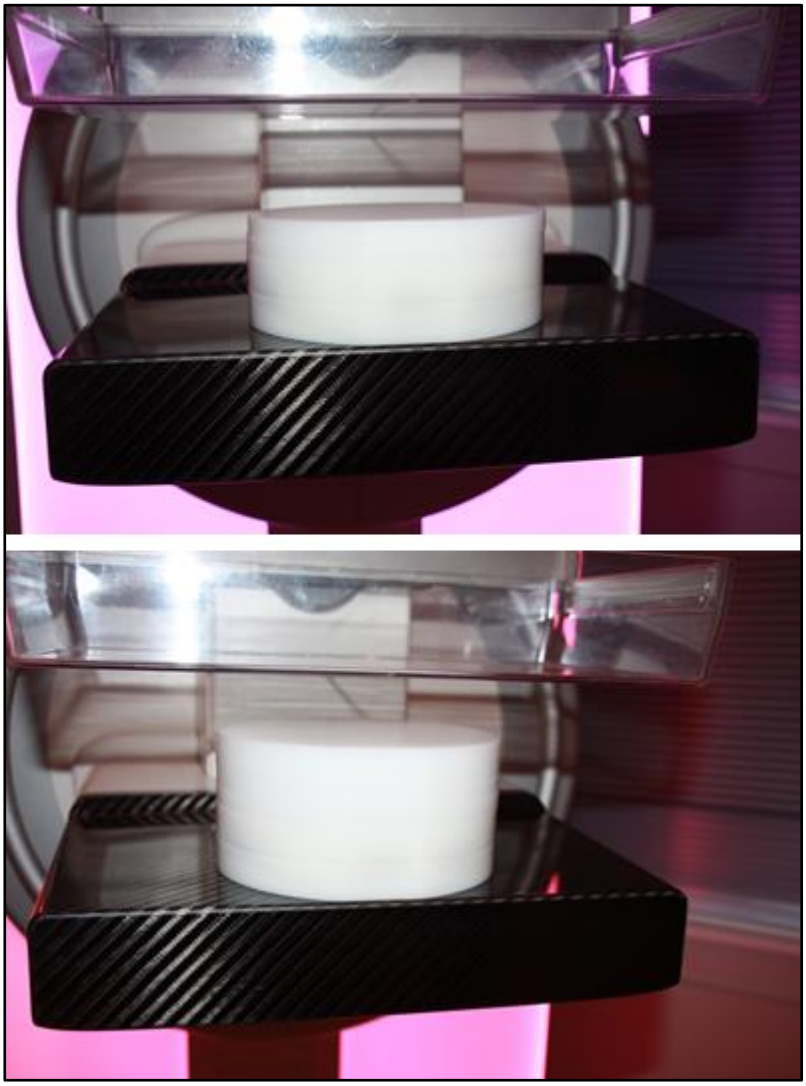

Figure A.26: a.) Phantom with 2 cm additional attenuator added on top of the phantom. b.) Phantom with 4 cm additional attenuator added on top of the phantom.

A.2.4.3 Load images into data analysis software

a. Export the raw obtained images from the mammography unit control console in Digital Imaging and Communications in Medicine (DICOM) format. Contact a technician or medical physicist to write a standing operating procedure (SOP) for doing this for your unit or department.
b. In the Phantom Scan application, click on File and select Open Image as shown in Figure A.27.

Figure A.27: Opening an image for analysis.

c. Select the image you wish to evaluate and click on Open. The image will now be displayed in the application, as shown in Figure A.28.

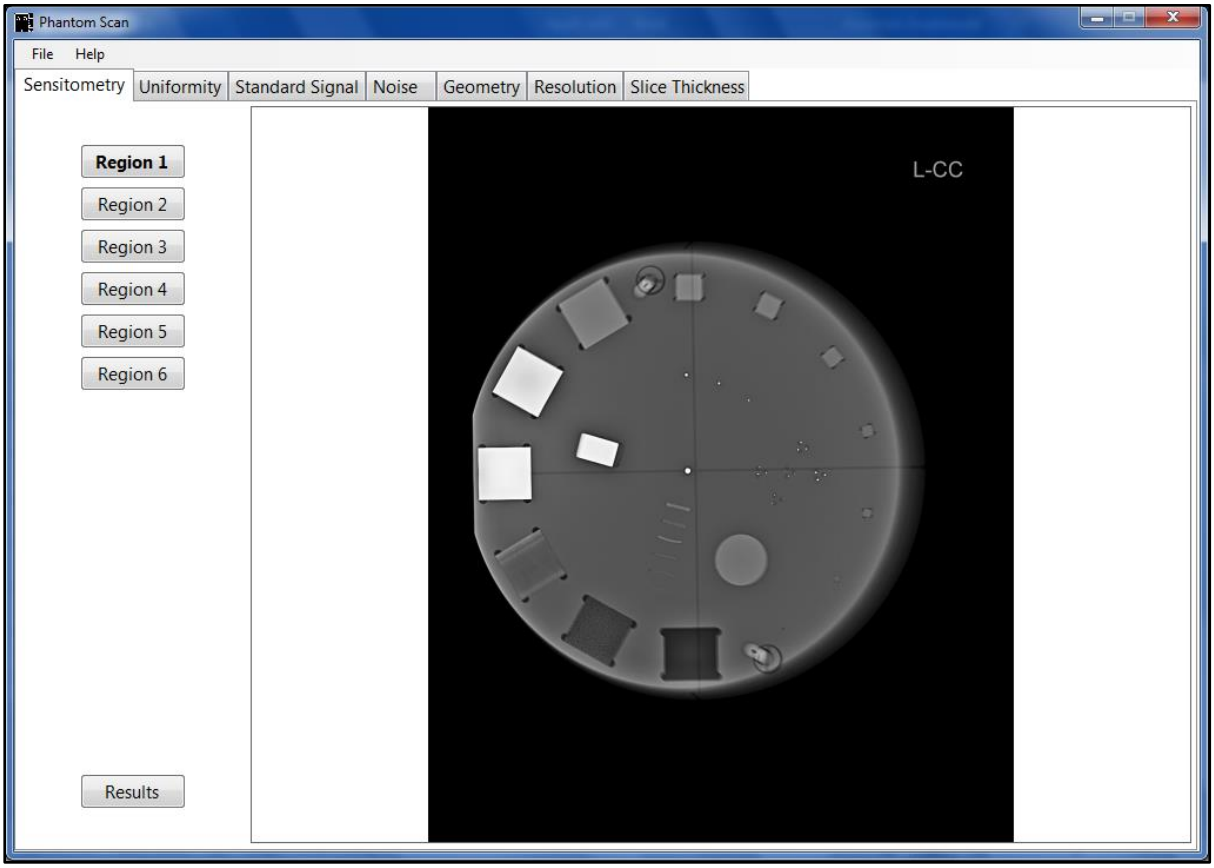

Figure A.28: Image opened in the application and ready for evaluation.

A.2.4.4 Visual inspection of the obtained images

Load the obtained images one by one into the data analysis software as explained in section A.2.4.3 above. In the software, view the loaded images and visually inspect each of the 4 obtained images to determine:

a. Low contrast detectability
   - Visually determine the smallest low contrast detectability insert that can be seen. Refer to Figure A.1 for the location of these blocks, labelled 1-8 in Figure A.1 b.).

- Record the size of the smallest visible block in the QC result page (at the end of the manual).
- If the result is out of tolerance, i.e. the limit in Table A.3 is exceeded, follow the steps in Figure A.2 for taking corrective action.

b. Positioning and alignment (x-ray / light beam centring)
   - For x-ray to light field coincidence, visually check that the entire phantom is captured in the image. The flat side of the phantom is placed at the edge of the bucky chest wall side. This is indicated in Figure A.25.
   - Record the results in the QC result page (at the end of the manual) and note the direction in which the deviation was observed.
   - If the result fails, i.e. the limit in Table A.3 is exceeded, follow the steps in Figure A.2 for taking corrective action.

c. Artefacts
   - Visually inspect the image for the presence of any artefacts, for example ghost images, lines, streaks, marks, spots, blur or any other unexpected appearance.
   - Record the artefact seen and where in the image it occurred in the QC result page (at the end of the manual).
   - If the result is out of tolerance, i.e. the limit in Table A.3 is exceeded, follow the steps in Figure A.2 for taking corrective action.

d. Image quality visual inspection
   - Visually inspect the image and note any visual obstructions, grey scale inversions, distortions or unexpected occurrences in the image.
   - Record the manifestation seen and where in the image it occurred in the QC result page (at the end of the manual).
   - If the result is out of tolerance, i.e. the limit in Table A.3 is exceeded, follow the steps in Figure A.2 for taking corrective action.

e. Fibres
   - Visually inspect the image and note the fibre inserts labelled number 19 in Figure A.1 b.).
   - Record the number of fibres seen in the QC result page (at the end of the manual).
   - If the result is out of tolerance, i.e. the limit in Table A.3 is exceeded, follow the steps in Figure A.2 for taking corrective action.

f. Masses
   - Visually inspect the image and note the masses inserts labelled 1-8 in Figure A.1 b.).

- Record the number of masses seen in the QC result page (at the end of the manual).
- If the result is out of tolerance, i.e. the limit in Table A.3 is exceeded, follow the steps in Figure A.2 for taking corrective action.

g. Micro-calcifications
   - Visually inspect the image and note the micro-calcification groups labelled 18 in Figure A.1 b.).
   - Record the number of groups seen in the QC result page (at the end of the manual).
   - If the result is out of tolerance, i.e. the limit in Table A.3 is exceeded, follow the steps in Figure A.2 for taking corrective action.

A.2.4.5 Data analysis software evaluation of the obtained images

Load the obtained images one by one into the data analysis software as explained in section A.2.4.3 above. Record the results obtained for the following tests.

a. Sensitometry & grey scale linearity (optical density consistency)
   - In the Sensitometry tab in the application, click on the Region 1 button and draw a region of interest (ROI) in the insert numbered 9, i.e. air, in Figure A.1 b.). The ROI should be of diameter approximately half the size of the insert, should not extend beyond the insert or touch the insert edges.
   - Click on the Region 2 button and draw a ROI in the insert numbered 10, i.e. lung, in Figure A.1 b.). The ROI should be of diameter approximately half the size of the insert, should not extend beyond the insert or touch the insert edges.
   - Repeat this for the Regions 3, 4, 5 and 6 buttons drawing ROIs in the inserts numbered 11, 12, 13 and 1 in Figure A.1 b.), i.e. supa wood, bone, Teflon and RGD. This is shown in Figure A.29.
     Note: First click on the Region button and then draw the ROI.
   - Click on the Results button.
   - The mean and standard deviation in each ROI is measured and displayed as shown in Figure A.30.

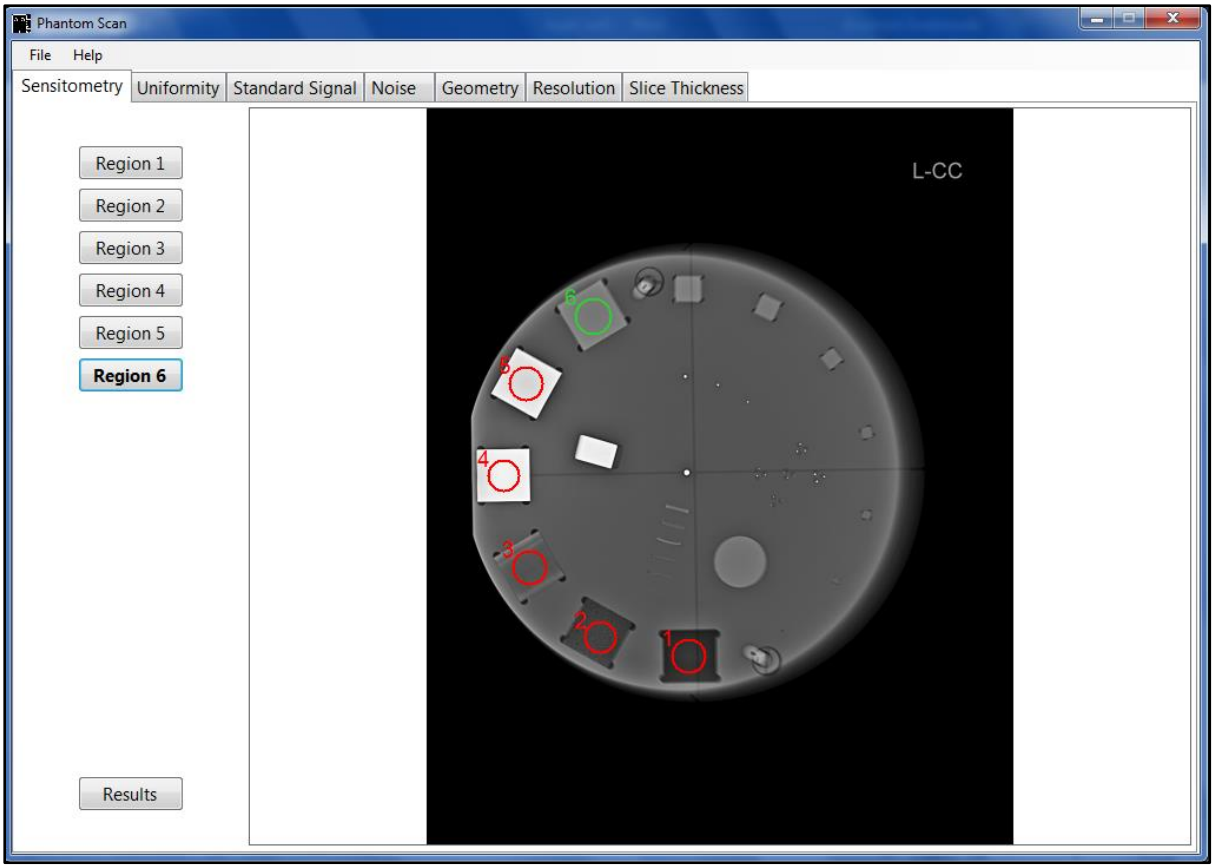

Figure A.29: Drawing the sensitometry ROIs.

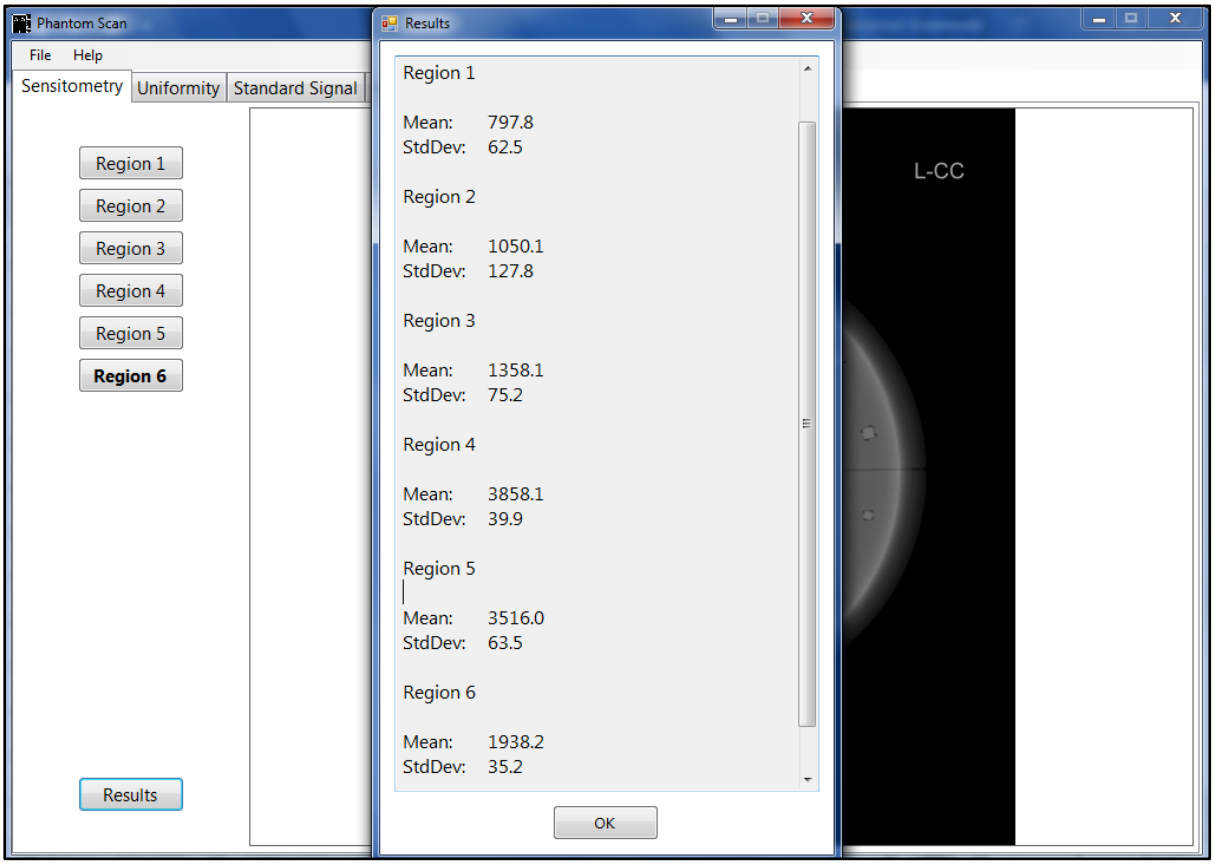

Figure A.30: Results for the sensitometry test.

- Record the results in the QC result page (at the end of the manual).
- If the result fails, i.e. the limit in Table A.3 is exceeded, follow the steps in Figure A.2 for taking corrective action.

b. Uniformity

- In the Uniformity tab in the application, click on the Region 1 button and draw a region of interest (ROI) in the HDPE housing material in a location that does not contain any other inserts.
- Click on the Region 2, 3 and 4 buttons and draw ROIs of similar size than in the first step in the remaining quadrants at locations with no other inserts. This is illustrated in Figure A.31.
- Click on the Results button. The mean and standard deviation in each ROI is measured as shown in Figure A.32.
- Calculate the largest difference in the mean value and record the result in the QC result page (at the end of the manual).
- If the result fails, i.e. the limit in Table A.3 is exceeded, follow the steps in Figure A.2 for taking corrective action.

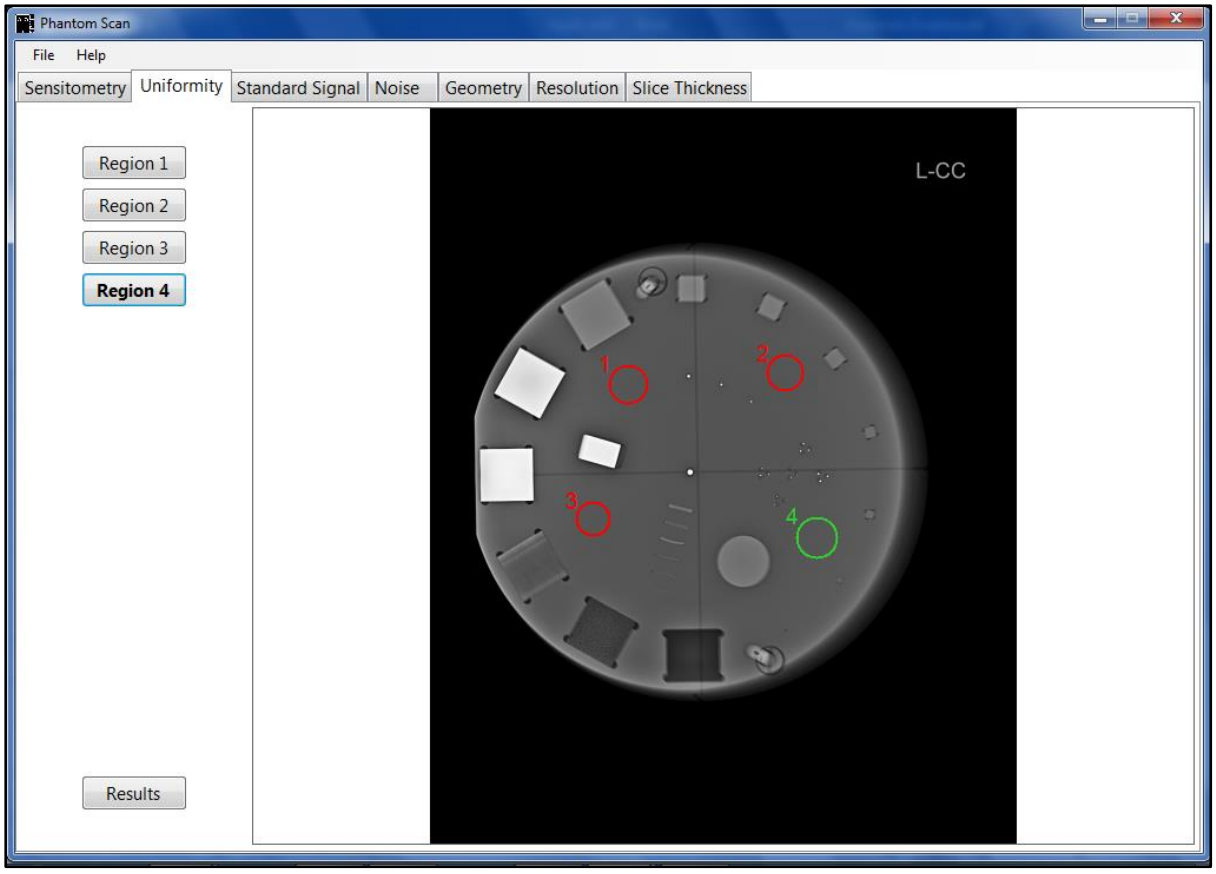

Figure A.31: Locations for ROIs for uniformity evaluation.

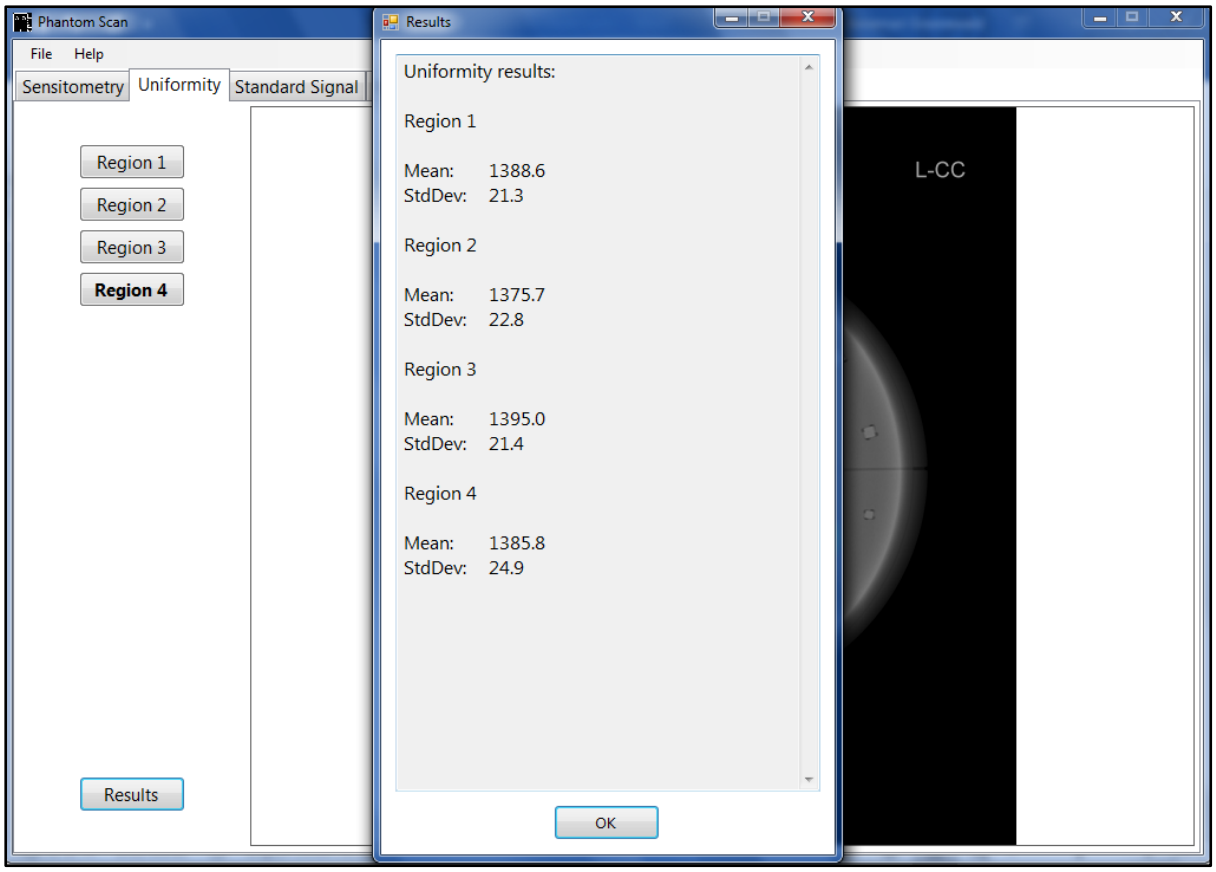

Figure A.32: Results for the uniformity test.

c. Resolution

- Determine the smallest ball visible from the inserts labelled number 21 in Figure A.1 b.).
- Click on the Point 1 button and draw a region of interest (ROI) around the ball. This is shown in Figure A.33.
- Click on the Results button. The data analysis software calculates the modulation transfer function (MTF) from the point spread function (PSF) of the ball. A MTF graph and the limiting spatial resolution are displayed. The limiting spatial resolution is the frequency where the MTF is at 10 %. This is indicated in Figure A.34.
- Record the results in the QC result page (at the end of the manual).
- If the result fails, i.e. the limit in Table A.3 is exceeded, follow the steps in Figure A.2 for taking corrective action.

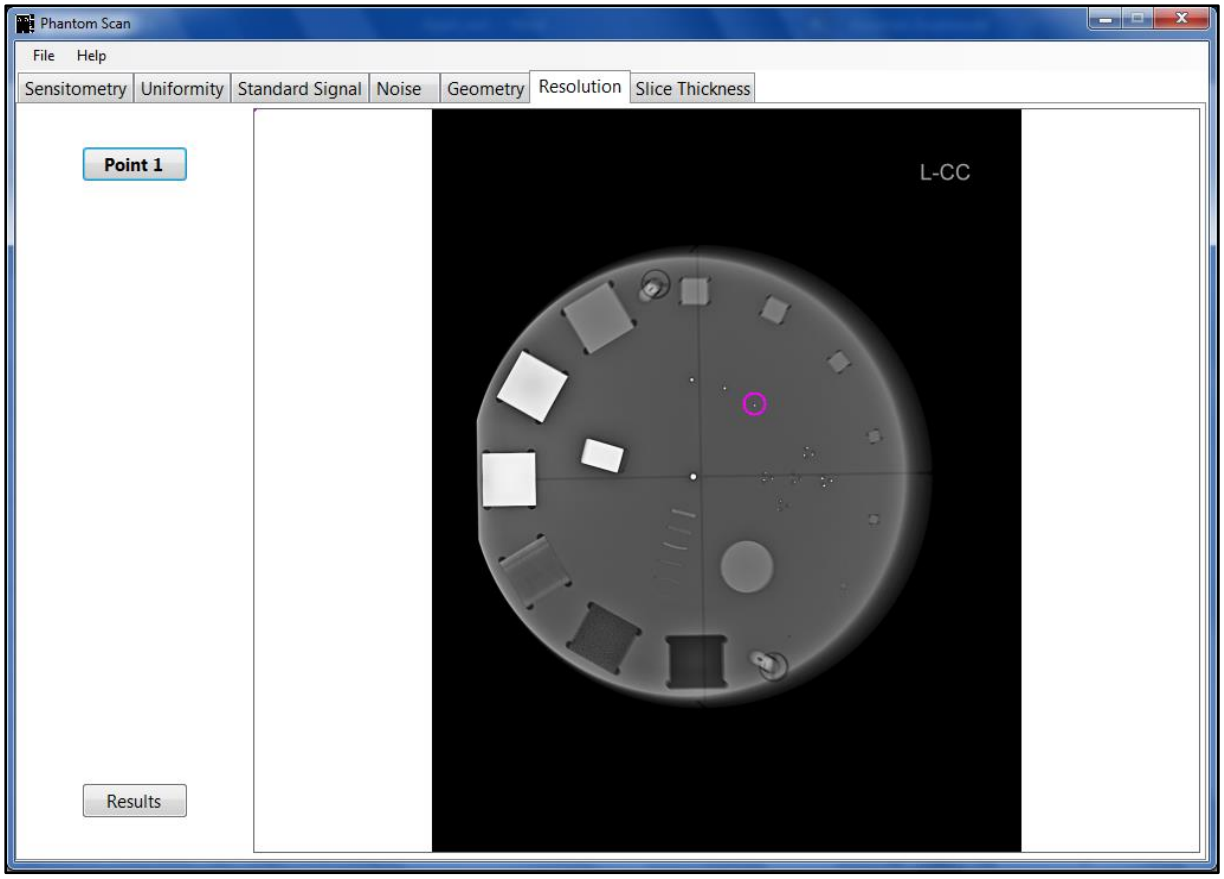

Figure A.33: Drawing a ROI around the smallest ball for resolution calculation.

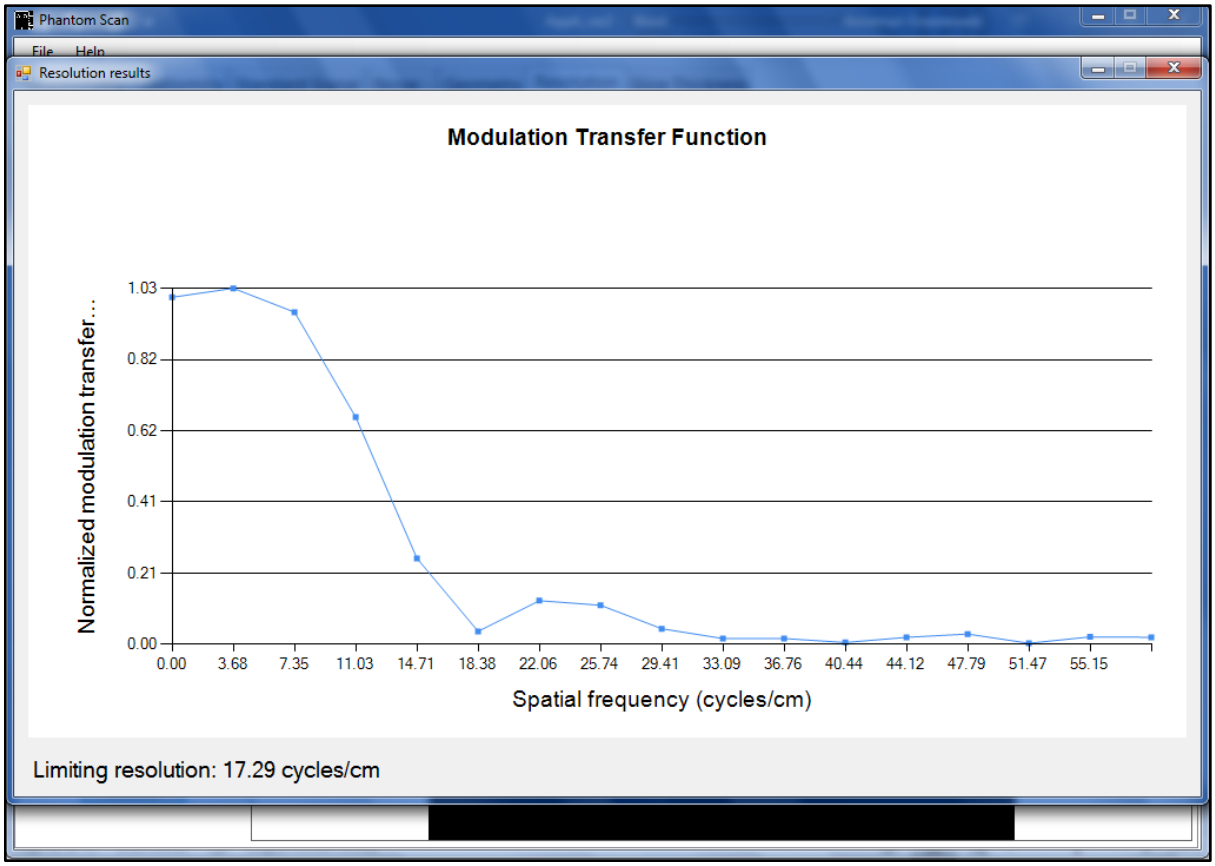

Figure A.34: Results for the resolution test.

d. Image noise

- In the Noise tab in the application, click on the Region 1 button and draw a region of interest (ROI) in the insert numbered 1 in Figure A.1 b.). The ROI should be of diameter approximately half the size of the insert, should not extend beyond the insert or touch the insert edges.
- Click on the Region 2 (background) button and draw a ROI of similar size to that of Region 1 next to the insert. This is shown in Figure A.35.
- Click on the Results button. The data analysis software shows the mean and standard deviations obtained in the ROIs and calculates the signal-to-noise ratio (SNR) and contrast-to-noise ratio (CNR) with Equations A.1 and A.2.

$$SNR = \frac{mean}{standard\ deviation} \quad \text{[Equation A.1]}$$

$$CNR = \frac{mean(a) - mean(b)}{standard\ deviation(b)} \quad \text{[Equation A.2]}$$

- Record the results, as shown in Figure A.36, in the QC result page (at the end of the manual).
- If the result fails, i.e. the limit in Table A.3 is exceeded, follow the steps in Figure A.2 for taking corrective action.

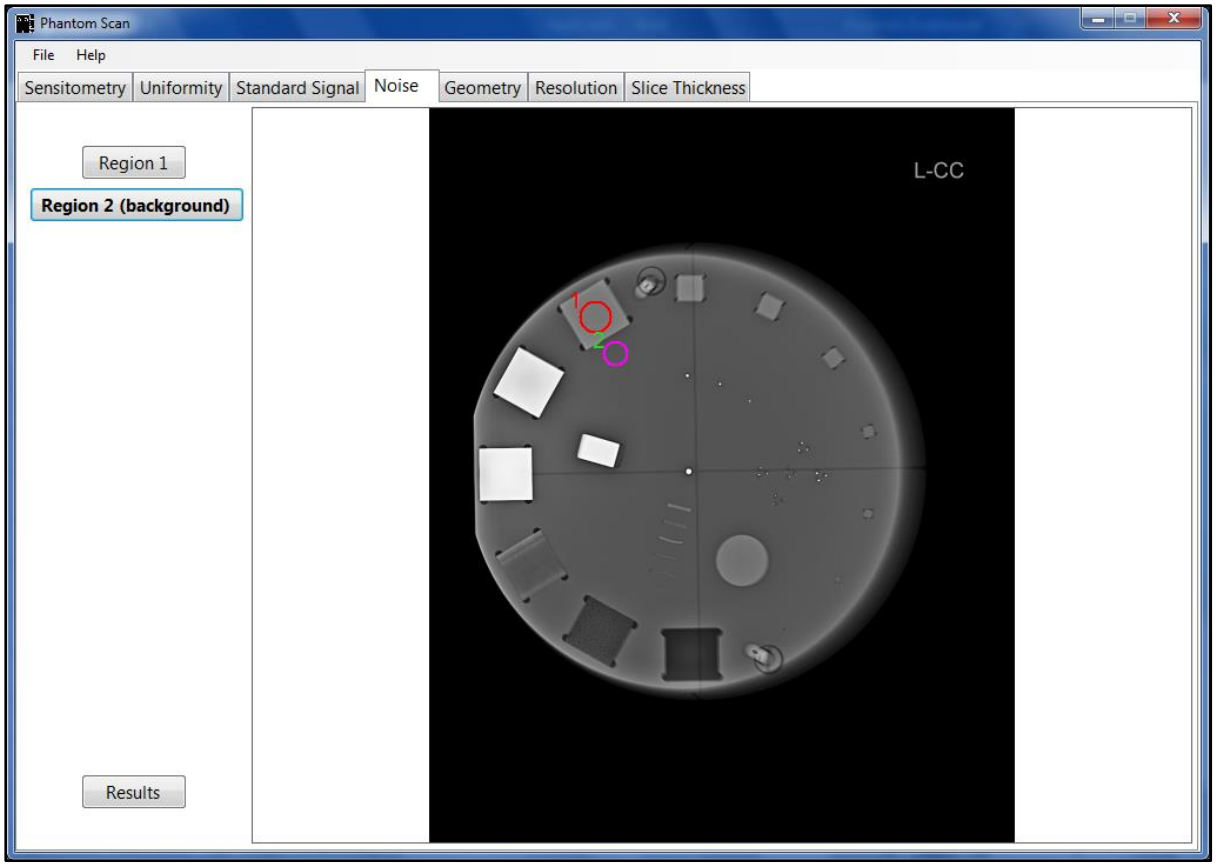

Figure A.35: Drawing ROIs for image noise analysis.

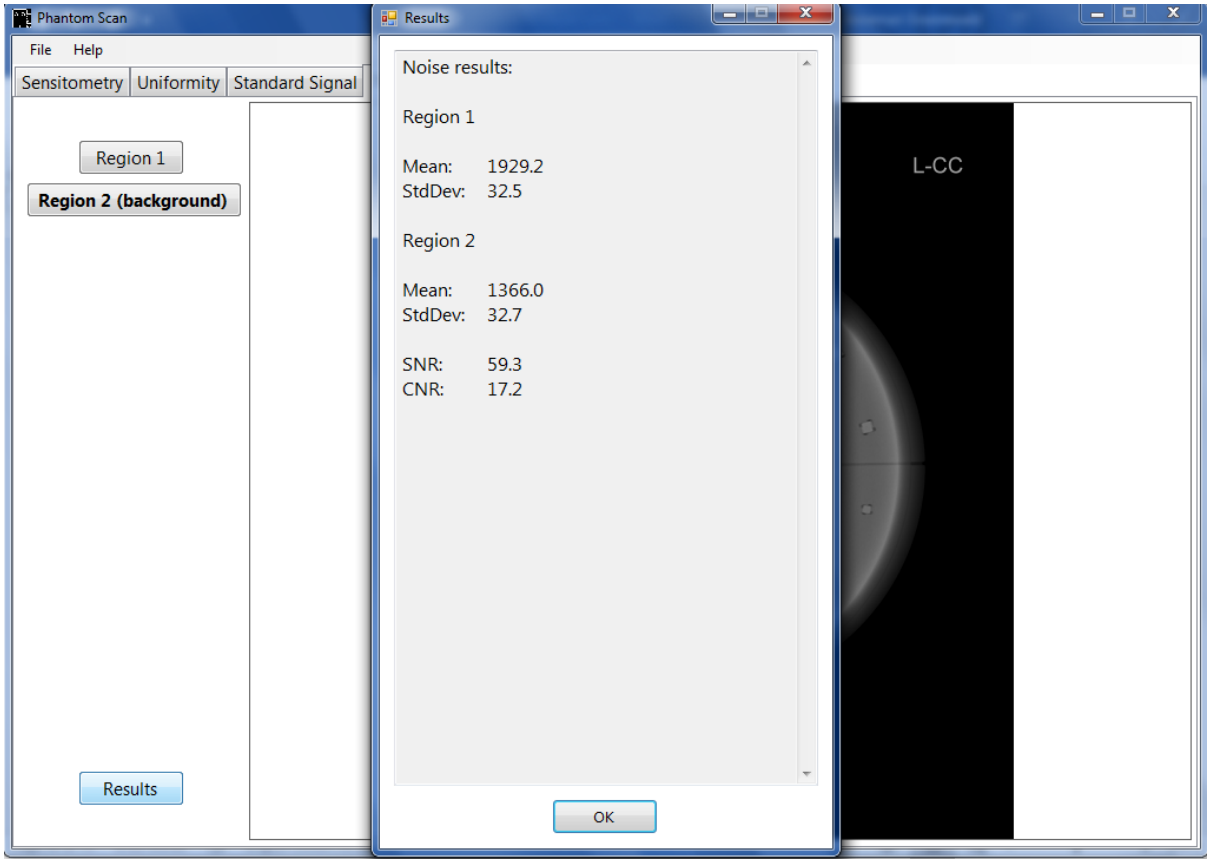

Figure A.36: Results for the noise test.

e. Geometry and measurement tools (distance accuracy / scaling errors)

- In the Geometry tab in the application, click on the Line 1 button and draw a vertical line from edge to edge in the insert numbered 17 in Figure A.1 b.).
- Click on the Line 2 button and draw a horizontal line from edge to edge in the same insert. This is shown in Figure A.37.
- Click on the Results button. The data analysis software measures the length of the drawn lines as indicated in Figure A.38.
- The actual size of the insert is 20 mm diameter. Compare the actual size of the insert to that measured with the software and calculate the difference.
- Record the results in the QC result page (at the end of the manual).
- If the result fails, i.e. the limit in Table A.3 is exceeded, follow the steps in Figure A.2 for taking corrective action.

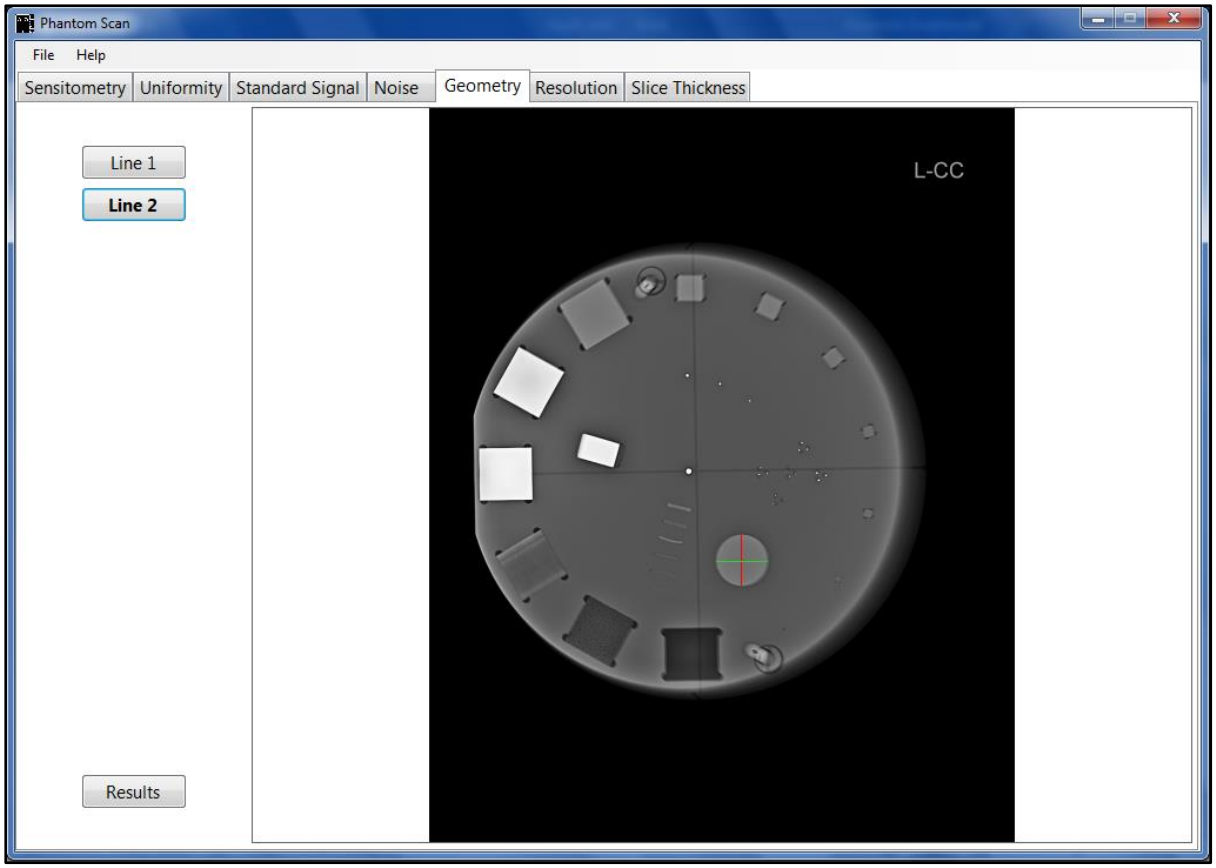

Figure A.37: Geometry measurement lines.

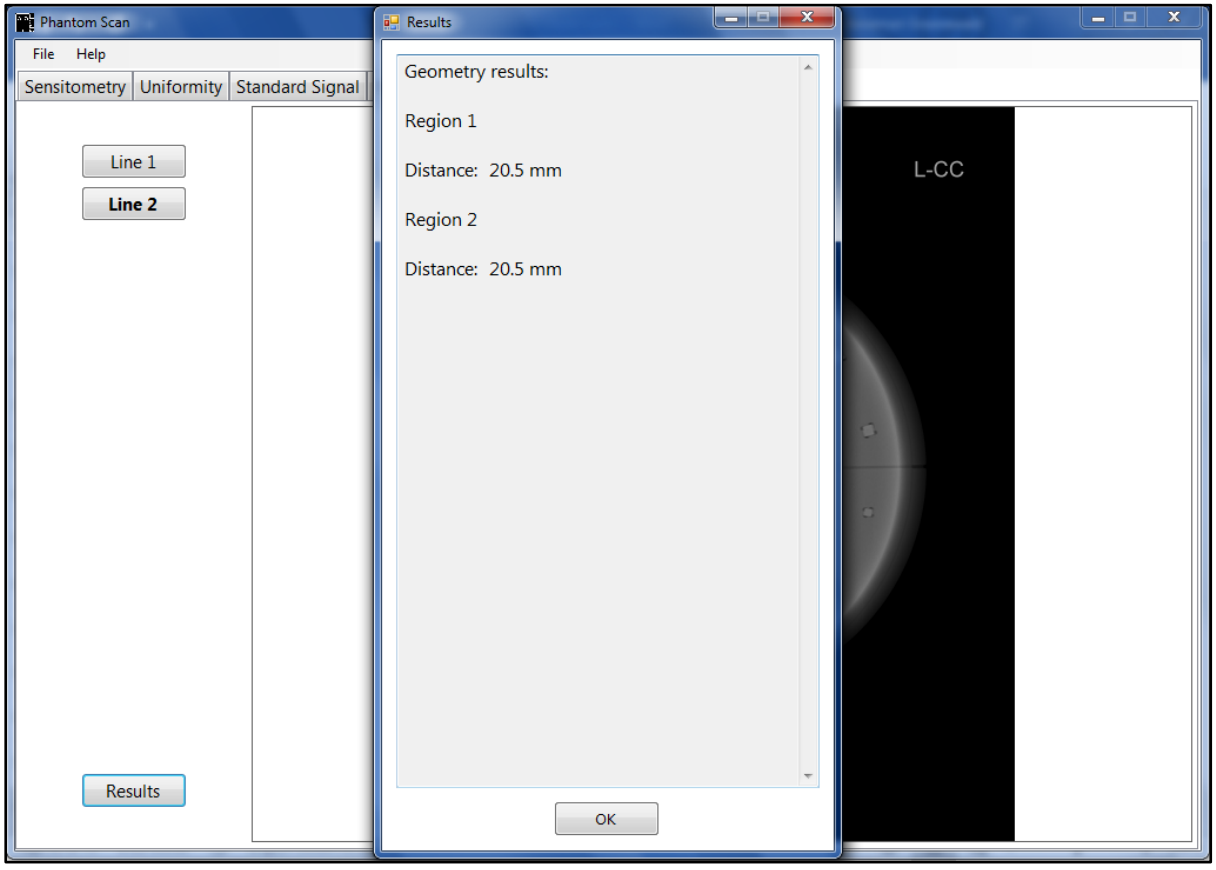

Figure A.38: Results for the geometry test.

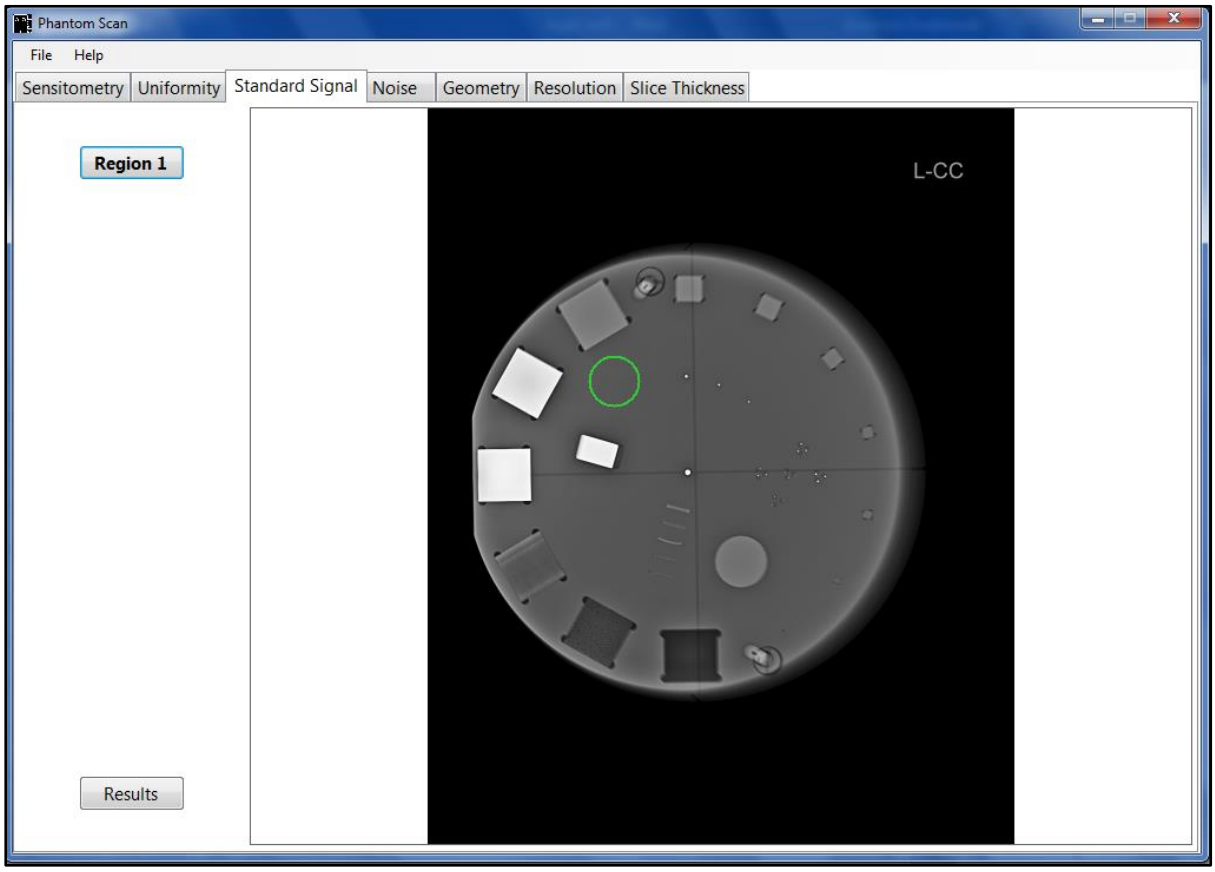

Figure A.39: Drawing a ROI for standard signal evaluation.

f. Standard signal

- In the Standard Signal tab in the application, click on the Region 1 button and draw a region of interest (ROI) in the HDPE housing material at the location labelled 15 in Figure A.1 b.). This is shown in Figure A.39.
- Click on the Results button. The software measures and displays the mean and standard deviation in the ROI as shown in Figure A.40.
- Record the results in the QC result page (at the end of the manual).
- If the result fails, i.e. the limit in Table A.2 is exceeded, follow the steps in Figure A.2 for taking corrective action.

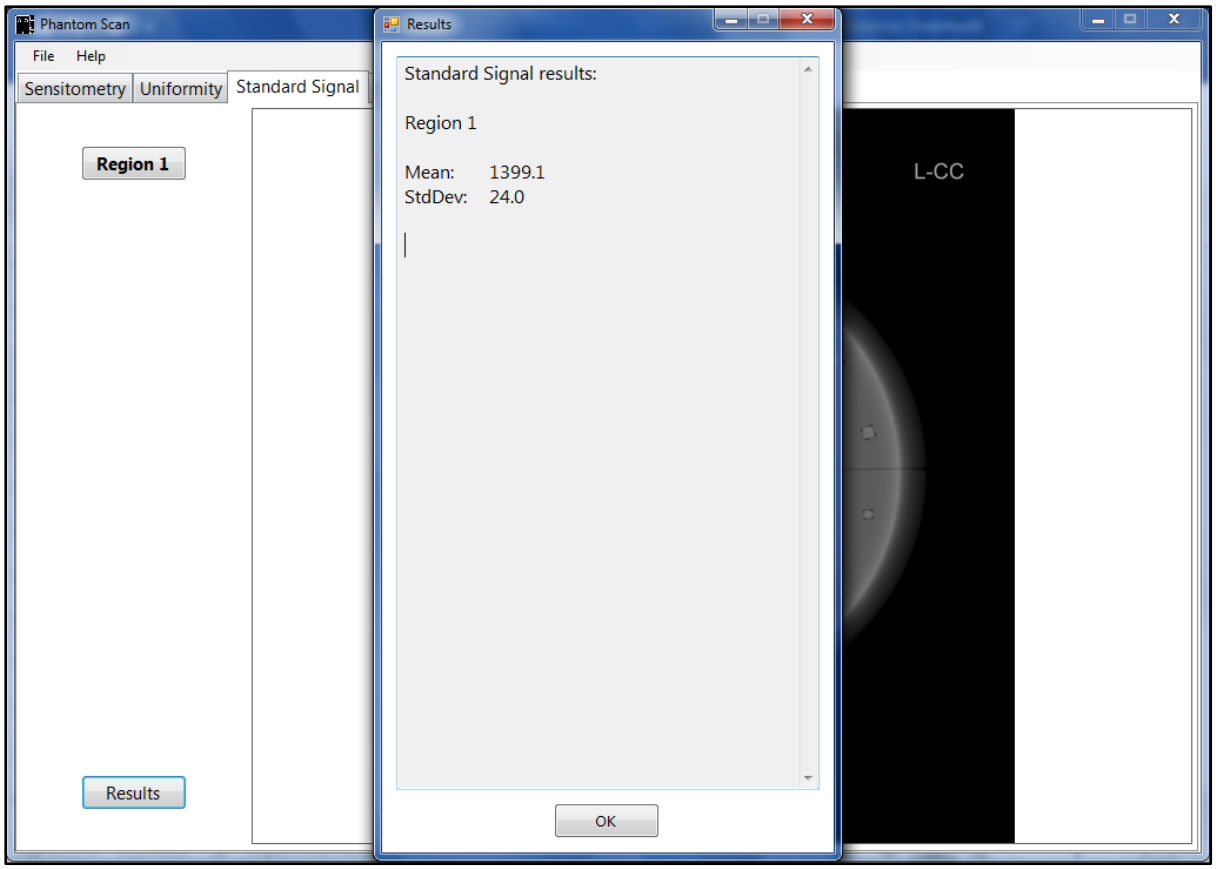

Figure A.40: Results for the standard signal test.

A.2.4.6 Automatic exposure control (AEC) results

a. AEC performance

- Repeat section A.2.4.4 a, c and d and A2.4.5 a, b, d and f for images obtained with AEC with 2 and 4 cm additional HDPE attenuator added.
- Compare the results for the different images.
- Record the results in the QC result page (at the end of the manual).
- If the result fails, i.e. the limit in Table A.3 is exceeded, follow the steps in Figure A.2 for taking corrective action.

b. AEC repeatability

- Repeat section A.2.4.4 a-d and A.4.3.5 a-f for three images obtained with AEC with the same thickness of additional HDPE attenuator added, e.g. perform 3 AEC exposures of the phantom only (0cm additional attenuator).
- Compare the results for the different images.
- Record the results in the QC result page (at the end of the manual).
- If the result fails, i.e. the limit in Table A.3 is exceeded, follow the steps in Figure A.2 for taking corrective action.

A.2.4.7 Saving and printing the results

- Click on File and select Save Results as shown in Figure A.41 a.).
- Enter a file name and choose the location where you want to save the results, as indicated in Figure A.41 b.).
- To print the results in hard copy, go to the selected save location, select the file name to be printed and double left click to open the file in Notepad.
- In Notepad, click on File and select Print. This is shown in Figure A.42 a.).
- Select the printer you want to use and click on Print, as shown in Figure A.42 b.).
- Sign and file the hard copy results.

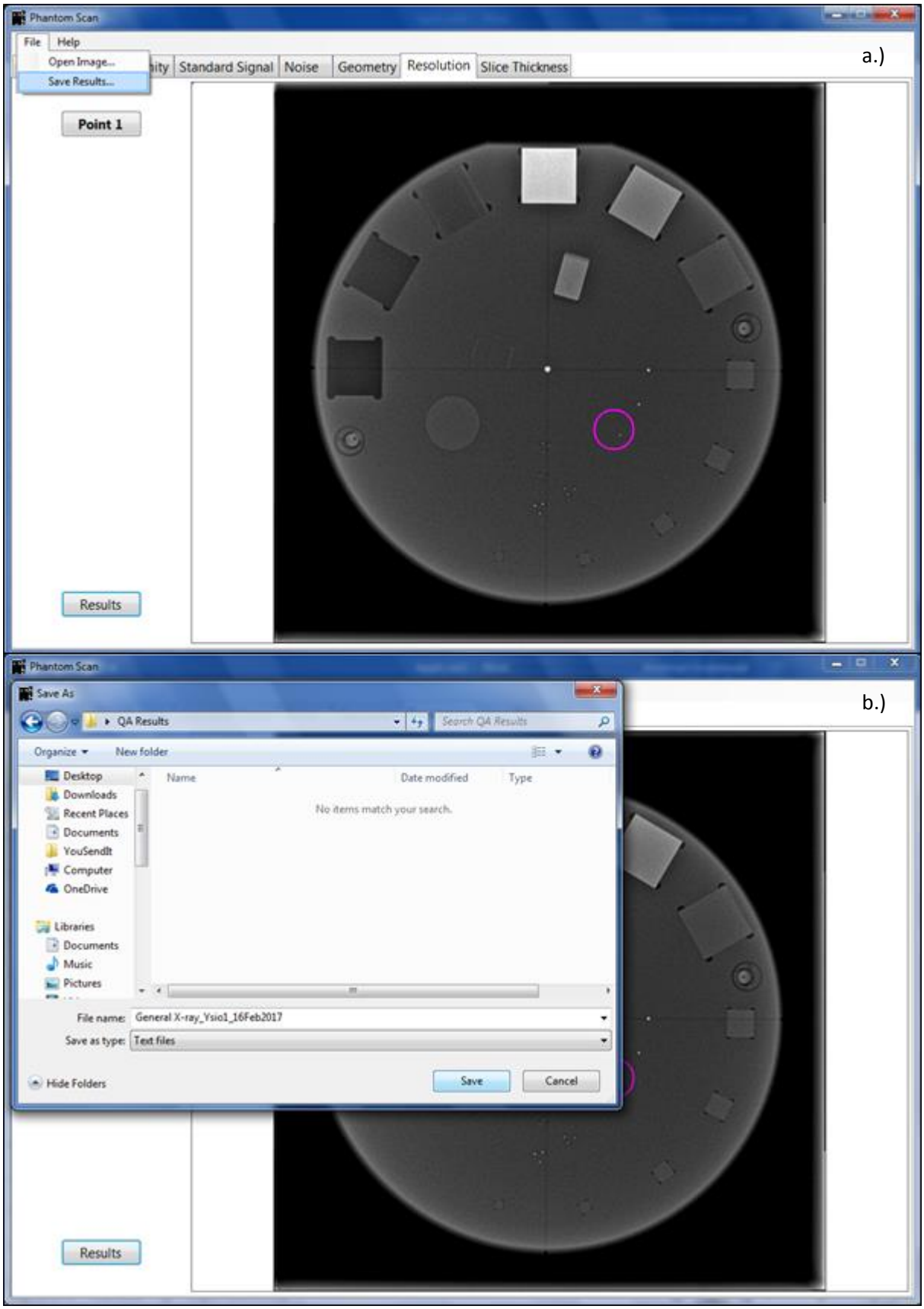

Figure A.41: Saving the obtained results. a.) Selecting the save option in the application. b.) Choosing the location to save to.

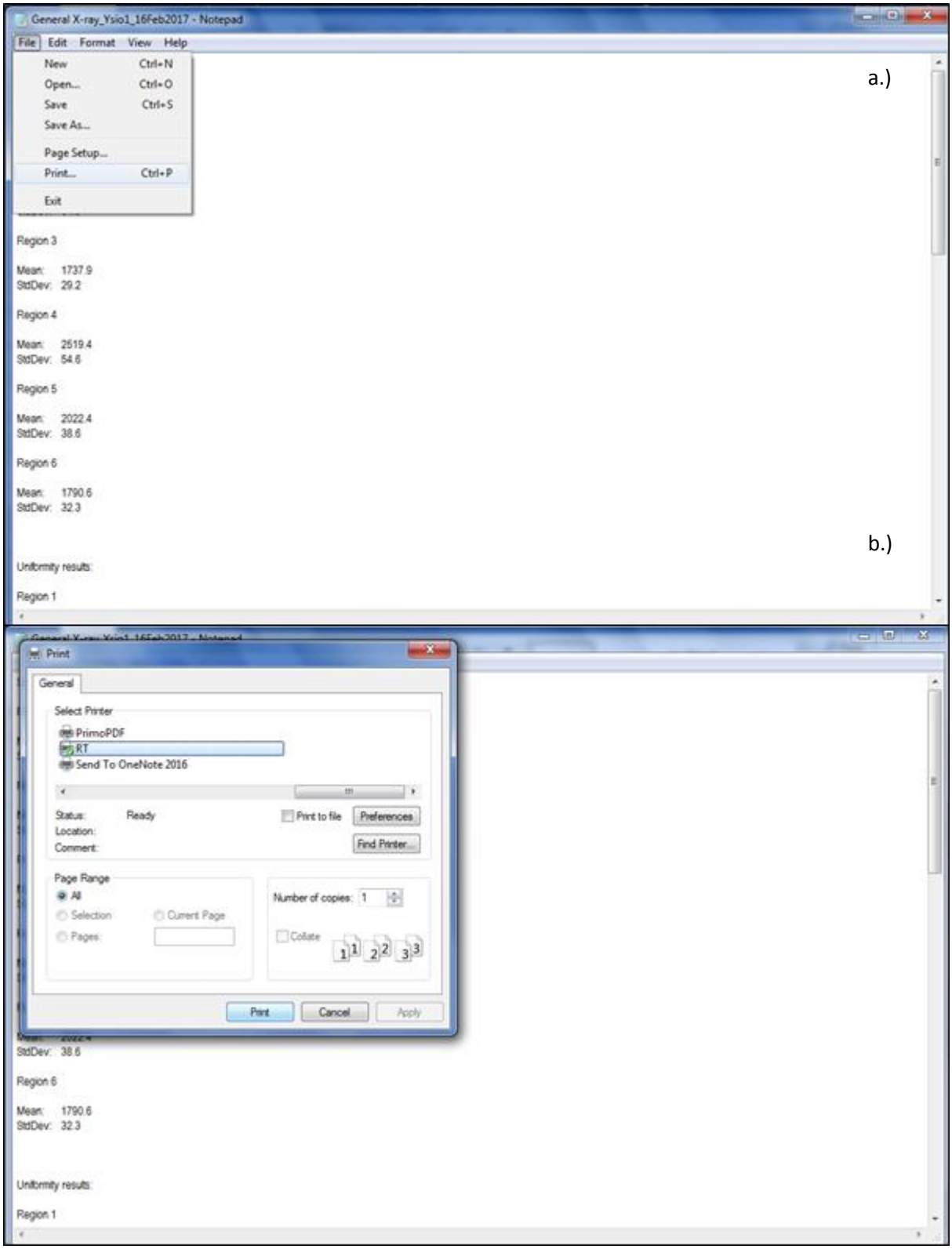

Figure A.42: Printing the results from Notepad. a.) Selecting the print option. b.) Selecting the printer.

A.2.5 Computed tomography scanning

These tests are performed for CT scanners. Table A.4 shows the tests required for comprehensive image quality assurance in CT scanning.

Table A.4: Tests required for comprehensive CT scanning image quality assurance. (Insert numbers in table refer to Figure A.1 b.))

Test	Objective	Method	Frequency	Limits
Sensitometry & grey scale linearity (HU / CT number linearity)	Maintain grey scale value for different object densities	ROI analysis with data analysis software using inserts 1, 9-13	Acceptance, daily	Baseline value ± 10 HU For universal phantom baseline value ± 10 %
Low contrast detectability	Distinguish objects of density similar to background as they become progressively smaller	Visual inspection of inserts 1-8 to determine smallest visible insert	Acceptance, 3 monthly	Baseline value +1 insert size
Uniformity	Ensure grey scale values across the image remain constant for the same material	ROI analysis with data analysis software using phantom housing 15	Acceptance, 3 monthly	Mean value ± 10 %
Resolution	Consistently distinguish objects as they become smaller and closer together	MTF analysis and plot with data analysis software using insert group 21	Acceptance, 3 monthly	Baseline value minus 25 %
Image noise	Quantum mottle is sufficiently low as to not degrade image quality unacceptably	ROI analysis with data analysis software using phantom housing 15 and Equations 1 and 2	Acceptance, 3 monthly	Baseline value ± 10 %
Positioning & alignment (zero slice position / scan plane localisation)	Checks that the slice the scan is zeroed on is at co-ordinates x=0, y=0, z=0	Visually check the coordinates of the slice with the central ball	Acceptance, 3 monthly	Zero ± 0.2 cm

Geometry and measurement tools (distance accuracy / scaling errors)	To ensure geometrical distortion and scaling does not occur	Comparing distances measured with data analysis software to know distances	Acceptance, 3 monthly	Obtained value ± 0.5 cm or ± 2 %, whichever is smaller
Artefacts	Check that the image is free of artefacts	Visually inspect images for lines, spots, blur, marks, etc	Acceptance, 3 monthly	No visible artefacts For universal phantom streak from central bead will be present, no other artefacts to be seen
Image quality visual inspection	Consistently maintains visual image quality	Visually inspect images noting inserts and artefacts seen	Acceptance, 3 monthly	Reproducible results
Standard signal	Keep the grey scale value of a certain material (HDPE) constant over time	ROI analysis with data analysis software using phantom housing 15	Acceptance, 3 monthly	Baseline grey scale value ± 10 HU
CT slice thickness	Determine if the set slice thickness is actually scanned	Data analysis software measures the slice thickness from the ramp labelled 20	Acceptance, yearly	Baseline value ± 20 % or ± 0.1 cm, whichever is smaller

A.2.5.1 Phantom set-up

a. Place the phantom on the provided stand with the scribe lines facing away from the gantry, as shown in Figure A.43 a.).
b. Align the phantom scribe lines with the CT scanner lasers. This is shown in Figure A.43 b.).
c. Zero the scan position.

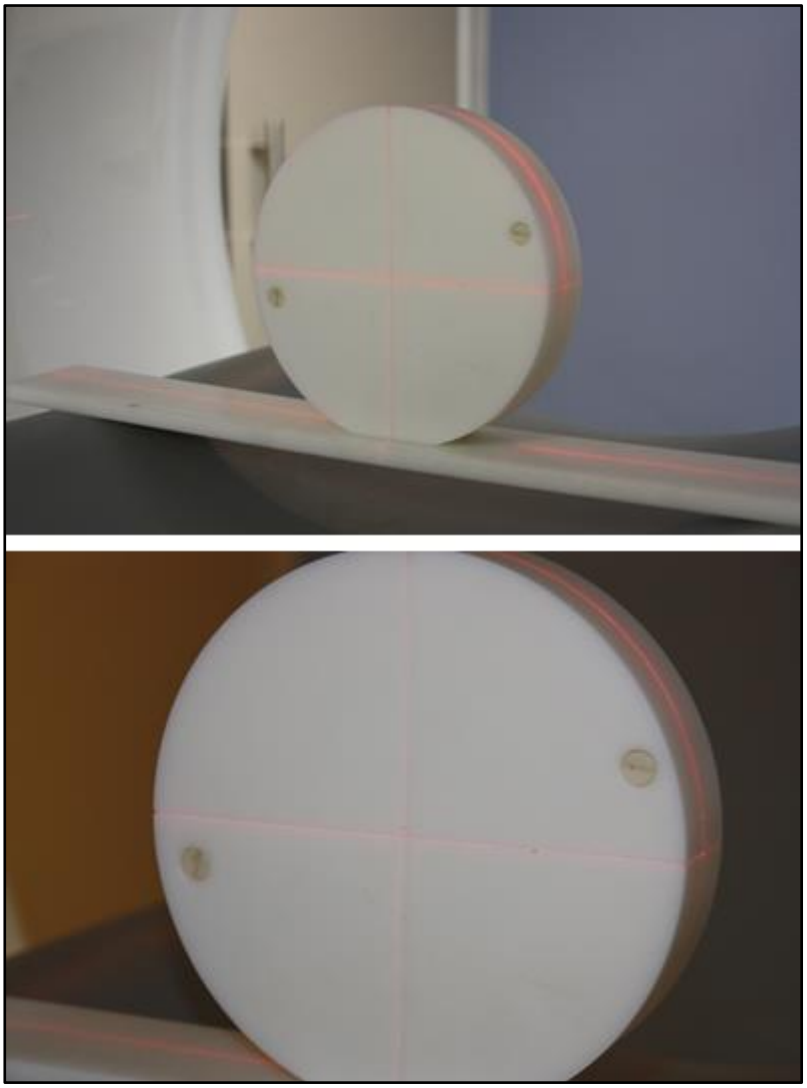

Figure A.43: a.) Phantom positioned on stand on CT scanner couch. a.) and b.) Phantom scribe lines aligned with lasers.

A.2.5.2 Phantom exposure

a. Use a head or brain scanning protocol with 5 mm slice thickness.
b. Perform the scan.
c. On the obtained image note the following details:
    i. Unit name
    ii. Test date
    iii. Technique factors used
    iv. Operator

A.2.5.3 Load images into data analysis software

a. Export the raw obtained images from the CT unit control console in Digital Imaging and Communications in Medicine (DICOM) format. Contact a technician or medical physicist to write a standing operating procedure (SOP) for doing this for your unit or department.
b. In the Phantom Scan application, click on File and select Open Image as shown in Figure A.44.

Figure A.44: Opening an image for analysis.

c. Select the zero-slice or central image from the CT data set and click on Open. The image will now be displayed in the application, as shown in Figure A.45.

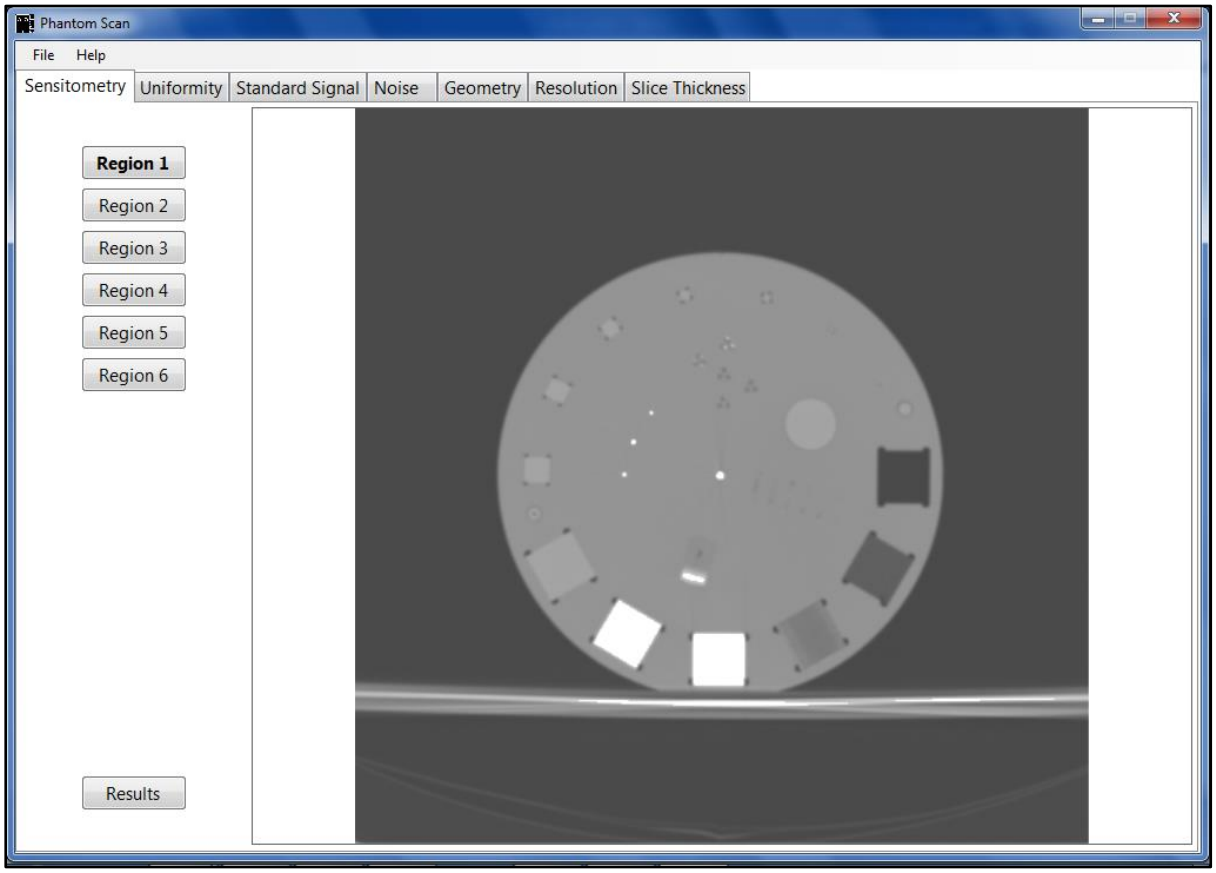

Figure A.45: Image opened in the application and ready for evaluation.

A.2.5.4 Visual inspection of the obtained images

Load the central or zero slice image into the data analysis software as explained in section A.2.5.3 above. In the software, view the loaded image and visually inspect the image to determine:

a. Low contrast detectability
   - Visually determine the smallest low contrast detectability insert that can be seen. Refer to Figure A.1 for the location of these blocks, labelled 1-8 in Figure A.1 b.).
   - Record the size of the smallest visible block in the QC result page (at the end of the manual).
   - If the result is out of tolerance, i.e. the limit in Table A.4 is exceeded, follow the steps in Figure A.2 for taking corrective action.

b. Positioning and alignment (zero slice position / scan plane localisation)
   - Visually check that the central ball appears on the slice located at co-ordinates x=0, y=0, z=0.
   - Record the results in the QC result page (at the end of the manual) and note the direction in which the deviation was observed.
   - If the result fails, i.e. the limit in Table A.4 is exceeded, follow the steps in Figure A.2 for taking corrective action.

c. Artefacts
   - Visually inspect the image for the presence of any artefacts, for example ghost images, lines, streaks, marks, spots, blur or any other unexpected appearance.
   - Record the artefact seen and where in the image it occurred in the QC result page (at the end of the manual).
   - If the result is out of tolerance, i.e. the limit in Table A.4 is exceeded, follow the steps in Figure A.2 for taking corrective action.

d. Image quality visual inspection
   - Visually inspect the image and note any visual obstructions, grey scale inversions, distortions or unexpected occurrences in the image.
   - Record the manifestation seen and where in the image it occurred in the QC result page (at the end of the manual).
   - If the result is out of tolerance, i.e. the limit in Table A.4 is exceeded, follow the steps in Figure A.2 for taking corrective action.

A.2.5.5 Data analysis software evaluation of the obtained images

Load the obtained zero slice image into the data analysis software as explained in section A.2.5.3 above. Record the results obtained for the following tests.

a. Sensitometry & grey scale linearity (CT number reproducibility)

- In the Sensitometry tab in the application, click on the Region 1 button and draw a region of interest (ROI) in the insert numbered 9, i.e. air, in Figure A.1 b.). The ROI should be of diameter approximately half the size of the insert, should not extend beyond the insert or touch the insert edges.
- Click on the Region 2 button and draw a ROI in the insert numbered 10, i.e. lung, in Figure A.1 b.). The ROI should be of diameter approximately half the size of the insert, should not extend beyond the insert or touch the insert edges.
- Repeat this for the Regions 3, 4, 5 and 6 buttons drawing ROIs in the inserts numbered 11, 12, 13 and 1 in Figure A.1 b.), i.e. supawood, bone, Teflon and RGD. This is shown in Figure A.46.
  Note: First click on the Region button and then draw the ROI.

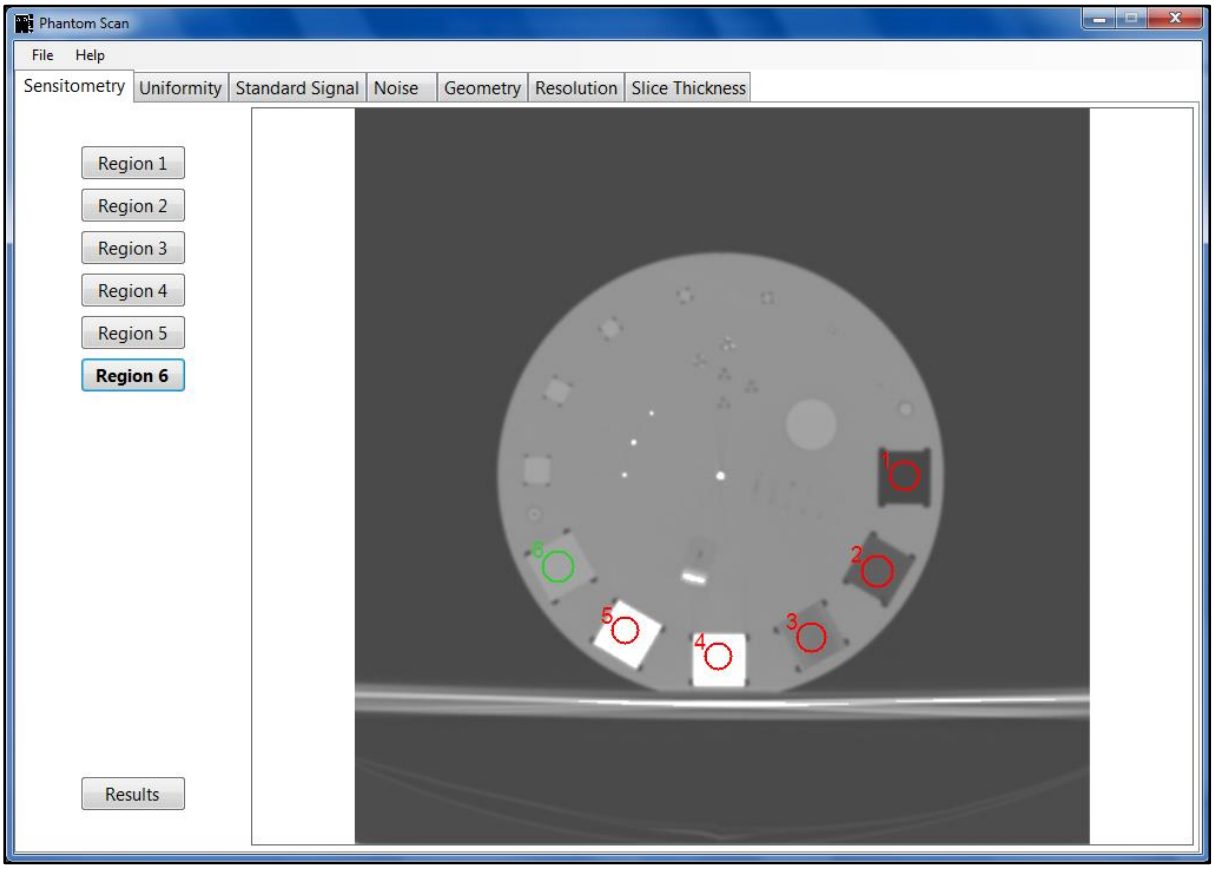

Figure A.46: Drawing the sensitometry ROIs.

- Click on the Results button.
- The mean and standard deviation in each ROI is measured and displayed as shown in Figure A.47.
- Record the results in the QC result page (at the end of the manual).
- If the result fails, i.e. the limit in Table A.4 is exceeded, follow the steps in Figure A.2 for taking corrective action.

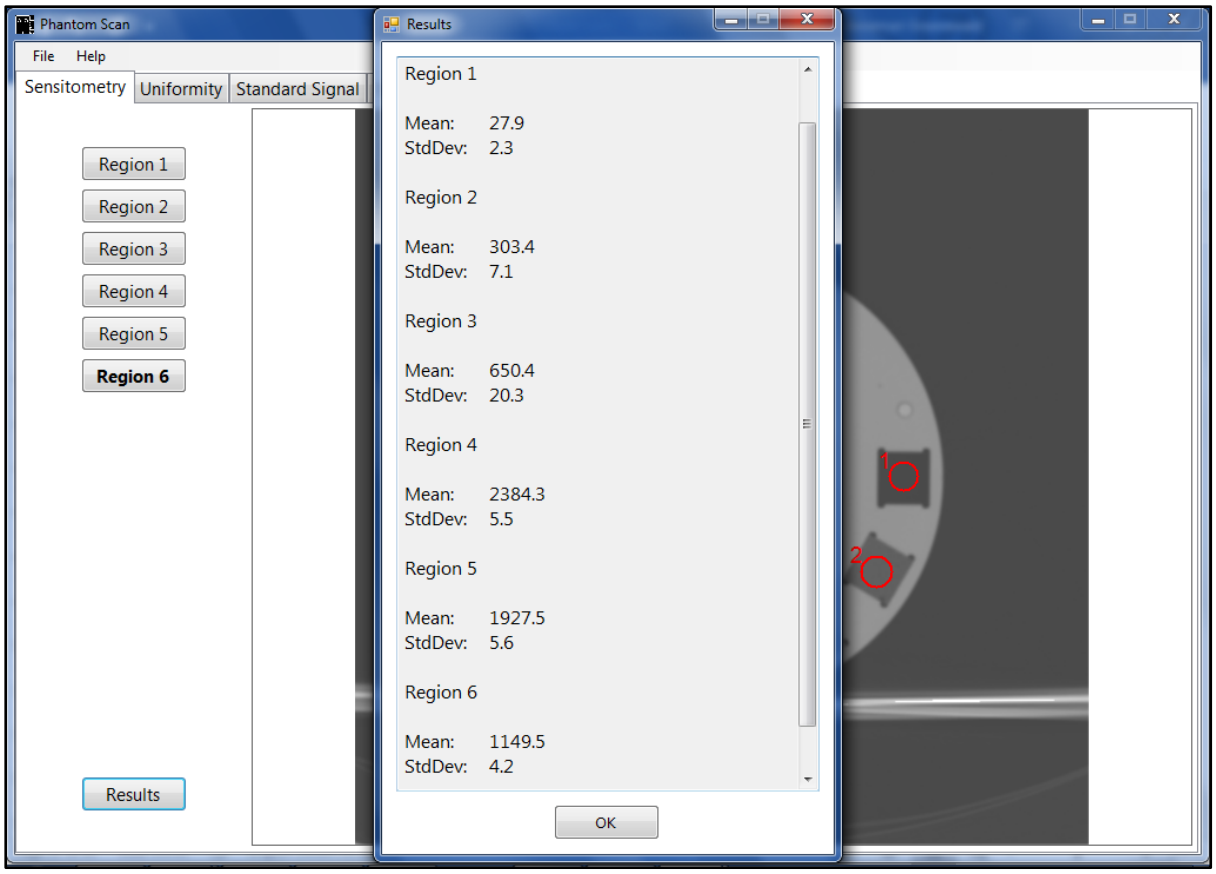

Figure A.47: Results for the sensitometry test.

b. Uniformity

- In the Uniformity tab in the application, click on the Region 1 button and draw a region of interest (ROI) in the HDPE housing material in a location that does not contain any other inserts.
- Click on the Region 2, 3 and 4 buttons and draw ROIs of similar size than in the first step in the remaining quadrants at locations with no other inserts. This is illustrated in Figure A.48.
- Click on the Results button. The mean and standard deviation in each ROI is measured as shown in Figure A.49.
- Calculate the largest difference in the mean value and record the result in the QC result page (at the end of the manual).
- If the result fails, i.e. the limit in Table A.4 is exceeded, follow the steps in Figure A.2 for taking corrective action.

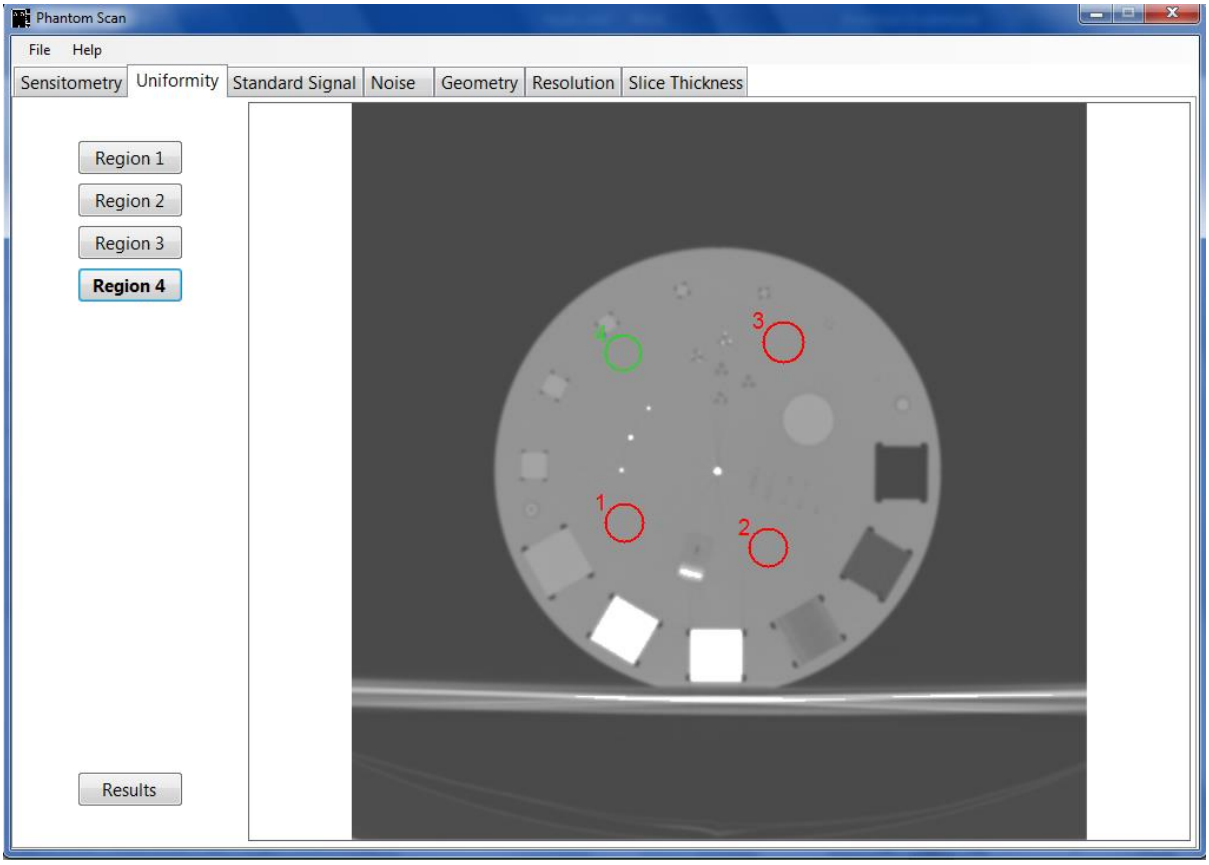

Figure A.48: Locations for ROIs for uniformity evaluation.

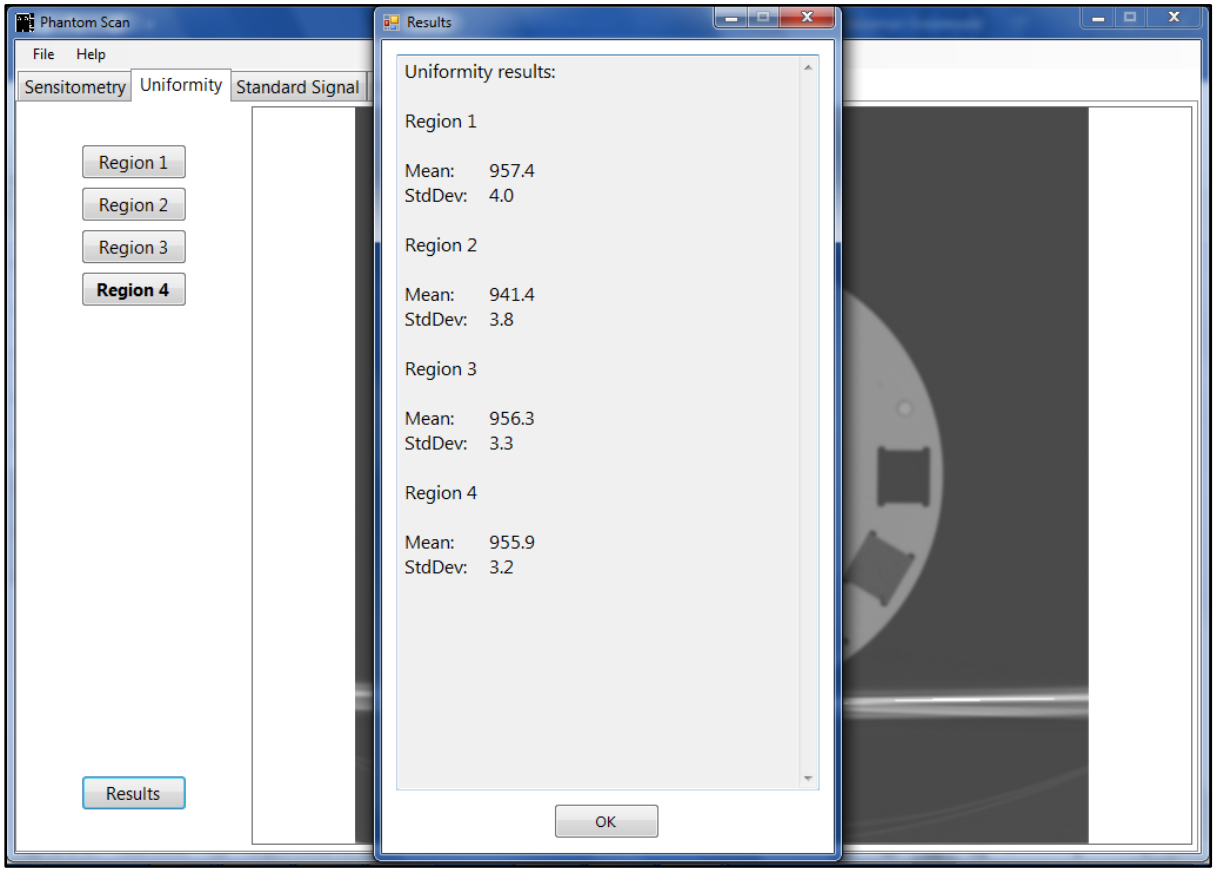

Figure A.49: Results for the uniformity test.

c. Resolution

- Determine the smallest ball visible from the inserts labelled number 21 in Figure A.1 b.).
- Click on the Point 1 button and draw a region of interest (ROI) around the ball. This is shown in Figure A.50.
- Click on the Results button. The data analysis software calculates the modulation transfer function (MTF) from the point spread function (PSF) of the ball. A MTF graph and the limiting spatial resolution are displayed. The limiting spatial resolution is the frequency where the MTF is at 10 %. This is indicated in Figure A.51.
- Record the results in the QC result page (at the end of the manual).
- If the result fails, i.e. the limit in Table A.4 is exceeded, follow the steps in Figure A.2 for taking corrective action.

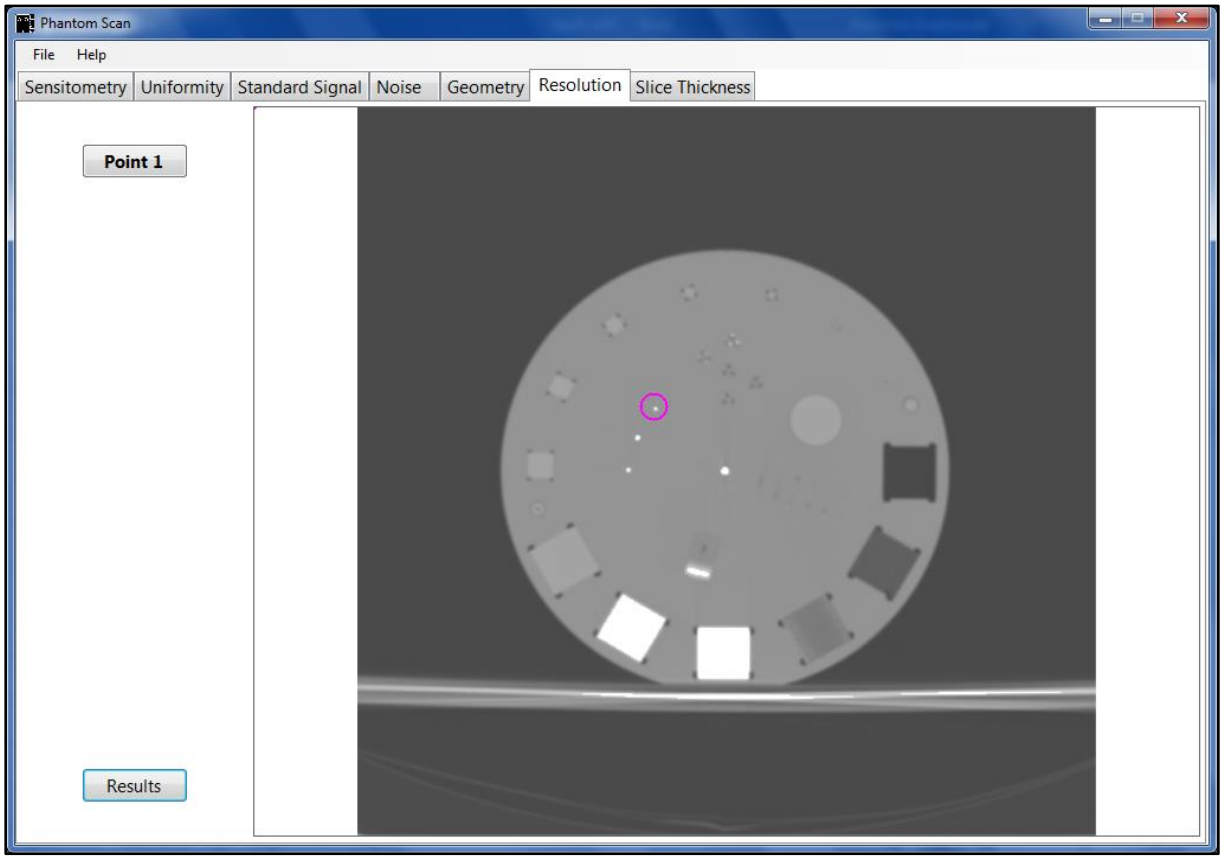

Figure A.50: Drawing a ROI around the smallest ball for resolution calculation.

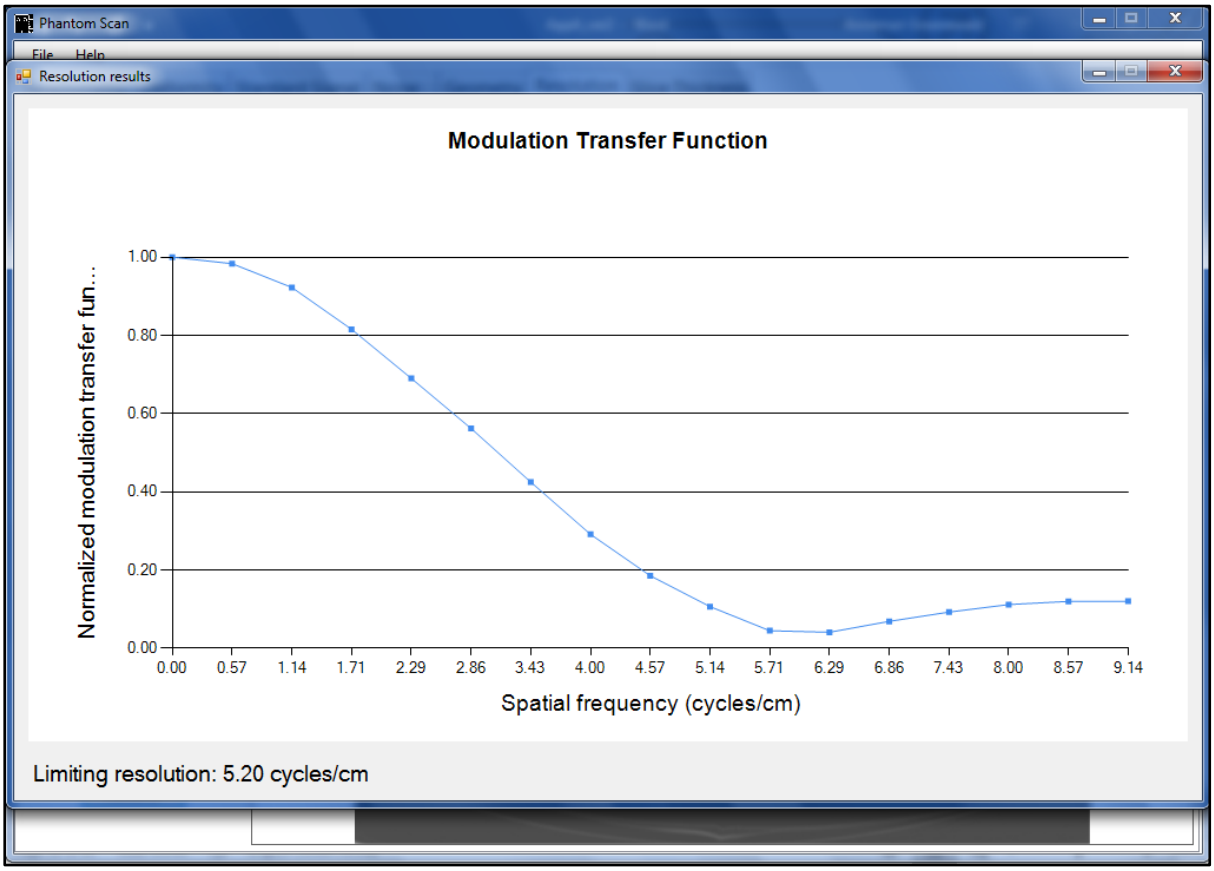

Figure A.51: Results for the resolution test.

d. Image noise

- In the Noise tab in the application, click on the Region 1 button and draw a region of interest (ROI) in the insert numbered 1 in Figure A.1 b.). The ROI should be of diameter approximately half the size of the insert, should not extend beyond the insert or touch the insert edges.
- Click on the Region 2 (background) button and draw a ROI of similar size to that of Region 1 next to the insert. This is shown in Figure A.52.
- Click on the Results button. The data analysis software shows the mean and standard deviations obtained in the ROIs and calculates the signal-to-noise ratio (SNR) and contrast-to-noise ratio (CNR) with Equations A.1 and A.2.

$$SNR = \frac{mean}{standard\ deviation} \quad \text{[Equation A.1]}$$

$$CNR = \frac{mean(a) - mean(b)}{standard\ deviation(b)} \quad \text{[Equation A.2]}$$

- Record the results, as shown in Figure A.53, in the QC result page (at the end of the manual).
- If the result fails, i.e. the limit in Table A.4 is exceeded, follow the steps in Figure A.2 for taking corrective action.

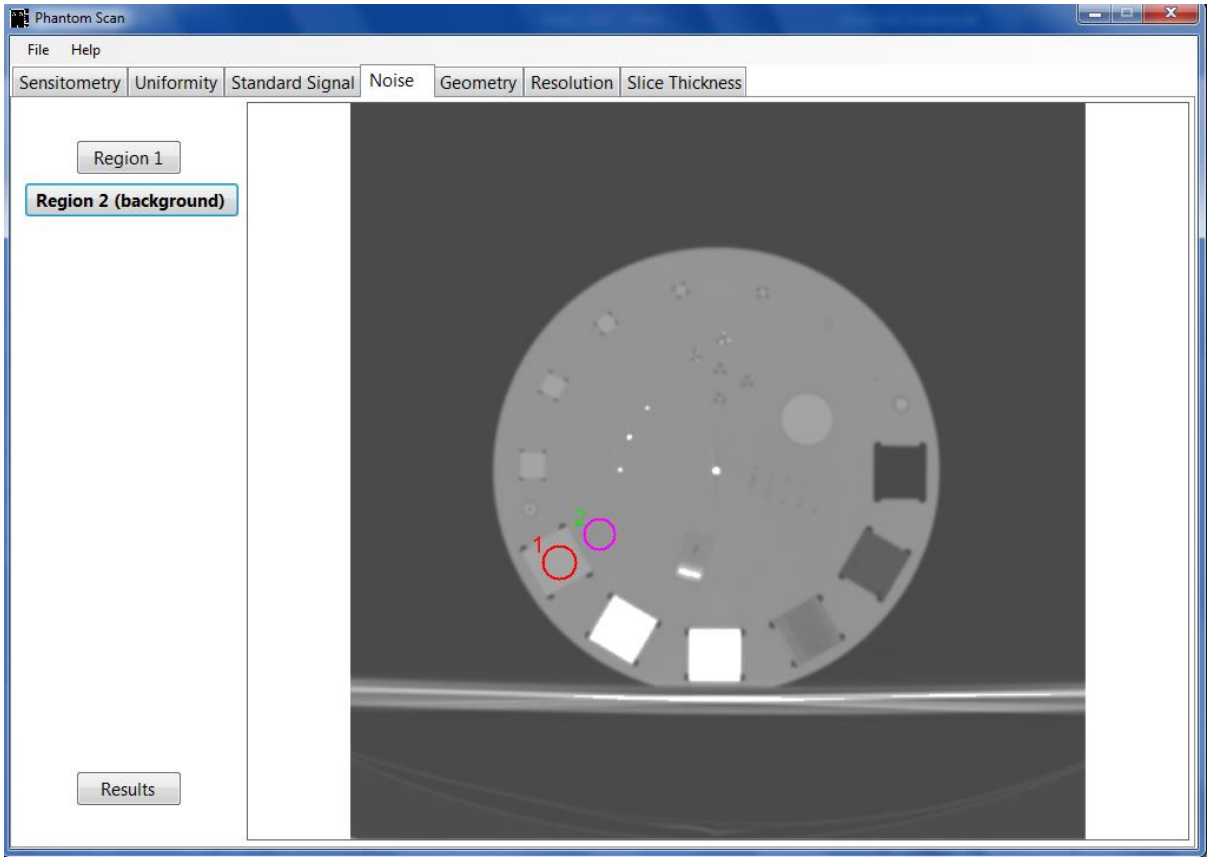

Figure A.52: Drawing ROIs for image noise analysis.

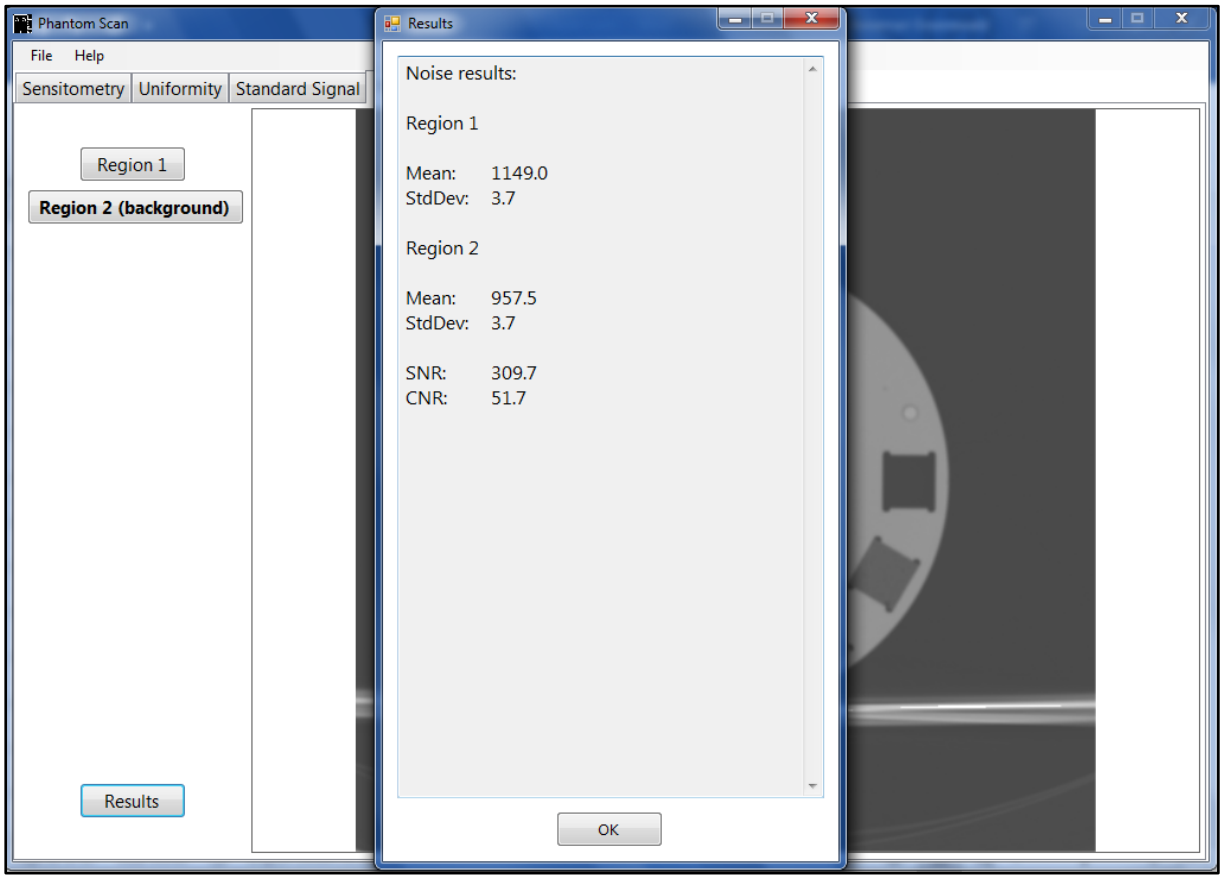

Figure A.53: Results for the noise test.

e. Geometry and measurement tools (distance accuracy / scaling errors)

- In the Geometry tab in the application, click on the Line 1 button and draw a vertical line from edge to edge in the insert numbered 17 in Figure A.1 b.).
- Click on the Line 2 button and draw a horizontal line from edge to edge in the same insert. This is shown in Figure A.54.
- Click on the Results button. The data analysis software measures the length of the drawn lines as indicated in Figure A.55.
- The actual size of the insert is 20 mm diameter. Compare the actual size of the insert to that measured with the software and calculate the difference.
- Record the results in the QC result page (at the end of the manual).
- If the result fails, i.e. the limit in Table A.4 is exceeded, follow the steps in Figure A.2 for taking corrective action.

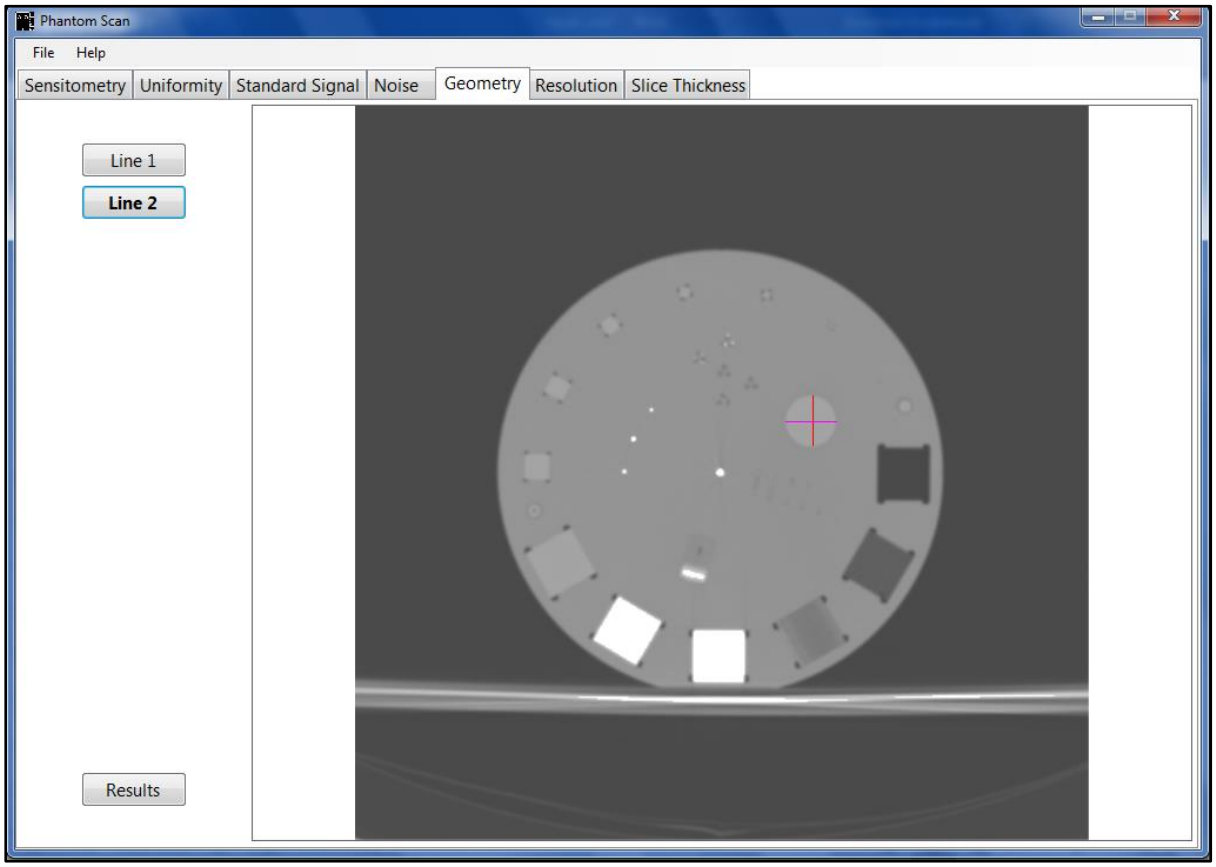

Figure A.54: Geometry measurement lines.

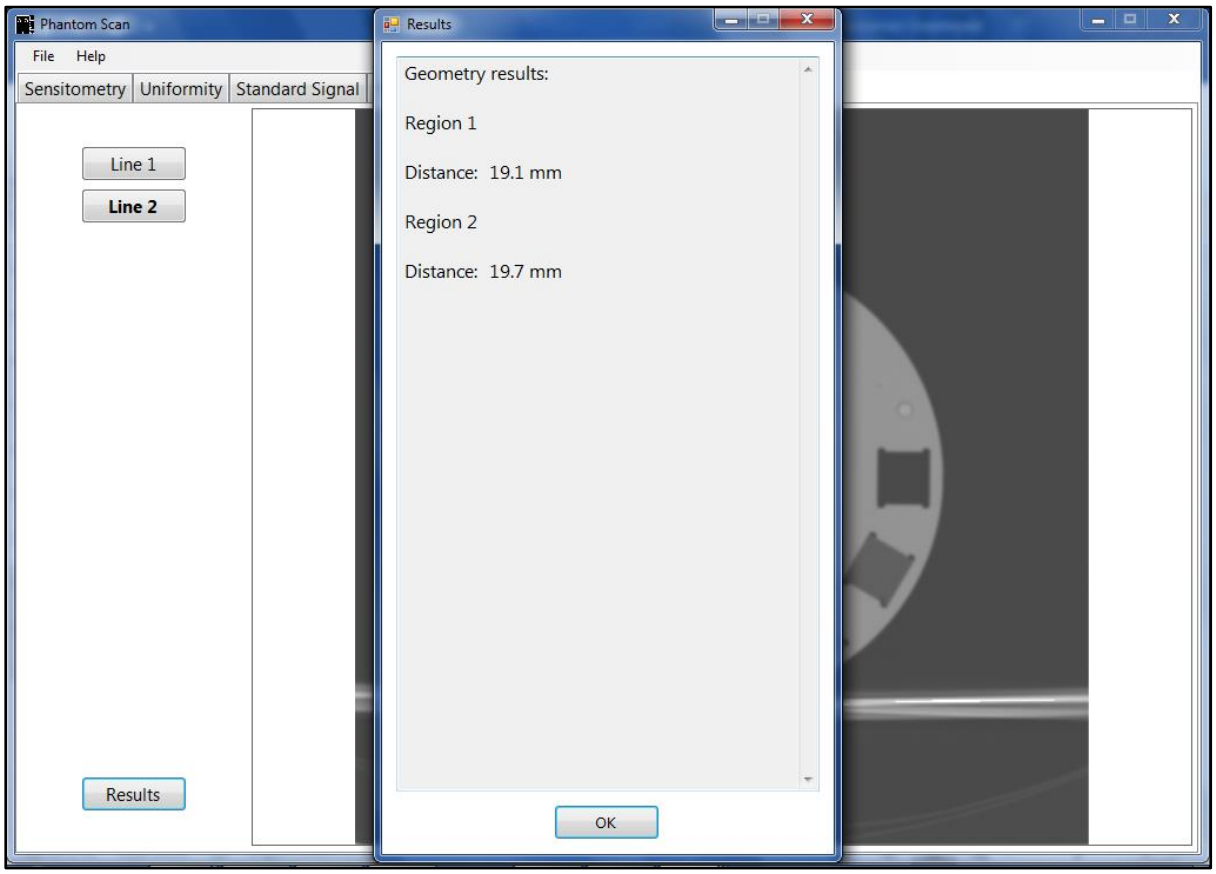

Figure A.55: Results for the geometry test.

f. Standard signal

- In the Standard Signal tab in the application, click on the Region 1 button and draw a region of interest (ROI) in the HDPE housing material at the location labelled 15 in Figure A.1 b.). This is shown in Figure A.56.
- Click on the Results button. The software measures and displays the mean and standard deviation in the ROI as shown in Figure A.57.
- Record the results in the QC result page (at the end of the manual).
- If the result fails, i.e. the limit in Table A.4 is exceeded, follow the steps in Figure A.2 for taking corrective action.

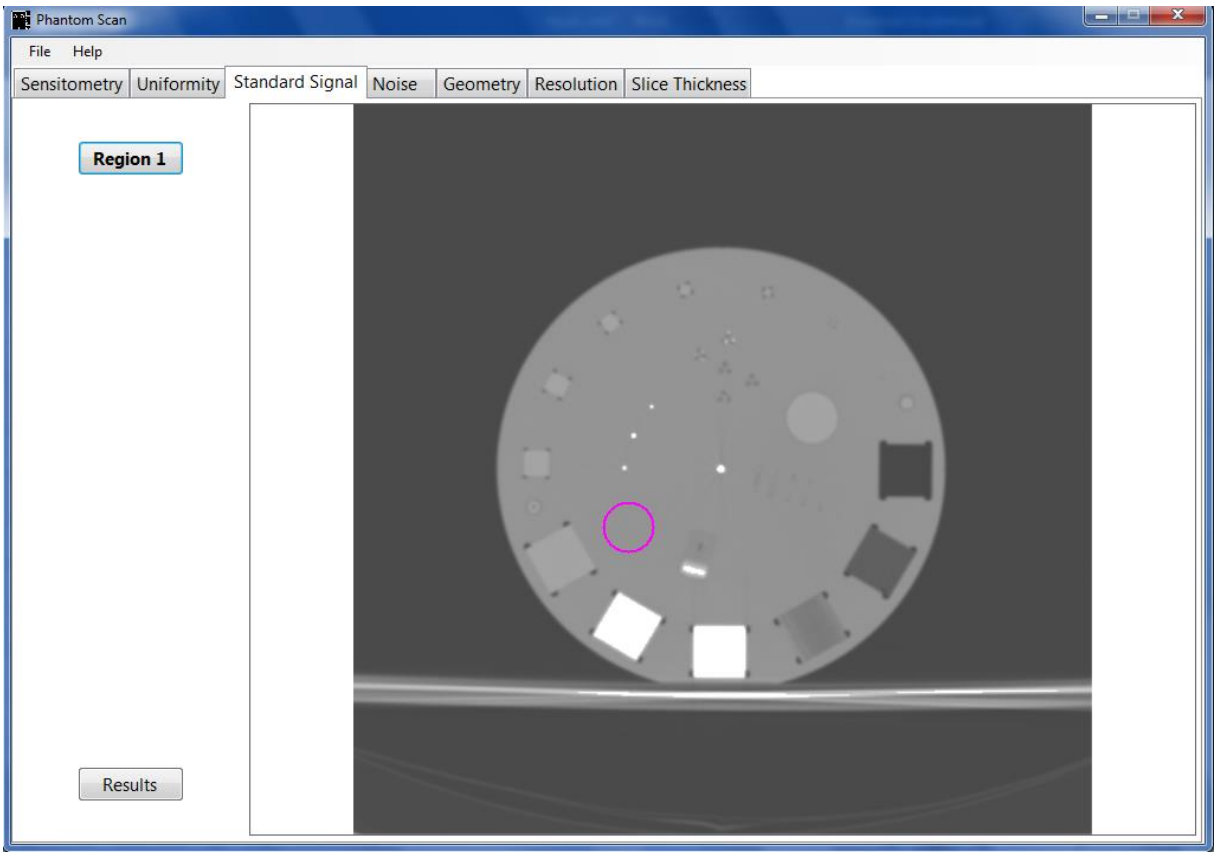

Figure A.56: Drawing a ROI for standard signal evaluation.

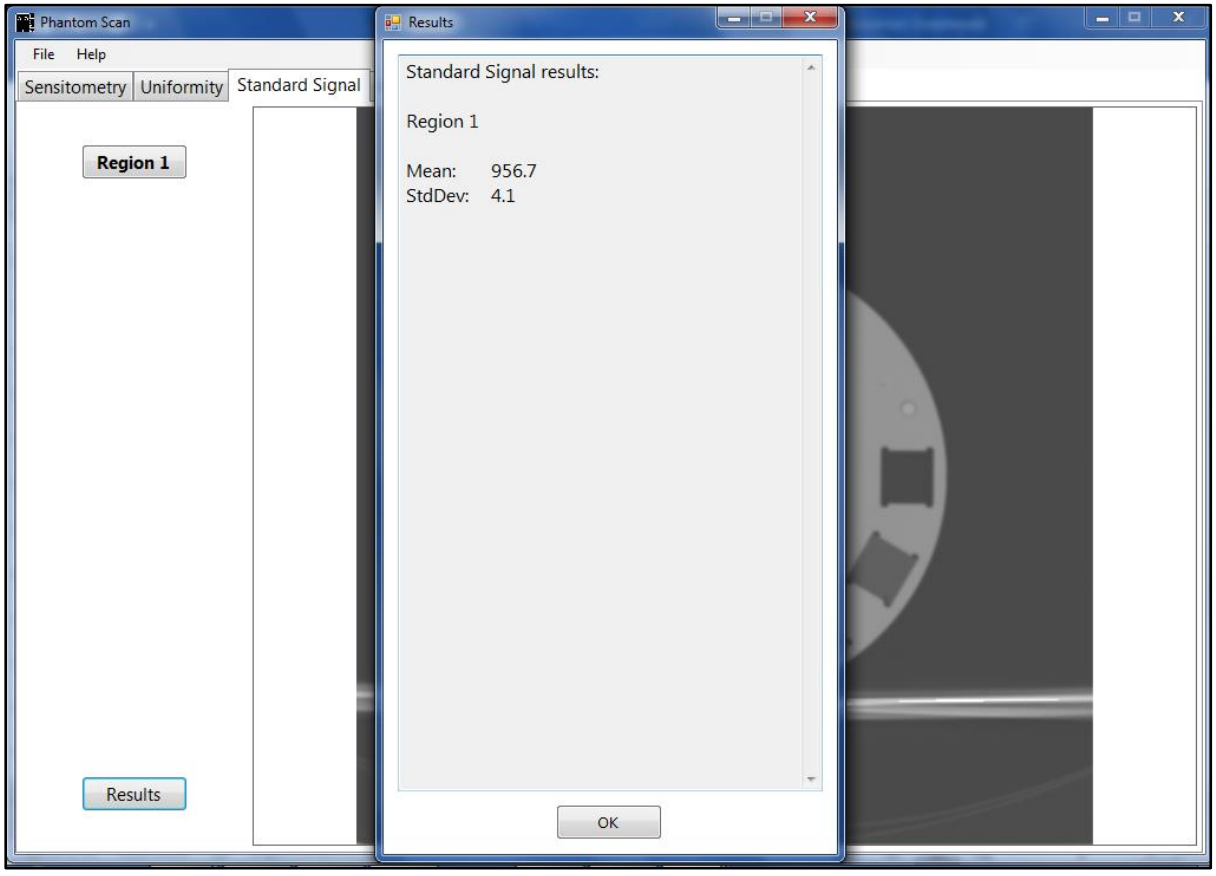

Figure A.57: Results for the standard signal test.

g. Slice thickness

- In the Slice Thickness tab in the application, click on the Select background button and draw a region of interest (ROI) next to the slice thickness ramp, labelled as number 20 in Figure A.1 b.). This is shown in Figure A.58.

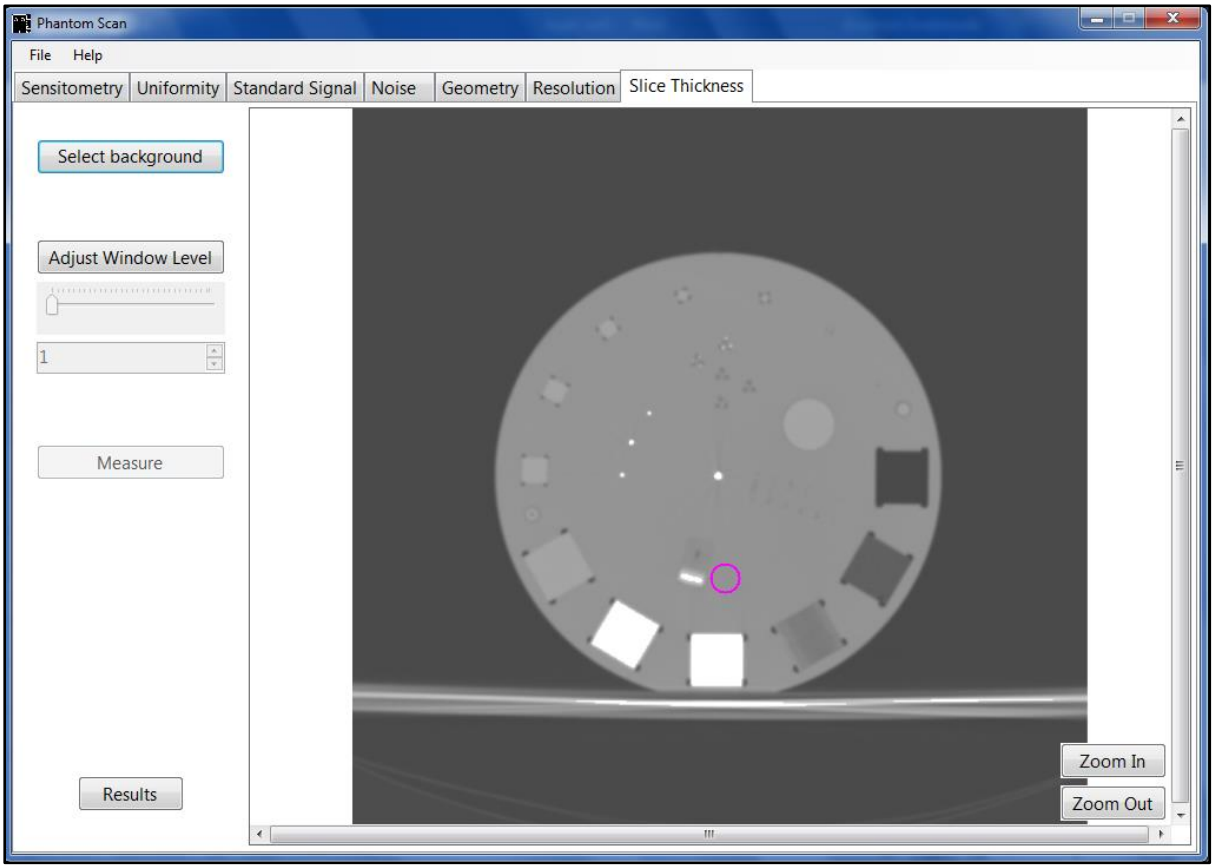

Figure A.58: Location of the background ROI.

- Click on the Adjust Window Level button. The image will become white as shown in Figure A.59.

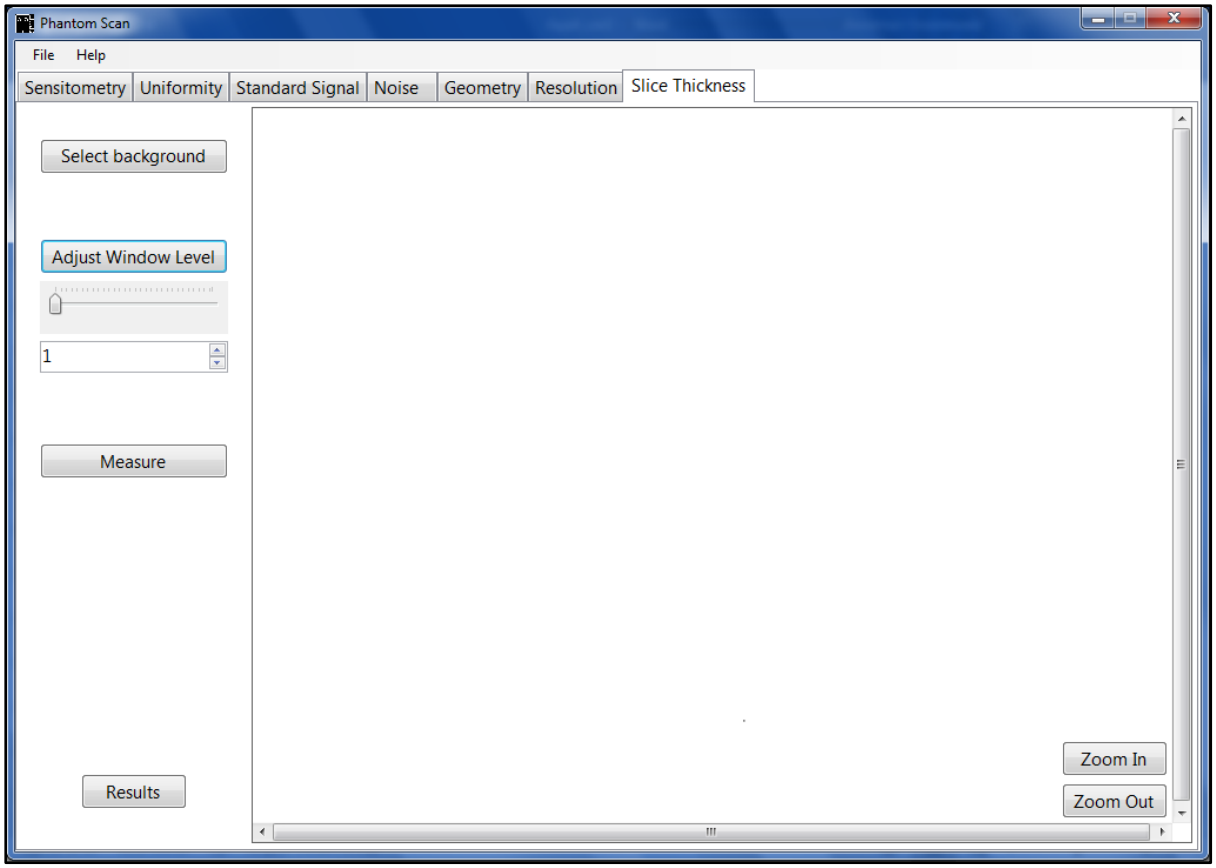

Figure A.59: White image after clicking on the Adjust Window Level button.

- Use the slider below the Adjust Window Level button and slide to the right until the slice thickness ramp, displayed as white, just disappears completely. This is illustrated in Figure A.60.

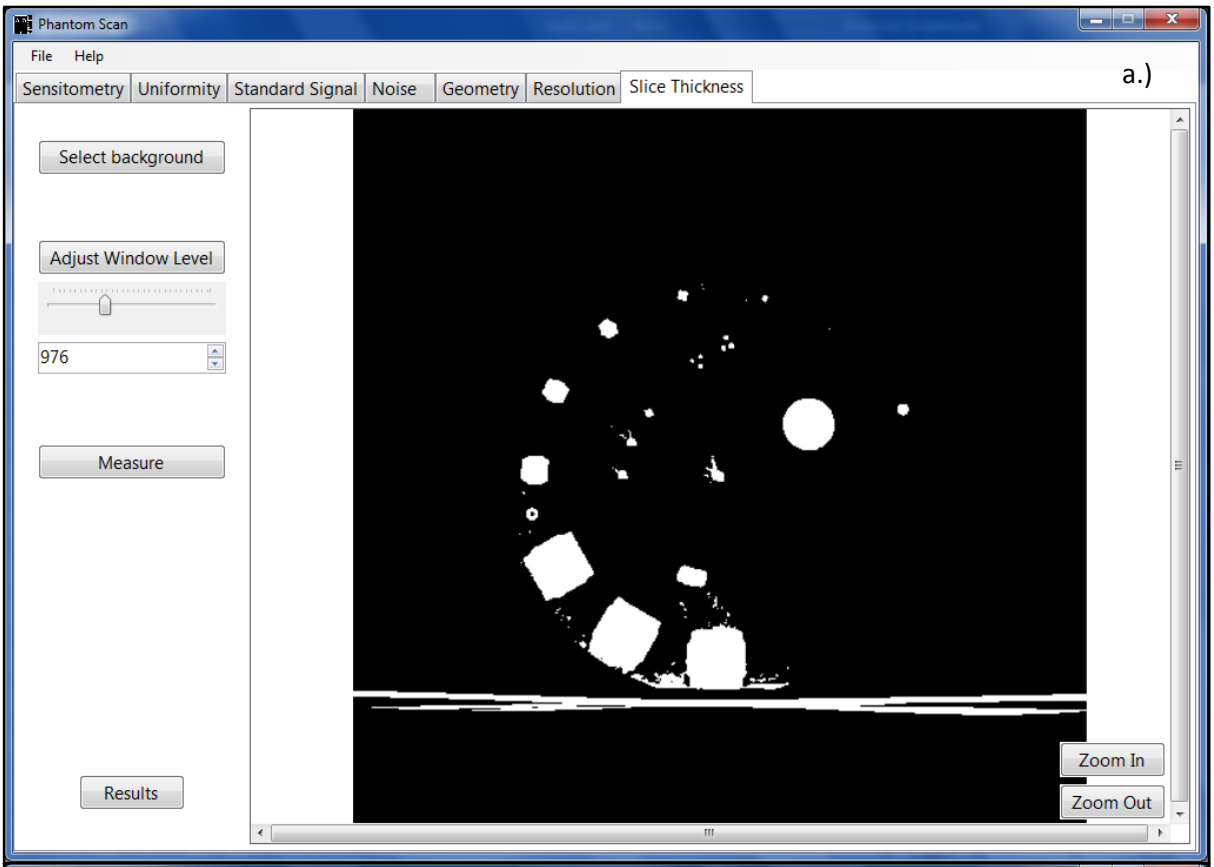

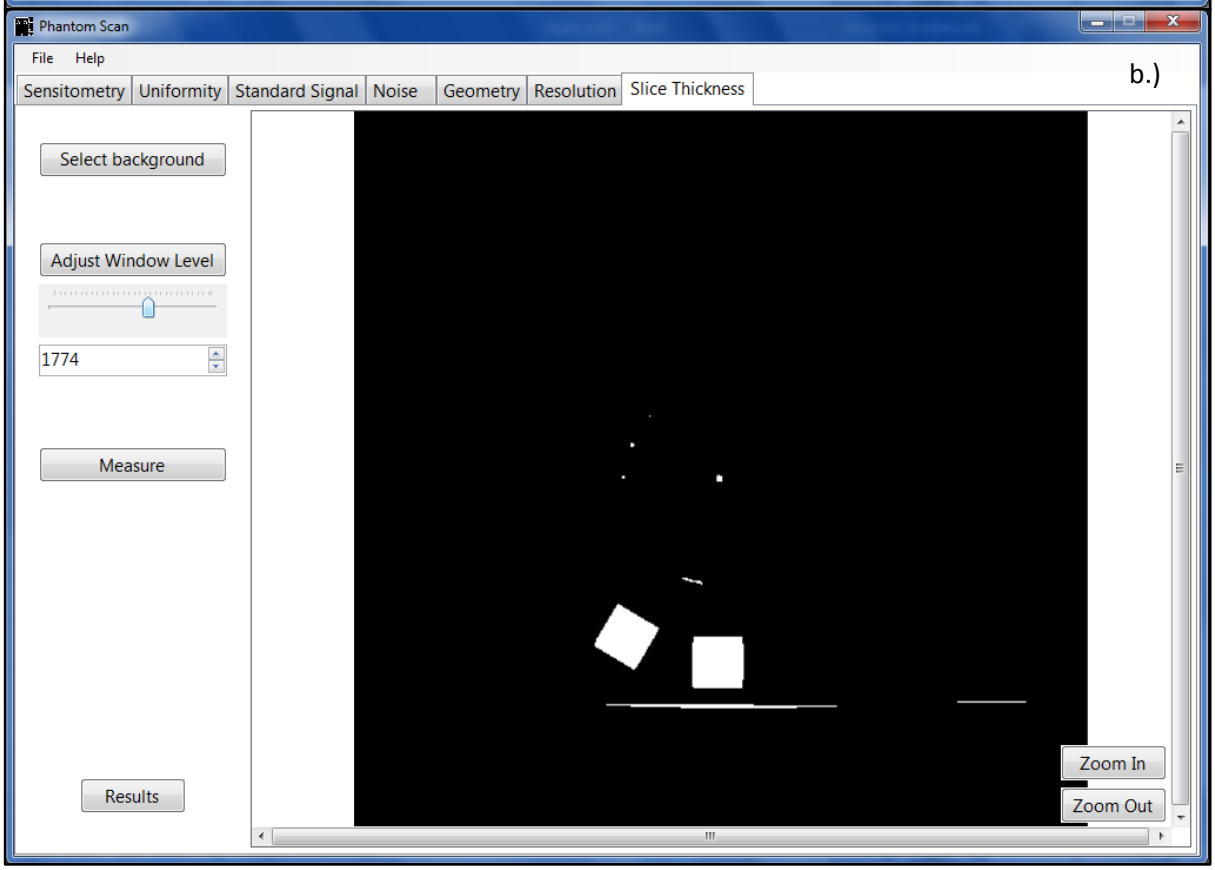

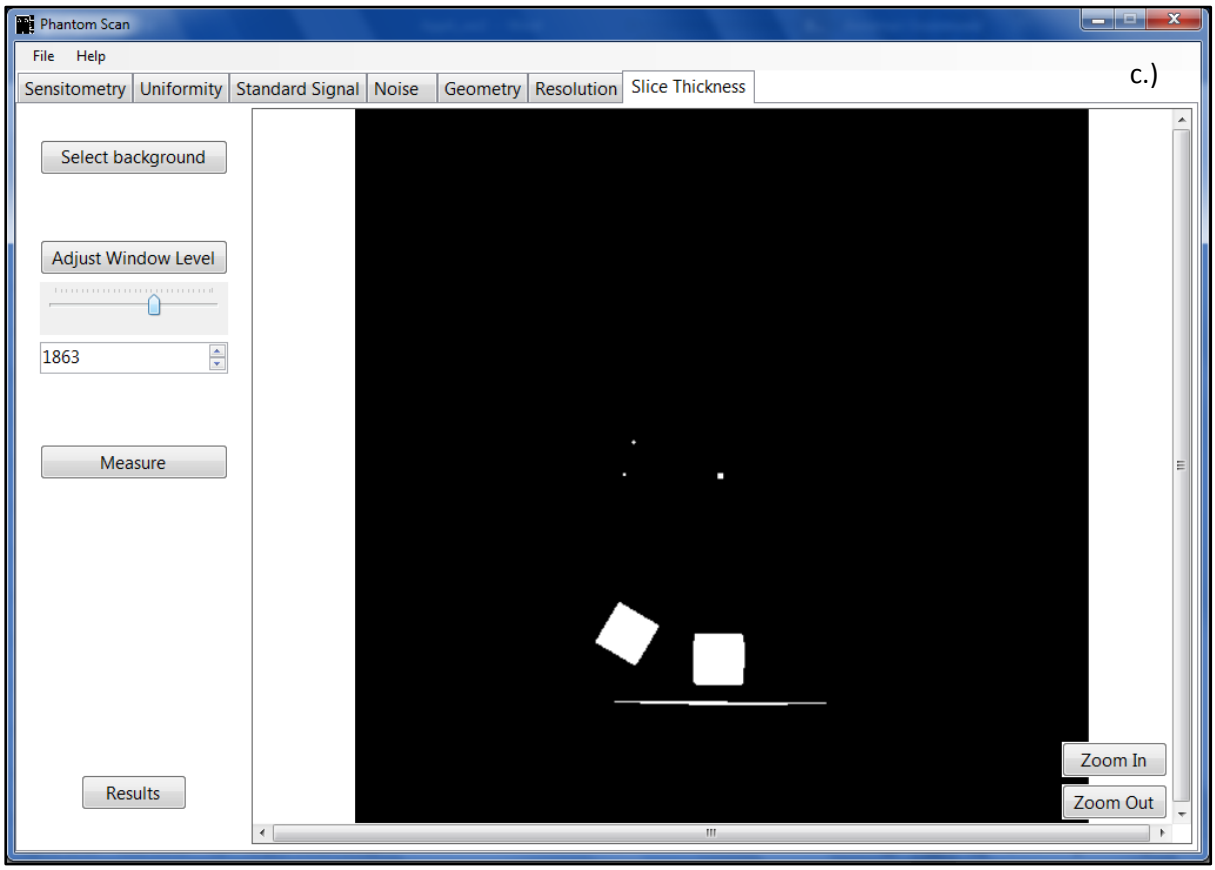

Figure A.60: Adjusting the window level using the slider. a.) Slice thickness ramp still large. b.) Slice thickness ramp becoming less visible. c.) Slice thickness ramp just disappeared.

- Click on the Measure button. The image will adjust to show the slice thickness ramp as shown in Figure A.61.
- Use the Zoom In and Zoom Out buttons and the vertical slider to zoom in on the ramp, as illustrated in Figure A.62.
- Draw a straight line across the displayed ramp as shown in Figure A.62.
- Click on the Results button. The measured slice thickness is displayed as shown in Figure A.63.
- Record the results in the QC result page (at the end of the manual).
- If the result fails, i.e. the limit in Table A.4 is exceeded, follow the steps in Figure A.2 for taking corrective action.

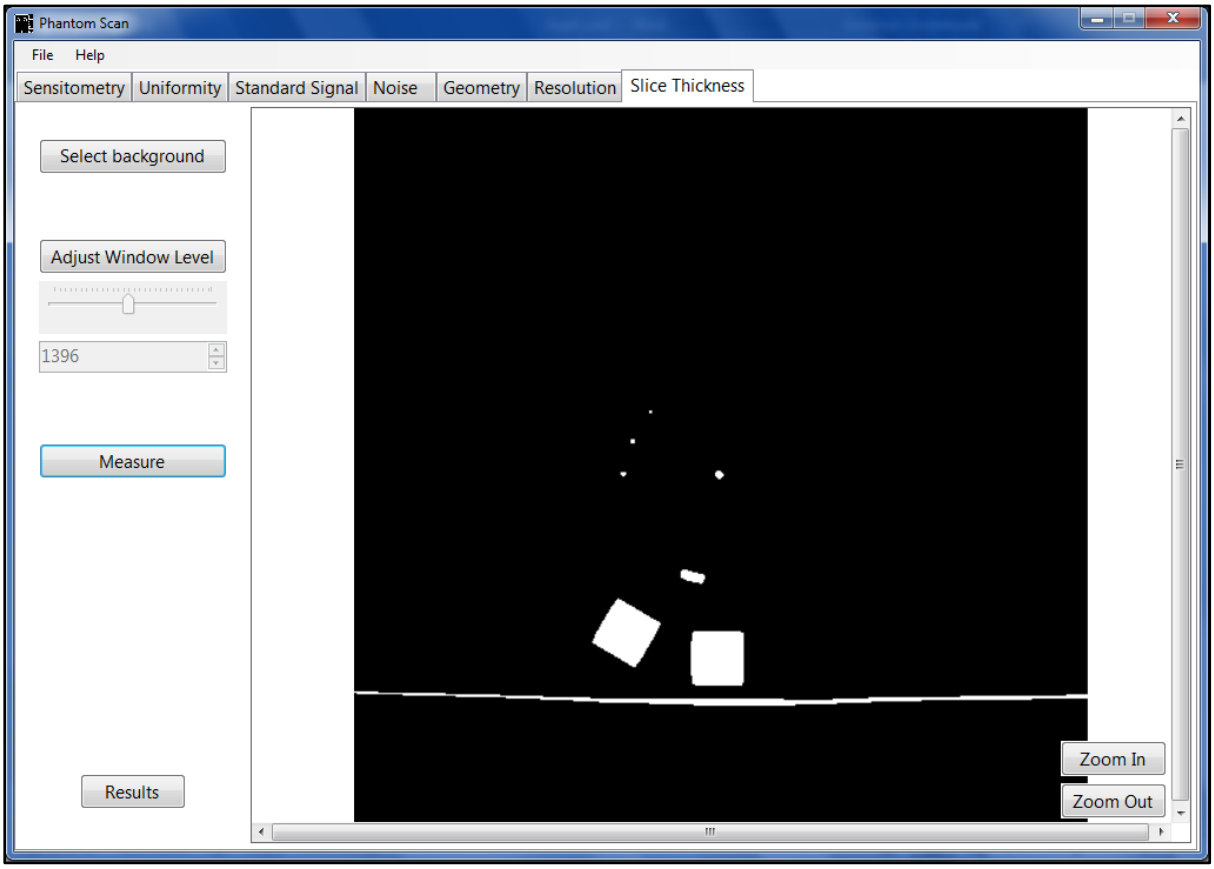

Figure A.61: Image corrected for slice thickness measurement.

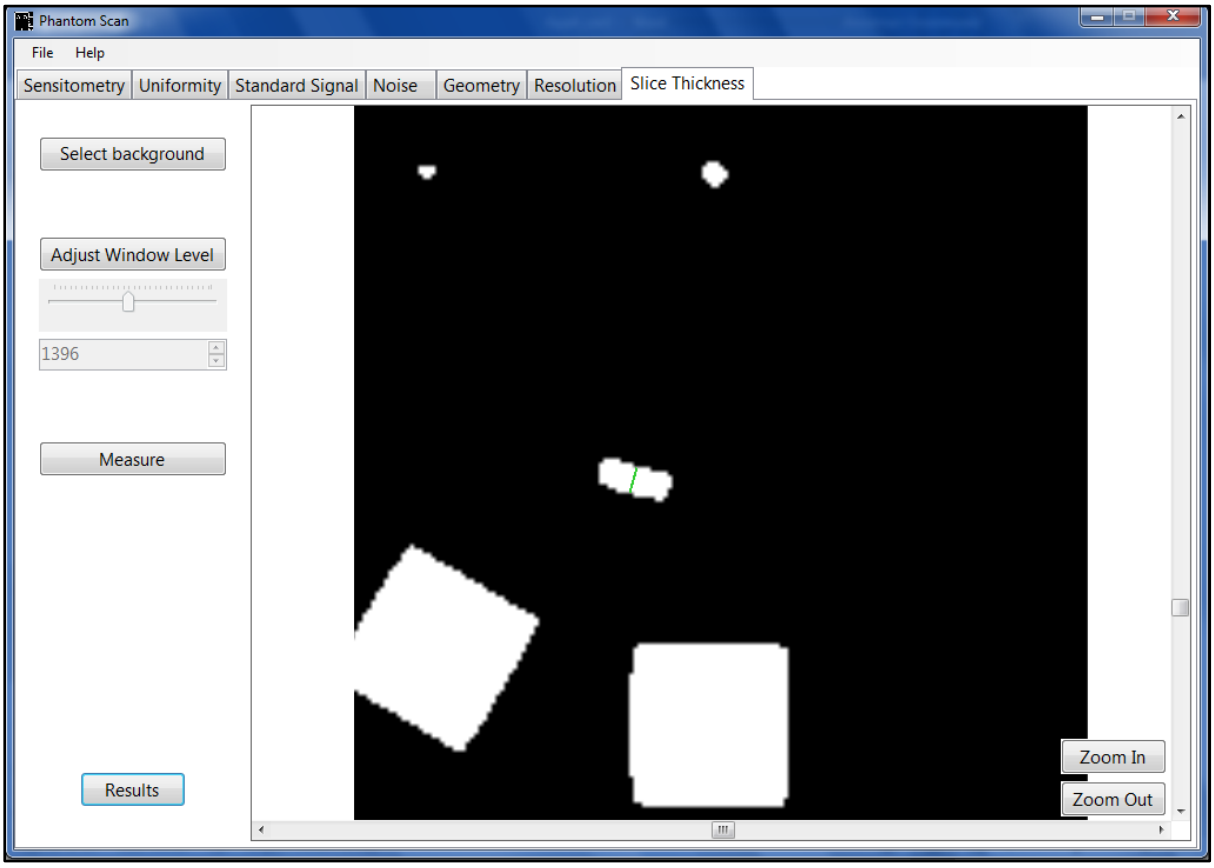

Figure A.62: Using the Zoom In function to visualise the slice thickness ramp and drawing the line (green) for measurement.

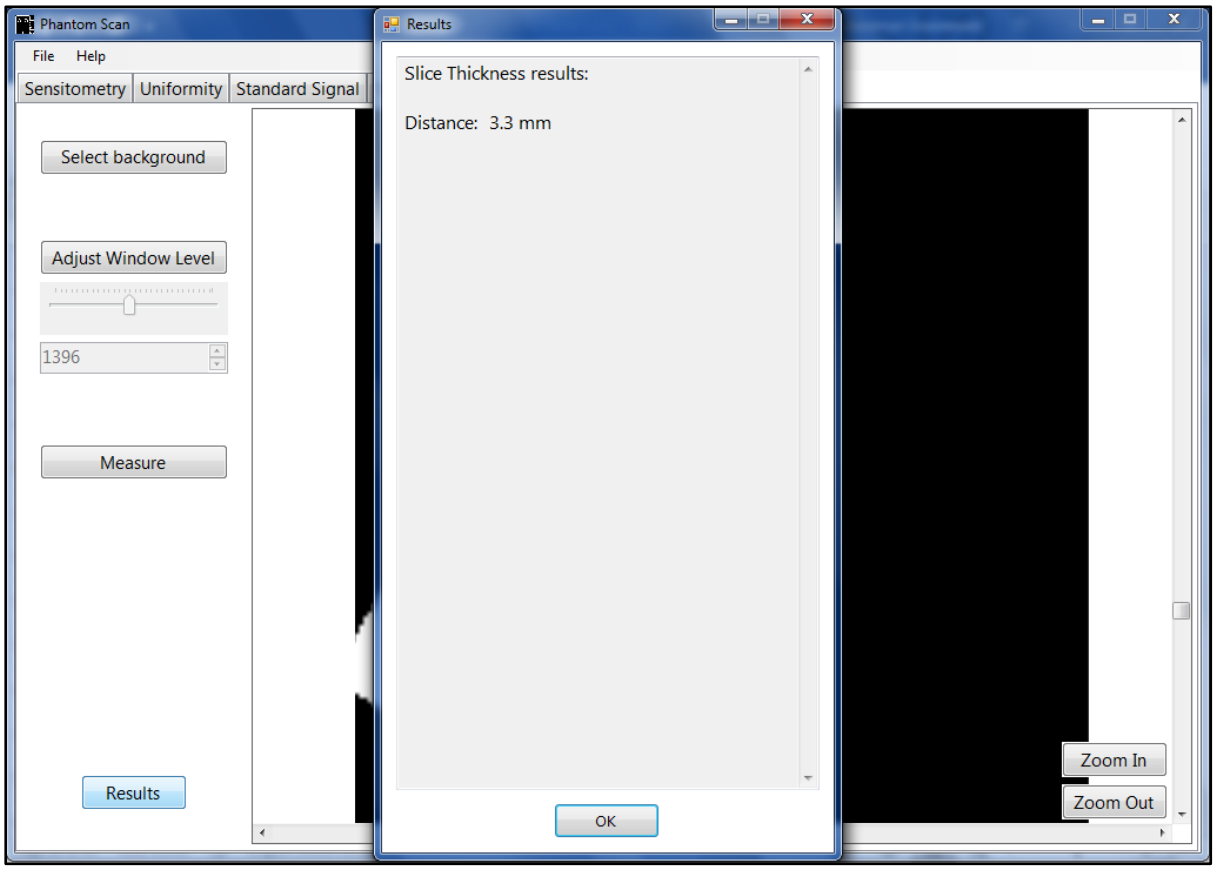

Figure A.63: Results for the slice thickness test.

A.2.5.6 Saving and printing the results

- Click on File and select Save Results as shown in Figure A.64 a.).
- Enter a file name and choose the location where you want to save the results, as indicated in Figure A.64 b.).
- To print the results in hard copy, go to the selected save location, select the file name to be printed and double left click to open the file in Notepad.
- In Notepad, click on File and select Print. This is shown in Figure A.24 a.).
- Select the printer you want to use and click on Print, as shown in Figure A.24 b.).
- Sign and file the hard copy results.

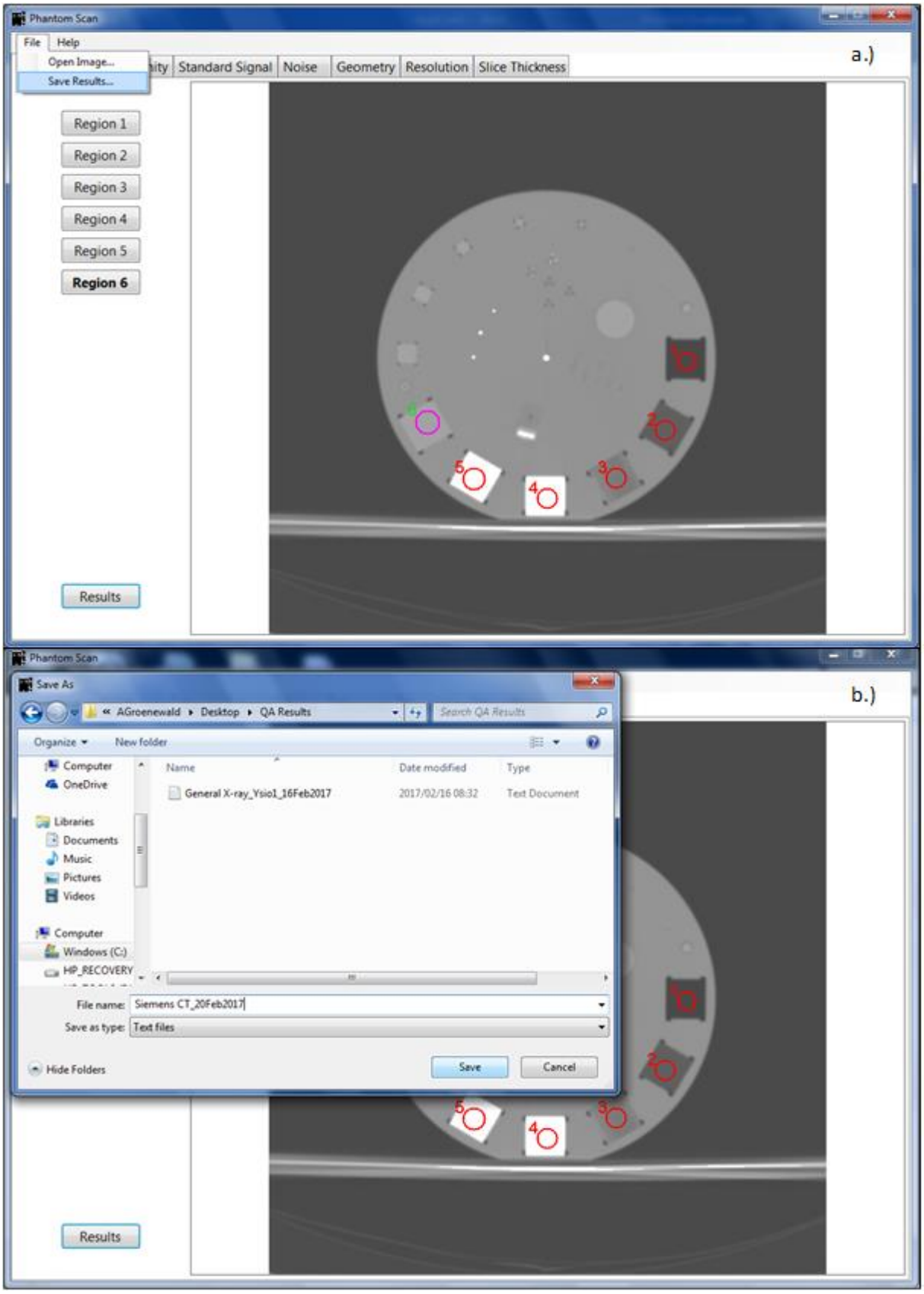

Figure A.64: Saving the obtained results. a.) Selecting the save option in the application. b.) Choosing the location to save to.

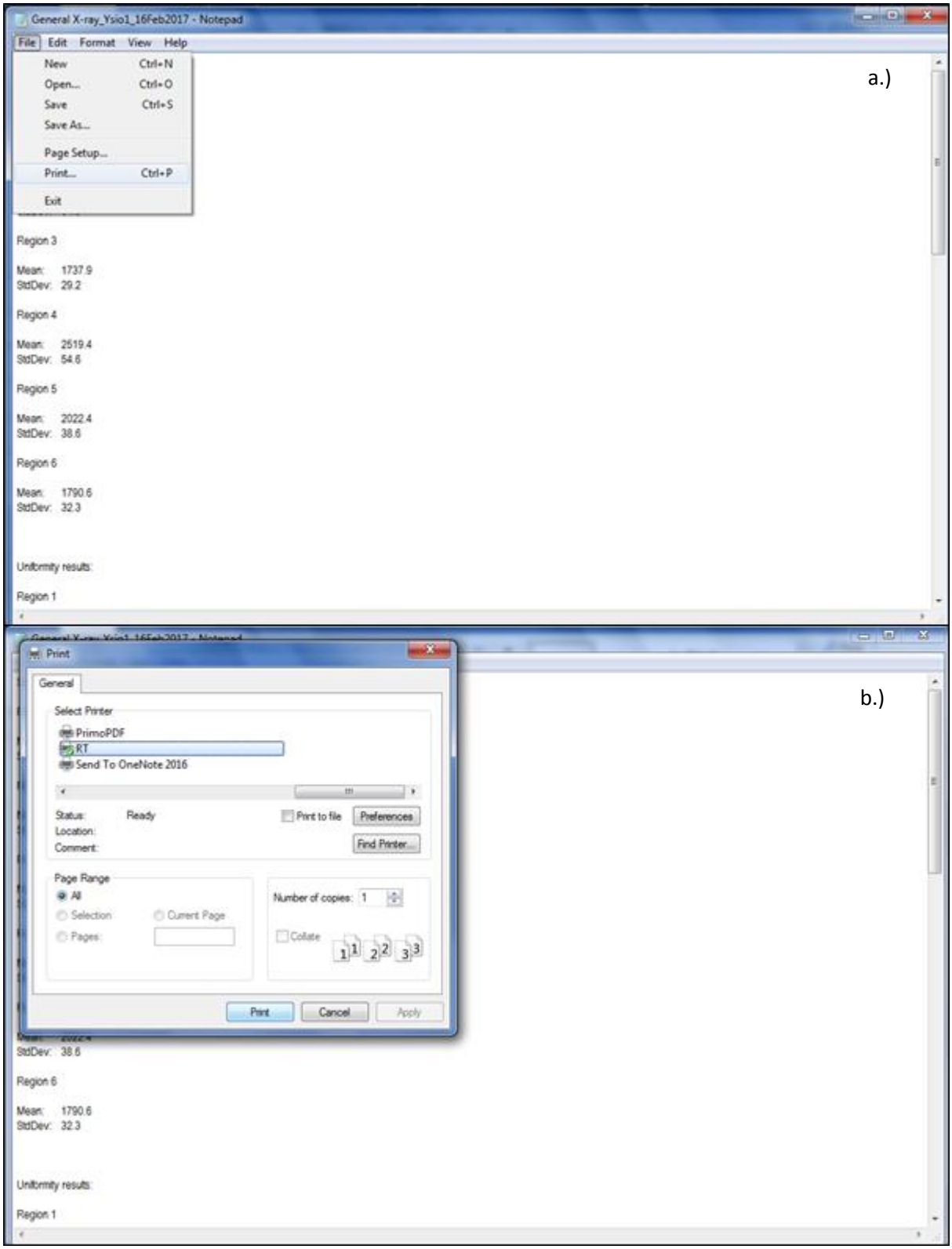

Figure A.24: Printing the results from Notepad. a.) Selecting the print option. b.) Selecting the printer.

A.3 Technical specifications

The technical data and specifications of the universal image quality assurance phantom are included in Table A.5.

Table A.5: Universal image quality assurance phantom technical specifications.

Description	Universal phantom specifications
Designer	Ms Annemari Groenewald.
Manufacturer	Gebrateq Advanced Engineering.
Patent	International Patent Application Number PCT/IB2016/051165.
Phantom housing material	High density polyethylene 170 mm diameter (167 mm at flat side), 20 mm thickness per half.
Attenuator blocks for sensitometry	20x20x10 mm^3 blocks of Gammex LN 300 Lung ®, Supawood, Gammex SB3 Bone ®, Teflon, 3D printed RDG240 and additional air filled void.
Attenuator blocks for low contrast assessment	20x20x10 mm^3, 10x10x10 mm^3, 8x8x8 mm^3, 6x6x6 mm^3, 4x4x4 mm^3, 3x3x3 mm^3, 2x2x2 mm^3, 1x1x1 mm^3 blocks of 3D printed RGD240.
Cylindrical insert	Polymethyl methacrylate 20 mm diameter, 10 mm thickness.
Fibre simulation inserts	Rubber bands of diameters 1.5, 1.3, 0.9, 0.6, 0.4 and 0.3 mm.
Micro-calcification simulation inserts	Metallic specs of diameters 0.5,0.4,0.3,0.2 and 0.1 mm.
Attenuator balls for point spread function and set up	Metallic balls of diameters 1.0, 0.7, and 0.5 mm.
Attenuator ramp	Gammex SB3 Bone ® of 20x10x3 mm^3 at an angle of 38^o.
Fixation screws	Nylon of 6 mm diameter and 40 mm length.
Attenuator plates	Two high density polyethylene plates of 170 mm diameter (167 mm at flat side) and 10 mm thickness and one high density polyethylene plates of 170 mm diameter (167 mm at flat side) and 20 mm thickness.
Set-up accessories	CT set-up plate/stand of high density polyethylene 600x50x10 mm with hinges.
Overall dimensions	170 x 167 mm semi-circle face with 40 mm thickness.
Weight	0.87 kg

The data analysis software is a Microsoft .NET application written in C# by Ernst Uys and is licensed to the developer as shown under About in the Help menu in the application. This is included in Figure A.65.

Figure A.65: Phantom Scan data analysis software licence.

A.4 Service manual

Caring for the universal image quality assurance phantom is explained in this section.

A.4.1 Cleaning

- The phantom housing can be cleaned by wiping it down with a water damp soft cloth.
- The phantom may not be immersed in water or another liquid.
- A mild soapy solution or common disinfectant can be used.
- No alcohol, corrosives or solvents may be used on the phantom.

A.4.2 Preventative maintenance

- Check the phantom housing for signs of mechanical damage prior to each use.
- If damages are noted, contact the manufacturer for repairs.
- Under normal conditions of use, the universal image quality assurance phantom is robust and therefore requires no preventative maintenance.
- Results from the data analysis program must be saved, backed up, printed and/or stored. This is the responsibility of the user.

A.4.3 Disposal

- The universal image quality assurance phantom contains no biohazardous substances.
- The materials of the universal image quality phantom are non-biodegradable.
- Most materials are plastic and can be re-cycled.

A.5 Quality Control Records

Example quality control (QC) record sheets are included. It is recommended that users copy these sheets, creating a record file for each of the different x-ray units in the department. The operator should also include as much detail about the exposure and obtained results as possible, with detailed comments. This assists in future evaluation and comparison of results, for a specific unit and for comparison between different units. It also aids technicians and medical physicists in fault finding when results are out of tolerance.

General x-ray quality control

Unit and exposure details

Unit name					
Unit licence number					
Date					
QC reason	Routine QC		Acceptance testing		After service QC
Technique factors used	AEC exposure		Manual exposure		
	kV		kV		
	mAs		mAs		
	SSD		SSD		
Casette / film used					
Reader / processor used					
Opperator name					

Quality control tests and results

Sensitometry & grey scale linearity (optical density consistency)	Air		Lung		Supawood	
	Mean	Std dev	Mean	Std dev	Mean	Std dev
	Bone		Tefon		RGD240	
	Mean	Std dev	Mean	Std dev	Mean	Std dev
Low contrast detectability	Smallest insert seen					
	20x20x10 mm^3		10x10x10 mm^3		8x8x8 mm^3	6x6x6 mm^3
	4x4x4 mm^3		3x3x3 mm^3		2x2x2 mm^3	1x1x1 mm^3
Uniformity	Largest difference in mean value					
Resolution	Limiting spatial resolution					
Image noise	Signal-to-npoise ratio (SNR)					
	Contrast-to-noise ratio (CNR)					

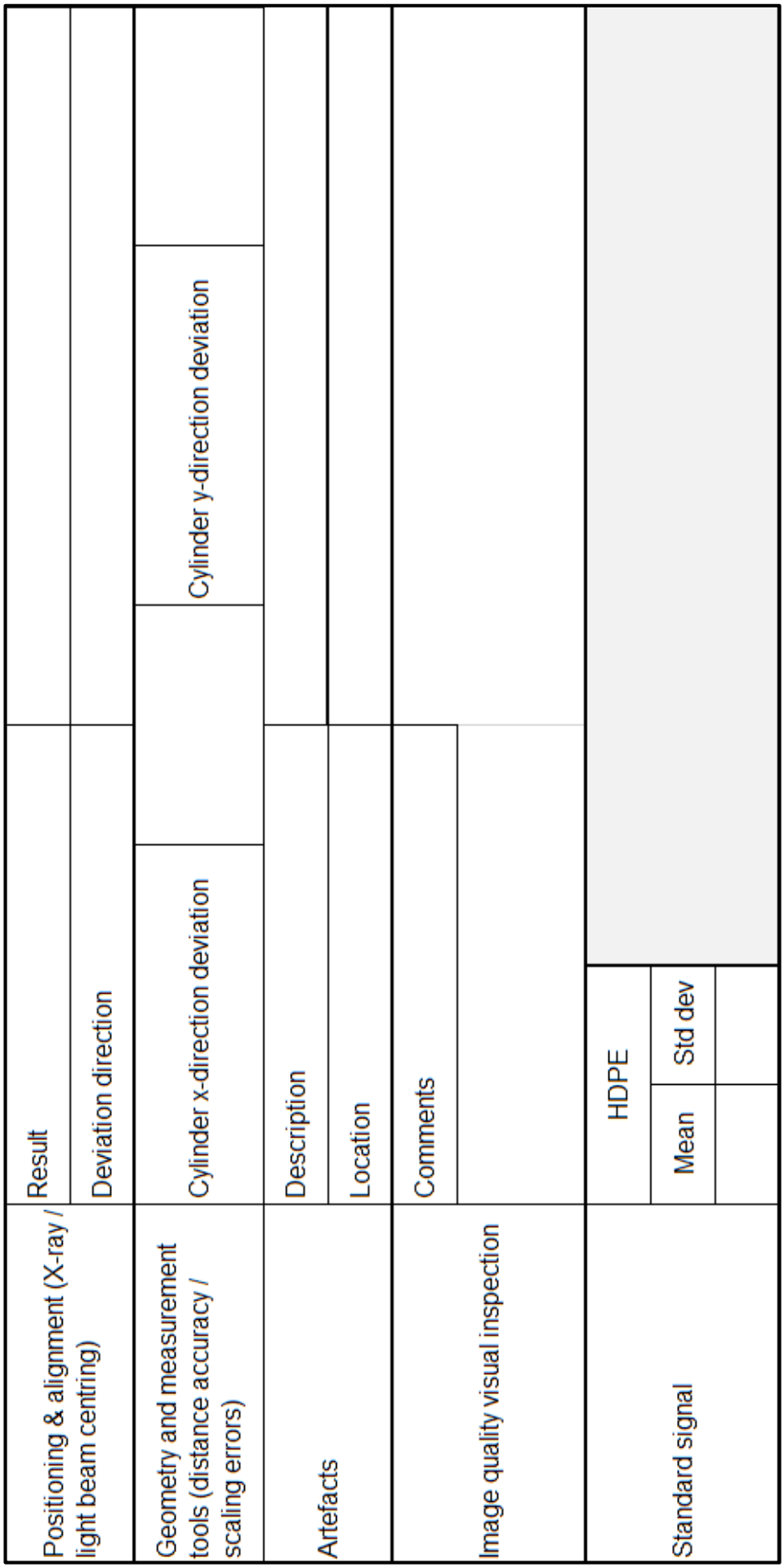

AEC image quality	0 cm additional attenuator comments	
	2 cm additional attenuator comments	
	4 cm additional attenuator comments	
AEC repeatability	Exposure 1 comments	
	Exposure 2 comments	
	Exposure 3 comments	
Additional comments		
Opperator signature		

Fluoroscopy quality control

Unit and exposure details			
Unit name			
Unit licence number			
Date			
QC reason	Routine QC	Acceptance testing	After service QC
Technique factors used	AEC exposure		
	kV		
	mAs		
	SSD		
Casette / film used			
Reader / processor used			
Opperator name			

Quality control tests and results

Sensitometry & grey scale linearity (optical density consistency)	Air		Lung		Supawood	
	Mean	Std dev	Mean	Std dev	Mean	Std dev
	Bone		Tefon		RGD240	
	Mean	Std dev	Mean	Std dev	Mean	Std dev
Low contrast detectability	Smallest insert seen					
	20x20x10 mm^3		10x10x10 mm^3		8x8x8 mm^3	6x6x6 mm^3
	4x4x4 mm^3		3x3x3 mm^3		2x2x2 mm^3	1x1x1 mm^3
Uniformity	Largest difference in mean value					
Resolution	Limiting spatial resolution					
Image noise	Signal-to-npoise ratio (SNR)					
	Contrast-to-noise ratio (CNR)					

Positioning & alignment (X-ray / light beam centring)	Result						
	Deviation direction						
Geometry and measurement tools (distance accuracy / scaling errors)	Cylinder x-direction deviation		Cylinder y-direction deviation				
Artefacts	Description						
	Location						
Image quality visual inspection	Comments						
Standard signal	HDPE	Mean		Std dev			

AEC image quality	0 cm additional attenuator comments	
	2 cm additional attenuator comments	
	4 cm additional attenuator comments	
AEC repeatability	Exposure 1 comments	
	Exposure 2 comments	
	Exposure 3 comments	
Additional comments		
Opperator signature		

Mammography quality control

Unit and exposure details

Unit name					
Unit licence number					
Date					
QC reason	Routine QC		Acceptance testing		After service QC
Technique factors used	AEC exposure		Manual exposure		
	kV		kV		
	mAs		mAs		
	SSD		SSD		
Casette / film used					
Reader / processor used					
Opperator name					

Quality control tests and results

Sensitometry & grey scale linearity (optical density consistency)	Air		Lung		Supawood	
	Mean	Std dev	Mean	Std dev	Mean	Std dev
	Bone		Tefon		RGD240	
	Mean	Std dev	Mean	Std dev	Mean	Std dev
Low contrast detectability	Smallest insert seen					
	20x20x10 mm^3		10x10x10 mm^3		8x8x8 mm^3	6x6x6 mm^3
	4x4x4 mm^3		3x3x3 mm^3		2x2x2 mm^3	1x1x1 mm^3
Uniformity	Largest difference in mean value					
Resolution	Limiting spatial resolution					
Image noise	Signal-to-npoise ratio (SNR)					
	Contrast-to-noise ratio (CNR)					

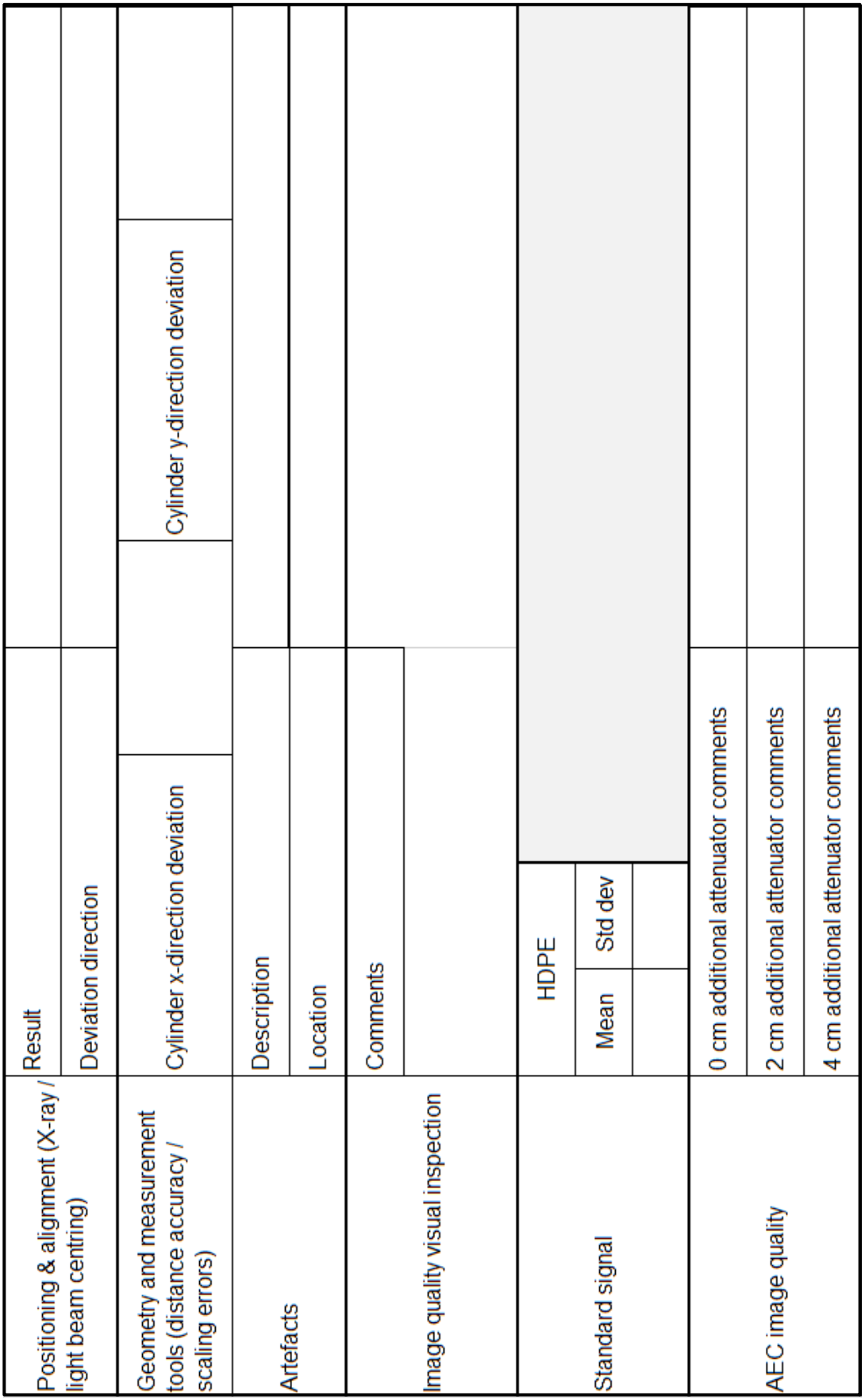

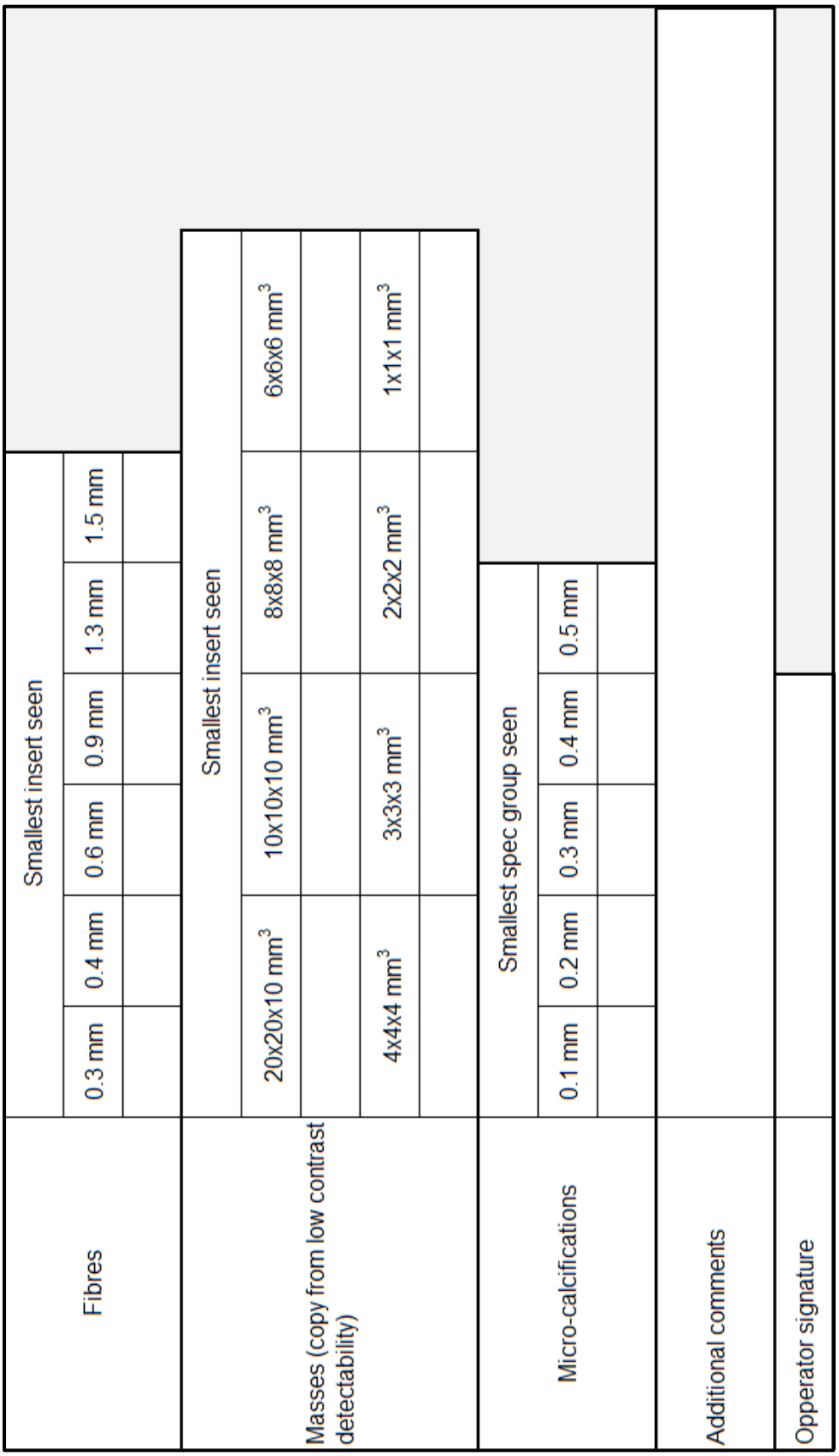

Computed tomography quality control

Unit and exposure details

Unit name					
Unit licence number					
Date					
QC reason	Routine QC		Acceptance testing		After service QC
Technique factors used	kV		Pitch		
	mAs		Slice width		
	SSD		FOV		
Opperator name					

Quality control tests and results

Sensitometry & grey scale linearity (optical density consistency)	Air		Lung		Supawood	
	Mean	Std dev	Mean	Std dev	Mean	Std dev
	Bone		Tefon		RGD240	
	Mean	Std dev	Mean	Std dev	Mean	Std dev
Low contrast detectability	Smallest insert seen					
	20x20x10 mm^3		10x10x10 mm^3		8x8x8 mm^3	6x6x6 mm^3
	4x4x4 mm^3		3x3x3 mm^3		2x2x2 mm^3	1x1x1 mm^3
Uniformity	Largest difference in mean value					
Resolution	Limiting spatial resolution					
Image noise	Signal-to-npoise ratio (SNR)					
	Contrast-to-noise ratio (CNR)					

Positioning & alignment (zero slice position / scan plane localisation)	Result								
	Deviation direction								
Geometry and measurement tools (distance accuracy / scaling errors)	Cylinder x-direction deviation		Cylinder y-direction deviation						
Artefacts	Description								
	Location								
Image quality visual inspection	Comments								
Standard signal	HDPE	Mean		Std dev					
Slice width	Result								
Additional comments									
Opperator signature									

Appendix B

Data analysis software

The data analysis software was developed by Ernst Uys, protected under copy right as in Figure B.1.

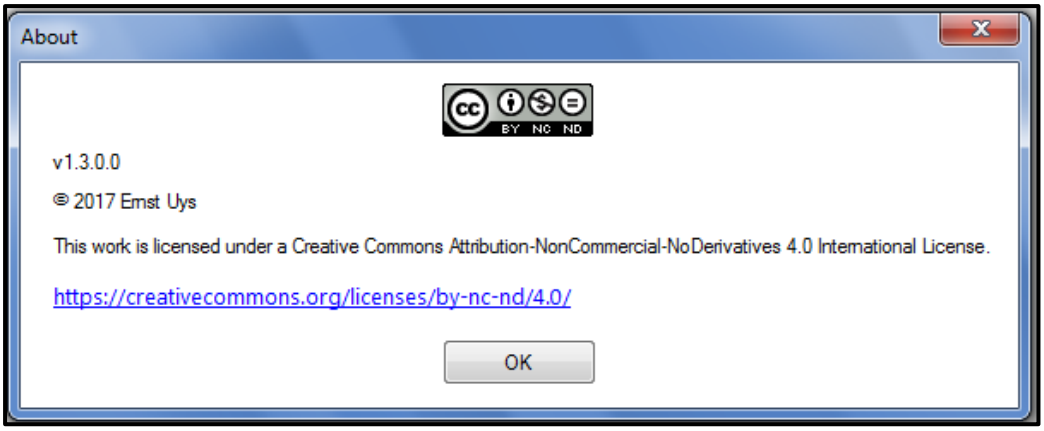

Figure B.1: Data analysis software copy right notice.

The application runs on Microsoft Windows (version 7 and higher) and is written in C# 7.0 (https://docs.microsoft.com/en-us/dotnet/articles/csharp), using .NET Framework 4.6.1 (https://www.microsoft.com/net). DICOM image parsing is done using the Fellow Oak DICOM library (https://github.com/fo-dicom/fo-dicom), which is licensed under the open source Microsoft Public License (https://opensource.org/licenses/MS-PL). The Math.NET Numerics library (https://numerics.mathdotnet.com/) is used for numerical computations and is licensed under the open source MIT/X11 license (https://numerics.mathdotnet.com/License.html).

Each high-level function, i.e. sensitometry, uniformity, standard signal, noise, geometry, resolution and slice thickness, is implemented in a separate module, as is DICOM image parsing and pre-processing. DICOM image pre-processing involves catering for the most common DICOM image modalities, including general x-rays, fluoroscopy, mammography and CT scanning, and rendering the DICOM image for

display, since the dynamic range of most DICOM images exceeds that of typical consumer-level monitors.

For sensitometry, uniformity and standard signal, ROIs are drawn specific inserts or locations in the phantom, as described in the user's manual in Appendix A. The software determines the mean and standard deviation in each of these ROIs. The results are displayed to one decimal place.

For noise analysis, ROIs are again used and SNR and CNR are calculated with Equations B.1 and B.2.

$$SNR = \frac{mean}{standard\ deviation} \qquad \text{[Equation B.1]}$$

$$CNR = \frac{mean(object) - mean(background)}{standard\ deviation(background)} \qquad \text{[Equation B.2]}$$

The mean and standard deviation values are displayed for the ROIs, together with the SNR and CNR, to one decimal place.

For the geometry module lines are drawn in the cylindrical insert and the length of the line is measured with the software and reported to one decimal place in mm.

Resolution is reported as a MTF plot showing the limiting spatial resolution as the cycles/cm value at 10 % MTF, to two decimal places. The software calculates the MTF from a PSF of a metallic bead, smaller than a pixel in size. By selecting a region around the specified bead, as described in Appendix A, the software creates a matrix of the obtained PSF. Background is measured in a ROI and this is subtracted from each matrix element to form a new matrix. The sum of the columns of this matrix is the LSF, which is plotted by giving each value a relative position. The Fourier transform of each LSF value is calculated in imaginary format. This is converted to real numbers by taking the absolute value. The absolute values are normalised by dividing by the maximum value to give the MTF values. The cycles/cm are calculated

as half of the size of the matrix used for imaging divided by the field of view. The MTF values are plotted against the cycles/cm values for the resultant graph.

For CT slice thickness the FWHM is determined. A background ROI is drawn next to the slice thickness ramp and the software measures the mean CT number in this ROI. The WW is then automatically adjusted to the minimum achievable by the software. The WL is then adjusted by the user to where the ramp just completely disappears from the image. This is the peak CT number. When the user now clicks the measure button, the software then calculates the net CT number as the peak CT number minus the background CT number. It then calculates 50 % of this net CT number and adds the background CT number to this result to obtain the FWHM value. It automatically adjusts the image to the FWHM value and the user can draw a line across the seen ramp. The software measures the length of this ramp and displays the result to one decimal place in mm. Here the software also provides a zoom in and zoom out functionality, so that the user can draw the line more accurately on a zoomed in image.

The image as displayed in the software is also visually inspected for low contrast detectability, artefacts, positioning and alignment, image quality visual inspection and masses, fibres and micro-calcifications in mammography.

Appendix C

Density calculations

C.1 Calculation of density of gasket rubber o-rings used for mammography fibre simulation

O-rings, used in watch manufacturing, were used to simulate mammography fibres in the phantom. Five o-ring were weighed on a Sartorius scale and were cut and the lengths and diameters measured with a Vernier calliper. The results are shown in Table C.1. The volume, V, of a cylinder is calculated with Equation C.1. Here π is the mathematical constant pie, r is the radius and h the height of the cylinder. Equation C.2, where ρ is the desnity, M is the mass and V is the volume, was used to calculate the density.

$$V = \pi r^2 h \qquad \text{[Equation C.1]}$$

$$\rho = \frac{M}{V} \qquad \text{[Equation C.2]}$$

Table C.1: Rubber o-ring density calculation values.

Description	Value
Average mass (g)	0.0796
Average diameter (cm)	0.0900
Average length (cm)	9.9500
Volume (cm^3)	0.0633
Density (gcm^{-3})	1.2575

C.2 Calculation of density of supawood used for sensitometry insert

The dimensions of the supawood block were measured with a Vernier calliper and its mass was weighed on a Sartorius scale. The obtained values are included in Table C.2. Equation C.2 as above was used to calculate the density, with the volume, V, calculated with Equation C.3, where l is the length, w the width and h the height of the block.

$$V = l \times w \times h$$

[Equation C.3]

Table C.2: Supawood density calculation values.

Description	Value
Mass (g)	5.982
Length (cm)	2.005
Width (cm)	2.009
Height (cm)	2.007
Volume (cm^3)	8.084
Density (gcm^{-3})	0.740

C.3 Calculation of density of Objet RGD240 3-D printing material used for low contrast detectability inserts

A Vernier calliper was used to measure the dimensions of one of the 3-D printed blocks. It was weighed on a Sartorius scale. Equations C.2 and C.3 as above were used and the density of the material was calculated with the values tabulated in Table C.3.

Table C.3: RGD240 density calculation values.

Description	Value
Mass (g)	4.761
Length (cm)	2.008
Width (cm)	2.010
Height (cm)	1.005
Volume (cm^3)	4.056
Density (gcm^{-3})	1.174

Appendix D

Publication and presentation

D.1 Publication

JOURNAL OF APPLIED CLINICAL MEDICAL PHYSICS, VOLUME 17, NUMBER 6, 2016

Development of a universal medical X-ray imaging phantom prototype

Annemari Groenewald[1a] and Willem A. Groenewald[2]

Equra Health,[1] Vergelegen Oncology Unit, 1 Arun Place, Sir Lowry's Pass Road, Somerset West, South Africa; Department of Medical Imaging and Clinical Oncology,[2] Stellenbosch University and Tygerberg Academic Hospital, Cape Town, South Africa annemari_korf@yahoo.com

Received 3 March, 2016; accepted 6 July, 2016

Diagnostic X-ray imaging depends on the maintenance of image quality that allows for proper diagnosis of medical conditions. Maintenance of image quality requires quality assurance programs on the various X-ray modalities, which consist of projection radiography (including mobile X-ray units), fluoroscopy, mammography, and computed tomography (CT) scanning. Currently a variety of modality-specific phantoms are used to perform quality assurance (QA) tests. These phantoms are not only expensive, but suitably trained personnel are needed to successfully use them and interpret the results. The question arose as to whether a single universal phantom could be designed and applied to all of the X-ray imaging modalities. A universal phantom would reduce initial procurement cost, possibly reduce the time spent on QA procedures and simplify training of staff on the single device. The aim of the study was to design and manufacture a prototype of a universal phantom, suitable for image quality assurance in general X-rays, fluoroscopy, mammography, and CT scanning. The universal phantom should be easy to use and would enable automatic data analysis, pass/fail reporting, and corrective action recommendation. In addition, a universal phantom would especially be of value in low-income countries where finances and human resources are limited. The design process included a thorough investigation of commercially available phantoms. Image quality parameters necessary for image quality assurance in the different X-ray imaging modalities were determined. Based on information obtained from the above-mentioned investigations, a prototype of a universal phantom was developed, keeping ease of use and reduced cost in mind. A variety of possible phantom housing and insert materials were investigated, considering physical properties, machinability, and cost. A three-dimensional computer model of the first phantom prototype was used to manufacture the prototype housing and inserts. Some of the inserts were 3D-printed, others were machined from different materials. The different components were assembled to form the first prototype of the universal X-ray

imaging phantom. The resulting prototype of the universal phantom conformed to the aims of a single phantom for multiple imaging modalities, which would be easy to use and manufacture at a reduced cost. A PCT International Patent Application No. PCT/IB2016/051165 has been filed for this technology.

PACS number(s): 87.57.C, 87.59.-e

Key words: image quality assurance, phantom, diagnostic radiology, X-ray imaging, prototype

[a] Corresponding author: Annemari Groenewald, Vergelegen Oncology Unit, 1 Arun Place, Sir Lowry's Pass Road, Somerset West, South Africa 7130; phone: (0027) 21 851 2255; fax: (0027) 21 852 3089; email: annemari_korf@yahoo.com

I. INTRODUCTION

Different imaging modalities are used in diagnostic radiology to diagnose and follow up a variety of disease conditions. In order to ensure that the images are of acceptable quality for accurate clinical diagnosis, image quality has to be evaluated and maintained. Image quality is a subjective concept that requires certain measures in order to be quantified; by using a phantom, for example. Currently modality-specific phantoms are used for image quality assurance in each of these imaging modalities. The commercially available phantoms for mammography include the American College of Radiology (ACR) mammography phantom that contains fibres (1.56, 1.12, 0.89, 0.75, 0.54, and 0.40 mm in diameter) and simulates tumorous masses with 2.00, 1.00, 0.75, 0.50, and 0.25 mm diameter hemispheres, as well as micro-calcifications with 0.54, 0.40, 0.32, 0.24, and 0.16 mm speck groups.[(1)] The ACR mammography phantom is 4.2 cm thick and consists of 3.5 cm Lucite and a 0.7 cm thick paraffin insert, which contains the image quality indicators.[(2)] The NORMI PAS phantom (PTW-Freiburg GmbH, Freiburg, Germany) is used for image quality assurance on digital mammography units. The base plate of the phantom is semicircular to simulate breast shape. Two rows of balls are used at chest-wall side to investigate image alignment. An aluminium step-wedge can be placed in a cutout in the base plate. The stepwedge consists of 14 steps 0–5.2 mm in thickness for sensitometry evaluation. Alternatively, a polymethyl methacrylate (PMMA) step-wedge with 14 steps of 0–39 mm thickness can be inserted in the cutout. Different test elements can be fitted into the cutout in the structure layer. The PMMA test element is used to assess optical density in a region of interest (ROI). The signal-difference-to-noise ratio (SDNR) is calculated from the SDNR test element, which is used to measure average pixel values for the calculation. The ACR test element contains fibres, microcalcifications, and tumorous masses for visual image quality evaluation. Fibres have diameters of 1.5, 1.1, 0.9, 0.7, 0.55, and 0.4 mm. Masses have thicknesses of 2.0, 1.0, 0.75, 0.5, and 0.25 mm. The speck groups used to simulate microcalcifications are 0.5, 0.4, 0.3, 0.2, and 0.12 mm in diameter. A dose detector can also be fitted in the phantom.[(3)]

For CT scanning the Catphan CT phantom (The Phantom Laboratory, Greenwich, NY) has two low-contrast modules. The supra-slice region has three groups of inserts, each with nine circular objects with diameters between 2 and 15 mm and contrast of 0.3%, 0.5%, and 1.0%. In the subslice module three groups of four inserts each are contained. Diameters range between 3 and 9 mm and contrast is fixed at 1.0%.[(4)] The Gammex ACR CT phantom (Gammex RMI, Middleton, WI) is made from Solid Water and has a 20 cm diameter and 16 cm length. It contains water-equivalent, bone-equivalent, acrylic, air, and polyethylene inserts for CT-number linearity assessment. A 0.011 mm diameter

tungsten carbide bead is used for modulation transfer function (MTF) calculation. Aluminium and polystyrene line pair material is used for resolution assessment with bar phantoms 4, 5, 6, 7, 8, 9, 10, and 12 line pairs per centimetre (lp/cm). Steel balls of 1 mm diameter are used for positioning and alignment checks and 0.28 mm ball bearings for distance measurements on an axial slice. A low-contrast rod module is used for low-contrast resolution with 6, 5, 4, 3, and 2 mm diameter cylinders at a contrast 0.6% different from background. Four cylinders of each diameter are included. CT-number uniformity is assessed with ROI analysis. Slice thickness is checked with two wire ramps evident in 0.5 mm z-axis increments.[5]

The CIRS Model 903 phantom (Radcal Corporation, Monrovia, CA) is used in radiography. It has low-contrast evaluation holes in an aluminium disk at 9.5 mm diameter and 1.73, 1.24, 0.89, 0.64, 0.46, 0.32, 0.23, 0.16, and 0.10 mm depths. High contrast is assessed with a mesh of 0.47, 0.63, 0.79, 0.94, 1.18, 1.57, 1.97, 2.36, and 3.15 line pairs per millimetre (lp/mm) and also contains a contrast detail insert.[6] The NORMI 13 phantom (PTW-Freiburg GmbH) is designed for acceptance and constancy tests for digital projection radiography. The phantom tests signal standardization by measuring the brightness of an image at a central area. It has seven dynamic steps, consisting of different thickness copper plates from 0.0 mm to 2.3 mm, for evaluation of contrast resolution. The steps should be separately identifiable. For low-contrast evaluation, six disks with contrasts of 0.8% to 5.6% are visually inspected at an image window setting where all seven dynamic steps are depicted differently. For homogeneity the optical density or luminance is measured in five different areas, at the center and at the four corners of the image. A lead foil test pattern is used to evaluate spatial resolution, using a magnifying glass. Image geometry is assessed by measuring the distances between different lines. These lines are also used to assess scaling and are checked for distortions. The variation between the light field and X-ray field is investigated using the different field size radiopaque field edge marker lines. The image is also evaluated for the presence of artifacts. An additional copper plate is supplied for use with higher kV setting (e.g., 100 kV). The phantom can also evaluate delivered radiation dose by establishing a dose indicator versus image brightness relationship at acceptance testing.[7]

The TOR CDRH Fluoroscopic phantom (Leeds Test Objects, Broughbridge, UK) has eight low-contrast test holes of the same diameter, 9.5 mm, and depths ranging between 0.16 to 1.73 mm.[8] The NORMI Rad/Flu phantom (PTW-Freiburg GmbH) is used for acceptance and constancy testing in fluoroscopy. It incorporates a copper step-wedge for sensitometry assessment, a resolution test pattern, a grid plate, and eight low-contrast detection inserts.[9] The resolution is assessed visually by reading the lp/mm resolved from the lead-foil roster. Resolutions from 0.6 to 5.0 lp/mm are included. Contrast is visually evaluated with a copper step-wedge, with 17 steps of thickness 0.00 to 3.48 mm at depths of 13 mm and 5 mm.[10] The readings and difference between the gray-scale values of two specified steps is recorded for signal standardization and contrast calculation. Contrast detail inserts are visually inspected for visibility.[11] Eight inserts of 10 mm diameter and depth of 0.4 to 4.0 mm are used as well as 16 inserts, one in each step-wedge step, of 4 mm diameter at 2.5 mm depth.[10] For position verification the distance between the mid-marks on the test object and the center of the radiation limiting field is measured. The diameter of the object is also measured.[11] All of these commercially available phantoms described are X-ray imaging modality specific. In addition, several exposures are needed for comprehensive image quality control with some of these phantoms (e.g., NORMI Rad/Flu and NORMI PAS), which have loose inserts for assessing different image quality parameters. Loose inserts can be lost or damaged. The Catphan is a modular phantom and hence several different slices

are needed for image quality control in CT scanning. A single modality nonspecific phantom, all-inclusive nonmodular phantom, requiring single exposure and single slice analysis, is not currently commercially available.

Image quality is defined in terms of three parameters: contrast, spatial resolution, and noise. Image contrast is the difference in the gray scales of adjoining regions in an image. It is affected by subject, detector, and display contrast. Subject contrast is differences in signal before it is registered as part of the image. Detector contrast describes how the detector converts the signal into output and digital image. Post-acquisition image processing affects display contrast.[12] Spatial resolution describes an imaging system's capability to distinguish two closely adjoining structures as separate as they become smaller and closer together (i.e., the amount of detail in the image). It is described by a point-spread-function (PSF), line-spread-function (LSF) or edge-spread-function (ESF) and these are used to calculate the MTF, which shows the percentage of an object's contrast as a function of its size.[12] Noise is a random "grainy" appearance in an image. Quantum noise is determined by the number of signals used to form the image and it influences the ability to detect low-contrast objects.[12] The image-quality parameters that have to be assessed with X-ray producing equipment in the diagnostic radiology environment include image reproducibility, circular symmetry, spatial linearity, high-contrast resolution, low-contrast detectability, image uniformity, spatial resolution, scaling, magnification, blurring, contrast-detail relationships, and the presence of artifacts.[13,14] Misdiagnosis due to poor image quality is possible, causing details such as small lesions and abnormalities to be missed. Image blurring, artifacts, high levels of image noise, and poor low-contrast detectability are examples of image-quality degradation contributory factors.

X-ray imaging modalities, including general X-rays, fluoroscopy, mammography, and CT scanning, employ X-rays for image formation. X-rays penetrate the body and interact with tissues in order to obtain useful information about the internal anatomy, as illustrated by the produced image.[15] Clinical performance of imaging systems may be assessed systemically with a good QA program. Routine image quality control (QC) compares results obtained at regular test intervals to the results obtained at acceptance testing of the equipment or to the determined baseline values. Deviations from the acceptance test or baseline values are indicative of changes in image quality. Routine QC provides a framework for continuous improvement through routine feedback and assists in identification of deviations from ideal performance (i.e., producing images with clinically relevant and diagnostically acceptable image quality). This could positively impact patient care.[16]

Three main problems are identified in the field of image quality assurance in resource-limited institutions. The biggest concern is cost. The commercially available image quality assurance phantoms are expensive. Each imaging modality currently uses dedicated phantoms, hence several different phantoms are needed for comprehensive image quality assurance. Secondly, human resource deficiency, including manpower and expertise, is a limiting factor. Many institutions do not employ sufficiently trained personnel (e.g., medical physicists) to work with and analyze data from complicated commercially available phantoms. The third problem is time constraints. Image quality assurance result analyses, and decisions on needed corrective action, take time. The lack of available data analysis time is amplified by the human resource deficiency problem in resource-limited institutions.

These limitations can be addressed by a universal phantom that would enable the required image quality assurance tests for all existing X-ray modalities to be done. A universal image quality assurance phantom that is user-friendly, robust, cheaper, compact, and allows for semiautomatic result analysis and recommendation of corrective action, with accompanying data analysis software, is needed. The universal image quality assurance package would include data analysis software and a user's manual explaining test objectives, phantom setup, procedures, and result analysis, as well as setting of baseline values for use in all the X-ray imaging modalities. The aim of this research is the design, development, and manufacturing of such a phantom, of which the prototype is described here.

II. MATERIALS AND METHODS

The image quality assurance parameters that were focused on included low-contrast detectability, high-contrast resolution, signal-to-noise ratios (SNR), contrast-to-noise rations (CNR), image uniformity, sensitometry for planar imaging (like general X-rays, fluoroscopy and mammography), Hounsfield unit (HU) or CT number linearity for CT scanning and the presence of artifacts. For CT scanning, zero-slice position and slice thickness should also be evaluated. In mammography microcalcifications, masses and fibres were assessed. The proposed phantom had to evaluate all these parameters without being a combination of the existing commercially available phantoms (i.e., it should be unique).

Routine QC compares obtained results to set baseline or acceptance testing values and the objective is identifying deviations from these initial values. Figure 1 shows the three-dimensional design of the first phantom prototype. The cubic inserts were arranged perpendicular to the X-ray beam central axis in the CT scanning (upright) and planar (flat) imaging orientations, along the periphery of the phantom. Cubes made from the same material but with different sizes were used for low-contrast detectability and mammography masses. The density of these cubes was selected to be slightly higher than that of the surrounding housing material. Cubes of the same size but made from different materials were used for HU linearity and sensitometry. Planar imaging sensitometry check assesses changes in the displayed gray scale for different materials, compared to set baseline or acceptance testing values. CT slice thickness was determined

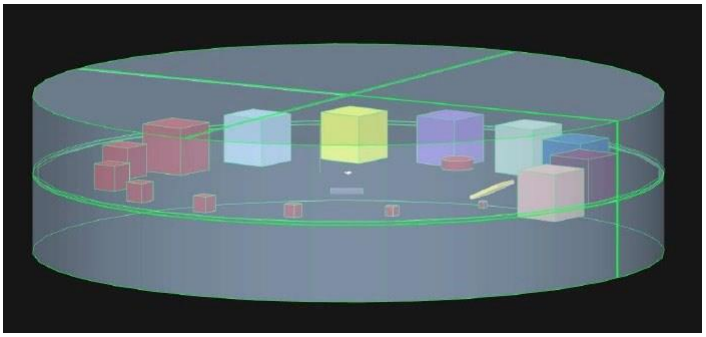

Fig. 1. First phantom prototype 3D illustration.

with a ramp placed in the phantom at a known angle. By using trigonometry, the slice thickness could be calculated. Mammography microcalcifications were simulated with metallic granules in different-sized clusters and rubber bands of different diameters were used to simulate mammography fibres. A cylinder was added to assess circular geometry using on-screen measuring tools available at X-ray imaging units. These were also used to determine distance accuracy by measuring the distance between different inserts and comparing it to the actual known distance.

Data analysis software would employ ROI analysis to calculate SNR, CNR, image uniformity, and the MTF from the PSF of a bead or point source that was smaller than the size of a pixel. The software would require the user to input the obtained image, which is extracted from the imaging system using a step-by-step written standard operating procedure developed by a suitably trained person (e.g., application specialist or computer assistant). Images would be visually inspected by the observer for the presence of artifacts; for example, streaks, ghost images, and blurring. Additional 4 cm attenuator plates, made from the same material as the phantom, will be supplied to simulate patient attenuation and evaluate automatic exposure control (AEC). The first phantom prototype would therefore measure all the image quality assessment parameters, as recommended in literature.
The development of the initial phantom concept into the first prototype resulted in the construction of the prototype. The sizes and materials of the different phantom inserts selected for the first phantom prototype are shown in Fig. 2.

The phantom housing was made from high-density polyethylene (HDPE) with a diameter of 200 mm and a density of 0.95 g/cm^3. This material was selected as it was affordable, easy to machine, and had a density suitably different from that of the low-contrast detectability cubes. The chosen diameter was sufficient to fit the inserts without interference. As the X-ray tube circularly rotates around the phantom in CT scanning, it was designed round. The cubes for low-contrast detectability and mammography masses were 3D printed from PMMA (density of 1.18 g/cm^3), in sizes of 2, 3, 4, 6, 8, 10, and 20 mm^3. The density of PMMA was 24.2 % higher than that of the HDPE housing material. HU linearity and sensitometry cubes included the 20 mm^3 PMMA cube. Additional 20 mm^3 cubes of Teflon (density of 2.20 g/cm^3), Gammex SB3 bone-equivalent plastic (density of 1.82 g/cm^3), Supawood (density of 0.74 g/cm^3) (Supawood Architectural Lining Systems, Robin Hill, Australia), Gammex LN300 lung-equivalent plastic (density of 0.30 g/cm^3) and air were incorporated. This gave six inserts ranging in density from air to bone for sensitometry assessment. Mammography fibres were simulated with 20 mm rubber bands, of density 1.26 g/cm^3, in diameters of 0.4, 0.6, 0.9, 1.2, and 1.5 mm. The CT slice thickness ramp was a 20 × 10 × 2 mm^3 slab of Gammex SB3 bone-equivalent plastic, placed in the phantom at 37°. The mammography microcalcifications were simulated with granules cut from metallic wires of diameter 0.2, 0.3, 0.4, and 0.5 mm. For MTF calculation from PSF, three metallic balls of diameters 0.35, 0.50, and 1.00 mm were included. The calculation would be done with the planned data analysis software. A 2.27 mm diameter ball bearing was included as central bead for cross-wire centering and zero-slice position evaluation. This ball was located exactly at the phantom center in 3D. Circular geometry was determined from a Perspex cylinder of 20 mm diameter, 20 mm length.

Figure 3 shows the construction drawings of the first phantom prototype, as drawn in SolidWorks 2015 Premium CAD 3-D design software (SOLIDWORKS Corp., Waltham, MA). Each of the halves was 250 mm thick. The cubic inserts, central bead, and cylinder were placed exactly on the middle plane between the two halves. The CT slice thickness ramp, mammography microcalcifications, and fibers and MTF beads were sunken into the bottom half of the first phantom prototype. In Fig. 2, semicircular cutouts are seen at the corners of the cubic inserts, due to round cutters being used to machine square voids. In the first prototype these cutouts were kept as air-filled voids, but it could be filled with wax, with a density of 0.93 g/cm^3, if necessary, due to image artifacts.

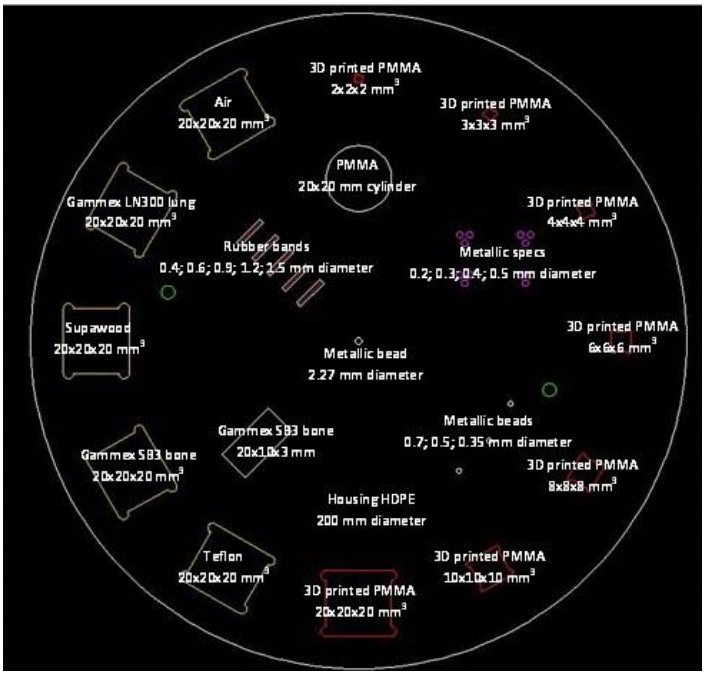

Fig. 2. Inserts of the first phantom prototype.

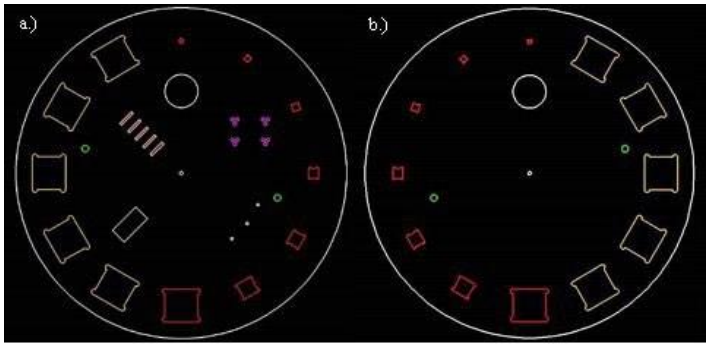

Fig. 3. Construction drawings of first prototype: (a) bottom half, (b) top half.

Voids were machined from a slab of phantom HDPE housing material, using a MultiCam 3000 series router (MultiCam Inc., Dallas, TX) for CNC routing. Cutting was done layer-bylayer and at a slow enough speed to prevent breaking of the cutters. However, cutting could not be done too slowly or else the HDPE would melt. This was done for the bottom and top halves of the phantom. Once all voids were in place, the circular phantom housing was cut from the HDPE slabs. The inserts were then fitted and the two halves were secured together using nylon screws. The process is illustrated in Fig. 4. Figure 5 shows the finished first prototype.

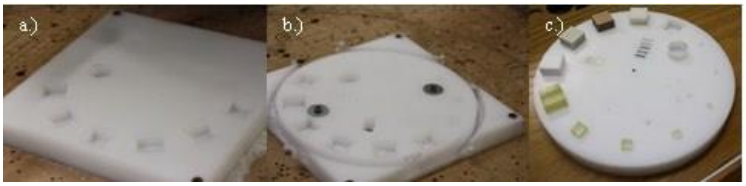

Fig. 4. The construction process: (a) machining voids from a 250 mm slab of HDPE, (b) cutting the round first prototype phantom housing from the slab of HDPE, (c) placing the inserts in the bottom half of the first prototype phantom housing.

Fig. 5. Completed first phantom prototype.

III. RESULTS AND DISCUSSION

The prototype was imaged for initial testing. Figure 6 shows the original images acquired with the first prototype. Figure 6(a) is an axial CT scan slice obtained with a Siemens Somatom Definition Edge CT (Siemens Healthcare GmbH, Erlagen, Germany) using a brain-imaging protocol; that is to say, 120 kV, 298 mA, 3.66 s, 235 cm field of view, pitch of 0.8, and 5 mm slices, and reconstruction with a medium smooth filter. A Siemens Ysio unit, at 40 kV, 2 mAs, 100 cm source-to-image distance, large focus, and with the cassette outside bucky, was used to produce the general X-ray image of the first phantom prototype, illustrated in Fig. 6(b). A Siemens Axiom Luminos DRF unit was used to produce the fluoroscopic image in Fig. 6(c), with technique factors of 62.3 kV, 10.2 mA, and 0.01 ms. The mammogram in Fig. 6(d) was obtained with a Siemens Mammomat Inspiration unit at 28 kV and 62.1 mAs, using automatic exposure control. Table 1 shows visual inspection results from the images in Fig. 6. All other results, including SNR, CNR, MTF, and uniformity calculations, as well as sensitometry, geometry, and slice thickness measurements, will be done with the data analysis software, which will only form part of the final phantom package.

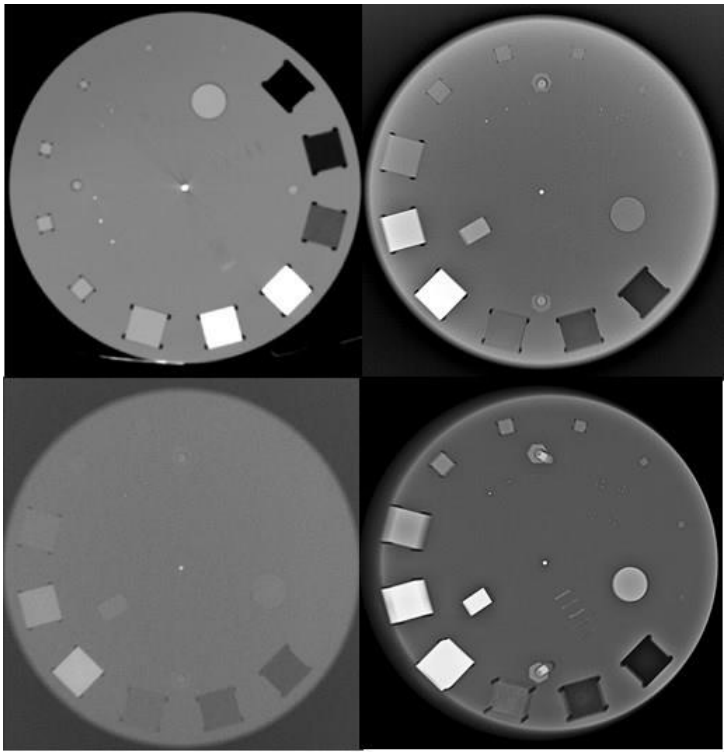

Fig. 6. First phantom prototype: (a) CT scan axial slice, (b) general X-ray, (c) image produced with fluoroscopy of the prototype, (d) mammogram of the prototype.

Table 1. Visual image quality assurance results from Fig. 6 images.

Imaging Modality	*Visual Image Quality Assessment Parameter*		
	Low Contrast Detectability	*Artifacts*	*Other*
Mammography	2×2×2 mm^3 mass seen	Geometrical distortion	0.4 mm fiber seen 0.2 mm specs seen
CT scanning	2×2×2 mm^3 mass seen	Streak artifact from central ball	Not applicable
General X-rays	2×2×2 mm^3 mass seen	None	Not applicable
Fluoroscopy	8×8×8 mm^3 mass seen	None	Not applicable

From the images in Fig. 6, the following recommendations and future improvements for subsequent phantoms were derived. The semicircular air voids at the corners of the cubic inserts did not produce significant artifacts. The nylon screws should be placed closer to the smaller cubic inserts, as these produced some interference in phantom halves fitting together. Machining should be done on a void-by-void basis, machining the voids marginally smaller than the actual inserts or size-to-size to ensure a tight fit. A 1 mm^3 3D-printed PMMA cube should be added to the low-contrast detectability and mammography mass simulation inserts.

Once these adjustments are made in the second phantom prototype, the prototype will then undergo vigorous testing, comparing its results to those from commercially available phantoms, to finalize the phantom design. The final phantom will be scientifically validated for each of the modalities to which it is intended to be applied. The validation process will include c areful comparison with existing modality specific phantoms. Table 2 compares the image quality parameters that can be assessed with the universal image quality assurance phantom prototype, compared to the capabilities of the

discussed commercially available phantoms. From this table it is clear that the universal image quality assurance phantom prototype is indeed an all-in-one image quality assurance phantom for general X-rays, fluoroscopy, mammography, and CT scanning.

Table 2. Summary of commercially available modality specific phantoms compared to the universal image quality assurance phantom prototype. X indicates the parameter the phantom can assess.

Image Quality Parameter	*Sensitometry*	*Low Contrast Detectability*	*Uniformity*	*Resolution*
ACR Mammo		X		
NORMI PAS	X	X		X
Gammex ACR CT	X	X	X	X
Catphan	X	X	X	X
CIRS 903 X-ray		X		X
NORMI 13		X	X	X
CDRH Fluoro		X		X
NORMI Rad/Flu	X	X		X
Universal phantom	X	X	X	X

Image Quality Parameter	*Noise*	*Positioning and Alignment*	*Geometry and Measurement Tools*	*Artifacts*
ACR Mammo	X			X
NORMI PAS	X	X		X
Gammex ACR CT		X	X	
Catphan	X	X	X	
CIRS 903 X-ray			X	
NORMI 13			X	X
CDRH Fluoro				
NORMI Rad/Flu		X	X	
Universal phantom	X	X	X	X

Image Quality Parameter	*Field Size*	*Standard Signal*	*High Contrast Resolution*	*Other*
ACR Mammo		X	X	X (Fibers)
NORMI PAS	X	X	X	X (Fibers)
Gammex ACR CT				X (Slice thickness)
Catphan				X (Slice thickness)
CIRS 903 X-ray				
NORMI 13	X	X	X	
CDRH Fluoro				
NORMI Rad/Flu		X	X	
Universal phantom	X	X	X	X (Fibers and slice thickness)

IV. CONCLUSION

Diagnostic radiology X-ray images should be clinically acceptable for disease follow-up and diagnosis. Routine image quality assurance, with a suitable phantom, ensures this. A universal phantom suitable to do quality assurance on the complete spectrum of X-ray imaging modalities was designed and a

prototype manufactured from the design. The initial images acquired with the prototype were satisfactory and showed that only small adjustments were needed to develop the prototype into a user-friendly universal phantom. The phantom prototype described above could be seen as the leading step towards developing a universal phantom, which will fill a gap in the existing market, with special emphasis on resource-limited institutions.

ACKNOWLEDGMENTS

The authors acknowledge Johan Braasch, of Gebrateq Advanced Engineering, who contributed substantially to the design and development of the first phantom prototype, and wish to thank Winelands Radiology in Vergelegen Medi Clinic for imaging of the first phantom prototype. This research is presented in partial fulfilment of the requirements for the degree of PhD (Medical Physics) in the Faculty of Medicine and Health Sciences at Stellenbosch University. The research proposal is the intellectual property of Stellenbosch University under the PCT International Patent Application No. PCT/IB2016/051165.

COPYRIGHT

REFERENCES

1. ACR Mammographic accreditation phantom model 156. Middleton, WI: Gammex RMI Inc; 2013. Available from: http://www.sunnuclear.com/solutions/diagnostic/mammography. Accessed 14 October 2013.
2. Argo WP, Hintelang K, Hintelang DE. A tissue-equivalent phantom series for mammography dosimetry. J Appl Clin Med Phys. 2004;5(4):112–19.
3. PTW. NORMI PAS user manual. Freiburg, Germany: PTW-Freiburg. Available from: http://www.ptw.de/ home_start.html?&no_cache=1. Accessed 11 February 2016.
4. Hernandez-Giron I, Geleijns J, Calzado A, Veldkamp WJ. Automated assessment of low contrast sensitivity for CT systems using a model observer. Med Phys. 2011;38 (Suppl 1):S25.
5. McCollough CH. CT accreditation program: image quality and dose measurements. The American Association of Physicists in Medicine. Available from: https://www.aapm.org/meetings/03AM/pdf/9785-27333.pdf
6. Computerized Imaging Reference Systems Inc. Radiography fluoroscopy QA phantom: Model 903. Ellicott City, MD: Medical Device Depot Inc.; 2014.
7. PTW. NORMI 13 user manual. Freiburg, Germany: PTW-Freiburg. Available from: http://www.ptw.de/normi_130. html. Accessed 11 February 2016.
8. CDRH Fluoroscopic phantom. Everett, WA: Fluke Biomedical; 2013 Available from: http://www.flukebiomedical.com/biomedical/usen/Diagnostic-Imaging-QUALITY%20ASSURANCE/Radiography/Fluoroscopy/07-649. htm?PID=54334. Accessed 4 September 2013.
9. PTW. NORMI Rad/Flu X-ray test object. Freiburg, Germany: PTW-Freiburg; 2015. Available from: http://www. ptw.de/typo3conf/ext/naw_securedl/securephp?u=0&file=ZmlsZWFkbWluL2ludGVybmFscy9kZ25fcmFkL05 PUk1JX1JBRF9GTFVfQnJvX2VuXzg1NzIxOTAwXzAzLnBkZg==&t=1458023697&hash=2ee6c62828d03c c3d958184fceca483e. Accessed 4 September 2013.
10. PTW. NORMI Rad/Flu. Freiburg, Germany: PTW-Freiburg; 2013. Available from: http://www.ptw.de/2856.html. Accessed 4 February 2016.
11. PTW. NORMI 4 Flu instruction manual. Freiburg, Germany: PTW-Freiburg. http://www.ptw.de/home_start. html?&no_cache=1. Accessed 11 February 2016.
12. Bushberg JT, Seibert JA, Leidholdt EM, Boone JM. The essential physics of medical imaging, third edition. Chapter 4. Philadelphia, PA: Lippincott Williams & Wilkins; 2012.
13. Suliman II, van Soldt RTM, Zoetelief J. Digital fluoroscopy quality control measurements. IFMBE Proc. 2007;14(3):1470–74.
14. Tsai MH, Chung CT, Wang CW, Chan YK, Shen CC. An automatic contrast-detail phantom image quality figure evaluator in digital radiography. Int J Innov Comput I. 2012;8(2):1063–75.
15. Dance DR, Christofides S, Maidment ADA, McLean ID, Ng KH. Fundamentals of atomic and nuclear physics, Chapter 1. In: Diagnostic radiology physics — a handbook for teachers and students, first edition. Vienna: IAEA; 2014. p.7.
16. Reis C, Pascoal A, Sakellaris T, Koutalonis M. Quality assurance and quality control in mammography: a review of available guidance worldwide. Insights Imaging. 2013;4(5):539–53.

D.2 Presentation

The prototype was presented at the 2016 South African Association of Physicists in Medicine and Biology (SAAPMB) congress and was awarded the Meditech prize for the person or group that develops new technology, including information technology, devices, or computer programmes in a research project. The accepted abstract is included below.

Design of a universal phantom for quality assurance in diagnostic radiology x-ray imaging – the prototype

Annemari Groenewald[a], Willem A Groenewald[b]

[a] *MScMedSc (Medical Physics), Equra Health, Vergelegen Oncology Unit, Somerset West*
[b] *PhD (Medical Physics), Radiodiagnosis Division, Faculty of Medicine and Health Sciences, University of Stellenbosch*

Introduction: In diagnostic radiology projection radiography, fluoroscopy, mammography and computed tomography (CT) are used in the diagnosis and follow-up of a variety of disease conditions. Diagnostically acceptable image quality is needed for proper diagnosis. A quality assurance (QA) programme enables the detection of image quality degradation, before clinically significant image defects occur. Currently expensive modality specific image quality assessment phantoms are available. Resource limited institutions are faced with time, man power and expertise and financial constraints. The aim of this study was to design a universal phantom, that could be used for x-ray image QA, which is robust, easy to use and affordable. The prototype of this phantom is presented here.

Materials and Methods: Commercially available phantoms were investigated, for example the Catphan in CT scanning, ACR mammo-phantom in mammography and the NORMI 13 and NORMI Rad/Flu phantoms in general x-rays and fluoroscopy. The image quality parameters necessary for image quality assurance were determined. The universal phantom concept was developed based on this knowledge, keeping ease of use and reduced cost in mind. Different possible phantom housing and insert materials were investigated, considering physical properties, machinability and cost. The prototype was drawn to scale three dimensionally.

Results: The three dimensional model of the prototype was used to manufacture the phantom housing and inserts. Some of the inserts were 3-D printed, others were machined from suitable materials. The first prototype of the universal x-ray imaging phantom was assembled. Imaging of the prototype provided satisfactory results.

Conclusion: The universal phantom prototype conformed to the aim of a single phantom for multiple imaging modalities. It addressed the identified constraints by significantly reducing manufacturing costs and being easy and quick to use.

International Patent Application No. PCT/IB2016/051165 has been filed for this technology.

Keywords: Image quality assurance, Phantom, Diagnostic radiology, X-ray imaging, Prototype

289 words

PLEASE DO NOT PUBLISH THIS ABSTRACT! Already submitted for publication in another journal.

The completed project will be presented at the 2017 SAAPMB congress, with the accepted abstract included below.

Introduction

Diagnostic radiology x-ray imaging requires image quality to be maintained at clinically acceptable levels for accurate disease diagnosis. This is achieved with routine image quality control (QC) using phantoms. Commercially available phantoms are imaging modality specific, expensive and often complicated to use. In resource limited institutions cost, man power and expertise and time constraints are identified as problems in image QC. A gap exists in the market for a cost and time saving, user friendly single universal image quality assurance (U-QA) phantom, capable of doing all required image QC tests for projection radiography, fluoroscopy, mammography and Computed Tomography (CT) scanning.

Aim

To design, manufacture and validate a compact, unique, universal and cost-effective U-QA phantom for diagnostic radiology x-ray imaging.

Materials and methods

The U-QA phantom was manufactured to include several inserts to asses sensitometry, uniformity, resolution, noise, geometry, standard signal, low contrast detectability, alignment, artefacts, visual image quality inspection, CT slice thickness and mammography masses, fibres and micro-calcifications. Data analysis software and a step-by-step user's manual was prepared. Reproducibility testing and independent validation of the phantom, software and manual was done.

Results

The U-QA phantom and data analysis software produced reproducible results complying with Department of Health tolerance levels for all imaging modalities. Independent validation confirmed that the phantom package was indeed compact, user friendly, versatile and cost effective.

Discussion and conclusion

The U-QA phantom, data analysis software and user's manual, offers an acceptable single phantom solution for medical x-ray imaging. It is a cost and time saver and fills a gap in the existing market.

This research was performed in partial fulfilment of the requirements for the degree of PhD (Medical Physics) at Stellenbosch University under patent PCT/IB2016/051165.